Regulation and Targeting of MCL-1 in Human Oral Cancers

By

Prasad Chandrakant Sulkshane

[LIFE09201004002]

Tata Memorial Centre

Mumbai

A thesis submitted to the
Board of Studies in Life Sciences
In partial fulfillment of requirements
for the Degree of

DOCTOR OF PHILOSOPHY

of

HOMI BHABHA NATIONAL INSTITUTE

MARCH, 2017

Homi Bhabha National Institute

Recommendations of the Viva Voce Committee

As members of the Viva Voce Committee, we certify that we have read the dissertation prepared by Mr. Prasad Chandrakant Sulkshane entitled "**Regulation and Targeting of MCL-1 in Human Oral Cancers**" and recommend that it may be accepted as fulfilling the thesis requirement for the award of Degree of Doctor of Philosophy.

M. M. Vaidya 29.03.2017

Chairman – Dr. Milind Vaidya Date:

T R Teni 29.03.2017

Guide/Convener – Dr. Tanuja Teni Date:

Sanjay 29/03/2017

Member 1 – Dr. Sanjay Gupta Date:

V. Prasanna 29/3/17

Member 2 – Dr. Prasanna Venkatraman Date:

29/03/17

Invitee – Dr. Nagaraj Balasubramanian Date:

D. KRN 29/03/2017

External Examiner – Dr. D. Karunagaran Date:

Final approval and acceptance of this thesis is contingent upon the candidate's submission of the final copies of the thesis to HBNI.

I hereby certify that I have read this thesis prepared under my direction and recommend that it may be accepted as fulfilling the thesis requirement.

T R Teni

Date: 29th March 2017
Place: Navi Mumbai

Dr. Tanuja Teni
Guide

STATEMENT BY AUTHOR

This dissertation has been submitted in partial fulfillment of requirements for an advanced degree at Homi Bhabha National Institute (HBNI) and is deposited in the Library to be made available to borrowers under rules of the HBNI. Brief quotations from this dissertation are allowable without special permission, provided that accurate acknowledgement of source is made. Requests for permission for extended quotation from or reproduction of this manuscript in whole or in part may be granted by the Competent Authority of HBNI when in his or her judgment the proposed use of the material is in the interests of scholarship. In all other instances, however, permission must be obtained from the author.

Prasad Sulkshane

DECLARATION

I hereby declare that the investigation presented in the thesis titled “Regulation and Targeting of MCL-1 in Human Oral Cancers” has been carried out by me. The work is original and has not been submitted earlier as a whole or in part for a degree/diploma at this or any other Institution / University.

Prasad Sulkshane

List of Publications arising from the thesis

Published:

BH3 mimetic Obatoclax (GX15-070) mediates mitochondrial stress predominantly via MCL-1 inhibition and induces autophagy-dependent necroptosis in human oral cancer cells. **Prasad Sulkshane,** Tanuja Teni. Oncotarget, August 2016 (DOI: 10.18632/oncotarget.11085).

Under submission:

Deubiquitinase USP9X stabilizes MCL-1 and contributes to tumor progression in human oral cancers. **Prasad Sulkshane,** Sushil Pawar, Sagar Pawar, Aniket Kamble, Harshada Sulkshane, Priyanka Rajput, Prajakta Kalkar, Rahul Patil, Tanuja Teni.

Conferences:

1. National Research Scholars Meet (NRSM), ACTREC, December, 2015.
2. 34th Annual convention of Indian Association for Cancer Research (IACR), Jaipur, 2015.
3. Gordon Research Conference (GRC) on "Cell death mechanisms at the interface of Health and Disease", West Dover, Vermont, USA, 2014.
4. All India Cell Biology Conference (AICBC) and Symposium on "Cell Dynamics and Cell Fate", Bangalore, 2013.
5. 32nd Annual convention of Indian Association for Cancer Research (IACR), Delhi, 2013.
6. Satellite meeting of the American Association for Cancer Research (AACR) "New Horizons in Cancer Research: Biology to Prevention to Therapy" Delhi NCR, 2011.

Prasad Sulkshane

Dedicated

to my

beloved family

ACKNOWLEDGMENT

I take this opportunity to thank the Almighty for the blessings, good health and mercy which helped me pursue my ambitions. First and foremost, I express my sincere gratitude to my mentor Dr. Tanuja Teni for this opportunity, her constant encouragement and supervision throughout the tenure. She has been extremely supportive through several difficult phases of the project. I also thank Dr. Shubhada Chiplunkar (Director), Dr. Sudeep Gupta (Deputy Director), Dr. Rajiv Sarin (Ex. Director) and Dr. Surekha Zingde (Ex. Deputy Director) for providing this wonderful opportunity to work in the institute. I am grateful to DBT, Govt. of India for providing the fellowship. I am also thankful to my Doctoral Committee members Dr. Milind Vaidya (Chaiperson), Dr. Sanjay Gupta, Dr. Prasanna Venkataraman, Dr. Nagaraj Balasubramanian (IISER, Pune), and Dr. Girish Maru (Ex. Chairperson) for their invaluable suggestions and critical analysis of the data.

I extend my sincere thanks to the staff of Animal house facility, ACTREC Digital imaging facility, Electron microscopy facility, Flow cytometry facility, Proteomics facility, Genomics facility and Common facility for providing the necessary infrastructure. I would also like to thank Administration Department, Accounts Department, HBNI Program office, Steno pool and other affiliated Departments for their timely assistance in processing various documents. I am extremely thankful to all the members of the Teni laboratory, my second family over the last few years: Staff: Mr. Sagar (for his timely scientific assistance), Mr. Yeshwant (for help with cell culture), Seniors: Dr. Vinayak (who taught me basic techniques in the lab), Dr. Rupa, colleague: Dr. Mohd. Yasser, Juniors: Rajashree, Dhanashree, Abhay, Dipti, Trainees: Harshada, Priyanka, Madhumitha, Heena, Aniket, Project staff: Prajakta, Rohit, Hrushikesh, Melissa, Ashish. Everyone has been extremely helpful and kind. Prajakta deserves a special mention as she has

always provided moral support throughout the turbulent times of the tenure. I wish to thank Dr. Sushil Pawar and Dr. Rahul Patil for their help with collection of oral tissue samples and providing demographic data of the individuals, performing IHC and data analysis. The 2010 batchmates (especially Crismita, Indrajit, Shyam, Poonam, Saikat, Richa, Asif and Rushikesh) have always been very supportive in terms of technical advice, reagent requirements or even nonscientific help.

This work wouldn't have been possible without the love, blessings, constant support and encouragement of my family. My grandfather (late), grandmother, father (late), mother, my loving sisters and every single individual of my family has got a share in this effort. Finally, I am grateful to all those who knowingly-unknowingly helped me through this voyage but couldn't mention them here due to space constraints. Thank you everyone!

Prasad Sulkshane

CONTENTS

	Page No.
Synopsis	12-25
List of Abbreviations	26-29
List of Figures	30-32
List of Tables	33
Chapter 1: Introduction	**34-39**
Chapter 2: Review of Literature	**40-73**
2.1 Oral cancer	41
2.2 Etiological factors associated with oral carcinogenesis	43
2.3 Current treatment modalities for the management of oral cancers	45
2.4 Apoptosis and its dysregulation in human cancers	48
2.5 The Intrinsic pathway of Apoptosis	49
2.6 The BCL-2 family	51
2.7 The BH3-only proteins	52
2.8 Myeloid Cell Leukemia-1 (MCL-1)	53
2.9 Autophagy	68
2.10 Necroptosis	72
Chapter 3: Aims and Objectives	**74-75**
Chapter 4: Materials and Methods	**76-106**
4.1 Materials	77-82
4.2 Methods	83-106
4.2.1 Mammalian cell culture	83

4.2.2 Cell viability assays 85

4.2.3 siRNA transfection 86

4.2.4 Flow cytometry 87

4.2.5 Fluorescence microscopy 88

4.2.6 Protein extraction and western blotting 91

4.2.7 Coimmunoprecipitation 95

4.2.8 Cycloheximide chase assay 96

4.2.9 Mitochondrial fractionation and cytochrome c release assay 96

4.2.10 RNA extraction, cDNA synthesis and real time PCR 97

4.2.11 Immunohistochemistry 99

4.2.12 *In vivo* studies 101

4.2.13 TUNEL assay 102

4.2.14 Coimmunoprecipitation coupled with mass spectrometry for identification of MCL-1-interacting proteins 103

4.2.15 Transmission Electron Microscopy (TEM) 105

4.2.16 Statistical analysis 106

Chapter 5: Results **107-180**

5.1 To assess the role of MCL-1-interacting partners that may contribute to its stability in human oral cancers **108-146**

5.1.1 To determine the basal levels of BCL-2 family proteins in human oral cancer cells 108

5.1.2 MCL-1 is rapidly degraded by the ubiquitin-proteasomal pathway 109

5.1.3 MCL-1 protein has a rapid rate of turnover and a short half-life as compared to BCL-2 and BCL-XL proteins 111

5.1.4. MCL-1 protein expression correlates with USP9X expression in oral cell lines and oral tissues 112

5.1.5 USP9X interacts with MCL-1 113

5.1.6 Standardization of siRNA transfection and siRNA mediated USP9X downregulation 114

5.1.7 USP9X downregulation lowers MCL-1 protein levels without affecting transcript expression 115

5.1.8 USP9X downregulation lowers MCL-1 protein levels by increasing its turnover 116

5.1.9 USP9X knockdown increases the radiosensitivity of OSCC cells 118

5.1.10 Deubiquitinase inhibitor WP1130 (Degrasyn) potently induces apoptosis in OSCC cells by causing rapid degradation of MCL-1 protein 119

5.1.11 WP1130 treatment triggers rapid accumulation of aggresomes in OSCC cells 122

5.1.12 *In vivo* efficacy of WP1130 in xenograft mouse models 123

5.1.13 MCL-1 expression correlates with USP9X expression in different oral histotypes 125

5.1.14 High MCL-1 expression correlates with a corresponding high USP9X expression in recurrent oral tumor samples 130

5.1.15 To investigate the role of Translationally Controlled Tumor Protein (TCTP) in stabilization of MCL-1 protein 133

5.1.16 MCL-1 and TCTP expression correlates in diverse oral histopathological types 135

5.1.17 Evaluation of E3-Ubiquitin Ligase MULE in regulating the stability of MCL-1 137

5.1.18 Identification of novel interacting partners of MCL-1 140

5.2 To assess the *in vitro/in vivo* effects of small molecule inhibitor of MCL-1 on human oral cancer cell lines 147-180

5.2.1 Obatoclax potently inhibits clonogenic potential of OSCC cells 148

5.2.2 Obatoclax does not alter the expression of BCL-2 family proteins but dissociate MCL-1/BAK interaction and induce BAX translocation to mitochondria 151

5.2.3 Obatoclax triggers caspase-independent cell death in OSCC cells 153

5.2.4 Obatoclax potently induces autophagy in OSCC cells 156

5.2.5 Obatoclax-induced autophagy culminates into cell death 158

5.2.6 Obatoclax causes a disturbance in autophagic flux leading to a defective autophagy in OSCC cells 160

5.2.7 Obatoclax-induced cell death in OSCC cells is mediated by necroptosis 164

5.2.8 Obatoclax induces extensive fragmentation of the mitochondrial network 167

5.2.9 Obatoclax induces mitochondrial oxidative stress and mitochondrial membrane depolarization in OSCC cells 170

5.2.10 Obatoclax-induced mitochondrial stress does not culminate into mitophagy 173

5.2.11 MCL-1 downregulation induces mitochondrial stress in SCC029B cells 175

5.2.12 Ultrastructural changes induced by Obatoclax 176

5.2.13 Obatoclax exhibits potent antitumor activity in xenograft mouse models 178

5.2.14 Obatoclax exhibits synergism with ionizing radiation to inhibit the clonogenic potential of OSCC cells 179

Chapter 6: Discussion **181-200**

6.1 Role of USP9X in stabilization of MCL-1 protein 183

6.2 Role of TCTP in stabilization of MCL-1 protein 187

6.3 Role of MULE in regulating the stability of MCL-1 protein 189

6.4 Identification of novel interacting partners of MCL-1 192

6.5 Efficacy and mode of action of Obatoclax against oral cancer cells 194

Chapter 7: Summary and Conclusions 201-205

Chapter 8: References 206-242

Chapter 9: Appendix 243-248

Chapter 10: Publication 249-270

Synopsis

Homi Bhabha National Institute

SYNOPSIS OF Ph. D. THESIS

1. Name of the Student: Mr. Prasad Chandrakant Sulkshane

2. Name of the Constituent Institution: ACTREC, Tata Memorial Centre

3. Enrolment No. : LIFE09201004002

4. Title of the Thesis: "Regulation and Targeting of MCL-1 in Human Oral Cancers".

5. Board of Studies: Life Sciences

SYNOPSIS

Background

Oral Squamous Cell Carcinoma (OSCC) is among the most prevalent cancers in the Indian subcontinent. It is estimated that OSCC alone comprises 30–40% of all malignancies among Indian males, the major risk factors being tobacco usage, betel quid chewing and alcohol consumption (Tandle et al. 2001). Indeed, a recent study revealed that tobacco-related cancers account for about 42% male and 18% female cancer deaths across India (Dikshit et al. 2012). About 40% OSCC patients die from loco-regional disease while 24% develop distant metastases (Notani et al. 2001). However, despite major improvements in cancer therapeutics, the 5-year survival rate of OSCC patients has not shown a significant improvement over the past several years (Lee et al. 2005).

The BCL-2 family

The intrinsic pathway of apoptosis is regulated by members of the BCL-2 family which are divided into three groups: Antiapoptotic members include BCL-2, BCL-XL, BCL-W, MCL-1, and A1 which contain multiple BH domains and antagonize apoptosis. The proapoptotic members include those containing multiple BH domains such as BAK, BAX and BH3-only members such as BID, BIM, PUMA, NOXA, BIK, BAD, HRK which promote apoptosis (Youle et al. 2008).

Apoptotic dysregulation and human oral cancers

Like many other human cancers, apoptotic dysregulation is believed to be the underlying cause for the progression of human oral cancers (Polverini et al. 1999). Previous studies from our lab has shown that antiapoptotic proteins of the BCL-2 family including Myeloid Cell Leukemia-1 (MCL-1) are overexpressed in human oral premalignant lesions and oral tumors as compared to normal oral mucosa (Mallick et al. 2009). We have also demonstrated that MCL-1 overexpression is associated with poor prognosis and reduced disease free survival in oral cancer patients treated with chemoradiotherapy indicating its potential role in chemo and radioresistance (Mallick et al. 2009, Palve et al. 2014, Palve et al. 2012). MCL-1 thus appears to be a potential therapeutic target in human oral cancers.

MCL-1: Myeloid Cell Leukemia-1

MCL-1, an antiapoptotic member of the BCL-2 family was identified as an immediate-early gene expressed during differentiation of a human myeloid leukemia cell line (Kozopas et al. 1993). It is primarily localized to the mitochondria (Craig et al. 1994). It is organised into BH1, BH2 and BH3 domains and a C terminus hydrophobic transmembrane domain (Yang et al. 1995). It contains a long N terminus domain (~170 amino acid residues) and contains two PEST domains

which are responsible for its characteristic rapid turnover and a short half-life. It not only provides survival advantage to the cancer cells but is important for the development and survival of important cell lineages (Zhou et al. 1997, Thomas et al. 2013, Opferman et al. 2003). MCL-1 deletion therefore is associated with peri-implantation lethality during mouse embryogenesis (Rinkenberger et al. 2000).

MCL-1 is overexpressed in many hematological cancers and solid tumours (Placzek et al. 2010). It imparts resistance to many chemotherapeutic drugs (Thallinger at al. 2004) and to radiation in many cancer cell lines (Skvara et al. 2005).

Therapeutic targeting of MCL-1 protein therefore provides great opportunities. However, due to its structural discrepancy from other antiapoptotic BCL-2 family members, therapeutic targeting of MCL-1 protein has largely been hindered (Nguyen et al. 2007). MCL-1 is well known to exhibit resistance to ABT-737 and ABT-263 which potently antagonize BCL-2, BCL-XL and BCL-W (Yecies et al. 2010). Nevertheless, newer generation pan-BCL-2 inhibitors such as Obatoclax and Sabutoclax which efficiently antagonize all the antiapoptotic BCL-2 family proteins including MCL-1 are actively being sought.

Regulation of MCL-1 expression

MCL-1 being a critical prosurvival protein, it is tightly regulated at multiple levels. Of these, the post-translational mode of MCL-1 regulation is the most pivotal which ultimately determines the stability and thus level of MCL-1 protein in the cell. MCL-1 is unique among the antiapoptotic members of the BCL-2 family in that it has a rapid rate of turnover mediated by the ubiquitin-proteasomal pathway which is responsible for its characteristic short half life. However, a tumor cell adopts several approaches to maintain its constitutively elevated levels (Ertel et al. 2013). The stability of MCL-1 protein is determined in a context-dependent manner in a cell which

includes a complex interplay of key kinases (such as ERK, GSK-3β), downstream E3-ubiquitin ligases (such as MULE/ARF-BP1, SCF^{FBW7}, β-TrCP) and deubiquitinases (such as USP9X). Not only does the level of these E3 ligases or deubiquitinases but also the extent of their interaction with MCL-1 determine the stability of MCL-1 protein.

The relevance and expected outcome of the proposed study

MCL-1 protein has a rapid rate of turnover (mediated by the ubiquitin- proteasomal degradation pathway), and thus has a short half-life. We have documented its overexpression in human oral premalignant lesions and oral cancers. It is therefore apparent that MCL-1 protein is stabilized in tumors through several mechanisms such as through the interaction with other proteins which could mediate its stabilization. We therefore intended to study the contribution of these interacting partners (such as the deubiquitinase USP9X and a small ubiquitously present protein TCTP) towards MCL-1 stabilization and of MULE (an E3-ubiquitin ligase specific for MCL-1) towards targeting it for proteasomal degradation. We also seek to identify novel interacting partners of MCL-1. In the second objective, we seek to target MCL-1 protein with a small molecule BH3 mimetic Obatoclax and assess the mode of its action in oral cancer cells.

Key questions:

1. Is the high expression of MCL-1 in oral cancers versus normal mucosa due to increased MCL-1 protein stability?
2. What are the binding partners of MCL-1 that contribute to its stability?
3. Using small molecule inhibitors can we target MCL-1 and/or its stabilizing partners?

Hypothesis:

We hypothesize that the overexpression of MCL-1 protein in human oral cancers may largely be contributed by its stabilization through interaction with pro-stabilizing partners. Moreover,

targeting MCL-1 protein with a small molecule BH3-mimetic pan-BCL-2 inhibitor Obatoclax could exhibit potent activity against OSCC cell lines.

Objectives:

1. To assess the role of MCL-1 interacting partners that may contribute to its stability in human oral cancers.
    a. Reported interacting partners (USP9X, TCTP and MULE)
    b. Novel interacting partners to be identified through MS.
2. To assess the *in vitro/in vivo* effects of small molecule inhibitor of MCL-1 on human oral cancer cell lines.

Cell lines used in the study:

Cell line	**Origin**
DOK	Dysplastic oral keratinocyte, derived from tongue epithelium
AW8507	Poorly differentiated SCC of tongue
AW13516	Epidermoid carcinoma of tongue
SCC029B	Human buccal mucosa carcinoma

Objective 1: To assess the role of MCL-1 interacting partners that may contribute to its stability in human oral cancers.

a. Reported interacting partners (USP9X, TCTP and MULE)

1) To deduce the mode of MCL-1 degradation in oral cancer cells

Several studies have shown that ubiquitin-dependent proteasomal degradation is the major mode of MCL-1 degradation. However, it is not the only mode of MCL-1 turnover. Certain other modes such as ubiquitin-independent degradation (Stewart et al. 2010), caspase-3 (Weng et al. 2005) and granzyme B mediated cleavage (Han et al. 2004) also contribute for MCL-1 turnover in a context-dependent manner. Our studies show that proteasomal degradation is the principal

mode of MCL-1 turnover in oral cancer cells.

2) To assess the turnover rate of MCL-1 in oral cancer cells

Cycloheximide chase assays revealed that MCL-1 protein has an average half-life of 150-180 minutes in oral cancer cells as compared to the reported half-life of <60 minutes in normal epithelial cells. It is indicative of increased stability of MCL-1 protein in oral cancer cells.

3) **To deduce the role of USP9X in stabilization of MCL-1**

We evaluated the expression of USP9X and MCL-1 in four oral cell lines (DOK, AW8507, AW13516 and SCC029B) and observed that expression of the two proteins correlate significantly (R^2=0.92, r=0.95, *p<0.05). This correlation was also evident across a set of normal-tumor paired oral tissue samples derived from oral cancer patients.

We then confirmed the direct physical interaction between MCL-1 and USP9X proteins by coimmunofluorescence/colocalization and coimmunoprecipitation assays.

We also evaluated the relative expression and correlation between MCL-1 and USP9X proteins by immunohistochemistry in normal oral mucosa (r=0.3850, **p=0.0058, n=50), Oral leukoplakia with epithelial dysplasia (r=0.6148, **p=0.0011, n=25), Oral submucous fibrosis (r=0.3954, p=0.0504, n=25) and Oral squamous cell carcinoma (r=0.6965, ***p<0.0001, n=50). There was a significant overexpression of MCL-1 in Oral leukoplakia with epithelial dysplasia (***p<0.0001), Oral submucous fibrosis (***p<0.0001) and Oral squamous cell carcinoma (***p<0.0001) as compared to normal oral mucosa. This was consistent with USP9X overexpression in Oral leukoplakia with epithelial dysplasia (***p<0.0001), Oral submucous fibrosis (*p<0.05) and Oral squamous cell carcinoma (***p<0.0001).

To establish the direct role of USP9X in stabilization of MCL-1 protein, we downregulated USP9X with siRNA. USP9X knockdown significantly lowered the MCL-1 protein levels but did

not affect the levels of BCL-2 or BCL-XL proteins. This was true even with the case of coimmunofluorescence assay, where USP9X downregulation also lowered MCL-1 expression. Further, to confirm whether USP9X prolong the half-life of MCL- 1 protein by reducing its turnover rate, we performed cycloheximide chase assay. We observed that USP9X downregulation significantly (***$p<0.0001$, MCL-$1_{1/2}$=1.28 Hours) reduced the half-life of MCL-1 protein as compared to control siRNA condition (MCL-$1_{1/2}$=3 Hours).

We then used a small molecule deubiquitinase inhibitor WP1130 to inhibit the activity of USP9X. Exposure of OSCC cells to WP1130 potently induced apoptosis in these cells evident from PARP and caspase-3 cleavage which was associated with a rapid decline in MCL-1 protein levels. Further, apoptosis was confirmed by DAPI staining of nuclei and detection of Annexin V-PI by flow cytometry. Immunofluorescence microscopy revealed that WP1130 treatment also induced appearance of numerous aggresomes (large aggregates of polyubiquitinated proteins marked by punctate staining of p62/SQSTM1). Electron microscopy also revealed the existence of numerous vesicles and electron dense proteinaceous inclusions detectable throughout the cytoplasm of WP1130 treated cells which probably are indicative of polyubiquitinated protein aggregates to be degraded by the proteasome.

Finally, we confirmed the antitumor efficacy of WP1130 against SCC029B cell line derived subcutaneous tumors in BALB/C nude mice. Not only does the drug treated animals exhibited a reduction in tumor burden but also revealed a significant (***$p<0.0001$) increase in percentage of cells positive for cleaved caspase-3 and TUNEL as compared to the control animals.

4) **To evaluate the role of TCTP in stabilization of MCL-1**

To assess the importance of TCTP in MCL-1 stabilization, we knocked down TCTP by using siRNA. However, TCTP knockdown neither affect the levels of MCL-1 protein nor did it altered

the turnover rate of MCL-1 degradation in OSCC cells.

However, when expression of TCTP was analyzed by IHC in different oral histotypes, we observed a significantly increased expression in Oral leukoplakia with epithelial dysplasia (***p<0.0001, n=25), Oral submucous fibrosis (***p<0.0001, n=25) and Oral squamous cell carcinoma (***p<0.0001, n=50) as compared to normal oral mucosa (n=50). Moreover, the expression of the two proteins correlated significantly in all of the four oral histotypes: normal oral mucosa (r=0.4904, ***p=0.0003, n=50), Oral leukoplakia with epithelial dysplasia (r=0.5323, **p=0.0062, n=25), Oral submucous fibrosis (r=0.6306, ***p=0.0007, n=25) and Oral squamous cell carcinoma (r=0.7997, ***p<0.0001, n=50).

TCTP also serve as a chaperone. So we seek to investigate its role in DNA repair pathway in response to exposure to ionizing radiation. Exposure of AW8507 cells to ionizing radiation increased TCTP levels concomitant with elevated MCL-1 levels. Furthermore, four hours post exposure to ionizing radiation, we observed extensive nuclear translocation of TCTP leading to foci formation in the nucleus. We also found that the TCTP forms foci along with MCL-1 at the DNA repair sites marked by γ-H2AX. All these observations highlight probable cooperative roles of MCL-1 and TCTP in repair of damaged DNA in response to ionizing radiation induced DNA damage.

5) Role of MULE in regulating the stability of MCL-1

MULE (MCL-1 **U**biquitinating **L**igase **E**3) is an E3-Ubiquitin ligase which mediates polyubiquitination of MCL-1 protein in response to apoptotic stimuli leading to the proteasomal degradation of MCL-1. In different oral histotypes, we observed a concomitant overexpression (***p<0.0001) of both MCL-1 and MULE proteins as compared to the normal oral mucosa. Notably, we anticipated a negative correlation between MCL-1 and MULE expression. However,

to our surprise, we observed a positive correlation between the two proteins in all tissue types including Oral leukoplakia with epithelial dysplasia (r=0.4681, *p=0.0183, n=25), Oral submucous fibrosis (r=0.5324, **p=0.0062, n=25) and Oral squamous cell carcinoma (r=0.32, *p=0.0235, n=50) except the normal oral mucosa (r=0.04645, p=0.7487, n=50).

These observations indicate that there is a greater stabilizing force on MCL-1 rather than the destabilizing forces which form the basis for elevated levels of MCL-1 protein in oral tissues.

b. Identification of novel MCL-1-interacting proteins through Mass Spectrometry

For the identification of novel MCL-1 interacting partners, we employed the approach of coimmunoprecipitation followed by mass spectrometry. The MS screen revealed several proteins associated with the ubiquitin Proteasomal pathway like E3 ubiquitin ligases and proteins associated with the regulation of cell cycle; although the scores were not significant. Only two proteins with significant scores were identified: alpha enolase (Score: 92) and NALP11 (Score: 60). Apart from these proteins, we could also detect several known MCL-1-interacting proteins such as BAX but with scores less than the significance value.

Objective 2: To assess the *in vitro/in vivo* effects of small molecule inhibitor of MCL-1 on human oral cancer cell lines.

We used a small molecule BH3 mimetic pan-BCL-2 inhibitor Obatoclax (GX15-070) which has a relatively higher affinity for MCL-1.

Obatoclax potently inhibits clonogenicity in OSCC cells:

DOK cell line which expressed significantly lower levels of MCL-1 protein exhibited a relatively higher sensitivity towards Obatoclax as compared to the other three cell lines. The level of MCL-

1 expression in these cells correlates significantly ($r=0.9692$, $*p<0.05$) with their relative sensitivities towards Obatoclax.

Obatoclax does not alter levels of BCL-2 family proteins in OSCC cells

We then assessed the expression of important BCL-2 family proteins upon exposure to Obatoclax by western blotting. However, there was no significant change in the expression of pro and antiapoptotic BCL-2 family proteins except for BIM and NOXA proteins both of which showed a reduced expression in response to Obatoclax treatment.

Obatoclax induced caspase-independent cell death in OSCC cells

We next showed that Obatoclax reduced the survival of OSCC cells in a dose and time dependent manner, characteristic of a small molecule drug mimetic and this cell death was primarily caspase-independent.

Obatoclax potently induced autophagy in OSCC cells

We then showed that Obatoclax potently induced autophagy in these cells evident by appearance of LC-3BII band in western blot and detection of LC-3B foci by immunofluorescence microscopy. We further showed that Obatoclax induced a massive accumulation of autophagosomes, a concomitant increase in the LC-3BII band intensity and sustained levels of p62 protein in a time dependent manner upon exposure to Obatoclax.

Obatoclax induced defective autophagy and a disturbed autophagy flux

Autophagy flux assay revealed that Obatoclax induced a late stage block in the autophagic degradative step and a defective clearance of the autophagic cargo. Further, Obatoclax induced autophagy leads to cell death in OSCC cells and is not prosurvival.

Obatoclax induced autophagy leads to cell death by necroptosis

We have shown that Obatoclax induced autophagy mediates cell death via necroptosis in OSCC cells evident from assembly of RIP1K, RIP3K and FADD in association with p62 at the "necrosome". Further, inhibition of RIP1K with Necrostatin-1 blocked Obatoclax mediated cell death, indicating that Obatoclax induced cell death in OSCC cells by "Necroptosis". Obatoclax also induced numerous ultrastructural changes in OSCC cells which includes appearance of numerous autophagic vesicles containing various cargos.

Obatoclax induced mitochondrial stress via MCL-1 inhibition

We observed that Obatoclax induced extensive fragmentation of the mitochondrial network, a reduction in the mitochondrial membrane potential ($\Delta\Psi m$), an increase in the mitochondrial oxidative stress and a reduction in the mitochondrial function. Apart from the canonical prosurvival function, MCL-1 protein is known to be important for normal mitochondrial organization and homeostasis. siRNA mediated downregulation of MCL-1 in SCC029B cells induced mitochondrial fragmentation, mitochondrial oxidative stress and reduced $\Delta\Psi m$. All these mitochondrial aberrations coincided with those observed when cells were exposed to Obatoclax, indicating that MCL-1 inhibition caused by Obatoclax mediated the mitochondrial stress.

Obatoclax exhibit *in vivo* antitumor activity and synergism with ionizing radiation

Finally, we demonstrated single agent *in vivo* efficacy of Obatoclax in Nude mice and a synergism of Obatoclax with ionizing radiation. A combination of Obatoclax and ionizing radiation significantly ($*p<0.05$) reduced the clonogenic potential of OSCC cells as compared to the either treatments alone.

Publications in Refereed Journal:

Prasad Sulkshane and Tanuja Teni. BH3 mimetic Obatoclax (GX15-070) mediates mitochondrial stress predominantly via MCL-1 inhibition and induces autophagy-dependent

necroptosis in Human Oral Cancer cells. Oncotarget, August 5, 2016 (DOI:10.18632/oncotarget.11085).

Manuscript under preparation:

Prasad Sulkshane, Sushil Pawar, Harshada Sulkshane, Aniket Kamble, Priyanka Rajput, Sagar Pawar, Rahul Patil, Tanuja Teni. Deubiquitinase USP9X stabilizes MCL-1 and contributes to progression of human oral carcinogenesis.

Conference presentations:

- **P Sulkshane** and T Teni. "BH3 mimetic Obatoclax induces autophagic cell death in human oral cancer cells". Platform presentation at the National Research Scholars Meet (NRSM) organized at ACTREC, Navi Mumbai between 17th and 18th December 2015.
- **P Sulkshane** and T Teni. "BH3 mimetic Obatoclax induces autophagy-dependent Cell Death in Human Oral Cancer cell lines". Poster presentation at the 34th Annual convention of Indian Association for Cancer Research (IACR) held at Jaipur, India between 19th-21st February 2015.
- **P Sulkshane** and T Teni. "BH3 mimetic Obatoclax inhibits clonogenic survival of Human oral cancer cell lines". Poster presentation at the prestigious Gordon Research Conference (GRC) on Cell death mechanisms at the interface of Health and Disease held in West Dover, Vermont, USA between 8th-13th June 2014.
- **P Sulkshane** and T Teni. "USP9X inhibition induces apoptosis in oral cancer cell lines through downregulation of MCL-1". Poster presentation at the All India Cell Biology Conference and Symposium on "Cell Dynamics and Cell Fate" held at IISC Bangalore, India between 22nd-24th December 2013.
- **P Sulkshane** and T Teni. "Regulation and Targeting of MCL-1 in Human Oral Cancers". Poster presentation at the 32nd Annual convention of Indian Association for Cancer Research (IACR) held at ACBR, University of Delhi between 13th-16th February 2013.

- V Palve, **P Sulkshane** and T Teni. "MCL-1 is a major radioresistance related factor in human oral cancer cells". Poster presentation at the satellite meeting of the American Association for Cancer Research (AACR) "New Horizons in Cancer Research: Biology to Prevention to Therapy" held in Gurgaon, New Delhi December 13th-16th, 2011.

Signature of student: P Sulkshane

Date: 30.08.2016

Doctoral committee

Sr. No.	Name	Designation	Signature	Date
1.	Dr. Milind Vaidya	Chairperson	M M Vaidya	30.08.16
2.	Dr. Tanuja Teni	Guide & Convener	T R Teni	30.08.16
3.	Dr. Sanjay Gupta	Member	Sanjay	30.08.16
4.	Dr. Prasanna Venkatraman	Member	P. Venkatraman	30.08.16
5.	Dr. Nagaraj Balasubramanian	Invitee	N Balasubramanian	30.08.16

Forwarded through:

S.V. Chiplunkar 2/9/16

Dr. S.V. Chiplunkar

Director, ACTREC

Chairperson, Academic & Training Programme

ACTREC

Dr. S. V. Chiplunkar
Director
Advanced Centre for Treatment, Research & Education in Cancer (ACTREC)
Tata Memorial Centre
Kharghar, Navi Mumbai - 410 210.

To

Dean-Academic

Dr. K. Sharma,

Director, Academics,

PROF. K. S. SHARMA
DIRECTOR (ACADEMICS)
TATA MEMORIAL CENTRE,
PAREL, MUMBAI

TMC

C.C. All doctoral committee members and reporting Student

Abbreviations

TNM	Tumor Nodal Metastasis
RT	Room Temperature
OSCC	Oral Squamous Cell Carcinoma
DNA	Deoxyribose Nucleic Acid
HPV	Human Papilloma Virus
Gy	Gray
EGFR	Epidermal Growth Factor Receptor
CDK	Cyclin-dependent Kinase
BCL-2	B-Cell Lymphoma-2
Rb	Retinoblastoma
MnSoD	Manganese Superoxide Dismutase
LA	Locoregionally Advanced
HNSCC	Head and Neck Squamous Cell Carcinoma
5-FU	5-fluorouracil
tKHSV	Thymidine Kinase of Herpes Simplex Virus
MDR1	Multi-Drug Resistance gene 1
DHFR	Dihydro Folate Reductase
MCL-1	Myeloid Cell Leukemia-1
OPMD	Oral Potentially Malignant Disorders
ROS	Reactive Oxygen Species
ADH	Aldehyde Dehydrogenase
IGF-1R	Insulin-like Growth Factor-1 Receptor

mTOR	mammalian Target of Rapamycin
PI3K	Phosphatidylinositol-4,5-bisphosphate 3-kinase
MOMP	Mitochondrial Outer Membrane Permeabilization
OMM	Outer Mitochondrial Membrane
IMM	Inner Mitochondrial Membrane
BH	BCL-2 Homology
BCL-XL	B Cell Lymphoma Extra Large
BCL-W/BCL-2L2	BCL-2 Like 2
BAK	BCL-2 Antagonist Killer
BAX	BCL-2-associated X protein
BOK	BCL-2-related Ovarian Killer protein
BAD	BCL-2 antagonist of cell death
BIK	BCL-2-interacting killer
BMF	BCL-2 Modifying Factor
BIM/BCL2L11	BCL-2 Like 11
tBID	Truncated BH3 Interacting-Domain Death Agonist
PUMA	p53 Upregulated Mediator of Apoptosis
BNIP3	BCL-2 Nineteen kilodalton Interacting Protein 3
ATR	Ataxia Telangiectasia and Rad3 related
ATM	Ataxia Telangiectasia Mutated
CHK1	Checkpoint Kinase 1
DNA-PK	DNA Activated Protein Kinase
ERK	Extracellularly Regulated Kinase

JNK	c-Jun N-terminal Kinase
MAPK	Mitogen Activated Protein Kinase
GSK-3	Glycogen Synthase Kinase-3
MULE	MCL-1 Ubiquitinating Ligase E3
ARF-BP1	ADP Ribosylation Factor-Binding Protein 1
SCF^{FBW7}	SKP1-cullin-1-F-box complex containing FBW7 as F-Box protein
FBW7	F-Box/WD repeat-containing protein 7
$SCF^{\beta\text{-TrCP}}$	SKP1-cullin-1-F-box complex containing β-TrCP as F-Box protein
β-TrCP	Beta Transducin Containing Protein
USP9X	Ubiquitin Specific Peptidase 9 X-linked
TCTP	Translationally Controlled Tumor Protein
ULK	Unc51-Like Kinase
ATG	Autophagy related Genes
LAMP	Lysosome Associated Membrane Protein
RIPK	Receptor-Interacting Protein Kinases
FADD	Fas-Associated Death Domain
MLKL	Mixed Lineage Kinase Like
TNFR	Tumor Necrosis Factor Receptor
TRADD	Tumor Necrosis Factor Receptor-Associated Death Domain
TRAF	Tumor Necrosis Factor Receptor-Associated Factor
GAPDH	Glyceraldehyde-3-Phosphate Dehydrogenase
Ct	Cross threshold
nm	Nanometer

nM	Nanomolar
µM	Micromolar
µm	Micrometer
TdT	Terminal deoxynucleotidyl Transferase
FITC	Fluorescein Isothiocyanate
TUNEL	Terminal deoxynucleotidyl transferase-mediated dUTP nick end labeling
MALDI-MS	Matrix Assisted Laser Desorption-Ionization Mass Spectrometry
TOF	Test Of Flight
r	Pearson's correlation coefficient
PARP	Poly(ADP-ribose) polymerase-1
TEM	Transmission Electron Microscope
IHC	Immunohistochemistry
OPMD	Oral Potentially Malignant Disorders
OSMF	Oral Submucous Fibrosis
OL	Oral Leukoplakia with Epithelial Dysplasia
PEG	Polyethylene Glycol
DMEM	Dulbecco's Modified Eagle's Medium
IMDM	Iscove's Modified Dulbecco's Medium
DUBs	Deubiquitinases

List of Figures **Page no.**

Figure 1: The pathways of apoptosis 49

Figure 2: The Mitochondrial Outer Membrane Permeabilization 50

Figure 3: The BCL-2 family 51

Figure 4: BH3-only proteins regulate MOMP 52

Figure 5: Molecular organization of MCL-1 54

Figure 6: Regulation of apoptosis by MCL-1 55

Figure 7: Role of MCL-1 in Mitochondria 57

Figure 8: Alternative splicing of MCL-1 pre mRNA 61

Figure 9: The N-terminus regulatory domain of MCL-1 62

Figure 10: The pathway of autophagy 71

Figure 11: The signaling mechanisms leading to the assembly of necrosomal complexes 73

Figure 12: Basal levels of BCL-2 family proteins 108

Figure 13: Ubiquitin-dependent proteasomal degradation is the major pathway for MCL-1 turnover 109

Figure 14: Determination of MCL-1 half-life by CHX chase assay 111

Figure 15: USP9X expression correlates with MCL-1 expression 112

Figure 16: USP9X interacts with MCL-1 113

Figure 17: Standardization of siRNA transfection 114

Figure 18: USP9X downregulation lowers MCL-1 protein levels 115

Figure 19: USP9X knockdown increases turnover of MCL-1 protein 116

Figure 20: USP9X contributes to radioresistance 118

Figure 21: WP1130 potently induces apoptosis in OSCC cells 119-121

Figure 22: WP1130 triggers aggresome formation 122

Figure 23: *In vivo* efficacy of WP1130 124

Figure 24: MCL-1 expression correlates with USP9X expression 129

Figure 25: MCL-1 and USP9X proteins are overexpressed in OPMD and OSCC 130

Figure 26: Recurrent oral tumor samples express high levels of MCL-1 and USP9X proteins 131

Figure 27: USP9X expression is an important predictor of prognosis in oral cancer patients 132

Figure 28: TCTP does not affect stabilization of MCL-1 protein 133

Figure 29: MCL-1 expression correlates with TCTP expression 135

Figure 30: MCL-1 and TCTP proteins are overexpressed in OPMD and OSCC 136

Figure 31: Analysis of MCL-1 and MULE protein expression in oral cell lines and oral tissues 137-139

Figure 32: Identification of MCL-1-interacting partners 140

Figure 33: Obatoclax potently inhibits the clonogenic potential of oral cancer cells 149-151

Figure 34: Effect of Obatoclax on the BCL-2 family proteins 152

Figure 35: Obatoclax triggers caspase-independent cell death in OSCC cells 154-155

Figure 36: Obatoclax potently induces autophagy in OSCC cells 157

Figure 37: Obatoclax-induced autophagy culminates into cell death 159

Figure 38: Obatoclax induces a defective autophagy in OSCC cells 161-163

Figure 39: Obatoclax induces necroptosis in OSCC cells 165-166

Figure 40: Obatoclax induces mitochondrial fragmentation in OSCC cells 168-169

Figure 41: Obatoclax induces oxidative stress and membrane depolarization in the 171-172

mitochondria of OSCC cells

Figure 42: Obatoclax does not induce mitophagy 174

Figure 43: MCL-1 downregulation induces mitochondrial stress in SCC029B cells 175-176

Figure 44: Ultrastructural changes induced by Obatoclax 177

Figure 45: *In vivo* efficacy of Obatoclax 178

Figure 46: Ionizing radiation treatment exhibits synergism when combined with Obatoclax 179-180

Figure 47: The proposed mode of Obatoclax action 200

List of Tables **Page no.**

Table 1: Antibodies used in the study. 81-82

Table 2: Instruments used in the study. 82-83

Table 3: Cell lines used in the present study. 84

Table 4: The conditions of siRNA transfection. 88

Table 5: Protein estimation by Bradford assay. 93

Table 6: Resolving gel composition. 94

Table 7: Stacking gel composition. 95

Table 8: Reaction mixture for a Reverse Transcription (RT) reaction. 99

Table 9: Thermal cycler program for a Reverse Transcription (RT) reaction. 99

Table 10: The sequence of the primers used for SYBR Green Real Time PCR. 100

Table 11: Demographic data for individuals with Normal Oral Mucosa. 127

Table 12: Clinicopathological characteristics of individuals with Oral Submucous Fibrosis. 127

Table 13: Clinicopathological characteristics of individuals with Oral leukoplakia with epithelial dysplasia. 128

Table 14: Clinicopathological characteristics of individuals with oral squamous cell carcinoma. 128-129

Table 15: Proteins identified through Mass Spectrometry screen. 143-147

Chapter 1
Introduction

1. Introduction

Most cancers of the head and neck region are squamous cell carcinoma and a majority of them are oral squamous cell carcinoma (OSCC) [1]. The cell of origin of oral cancer is the oral keratinocyte [1]. Oral cancer or OSCC is the sixth most common cancer in the world [2]. In India, oral cancer is the most prevalent cancer type among men and third most common cancer in women. The major risk factors include tobacco usage (primarily chewing and/or smoking habit), betel-quid chewing and alcohol consumption [3, 4]. Recently, HPV infection has also been implicated in oral carcinogenesis [5, 6]. Other determinants for predisposition to oral cancer includes micronutrient deficiency, genetic constitution of the individual which determines carcinogen metabolizing potential, oral hygiene, occupational risks and immunosuppression [4, 7]. The major oral subsites affected in oral cancer includes tongue, buccal mucosa, gingivae, palate, retromolar trigone, lower alveolus and floor of mouth [8]. Clinically, the precancerous lesions (includes leukoplakia, erythroplakia, erythroleukoplakia and submucous fibrosis) precedes the malignant form of OSCC [9]. The TNM stage of the primary tumor correlates well with the survival rate. The 5-year survival rate of patients with early-stage OSCC ranges between 80-90% whereas for the advanced stage patients, it is merely 40% [1]. About 40% OSCC patients die from loco-regional disease while 24% develop distant metastases [10]. Early stage detection of OSCC therefore is important for the improved management and better prognosis of OSCC patients. Some of the diagnostic methods used for the detection of OSCC includes vital staining with Toluidine blue and optical techniques to improve visualization of the biopsy, cytology, DNA ploidy, molecular markers and salivary biomarkers [1]. Despite the fact that oral cavity is readily accessible to complete clinical examination, OSCC is frequently diagnosed at a late stage either due to ignorance, lack of awareness or inaccessibility of medical care [11].

Although surgery remains the primary treatment modality for oral cancers, a multimodal approach including postoperative radiotherapy or chemotherapy is administered for advanced-stage disease [12]. In ~20-30% OSCC cases, surgical resection of the primary tumor with surrounding ~5 mm tumor free margins often develop local recurrence or even distant metastases and therefore needs administration of post-operative chemoradiotherapy [13]. The selection criteria for a particular treatment modality is determined by the nature of the carcinoma (includes specific oral subsites affected, the clinical size, extent of local invasion, histopathological characteristics, regional lymph node and distant metastasis) and general condition of the patient (includes age, general health status, clinical history and high-risk habits) [2].

Radiotherapy forms an integral part of the treatment modality for the management of human oral cancers either alone or as an adjuvant mode of treatment with chemotherapy [14]. Standard radiotherapy protocol for oral cancer involves daily exposure of 2Gy fractionated ionizing radiation dose for few weeks so that patients receive a cumulative dose of 50 to 70Gy during the course of fractionated radiotherapy [15]. This treatment kills rapidly dividing tumor cells whilst sparing the normal cells [16]. However, radiotherapy often fails as the tumor cells become refractory to radiation and develop radioresistance, thereby limiting the success of the therapy [17].

Chemotherapy is administered to patients with locoregionally advanced (LA) HNSCC either concurrently with ionizing radiation or as induction chemotherapy prior to local treatment or as palliative therapy in patients with recurrent and/or metastatic disease. Cisplatin-based chemoradiation remains the standard treatment modality for LA tumors. For induction chemotherapy, Cisplatin/infusional 5-FU/Docetaxel has emerged as a standard chemotherapy regimen. A combination therapy regimen including Methotrexate, Cisplatin and 5-FU has shown

better overall survival as compared to single agents in recurrent/metastatic conditions. A combination of Cetuximab (blocks EGFR) with platinum based drugs/5-FU has shown an increased overall survival as compared to the prevailing standard platinum-based therapy [18]. In cases of recurrent OSCC, EGFR inhibitors are often combined with conventional chemotherapy as a frontline treatment approach [9]. Although several targeted therapies are available currently, their full potential can only be evaluated upon rational combination with standard chemotherapy and/or radiotherapy in case of OSCC [1, 19]. However, despite major improvements in cancer therapeutics, the 5-year survival rate of OSCC patients has not shown a significant improvement over the past several years [20].

Like many other human cancers, OSCC is marked with frequent genomic alterations in tumor suppressor genes (such as p53, p16, $p21^{CIP}$, pRb) and proto-oncogenes genes (c-myc, CDKs, Cyclins, EGFR, BCL-2 family) which drives tumorigenesis [21]. Therefore, clinical implications of the gene therapy have actively been sought recently. It uses a viral vector (Adenovirus, Retrovirus, Adenoassociated virus, Herpesviruses) to manipulate the existing genetic material or introduce new genetic material into cancer cells without damaging normal healthy cells. A number of clinical trials involving gene therapy for the management of OSCC are currently underway which target important oncogenes and tumor suppressor genes such as p53, Rb, MnSoD, tKHSV, MDR1, DHFR [22].

Previous studies from our laboratory have demonstrated altered expression of BCL-2 family members and overexpression of antiapoptotic MCL-1 transcript and protein in human oral premalignant lesions, oral tumors and oral cancer cell lines [23]. Moreover, overexpression of antiapoptotic MCL-1 is associated with poor prognosis and a reduced disease free survival in oral cancers patients treated with definitive radiotherapy [24]. Subsequent studies showed that

the antiapoptotic MCL-1 is an important prosurvival and radioresistance related protein in oral cancer cell lines [25]. Further, it was shown that overexpression of MCL-1 is associated with chemoresistance and poor prognosis in oral cancer patients [26]. MCL-1 protein therefore appears to be an important therapeutic target in oral cancers.

MCL-1 overexpression has been implicated in a variety of human cancers including the hematological malignancies and solid tumors [27]. Moreover, MCL-1 overexpression is associated with therapy resistance and poor prognosis in several human cancers, thus highlighting it as a potential therapeutic target [28, 29]. Being an important prosurvival protein, it's expression is tightly regulated at multiple levels in a mammalian cell [30]. MCL-1 is unique among the antiapoptotic members of the BCL-2 family, because it has a rapid rate of turnover and a short half-life attributed by the ubiquitin-dependent proteasomal degradation [31, 32]. However, tumor cells tend to maintain sustained elevated levels of MCL-1 protein by adopting several approaches which could form the basis of its therapeutic targeting [33]. Alternatively, MCL-1 protein can be directly targeted by BH3-mimetic small molecule inhibitors which may induce apoptosis and therefore may prove to be important chemotherapeutic agents with great potential.

Although significant information is available in the literature about the regulation of MCL-1 expression in normal cells, little is known about the mechanisms which favor its elevated levels in tumors. Altered regulatory mechanisms which account for overexpression of MCL-1 protein in human oral cancers has not been discussed previously. Moreover, targeting MCL-1 with a small molecule BH3-mimetic inhibitor may provide new therapeutic opportunities for the management of human oral cancers.

Therefore, in the present study, we investigated the regulation of MCL-1 protein at the post-translational level in human oral cancer cell lines and assessed the importance of MCL-1-interacting proteins in maintaining its sustained elevated levels. We also evaluated the efficacy and mechanism of action of a small molecule BH3-mimetic pan-BCL-2 inhibitor Obatoclax (GX15-070, which has a high affinity for MCL-1 protein) in oral cancer cell lines *in vitro* and *in vivo*. The outcome of the study may help devise new therapeutic strategies for efficiently targeting MCL-1 in human oral cancers.

Chapter 2
Review of Literature

2.1 Oral cancer

2.1.1 Incidence and epidemiology

Oral cancer is the sixth most prevalent cancer in the world and is a serious health issue in many parts of the world especially in the Southeast Asia. In high risk countries including India, Pakistan, Sri Lanka, Bangladesh and Taiwan, it is the most common cancer among men and accounts for about 25% of all cancers [8]. According to a recent nationally representative survey, oral cancer is the leading cause of death (~23%) among Indian men primarily due to use of tobacco. Indeed, tobacco-related cancers accounted for 42% cancer associated mortality in men and 18% in women across India [3].

2.1.2 Pathogenesis

OSCC arise from DNA mutations in the oral keratinocyte caused by various carcinogens (Chemical, Physical or Microbial) which brings about its transformation from a normal keratinocyte to a pre-malignant or a potentially malignant keratinocyte characterized by uncontrolled proliferation ultimately resulting into cancer [1].

2.1.3 Oral Potentially Malignant Disorders (OPMD)

The oral lesions with a predisposition to malignant transformation are described by the term ‘‘Oral Potentially Malignant Disorders” which include Leukoplakia, Erythroplakia and Oral Submucous Fibrosis [34].

A) Leukoplakia

It represents ‘‘A white plaque of questionable risk having excluded (other) known diseases or disorders that carry no increased risk for cancer”. It is more common in individuals with smoking habit and/or alcohol consumption; although its association with HPV infection is debatable. It is

further categorized into Homogenous type (flat, thin, uniform white in color) and Non-homogeneous type (erythroleukoplakia and Verrucous leukoplakia). Histopathologically, it is distinguished between dysplastic and non-dysplastic leukoplakia. Its prevalent rate is ~2% and malignant transformation rate is ~1% [34].

B) Erythroplakia

It is represented by ‘‘A fiery red patch that cannot be characterized clinically or pathologically as any other definable disease”. Clinically, it appears as flat or even depressed with a smooth or granular surface. The major etiological factors being Tobacco and alcohol; although the role of *Candida albicans* infection is debatable. Histopathologically, it commonly shows at least some degree of dysplasia and often even carcinoma *in situ* or invasive carcinoma. It has a high risk potential as a majority of erythroplakia will undergo malignant transformation. The incidence rates of erythroplakia are ~0.83% in Southeast Asia [34].

C) Oral submucous fibrosis (OSMF)

It is the most prevalent OPMD in Southeast Asia and is causally linked to tobacco, betel quid and areca nut chewing habit. Clinically, it is characterized by a burning sensation, blanching and stiffening of the oral mucosa, oropharynx, and trismus. In advanced stages, vertical fibrous bands appear in the cheeks, faucial pillars, and encircle the lips resulting in difficulty in opening the jaw. The annual malignant transformation rate for OSMF is ~0.5% [34].

2.1.4 Oral squamous cell carcinoma (OSCC)

Being a leading cause of mortality, OSCC constitutes a major health concern in the developing countries. It is often preceded by a pre-invasive stage that may last for several years before attaining full malignant phenotype. The tumor progression in epithelia has been classified as

normal, hyperplastic (non-dysplastic), dysplastic carcinoma *in-situ* and invasive carcinoma [35]. The major oral subsites affected includes tongue, alveolus, floor of mouth and lips in the Western world whereas in India, Gingiovobuccal region (comprising of buccal mucosa, retromolar trigone and lower gum) is most commonly affected due to prevalent habit of holding tobacco within the mouth at these oral subsites [8].

2.2 Etiological factors associated with oral carcinogenesis

Several lifestyle behaviors are associated with progression of human oral cancers with convincing evidence which include tobacco use, betel quid chewing, alcohol consumption, dietary and nutrient deficiencies, oral hygiene and HPV infection [36]. The major risk factors associated with oral cancer progression are discussed below in detail.

A) Tobacco

Tobacco is perhaps the most important prognostic factor causally linked to oral cancer with sufficient evidences. Tobacco is addictive because of presence of a psychoactive alkaloid "Nicotine" in the leaves of Tobacco plant, which increases heart rate, causes vasoconstriction, anxiety and alertness [37]. In the western countries, Tobacco is mostly used in the form of cigarette smoking [38] whereas in the Southeast Asian countries, it is mainly used in chewing form (tobacco consumed without combustion and placed inside the oral cavity as "Quid" in contact with the mucous membranes where the nicotine is absorbed to provide the desired effect) with or without smoking habit [39]. More than 60 carcinogens have been identified in cigarette smoke and at least 16 in the smokeless form of tobacco, the most important being 4-(methylnitrosamino)-1-(3-pyridyl)-1-butanone (NNK) and N-nitrosonornicotine (NNN), polycyclic aromatic hydrocarbons (PAH) such as benzo[a]pyrene and aromatic amines. In particular, NNK, NNN and PAH form DNA adducts and have been causally linked to oral cancer

[40]. Use of tobacco (in smoking or smokeless form) along with alcohol consumption greatly increases the risk of oral cancer. Although the association between tobacco consumption and oral cancer is dose-dependent, genetic determinants such as carcinogen metabolizing, DNA repair, cell cycle regulatory genes play decisive roles [41].

B) Betel quid

It is commonly consumed in many parts of the Southeast Asia in the form of an envelope of a leaf of the plant betel (*Piper betle*) containing other components such as areca nut, slaked lime, and catechu [42]. It is mainly chewed to extract out alkaloids such as arecoline (similar to nicotine), arecaidine, guvacoline, guvacine which interact mainly with muscarinic receptors and functions via acetylcholine. The alkaloids from areca nut and betel leaves serve as stimulants and together brings about many physiological changes which increases capacity to work with euphoric effects and heightened alertness [42]. Betel quid chewing results in the production of potentially carcinogenic nitrosamines and ROS due to auto-oxidation of polyphenols contained in areca nut and enhanced by the alkaline pH from slaked lime [43].

C) Alcohol

The main constituent of diverse alcoholic beverages is ethanol which varies in concentration from 3-18%. It acts in the central nervous system by modulating the activities of key neurotransmitters [36]. Alcohol consumption has a dose-dependent relationship with risk of oral cancer, where about 7-19% oral cancer cases are attributable to heavy alcohol consumption. Alcohol consumption further increases the risk of oral cancer in individuals with tobacco/betel quid chewing habits [44]. Alcohol dehydrogenase oxidizes ethanol to acetaldehyde, and aldehyde dehydrogenase (ADH) detoxifies acetaldehyde to acetate. Acetaldehyde exerts the carcinogenic effects of ethanol on DNA and is responsible for the oral carcinogenic effects of

ethanol. Presence of a defective ADH allele therefore greatly increases the risk of oral cancer in individuals consuming alcohol [45]. Apart from ethanol, other components of alcoholic drinks such as nitrosamines, acrylamide, and oxidized polyphenols are probably carcinogenic to humans [46].

D) Dietary deficiencies

About 10-15% oral cancer cases are attributable to low dietary fruit and vegetable intake [47]. As natural foods are rich in agents with antioxidant and anti-carcinogenic properties (such as vitamins A, C and E, other carotenoids, flavonoids, phytosterols, folates and fibres), their dietary deficiency may greatly increase susceptibility to cancer causing agents [48].

E) Microorganisms

The association of HPV with oropharyngeal cancers has been shown in a number of studies [49, 50]. Not only the role of HPV but some herpes viruses is evident in oropharyngeal cancers [51, 52]. Microbial infections such as candidosis and syphilis and poor oral hygiene have also been implicated in oral cancers [53-55].

2.3 Current treatment modalities for the management of oral cancers

The aim of therapy in the management of oral cancers is to eradicate the tumor, stop the locoregional and metastatic spread, and prevent disease recurrence whilst restoring the overall form and physiological functions of the affected subsite. Surgery, Radiotherapy, Chemotherapy and their rational combination still remain the preferred therapeutic modalities for the management of oral cancers in the clinics. Several factors that determine the choice of therapeutic modalities include patient related factors (such as age, overall health, medical history of the patient and any high-risk habits), nature of the carcinoma (includes the oral subsite

affected, the clinical size of the tumor, the extent of local invasion, histopathological features, regional lymph node involvement and distant metastasis) and Physician factors (a multidisciplinary team for making selection of the most appropriate initial definitive treatment, rehabilitation services, dental and prosthetic support, and psycho-social support) [2].

2.3.1 Surgery

Surgery is the most well established mode of initial definitive treatment for a majority of oral cancers. Certain tumor factors such as size of the primary tumor, its depth of infiltration, its site (that is anterior versus posterior location), and proximity of the tumor to mandible or maxilla determine the choice of a particular surgical approach for primary tumors of the oral cavity. To rule out the possibility of bone invasion, radiographical imaging of the mandible are routinely performed (include Orthopantomogram, CT scan, Denta scan). MRI scan allows a detailed assessment of the extent of tumor infiltration in the underlying soft tissue. Peroral, mandibulotomy, lower cheek flap approach, visor flap approach or upper cheek flap approach are the most routinely used surgical approaches for surgical resection of the primary tumor of oral cavity. A reconstructive surgery is necessary when resection of a primary tumor in the oral cavity leads to functional or aesthetic loss of structures (such as loss of a significant part of the tongue, floor of mouth or buccal mucosa, and loss of a segment of the mandible) in the oral cavity. The outcome of the surgical treatment is determined by the stage of the disease at the time of diagnosis, with early stage cancers showing better response as opposed to late stage disease [2].

2.3.2 Radiation

Radiotherapy plays a key role in the management of early stage and locally advanced HNSCC either alone or, more frequently combined with surgery and/or chemotherapy. Ionizing radiation

(which constitutes high-energy gamma radiation) causes cellular damage mainly in two ways: (A) Direct by inducing a variety of DNA lesions, including oxidized base damage, abasic sites, single-strand breaks (SSBs) and double-strand breaks (DSBs). These lesions, if unrepaired, ultimately result in cell death through mitotic catastrophe and apoptosis [56]. (B) Indirect DNA damage & cell death by forming free radicals and ionization of oxygen molecules [57]. Currently, radiation treatment is administered in multiple fractions of 2 Gy each daily over a period of several weeks which could help limit toxicity and increase the total dose thereby improving its efficacy. In cases of LA HNSCC, concomitant chemoradiotherapy (CT-RT) is often preferred. Recently, molecular targeted therapies such as EGFR inhibitors when combined with radiotherapy have shown promising results [58].

2.3.3 Chemotherapy

Chemotherapy is often administered in HNSCC patients with LA cancer either concurrently as CT-RT or as induction chemotherapy prior to local treatment or as palliative therapy in patients with recurrent and/or metastatic disease [18]. Cisplatin, Paclitaxel, 5-FU, Docetaxel, Methotrexate, Vincristine, and Bleomycin are most commonly employed in the management of HNSCC either individually, sequentially or in a rational combination. Nevertheless, chemotherapy is associated with several side effects and toxicities including neutropenia, thrombocytopenia, diarrhoea, mucositis which limit dose escalations [18].

2.3.4 Targeted therapies

Targeted therapies provide an exciting solution for the limitations associated with conventional chemoradiotherapy evident from the use of EGF/Erb-B receptor inhibitors/monoclonal antibodies in several clinical trials in HNSCC either individually or in combination with existing therapeutic agents in case of recurrent disease setting [59]. Apart from EGFR, IGF-1 receptor

targeting have been explored in the management of HNSCC due to its key role in cancer progression and metastasis [60]. Similar to EGFR, small molecule inhibitors and monoclonal antibodies against IGF-1R are being explored for their efficacy against HNSCC either individually or in combination in several clinical trials. Further, key signaling molecules (such as Ras, Raf, mTOR), Angiogenesis and cell cycle regulators, inducers of apoptosis, and protein degradation machinery are actively being sought as potential therapeutic targets in HNSCC [19].

2.4 Apoptosis and its dysregulation in human cancers

Apoptosis is an ordered and orchestrated sequence of molecular and cellular events which occurs in physiological (for maintenance of tissue homeostasis) and pathological conditions leading to the death of a mammalian cell [61, 62]. Evasion of apoptosis is one of the eight hallmarks of cancer cells which allows them to resist the death-inducing stimuli [63]. Impaired apoptosis is both critical in cancer development and a major barrier to anticancer therapeutics [62, 64, 65]. The apoptotic machinery is composed of both upstream regulators and downstream effector components. The regulators are further categorized into two principal circuits: A) The extrinsic or death receptor pathway which receives and processes the extracellular death-inducing stimuli (e.g. The Fas receptor/FasL and TNF receptor/TNF) B) The intrinsic or mitochondrial pathway which senses and integrates various intracellular stimuli. Both pathways eventually culminate into activation of precursor cysteine proteases called “Caspases” in a cascade which executes the death sentence and foster the characteristic features of a cell undergoing apoptosis including DNA fragmentation, chromatin condensation, loss of plasma membrane asymmetry and blebbing (Figure 1). To date, the intrinsic cell death pathway has been widely implicated in a variety of human cancers and has been a focus of novel therapeutics aimed at targeting the apoptosis machinery [66].

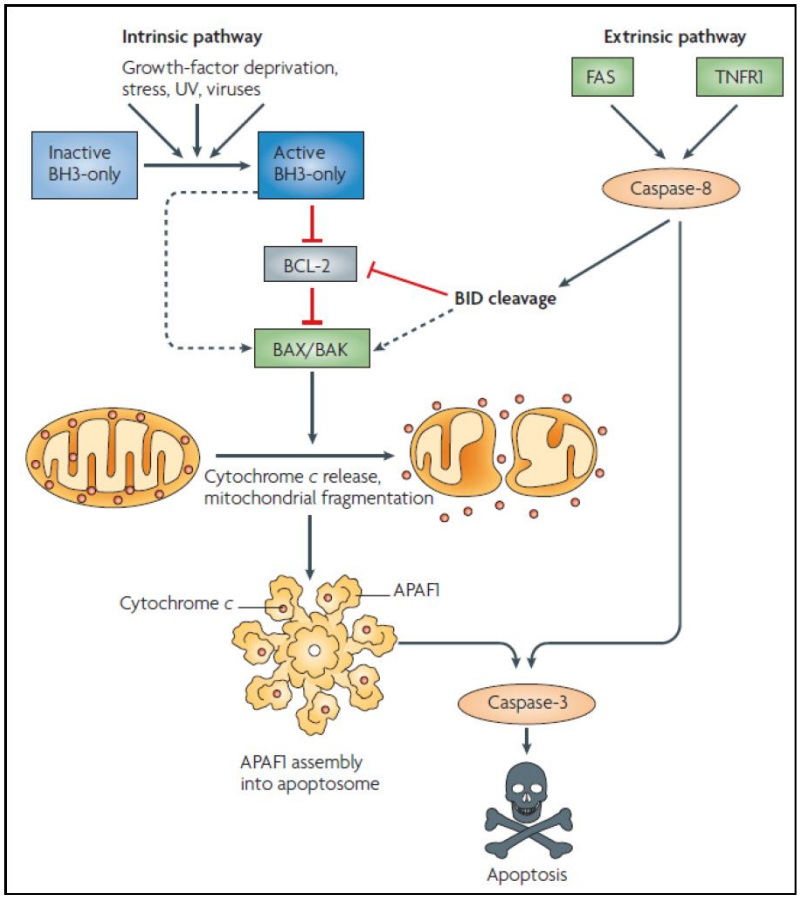

Figure 1: The pathways of apoptosis. Internal death stimulus activates the intrinsic (Mitochondrial) pathway of apoptosis. Alternatively, the extrinsic (death receptor) pathway receives and processes the extracellular death-inducing stimuli. Both pathways unite at a focal point leading to the activation of Caspases [67].

2.5 The Intrinsic pathway of Apoptosis

The intrinsic pathway of apoptosis integrates various internal stress signals such as DNA damage, cytoskeletal damage, ER stress, loss of adhesion, growth factor withdrawal, macromolecular synthesis inhibition, etc [68]. As discussed above, upon activation in a cascade, Caspases mediate proteolysis of numerous specific cellular substrates which ultimately brings

about the characteristic morphological changes in a cell. Caspase activation necessitates an upstream event called as 'Mitochondrial Outer Membrane Permeabilization (MOMP)' which involves release of cytochrome c from the mitochondrial intermembrane space to the cytosol (Figure 2). Once in the cytosol, cytochrome c forms a complex with APAF-1 and procaspase-9 called as 'Apoptosome' leading to the activation of caspase-9 (initiator caspase) and downstream activation of caspase-3 (executioner caspase) [69, 70]. BCL-2 family proteins have long been regarded as apical regulators of the intrinsic pathway of apoptosis [71]. Diverse members of this family engage in a coordinated interplay to bring about MOMP, ultimately leading to caspase activation or if this pathway is inhibited, leads to a caspase-independent cell death (CICD). MOMP is actuated by formation of membrane-spanning pores or hydrophilic channels allowing the release of cytochrome c to the cytosol [72].

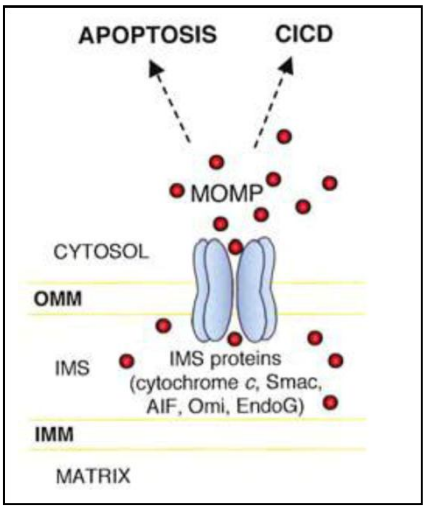

Figure 2: The Mitochondrial Outer Membrane Permeabilization. Under stressful conditions, proapoptotic members of the BCL-2 family coordinate to bring about release of mitochondrial intermembrane space proteins such as cytochrome c to the cytosol leading to the activation of caspases and ultimately apoptosis or alternatively induce a caspase-independent cell death (CICD) [73].

2.6 The BCL-2 family

The BCL-2 family of apoptosis regulators is categorized into three subfamilies based on their constitution of BCL-2 Homology domains (BH Domains). The antiapoptotic subfamily members contain four BH domains (BH1-4) and include BCL-2, BCL-XL, MCL-1, BCL-W, A1 which antagonize apoptosis by interacting with and sequestering the proapoptotic members. The multidomain (contains BH1-3) proapoptotic subfamily includes BAK, BAX and BOK which serves as effector proteins by oligomerizing in the OMM thereby forming hydrophilic channels leading to cytochrome c release. Members of the BH3-only proapoptotic subfamily serves as stress sensors of the intrinsic pathway (Figure 3) [74].

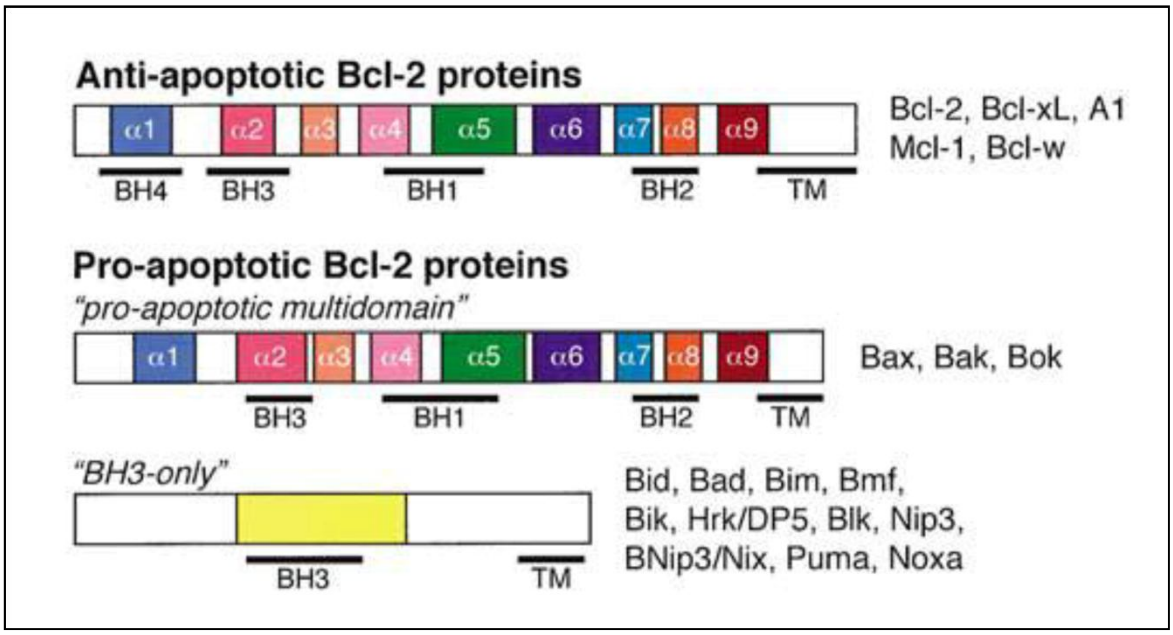

Figure 3: The BCL-2 family. The BCL-2 family of apoptosis regulators is categorized based on their activities and composition of their BH domains. The anti-apoptotic members antagonize apoptosis and contain multiple BH domains whereas, the pro-apoptotic members which promote apoptosis either constitute multiple BH domains or only the BH3 domain [73].

2.7 The BH3-only proteins

The BH3-only proteins are the most apical regulators of apoptosis, and are further categorized into: A) "Derepressors (or Sensitizers)" (include NOXA, BAD, BIK, BMF) which interact with antiapoptotic members of the BCL-2 family and thereby neutralize them. B) Direct activators (include BID, BIM, PUMA) interact with BAK and BAX leading to their activation by bringing about conformational changes in them. They are activated by multiple stimuli from inside or outside the cell to initiate the apoptotic response and are regulated transcriptionally and by various post-translational modifications [75]. Their BH3 domain is an amphipathic α-helix that serves as a binding motif for interaction with a hydrophobic groove on either multidomain anti- or proapoptotic BCL-2 family members. This interaction either antagonizes the survival activity of anti-apoptotic proteins or activates proapoptotic BAX and BAK and these two activities may cooperate to execute apoptosis. Furthermore, the BH3-only proteins exhibit binding specificities for particular multidomain proapoptotic and anti-apoptotic BCL-2 family members which in turn is determined by their BH3 domains [74]. Moreover, activation of a single BH3-only protein is not sufficient to induce MOMP as it is likely to be sequestered by multiple antiapoptotic members of the BCL-2 family. Instead, simultaneous activation of multiple derepressor BH3-only proteins may be required [67, 73].

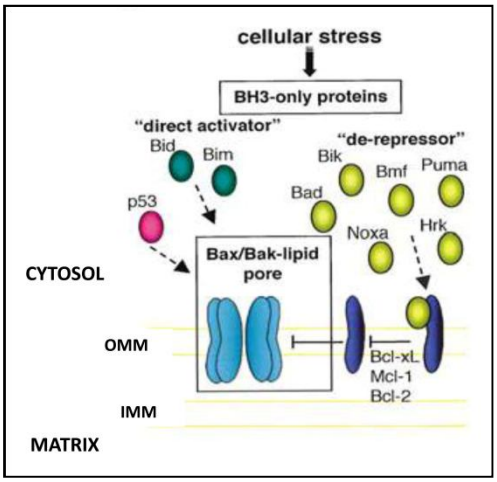

Figure 4: BH3-only proteins regulate MOMP. BH3-only proteins serves as sensors for various stressful stimuli and bring about MOMP either by interacting with multidomain proapoptotic proteins, thereby bringing about conformational change leading to their oligomerization in the OMM (so termed as "Direct activators") or by interacting with and neutralizing the activities of anti-apoptotic proteins (so termed as "De-repressors") [73].

2.8 Myeloid Cell Leukemia-1 (MCL-1)

MCL-1 is an antiapoptotic member of the BCL-2 family, first characterised in 1993 as an immediate-early gene expressed during phorbol ester-induced differentiation of a human myeloid leukemia cell line [76]. It has sequence, structural and functional homology to BCL-2 and was mapped to the chromosome 1q21 which is frequently involved in chromosomal aberrations in many cancers [77].

2.8.1 Structure

Structurally, it is composed of 350 amino acid residues and contains BH1, BH2 and BH3 domains. Despite its similarity, it is radically distinct from other BCL-2 antiapoptotic members in its N terminus domain which is much longer (~170 amino acid residues) and contains two PEST domains which contribute to its characteristic rapid turnover and a short half-life [76]. Its C terminus hydrophobic domain anchors it to the cellular membranes, mainly to the OMM and is similar to BCL-2 (Figure 5) [78]. Furthermore, unlike other BCL-2 family members, MCL-1 is rapidly induced in response to survival signals and downregulated when apoptotic signals are received, thus making it an ideal switch that can rapidly modulate the response of a cell to environmental cues [79, 80] and is therefore tightly regulated [30].

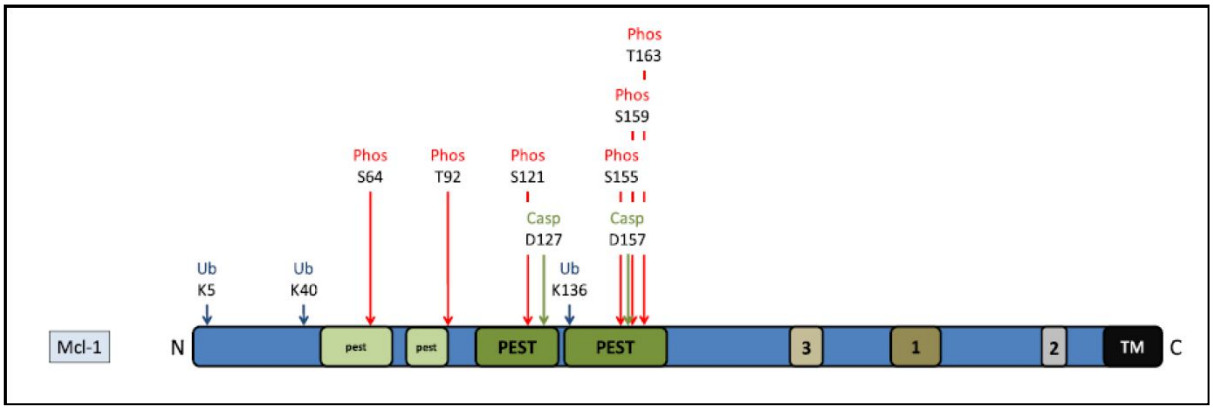

Figure 5: Molecular organization of MCL-1. The C-terminus of MCL-1 contains BH domains and a transmembrane domain. Whereas the N-terminus is unique to MCL-1 and contains several Phosphorylation, Polyubiquitination and caspase cleavage sites within the PEST sequences [30].

2.8.2 Physiological functions

MCL-1 deletion in mice leads to peri-implantation lethality highlighting its indispensable role during embryonic development [81]. It is also important for the survival of hematopoietic stem cells [82] and cells of both lymphoid [83] and myeloid lineages [84]. MCL-1 protects hematopoietic cells from undergoing apoptosis under various stressful conditions [85]. MCL-1 upregulation is also important for the survival of human melanoma cells under stressful conditions [86]. Thus, MCL-1 is not only critical during the normal development but is an important prosurvival molecule for many cell types.

2.8.3 Regulation of Apoptosis by MCL-1

BAX is sequestered in the cytosol in a latent monomeric state and undergoes conformational changes in response to apoptotic stimuli induced by binding of activator BH3-only proteins followed by its membrane insertion and oligomerization in the OMM [87]. MCL-1 is known to

bind and sequester BAX. Whereas BAK is constitutively sequestered in an inactive monomeric conformation through its interaction with MCL-1 in the OMM [88]. The BH3 domain of BAK binds to the hydrophobic groove of MCL-1 with a high affinity [74, 89]. Following an apoptotic stimulus, BH3-only members are activated which release BAK from MCL-1 and promotes degradation of the latter [88]. However, this event is not sufficient to promote apoptosis but requires another stimulus to activate BAK and BAX to be able to oligomerize causing the release of cytochrome c from mitochondria [90]. NOXA, a BH3-only protein binds MCL-1 with a high affinity by disrupting MCL-1-BAK interaction thus releasing BAK to promote apoptosis and mediate MCL-1 degradation (Figure 6) [89, 91].

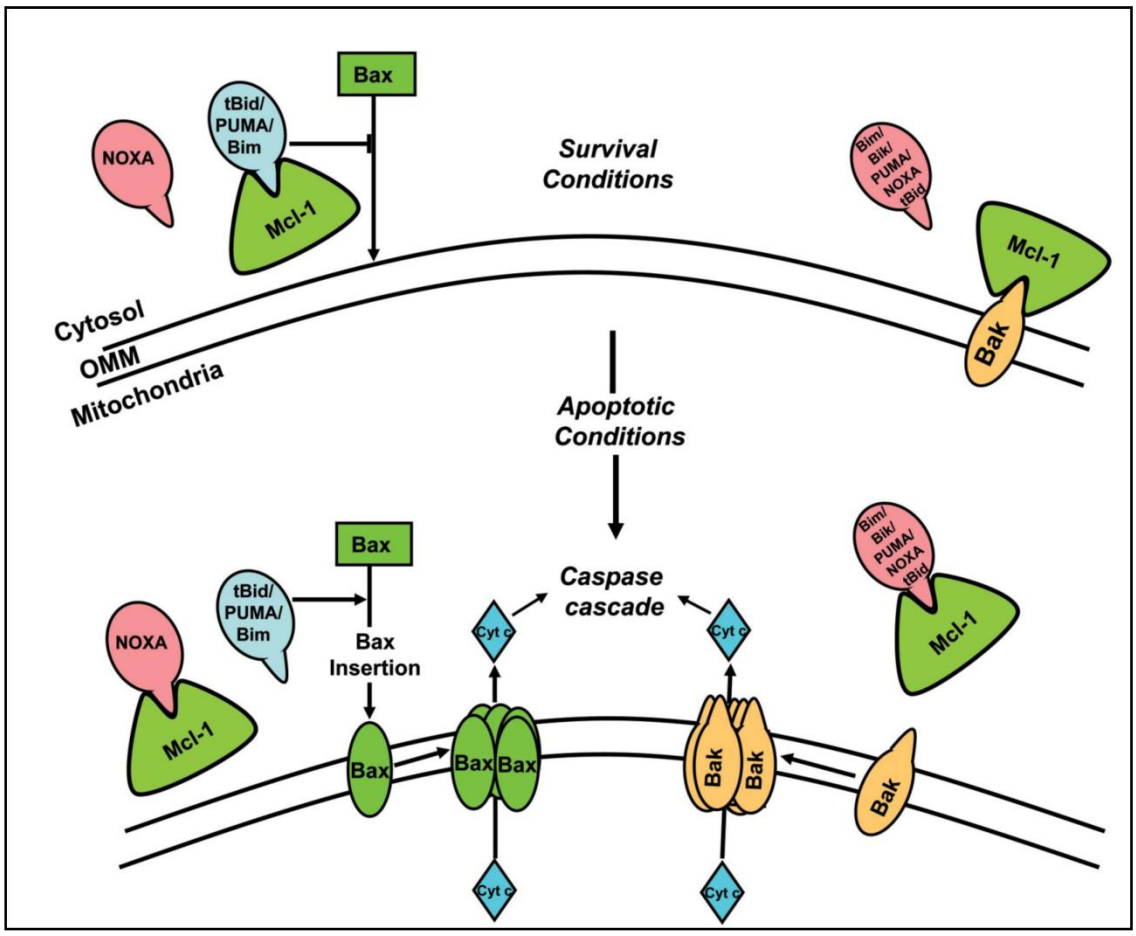

Figure 6: Regulation of apoptosis by MCL-1. Under survival conditions, MCL-1 is constitutively engaged in an interaction with BAK in the OMM which does not allow BAK to oligomerize. Alternatively, MCL-1 interacts with and antagonizes the "Direct activator" BH3-only proteins, thereby restricting their ability to interact with BAX which thus cannot translocate to the OMM and unable to oligomerize. When apoptotic stimuli are received by a cell, "De-repressor" BH3-only proteins are activated which neutralize MCL-1. BAK can now oligomerize in the OMM. Simultaneously, NOXA displaces "Direct activator" BH3-only proteins from MCL-1 which promote BAX activation, its translocation to the OMM resulting into its oligomerization. These events bring about MOMP leading to cytochrome c release into the cytosol and ultimately caspase activation [28].

2.8.4 Noncanonical functions of MCL-1

The versatility of physiological roles of MCL-1 extends way beyond its canonical prosurvival function. Several noncanonical functions of MCL-1 are recently being uncovered which are described below in detail.

A) Maintenance of Mitochondrial Homeostasis

Unlike the MCL-1 located within the OMM which performs a prosurvival function, Perciavalle et al documented the critical role of a distinct species of MCL-1 in the maintenance of mitochondrial integrity and function. During mitochondrial import, the full length MCL-1 is truncated at its N-terminus and is inserted within the IMM facing the mitochondrial matrix (Figure 7) [92]. This truncated form of MCL-1 appears to be essential for the assembly of F_1F_0-ATP synthase into oligomers, to maintain the ultrastructure of cristae and for normal

mitochondrial fragmentation which happens to be necessary for the maintenance of normal mitochondrial DNA (mtDNA) levels. It is also required for the assembly of electron transport chain components into higher order functional complexes which improves electron transport efficiency and thus energy production. Evidently, this novel function of MCL-1 supports tumor cell survival and proliferation by fuelling its mitochondria [92]. Recently, the involvement of MCL-1 in mitochondrial dynamics has also been shown to be associated with apoptosis [93].

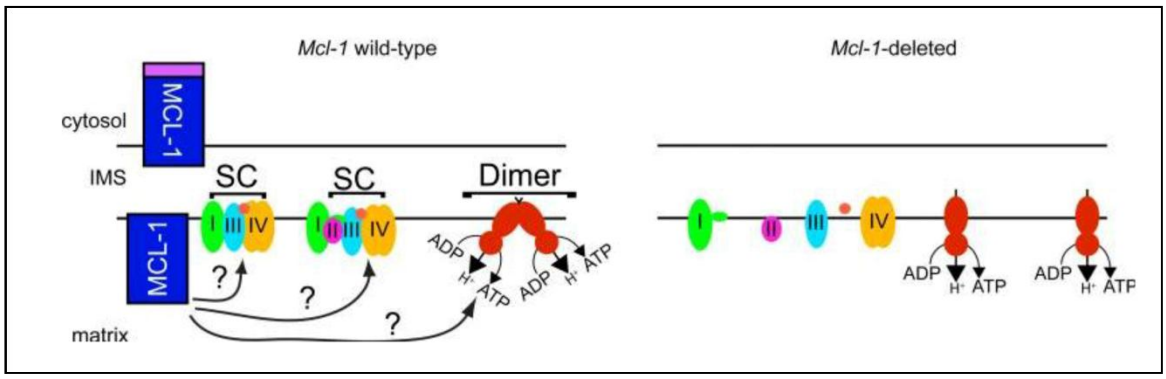

Figure 7: Role of MCL-1 in mitochondria. An N-terminally truncated species of MCL-1 localizes to the mitochondrial matrix and is important to maintain mitochondrial cristal ultrastructure, promotes the assembly of the electron transport chain (ETC) complexes into higher-order assemblies known as supercomplexes (SCs) which increases electron transport efficiency and energy output. It also facilitates the higher order assembly of the ATP synthase complexes into oligomers [94] **.**

B) DNA repair

The critical role of MCL-1 in radioresistance of a variety of human cancers is well known including oral cancers [24, 25], melanoma [95] and pancreatic carcinoma [96]. The exact

molecular mechanism by which MCL-1 contributes to radioresistance is still being explored. Jamil et al demonstrate that a short nuclear form of MCL-1 (snMCL-1) mediates ATR-dependent Chk-1 phosphorylation independent of ATM or DNA-PK [97]. Moreover, MCL-1 was shown to be directly recruited to the sites of DNA damage along with other DNA damage response proteins. MCL-1 null cells accumulated greater chromosomal abnormalities and were unable to efficiently repair the damaged DNA as compared to the wild-type cells [98].

C) Autophagy

Autophagy represents physiological response of a cell to stressful conditions such as nutrient deprivation which enables the cell to breakdown its organelles or macromolecules and recycling the resulting metabolites for energy production. The regulatory circuits of autophagy, apoptosis and cellular homeostasis are closely associated [99]. Beclin-1 is an important component of the autophagic pathway which bears BH3 domain and is associated with the antiapoptotic members of the BCL-2 family including MCL-1 [100, 101]. Furthermore, MCL-1 protein has recently been shown to regulate the balance between apoptosis and autophagy [102, 103]. MCL-1 is also important for normal autophagy, loss of which leads to impaired autophagy and heart failure [104].

2.8.5 Regulation of MCL-1

Evidently, MCL-1 being such a critical prosurvival molecule, it is tightly regulated by a cell at multiple levels in a context-dependent manner [30]. Ertel et al reviewed several strategies a tumor cell adopts to maintain constitutively high levels of MCL-1 [105].

A) At genomic level

MCL-1 gene is located on a chromosomal region (1q21) that is frequently associated with chromosomal aberrations [106]. Moreover, genome wide screening across diverse tumor types have elucidated that MCL-1 gene is subject to increased copy number [107]. Certain promoter alterations [108, 109] and epigenetic modifications have also been implicated in the enhanced expression of MCL-1 gene [110].

B) At the level of transcription

MCL-1 expression at the level of transcription is rapidly induced in response to survival and differentiation signals through the activation of JAK/STAT [111, 112], PI3K/Akt/mTORC1 [113] and MAPK/ERK [114] pathways. MCL-1 promoter has consensus binding sites for many transcription factors which are involved in its upregulation and include STAT3 [111, 112], STAT5 [115], CREB [113], PU.1 [116], and HIF-1α [117]. The role of transcription factors Ets-1 [118], IRE1α and ATF6 [119] in the upregulation of MCL-1 in human melanoma cells upon ER stress have also been documented. Conversely, E2F1 represses the MCL-1 promoter either in p53-dependent or independent manner [120]. p53 is also reported to transcriptionally repress MCL-1 expression through inhibition of Sp1 binding to the basic transcription factor binding sites in the MCL-1 promoter [121].

C) At posttranscriptional and translational level

MCL-1 mRNA has a short life and its rapid turnover is also a key regulatory mechanism [122] primarily modulated by a repertoire of miRNAs. miR-29 [123] and miR-133B [124] are known to repress the translation of MCL-1 mRNA through binding to its 3'UTR. miR-29B is found to be downregulated in tumors and correlate to elevated MCL-1 protein levels [123]. miR-139 is also known to inhibit MCL-1 expression in glioma cells and sensitize the cells to temozolomide

[125]. CUGBP2, an RNA binding protein binds to the 3' UTR of MCL-1 mRNA and inhibit its translation [126]. Adding to the complexity of its regulation, the MCL-1 precursor mRNA is alternatively spliced skipping the central exon 2 resulting in a corresponding shift in the reading frame downstream to yield two distinct isoforms viz. the less abundant proapoptotic short isoform (S) which resemble BH3-only proteins because it contains only a BH3 domain and the predominant antiapoptotic long isoform (L) which retains all the three BH domains and a C terminus transmembrane domain [127]. MCL-1S itself interacts with MCL-1L as shown by the yeast two hybrid systems and coimmunoprecipitation assays. The proapoptotic action of MCL-1S is neutralised by MCL-1L. The relative balance and interactions between these two isoforms determines the fate of a cell which depend on MCL-1 for survival [128]. Evidently, our own reports in oral cancer cell lines and tumors shows significantly high levels of antiapoptotic MCL-1L transcript versus the pro-apoptotic MCL-1S which might contribute to transformation and tumorigenesis [23]. Recently, a third spliced isoform of MCL-1 has been discovered, termed MCL-1 Extrashort (ES) which also interacts with MCL-1L, antagonise it and thus promote apoptosis, again delineating the importance of alternative splicing in determining the fate of a cell [129].

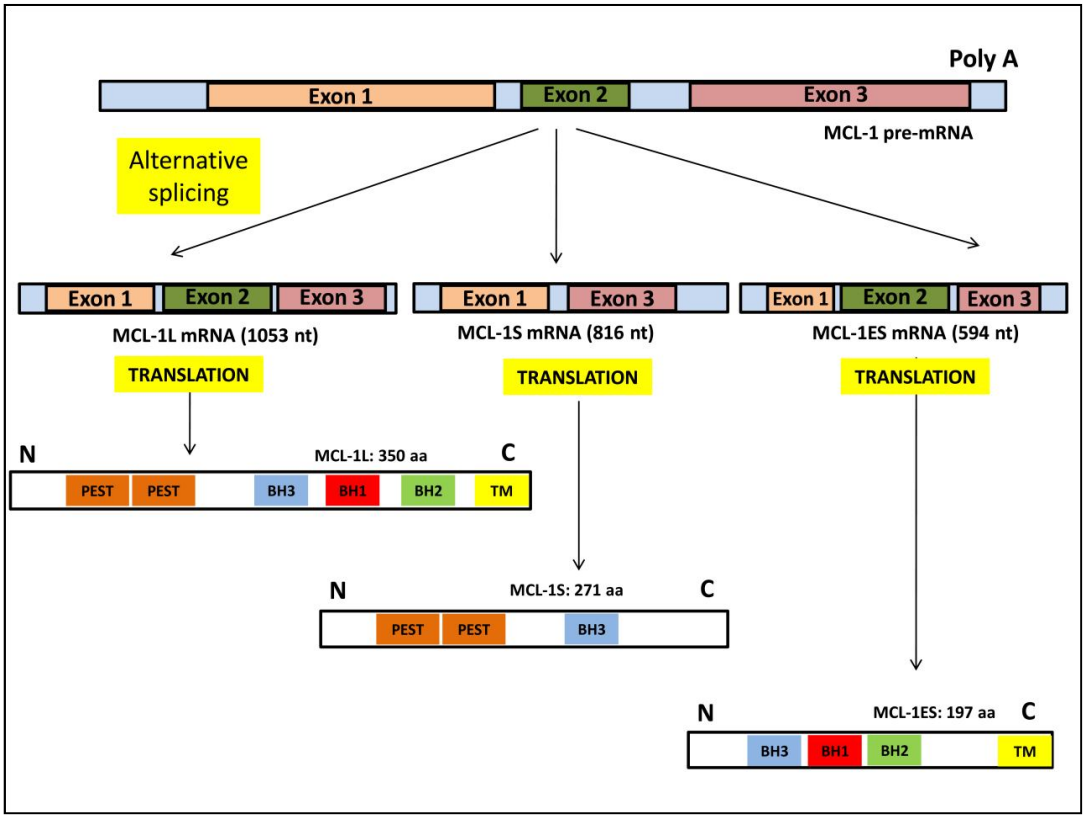

Figure 8: Alternative splicing of MCL-1 pre mRNA. The MCL-1 precursor mRNA is alternatively spliced to give rise to three isoforms: MCL-1L (Long isoform, the predominant form which is antiapoptotic in nature), MCL-1S (Short isoform, proapoptotic) and MCL-1ES (Extrashort isoform, proapoptotic).

D) At posttranslational level

i) Regulation of MCL-1 stability by phosphorylation

Perhaps the most pivotal mode of MCL-1 regulation is at the posttranslational level. Unique to MCL-1 is its long unstructured N-terminus regulatory region which critically regulates its turnover. This region has several phosphorylation sites within the PEST domains and the different phosphorylation states of these residues have different effects on the fate of MCL-1 protein (Figure 9). ERK-1 mediated phosphorylation at T92 in conjunction with phosphorylation

at T163 stabilizes MCL-1 [130]. Phosphorylation of MCL-1 at S121 in conjunction with T163 by JNK/p38 stabilizes it [131]. GSK-3 mediated phosphorylation at S155 [132] and S159 [133] in association with T163 decreases MCL-1 stability through its polyubiquitination. T163 is a target of phosphorylation for ERK, GSK-3 and JNK and is a priming residue for phosphorylation at many other sites of MCL-1 [134]. A protein kinase Cδ catalytic fragment (PKCδ cat) is also reported to phosphorylate MCL-1 and promote its proteasome-mediated degradation [135].

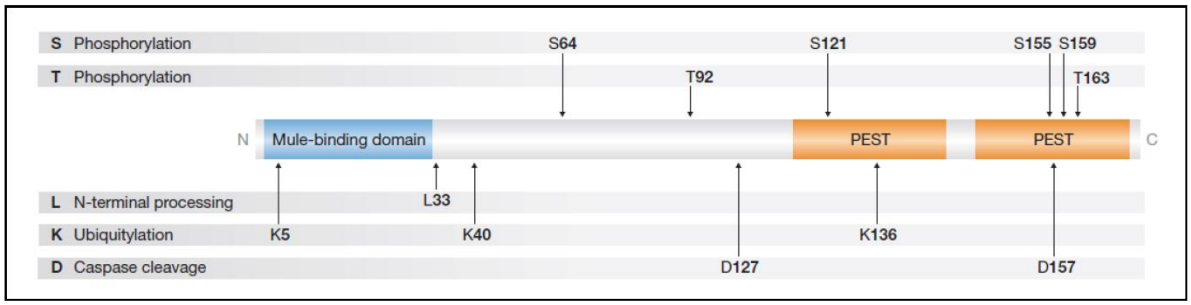

Figure 9: The N-terminus regulatory domain of MCL-1. Unique to MCL-1 is its long N-terminus regulatory domain which contains several phosphorylation, polyubiquitination and caspase-3 cleavage sites. Phosphorylation of various residues in the PEST sequences by various kinases determine the stability and thus half-life of MCL-1 [33].

ii) Proteasomal degradation of MCL-1

Proteasomal degradation is the major mode of MCL-1 turnover. MCL-1 protein contains three major polyubiquitination sites at the N-terminus, namely Lys^{5}, Lys^{40} and Lys^{136}. A HECT domain containing E3-ubiquitin ligase MULE interacts with MCL-1, polyubiquitinate it and thus promote its proteasomal degradation [136]. BIM competes with MULE for binding to MCL-1 and thus may protect it from degradation [137]. $SCF^{\beta\text{-}TrCP}$ is another E3-ligase which specifically

targets MCL-1 following its GSK-3-mediated phosphorylation [132]. A more recent finding suggests that in a T-ALL setting, MCL-1 is polyubiquitinated by an E3 ubiquitin ligase SCF^{FBW7} followed by its proteasomal destruction in a GSK-3-mediated phosphorylation-dependent manner [138]. During a prolonged mitotic arrest, MCL-1 degradation is essential for apoptosis to occur. CDK1/Cyclin-B complex phosphorylates MCL-1 at T92 followed by its polyubiquitination by a multi-subunit RING E3 ligase APC/C^{cdc20} leading to its proteasomal destruction [139]. Xu et al demonstrated that the ATPase domain of AAA-ATPase p97 is essential for the export of MCL-1 from mitochondria to the cytosol for its proteasomal degradation and several reports have implicated this protein in cancers although a direct correlation with MCL-1 levels is yet to be established [140].

iii) Non-proteasomal modes of MCL-1 degradation

Apart from proteasome mediated destruction, MCL-1 is also cleaved by Caspases-3 and Granzyme B. Caspase-3 cleaves MCL-1 at Asp^{127} and Asp^{157} during apoptosis and the C-terminal fragments thus generated exhibit proapoptotic activity [141]. Granzyme B cleaves MCL-1 at a site different than Caspase-3 and interferes with Bim sequestration by MCL-1 [142]. Stewart et al reported ubiquitin-independent degradation of MCL-1. In a system where MCL-1 mutant was lacking lysine residues required for its polyubiquitination, the turnover of mutant MCL-1 was similar to that of the wild type MCL-1. The MCL-1 turnover was found to be unaffected even when E1 ubiquitin activating enzyme was blocked [143].

2.8.6 Mechanisms stabilising MCL-1

Not surprisingly, in tumors where MCL-1 levels are often elevated, apparently it is the protein that is being stabilised in addition to its transcriptional upregulation. One way this is achieved is through the interaction with several proteins (such as a deubiquitinase USP9X and a small

ubiquitously expressed protein TCTP) that enhance the stability of MCL-1. Alternatively, reduced association with the E3-ligase MULE may contribute to elevated levels of MCL-1 protein. Furthermore, N-terminal truncation of the newly synthesized MCL-1 protein in the OMM removes a portion that is necessary for its interaction with MULE and thus the two cannot interact thereby stabilizing MCL-1 [144, 145]. Deletion of the N-terminal 79 residues of MCL-1 impairs the mitochondrial localization and thus its antiapoptotic function and also increases its anti-proliferative activity. Conversely, expression of this domain promotes the mitochondrial localization and thus increases its antiapoptotic activity and cell proliferation [146]. Furthermore, BIM and PUMA interacts with MCL-1 through their BH3 domains preventing the interaction between MCL-1 and MULE thereby stabilising it [147, 148].

In the present study, we therefore evaluated the critical role of three non-BCL-2 family interacting partners of MCL-1 which are directly associated with its ubiquitin-proteasomal mode of degradation:

A) USP9X (Ubiquitin Specific Peptidase 9 X-linked)

Ubiquitination is a reversible post-translational modification of proteins, carried out by certain E3-ubiquitin ligases which is critical for the regulation of protein stability, activity and interactions [149]. Deubiquitinases (DUBs) are proteases that cleave the isopeptide linkage between the protein substrate and the ubiquitin (Ub) residue, thereby terminating Ub-dependent signaling. They belong to the superfamily of peptidases, specifically to the cysteine- and metallo-peptidase families [150]. DUBs perform a variety of cellular functions including Ub-recycling in association with proteasome, remodeling the Ub content of target proteins (known as Ub-editing) and regulation of multiple cellular signaling pathways [151]. Because of their key role in regulation of cell fate, DUBs have been assigned both oncogenic and tumor suppressor roles

[152]. Their aberrant expression in several human cancers therefore may contribute to tumorigenesis and represent novel therapeutic targets [153, 154]. USP9X, a deubiquitinase was found to interact with and catalyze the removal of Lys^{48}-linked polyubiquitin chains from MCL-1, thus stabilising it. Elevated USP9X levels correlated significantly with increased MCL-1 levels in human follicular lymphomas, and diffuse large B-cell lymphomas and are associated with a poor prognosis. USP9X may therefore serve as an important prognostic and therapeutic target [155].

B) Translationally Controlled Tumor Protein (TCTP)

TCTP (Translationally Controlled Tumor Protein) is a highly conserved protein widely expressed in all eukaryotic organisms. Based on its structure, TCTP is closely related to a family of small chaperone proteins. Its expression is tightly regulated both at the transcriptional and translational level in response to a wide range of extracellular signals. TCTP has been implicated in important cellular processes, such as cell growth, cell cycle progression, malignant transformation, extracellular cytokine-like function and in the protection of cells against various stress conditions and apoptosis [156]. TCTP is predicted to interact with MCL-1 and stabilize it by interfering with the ubiquitin proteasomal pathway, although the exact mechanism is not known. It may therefore serve as a chaperone for MCL-1 [157]. TCTP is also reported to be overexpressed in many cancers as compared to the corresponding normal tissues [158, 159].

C) MULE (MCL-1 Ubiquitinating Ligase E3)

The steady state levels of MCL-1 protein are meticulously maintained in a cell by its ubiquitination-dependent proteasomal degradation and deubiquitination. MULE (ARF-BP1 or LASU1) is a 482 KDa HECT-Domain containing E3-ubiquitin ligase which is both required and sufficient to bring about the polyubiquitination of MCL-1. It harbors a BH3 domain by virtue of

which it interacts with MCL-1. MULE polyubiquitinates at five lysine residues (Lys^{5}, Lys^{40}, Lys^{136}, Lys^{194}, Lys^{197}) in the N-terminus domain of MCL-1 [160]. Under apoptosis-stimulating conditions, GSK-3 phosphorylate MCL-1 at a consensus site Ser^{159} in the N-terminus regulatory domain of MCL-1 leading to its increased polyubiquitination and proteasomal degradation [80].

2.8.7 MCL-1 in cancers

Being a critical prosurvival molecule, MCL-1 is under tight regulation in normal cells. However, it is often overexpressed in a variety of human cancers owing to the deregulation of multiple signaling pathways that regulate its expression [28]. MCL-1 expression is shown to be elevated in many solid tumors including hepatocellular carcinoma [161], prostate cancer [162], pancreatic cancers [163] and oral cancers [23] among several others. MCL-1 overexpression has also been documented in hematological malignancies [115, 164, 165]. Placzek et al documented predominant overexpression of MCL-1 over other BCL-2 family proteins in a variety of human cancer cell lines [27]. MCL-1 overexpression is also reported to be associated with acquired chemo and radioresistance in many cancers [90, 95, 166]. Indeed, studies from our laboratory indicates that MCL-1 is a major radioresistance related protein and its targeted downregulation increases radiosensitivity of oral cancer cell lines [25]. Furthermore, oral cancer patients showing elevated levels of MCL-1 were associated with poor prognosis and reduced disease free survival when treated with definitive radiotherapy [24]. MCL-1 overexpression is also associated with chemoresistance in oral cancer patients and its pharmacological inhibition sensitizes the cells to Cisplatin-induced cell death [26]. Targeted downregulation of MCL-1 also induces significant cell death in many cancer cell types [164, 167-169]. All these reports suggest that MCL-1 is an important prosurvival molecule in many types of cancers and is thus a potential therapeutic target.

2.8.8 Targeting MCL-1: Therapeutic potential

Two principal therapeutic strategies can be employed to tackle the overexpression of MCL-1 in cancers and its associated resistance to existing therapeutic agents. It includes A) Targeting pathways that will ultimately lead to downregulated expression of MCL-1 protein. B) Direct chemical antagonism of MCL-1 protein using small molecule BH3-mimetic inhibitors.

A) Therapeutic strategies that modulate MCL-1 expression

Targeting the mechanisms that modulate MCL-1 expression in tumors offers a great promise in cancer therapeutics. Xu et al in small cell lung cancer cell lines reported that actinomycin D decreases MCL-1 levels, increases the NOXA levels and thereby increases effectiveness of ABT-737 synergistically [170]. Seliciclib (CYC202) downregulated MCL-1 levels through the inhibition of transcription and protein expression by inhibiting STAT3 phosphorylation. Seliciclib has a dual mode of action in that it inhibits RNA Pol II-dependent transcription and also serves as a CDK inhibitor [171]. Sorafenib (BAY43-9006) decreases MCL-1 levels through translational inhibition in leukemic cell lines [172]. Flavopiridol induces apoptosis in lung cancer cell lines through upregulation of E2F1 and subsequent transcriptional repression of MCL-1 [173]. Simultaneous inhibition of mTORC and PI3K downregulated MCL-1 in mantle cell carcinoma cell lines and enhanced their sensitivity to rapamycin [174]. USP9X overexpression is also frequently reported in several types of tumors which contributes to elevated MCL-1 levels [175]. USP9X thus appears to be an important target. WP1130, a small molecule inhibitor of USP9X significantly lowers MCL-1 levels and thus induces apoptosis in tumor cells [176].

B) Direct chemical antagonism of MCL-1

ABT-737, an effective inhibitor of BCL-2, BCL-XL and BCL-W does not exhibit potency against MCL-1 [177]. Similarly, ABT-263 (Navitoclax) which is an orally bioavailable analog of

ABT-737 efficiently neutralizes BCL-2 and BCL-XL but is unable to antagonize MCL-1 [178]. Lee et al characterised a BH3-like ligand BIMs2A which selectively binds to MCL-1 without triggering its degradation [179]. Obatoclax (GX15-070) is a pan-BCL-2 inhibitor able to effectively antagonize all the antiapoptotic BCL-2 family members including MCL-1 and thus induces apoptosis in a wide variety of cell lines. Through competitive binding, it potently inhibits the interaction between MCL-1 and BAK thus facilitating MOMP. Obatoclax also overcomes MCL-1-mediated resistance to Bortezomib in melanoma model and to ABT-737 [90]. The *in vitro* and *in vivo* potency of Obatoclax has been demonstrated against a variety of human cancer cell lines [90, 180-182] and in several clinical trials against diverse tumor types [183-185]. Zhang et al reported the identification of S1 as a small molecule BH3 mimetic capable of antagonising BCL-2, BCL-XL and MCL-1 and induces apoptosis dependent on BAK and BAX by dissociating the BCL-2/BAX and MCL-1/BAK interaction [186]. An apogossypol derivative named Sabutoclax (BI-97C1) was also found to inhibit MCL-1 and induce apoptosis in prostate cancer cells [187], lung cancer cells [188], OSCC cells [189] and prostate cancer xenografts *in vivo* [190]. More recently, Doi et al, characterised a natural product, Maritoclax as a novel MCL-1 specific inhibitor. It inhibits the interaction between MCL-1 and BIM and induces MCL-1 degradation. Thus it selectively kills MCL-1-dependent but not BCL-2 or BCL-XL dependent cells [191]. Rationally combining these agents with the established therapeutics may yield better antitumor efficacy.

2.9 Autophagy

Autophagy is an evolutionarily conserved mechanism which enables eukaryotic cells to recycle their intracellular macromolecules and organelles for generation of energy under conditions of stress and starvation [192]. A basal level of autophagy is always on which is responsible for

turnover of long-lived proteins and damaged organelles. However, autophagy is triggered by stressful conditions such as nutrient depletion. Autophagy has long been recognized as a survival mechanism under conditions of nutrient starvation by bulk degradation of cytoplasmic material to generate both nutrients and energy in starving cells to sustain cell viability [193]. However, recent evidences show that sustained autophagy in response to persistent stress often leads to a non-apoptotic type 2 programmed cell death called as "Autophagic cell death" [194-196]. Moreover, autophagy has been implicated in a number of pathophysiological conditions in the human body including ageing, heart diseases, diabetes, cancer and neurodegenerative diseases [197-199]. Owing to the prosurvival nature of autophagy, it has been associated with therapy resistance in a variety of human cancers and therefore, targeting autophagy has great therapeutic implications [200, 201].

2.9.1 Pathway of autophagy

Autophagy is a complex multi-step process involving a plethora of molecules.

1) Initiation:

Nutrient deprivation leads to inhibition of mTOR kinase-induced phosphorylation of a serine/threonine kinase complex (consisting of ULK, ATG13 and FIP200) which liberates the kinase activity of ULK. ULK in turn phosphorylates itself, ATG13 and FIP200. The ULK complex then accumulates at the initiation focus of the isolation membrane/phagophore.

2) Autophagosome formation:

Vesicle nucleation: class III phosphoinositide 3-kinase (PI3K-III) hVps34, Beclin-1 and p150/hVps35 are required for the further development of the isolation membrane/phagophore.

Vesicle elongation and completion: Two ubiquitin-like conjugation systems ATG12 and ATG8 are required for this step**.** For its activation, ATG12 forms a multimeric complex (ATG12-

ATG5-ATG16) with ATG7, ATG5, ATG10, ATG16. ATG8 has a mammalian homolog called as LC-3 which serves as an autophagosomal marker. LC-3 is synthesized as a precursor protein proLC-3 which is processed to LC-3I by ATG4. LC-3 maturation requires reversible conjugation of phosphatidylethanolamine at the C-terminus of LC-3I by ATG3 and ATG7 to form LC-3II which is then incorporated within the autophagosomal membranes. LC-3 controls the expansion of phagophore and its amount directly correlates with the size of the autophagosomes.

3) Maturation and degradation:

It involves fusion of autophagosomes with lysosomes to form autophagolysosomes or autolysosome. The autophagosome maturation process involves key role of lysosomal membrane proteins (LAMP1 and LAMP2), small GTPases Rab7 and UVRAG. Within autolysosome, the lysosomal hydrolases, particularly Cathepsins degrade the intracellular material and the metabolites resulting from the process fuel the energy demands of the cell under conditions of starvation [202].

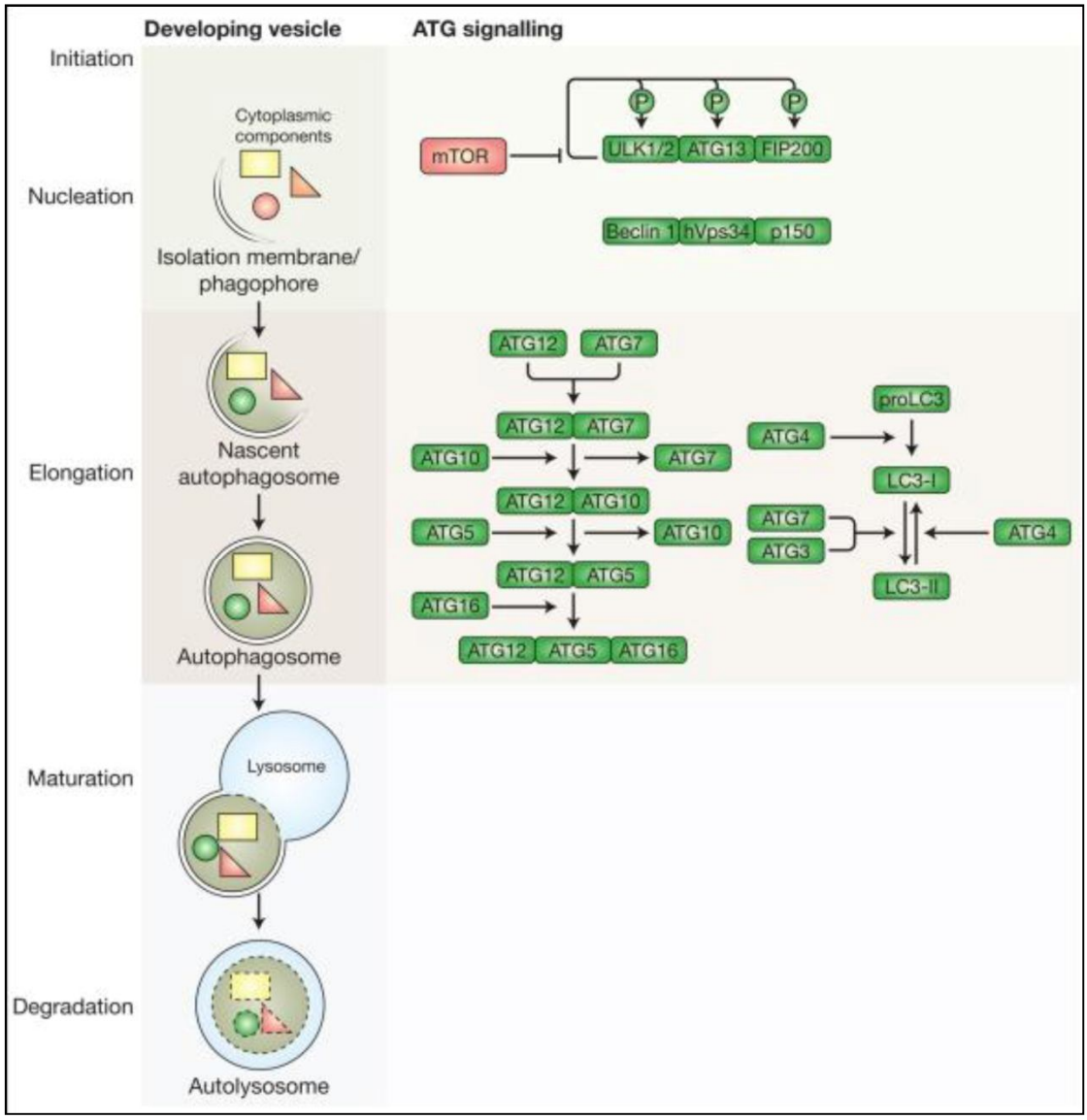

Figure 10: The pathway of autophagy. Following a stress stimuli, the initiation of autophagosome formation and its assembly requires the activity of several important kinases such as ULK and a set of ATG proteins. The mature autophagosome carrying various cargos in the later stages fuses with a lysosome. The lysosomal enzymes brings about digestion of the autophagosomal cargo ultimately releasing the metabolites to the cytosol to meet cells' immediate energy demands under stressful conditions [202].

2.10 Necroptosis

Necroptosis is a programmed pathway of necrotic cell death which involves a critical role of serine/threonine kinases called as Receptor-interacting protein (RIP) kinases. It is linked to defective autophagy in response to a variety of stress stimuli [203, 204]. Necroptosis has a central pathophysiological relevance in myocardial infarction, stroke, atherosclerosis, ischemia-reperfusion injury, pancreatitis, inflammatory bowel disease and many other common clinical disorders [205]. The most upstream and a key member of the necroptosis pathway is RIP1 kinase (RIP1K). An upstream signal triggers dimerization and autophosphorylation of RIP1 which leads to its activation and recruitment of downstream signaling proteins such as RIP3 kinase (RIP3K), and FADD in a complex called as "Necrosome". RIP3K further downstream recruits and phosphorylates its substrate MLKL which is proposed to execute necroptosis by mediating mitochondrial fission, generation of Reactive oxygen species (ROS) in mitochondria and recruitment of Ca^{2+} and Na^{+} ion channels or pore-forming complexes at the plasma membrane [206, 207].

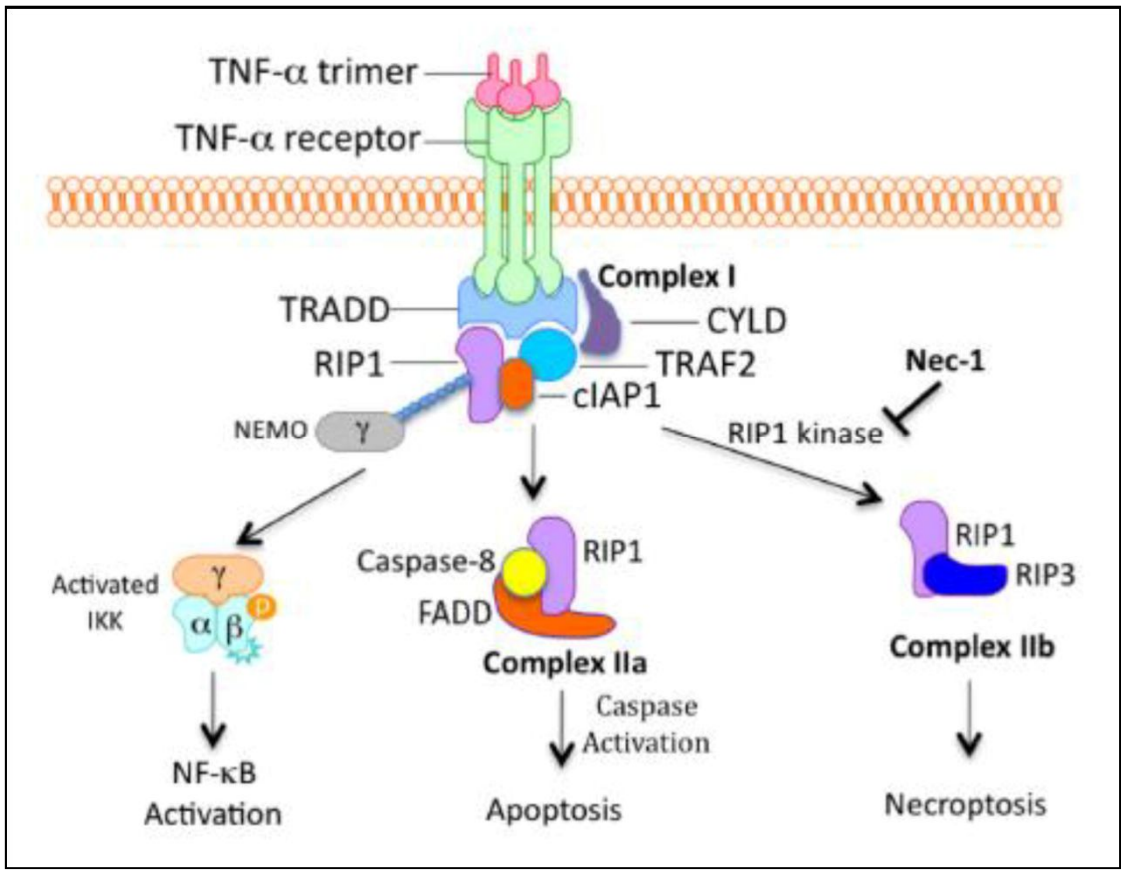

Figure 11: The signaling mechanism leading to the assembly of necrosomal complexes. Stimulation of TNFR1 by TNFα leads to the formation of an intracellular complex at the cytoplasmic membrane (complex I) that includes TRADD, TRAF2, RIP1 and cIAP1. Ubiquitination of RIP1 at K377 by cIAP1 leads to the recruitment of NEMO, a regulatory subunit of IKK complex that in turn activates NF-κB pathway. RIP1 is also involved in the formation of complex IIa including FADD and caspase-8 to activate a caspase cascade to mediate apoptosis. Under apoptosis deficient conditions or when cells are infected by certain viruses, RIP1 interacts with RIP3 to form complex IIb which is involved in mediating necroptosis. The formation of complex IIb requires the kinase activity of RIP1 that is inhibited by Necrostatin-1.

Chapter 3
Aims and Objectives

The objectives of the study are as follows:

1. To assess the role of MCL-1-interacting partners that may contribute to its stability in human oral cancers.
   a. Reported interacting partners (USP9X, TCTP and MULE).
   b. Novel interacting partners to be identified through Mass Spectrometry.
2. To assess the *in vitro/in vivo* effects of small molecule inhibitor of MCL-1 in human oral cancer cells.

Chapter 4
Materials and Methods

4.1 Materials

The following chemicals/reagents/kits/enzymes were obtained from:

Sigma: Paraformaldehyde (PFA), Sodium Orthovandate (Na_3VO_4), Acrylamide, N-N' Methylene Bis-Acrylamide, β-mercaptoethanol (BME), Bovine Serum Albumin (BSA), Ethylenediaminetetraacetic acid (EDTA), Glycine, Sodium Dodecyl Sulphate (SDS), Tween-20, Triton X-100, Tris, Trypsin, N,N,N',N'-Tetramethylethylenediamine (TEMED), Dithio Thritol (DTT), Iodo-Acetamide (IAA), Bromophenol Blue, Coomassie brilliant blue (CBB), Dimethyl Sulfoxide (DMSO), Diethyl Pyrocarbonate (DEPC), Ethidium Bromide (EtBr), Proteinase K, Glutaraldehyde, TRI reagent, Tri-fluoro acetic acid (TFA), Low melting agarose, Erythrosine B, Ponceau stain, Fast Green stain, 4',6-diamidino-2-phenylindole (DAPI), Tri-Sodium citrate, 3-(4,5-Dimethylthiazol-2-yl)-2,5-diphenyltetrazolium bromide (MTT) and Sulforhodamine B (SRB) dyes, Trypan blue, 3,3′-Diaminobenzidine (DAB).

Drugs/inhibitors: Cycloheximide and Chloroquine (Sigma), MG132 (Calbiochem), Obatoclax and WP1130 (Selleck Chemicals), z-VAD-FMK (Abcam).

Hi-Media laboratories: Crystal Violet, Hanks Balanced Salt Solution (HBSS)

Qualigens: Boric acid, Disodium hydrogen phosphate, $MgCl_2$, NaOH pellets, Sodium dihydrogen orthophosphate, Tri-sodium citrate, Glacial acetic acid, Glycine, Xylene, DPX mountant.

SISCO Research Laboratories: Chloroform, Folin Ciocalteu reagent, Isopropanol, Isoamyl alcohol, Methanol, Molecular biology grade ethanol, Phenol, Sodium chloride, Sodium acetate, Trichloro acetic acid (TCA).

MBI Fermentas: First strand cDNA synthesis kit, 6X loading dye, 25mM $MgCl_2$, Protein ladder, 10X PCR buffer, Taq polymerase, Proteo-block protease Inhibitor cocktail, Proteo-jet Mammalian cell lysis reagent.

Gibco: Fetal Bovine Serum (FBS), DMEM, IMDM, Ampicillin.

Invitrogen: Lipofectamine-2000, TRIzol reagent.

Applied Biosystems: High Capacity cDNA Reverse Transcription Kit, Power SYBR Green PCR Master Mix

Molecular probes, Invitrogen: MitoTracker Green FM, MitoTracker Red CMXRos, MitoSOX Red dyes

eBiosciences: JC-1 dye mitochondrial probe

Roche: dNTPs, Taq DNA polymerase.

GE Life sciences: Enhanced Chemiluminescence Kit, Protein G Sepharose beads.

Merck Millipore: PVDF membrane.

SD Fine: Acetonitrile (Mass spectrometry grade), Prestained protein ladder (10-250 KDa range).

Nunc and BD-Falcon: Tissue culture plates and flasks.

Axygen and Tarson: Nuclease free disposable tips and eppendorf tubes.

Dharmacon (GE Life sciences): siRNA against TCTP and USP9X, siGlo (to check transfection efficiency), Control/Non-target/scrambled siRNA, 5X siRNA resuspension buffer

Thermo Scientific: Super signal West Femto, Mitochondria Isolation Kit for Cultured Cells

Kodak: X-ray films.

Vector labs (USA): Vectashield (Fluorescence anti-quench mounting medium), VectaStain ABC kit for IHC.

BD Pharmingen: FITC Annexin V Apoptosis Detection Kit I

Takara: *In situ* Apoptosis Detection Kit

Plasmid constructs: pBABE-puro mCherry-EGFP-LC3B (Addgene plasmid repository; deposited by Dr. Jayanta Debnath).

Water used for the preparation of all solutions and reagents was obtained from MilliQ water plant (Millipore).

Table 1: Antibodies used in the study

Antibody	**Clone**	**Catalogue no.**	**Company**
MCL-1	Rabbit polyclonal	sc-819	Santa Cruz
MCL-1	Rabbit polyclonal	sc-20679	Santa Cruz
MCL-1	Rabbit polyclonal	554103	BD Pharmingen
TCTP	Rabbit polyclonal	sc-30124	Santa Cruz
USP9X	Mouse monoclonal	sc-100628	Santa Cruz
MULE/ARF-BP1	Rabbit polyclonal	ab70161	Abcam
BCL-2	Rabbit polyclonal	sc-492	Santa Cruz
BCL-XL	Rabbit monoclonal	2764	Cell Signaling
BAK	Rabbit polyclonal	sc-832	Santa Cruz
BAX	Rabbit polyclonal	A3533	Dako
NOXA	Goat polyclonal	sc-26917	Santa Cruz
PUMA	Rabbit polyclonal	ab9643	Abcam
BID	Goat polyclonal	sc-6538	Santa Cruz
BIM	Rabbit monoclonal	2933	Cell Signaling
PARP	Rabbit polyclonal	9542	Cell Signaling
Caspase-3	Rabbit polyclonal	ab90437	Abcam
Caspase-8	Mouse monoclonal	9746	Cell Signaling
Actin	Rabbit polyclonal	sc-1616	Santa Cruz
Ubiquitin	Mouse monoclonal	U0508	Sigma
Beclin-1	Rabbit polyclonal	sc-11427	Santa Cruz

p62/SQSTM1	Rabbit polyclonal	5114	Cell Signaling
LC-3B	Rabbit polyclonal	ab51520	Abcam
GRP78	Mouse monoclonal	610978	BD Pharmingen
LAMP-1	Mouse monoclonal	Culture supernatant of mouse hybridoma	
ATG5	Rabbit monoclonal	12994	Cell Signaling
RIP1	Rabbit polyclonal	4926	Cell Signaling
RIP3	Rabbit monoclonal	13526	Cell Signaling
HSP60	Rabbit monoclonal	12165	Cell Signaling
Cytochrome c	Mouse monoclonal	IMG-101A	Imgenex
anti-mouse IgG-HRP	Goat polyclonal	sc-2005	Santa Cruz
anti-rabbit IgG-HRP	Goat polyclonal	sc-2004	Santa Cruz
anti-goat IgG-HRP	Donkey polyclonal	sc-2020	Santa Cruz
anti-mouse Alexa fluor 488	Goat polyclonal	11059	Invitrogen
anti-rabbit Alexa fluor 488	Goat polyclonal	11008	Invitrogen
anti-rabbit Alexa fluor 568	Goat polyclonal	11011	Invitrogen

Table 2: Instruments used in the study

Instrument	**Model**	**Company**
Vertical electrophoresis assembly for SDS-PAGE	Mini-PROTEAN Tetra Cell	Bio-Rad, USA
Electroblotting	Trans-Blot Cell	Bio-Rad, USA
Electrophoresis Power packs	EPS-301	Amersham, UK

Flow cytometer	FACS Caliber	Becton Dickinson, USA
ELISA reader	Spectra Max 190	Molecular Devices, USA
Speedvac concentrator	SVC 1000, AES 1000	Savant, USA
Mass Spectrometry MALDI Instrument	Ultra Flex-2	Bruker, Germany
Real Time PCR machine	Quant Studio 12K Flex	Applied Biosystems, USA
pH meter	Orion	Thermo scientific, USA
X-ray film developing machine	Optimax	Pro-Tec, Germany
Microfuge	G Fuge	Genetix Biotech, India
Table top microcentrifuge	MIKRO 120	Hettich, Germany
Cooling centrifuge	Heraeus Multifuge X3R	Thermo Scientific, USA
Fluorescence confocal microscope	LSM 510 Meta and LSM 780 Meta	Zeiss, Germany
Inverted microscope	Axiovert-200M	Zeiss, Germany
Upright microscope	Axio Imager Z1	Zeiss, Germany
Cryotome	CM1950	Leica, Germany
Ultramicrotome	EM UC7	Leica, Germany
Transmission electron microscope (TEM)	100-CX-II	Jeol, UK
Microtome	RM2245	Leica, Germany

4.2 Methods

4.2.1 Mammalian cell culture:

Four human oral cell lines were used in the study as outlined below. All the cell lines except DOK were cultured in IMDM medium containing 10% FBS and antibiotics. DOK cells were grown in DMEM medium containing 5 µg/ml hydrocortisone, 10% FBS and antibiotics. The cells were maintained in a humidified CO_2 incubator at 37^{o}C and 5% CO_2.

Table 3: Cell lines used in the present study

Cell line	Origin/oral subsites derived from	Reference
DOK	Dysplastic oral keratinocyte, derived from tongue epithelium	[208]
AW8507	Poorly differentiated Squamous Cell Carcinoma of tongue	[209]
AW13516	Epidermoid carcinoma of the tongue	[209]
SCC029B	Buccal mucosa carcinoma	[210]

4.2.1.1 Passaging the cells

Exponentially growing cells (~80% confluence) were washed with PBS twice followed by incubation with trypsin-EDTA until the cells detach from the culture plate. The cells were then resuspended in twice the volume of complete medium (i.e. containing serum) as the trypsin-EDTA solution. The cell suspension was then centrifuged at 1000 rpm for 5 minutes at RT. The cell pellet thus obtained was again resuspended in complete medium and either subjected to cell counting followed by downstream assays or freezing.

4.2.1.2 Cryopreservation of cells

Cells were harvested by trypsinization as described above. The cell pellet was resuspended in a freezing mixture (90% FBS+10% DMSO) and aliquoted into freezing vials. DMSO serves as a cryoprotectant. Initially, the cells were gradually frozen in liquid nitrogen vapors for a couple of hours and then immersed in liquid nitrogen in cryoboxes placed in designated positions in canisters.

4.2.1.3 Revival of cryopreserved cells

The frozen vial was carefully withdrawn from the liquid nitrogen cylinder and placed on a table top for a few minutes. The vial was then immersed in a warm water bath until its contents appear thawed. The cell suspension was thoroughly resuspended in 5 ml complete medium and centrifuged at 1000 rpm for 5 minutes at RT. The cell pellet thus obtained was again resuspended in complete medium and seeded in fresh culture plate or flask. The cells were subcultured as described above for at least two passages before being used for experiments or assays.

4.2.1.4 Cell counting

The cell suspension is appropriately diluted in complete medium and maintained on ice throughout the cell counting procedure. Briefly, the cell suspension was mixed with 0.4% Erythrosin B or Trypan blue dye in 1:1 proportion and loaded onto the Neubaur's chamber (Hemocytometer) slide under a coverglass and placed under a light microscope. The dead cells appear stained whereas the live cells appear unstained. The cells were then counted in peripheral four WBC chambers to give a total cell count from which an average count per square was determined. The cell count was then determined as:

Total number of cells per ml = the average cell count per square X dilution factor X 10^4

4.2.2 Cell viability assays

4.2.2.1 Clonogenic assays

Cells growing in exponential phase were harvested by trypsinization followed by cell counting. An equal number of cells were seeded in individual wells of a 6-well plate or individual culture plates. The cells were allowed to grow overnight (~16 to 20 hours) and were then exposed to the desired treatment (radiation or a drug) at a specified dose for the indicated duration, following which the medium was replaced with fresh culture medium. The plates were incubated for a period of 8-10 days until visible colonies appear, after which the culture media was carefully decanted off and the colonies were thoroughly washed twice with PBS. The colonies were then fixed with 90% methanol (v/v) for 5 minutes at RT and then stained with 0.5% Crystal violet (w/v) in 90% methanol for 5 minutes at RT. The Crystal violet solution was then carefully decanted off and the plates were immersed into a tray containing tap water and washed thoroughly to remove the Crystal violet dye. The plates were then allowed to air dry and the colonies were scored manually.

4.2.2.2 MTT assay

2000 cells were seeded in individual wells of a 96-well plate and allowed to grow overnight. Next day, the cells were exposed to the designated concentrations of the inhibitors for the indicated time. At the end of the incubation period, 20 µl MTT reagent (from 5 mg/ml w/v in PBS stock) was added to each well and the plates were again incubated for 4 hours, following which the plate was centrifuged at 1000 RPM for 2-3 minutes. The plates were then carefully inverted so as to decant off the culture medium. The formazon crystals were dissolved by addition of 100 µl DMSO per well. The absorbance was then recorded on a microplate reader at

540 nm with a reference wavelength of 690 nm. The viability of the cells was expressed as percent viability as compared to vehicle control cells (which was designated as 100% viability).

4.2.2.3 SRB assay

The cells were seeded and treated with desired inhibitors similar to MTT assay as mentioned above. At the end of the treatment period, the cells in each well were fixed by addition of 100 µl 30% (w/v) Trichloroacetic acid (TCA) followed by incubation for 1 hour at 4^{o}C. The plates were then washed with water and then air dried. At this point, the plates can be stored for several months. The fixed cells were stained with 50 µl 0.05% (w/v) Sulforhodamine B (SRB) dye for 30 minutes at RT. Excess dye was removed by washing the wells repeatedly with 1% acetic acid (v/v) and the plates were again air dried. Finally, the protein-bound dye was solubilized by addition of 10 mM Tris (pH 10) and absorbance was recorded at 540 nm with a reference wavelength of 690 nm on a microplate reader.

4.2.3 siRNA transfection

Cells were seeded in culture plates and allowed to grow overnight. Next day, the cells were transfected with the siRNA oligos. Briefly, siRNA oligos (gene specific/control/siGlo) were mixed with the transfection reagent Lipofectamine 2000 in incomplete medium (i.e. without serum) and incubated at RT for 20 minutes. This transfection mixture (i.e. siRNA+Transfection reagent) was then added to the cells and then replenished with fresh medium. The culture medium was then replaced with fresh medium 6 hours post transfection. The siRNA oligos consisted of a pool of 3 different oligos targeting three distinct regions of the same mRNA sequence (siGenome SMARTPool siRNA from Dharmacon). siGlo is a fluorescent (labeled with a Cy3 analog DY-547) oligonucleotide duplex that localizes to the nucleus, thus permitting

unambiguous visual assessment of uptake into mammalian cells and allows to determine the optimal siRNA transfection conditions.

Table 4: The conditions of siRNA transfection

Culture plate size	**Vol. of Lipofectamine 2000 per well**	**Total vol. of culture medium per well**	**vol. of dilution medium**
24-well plate	2 µl	500 µl	2X50 µl
12-well plate	4 µl	1000 µl	2X100 µl
6-well plate	8 µl	2000 µl	2X250 µl

The siRNA was resuspended in siRNA reconstitution buffer to a final stock concentration of 20 µM and stored at -20^{o}C which is then appropriately diluted at desired working concentrations. The siRNA concentration was standardized by transfecting the cells with increasing doses of the siRNA (viz., 12.5 nM, 25 nM, 50 nM, 75 nM, 100 nM). 48 hours post transfection, the cells were harvested by trypsinization and analyzed for the efficiency of target gene or protein knockdown by real time PCR or western blotting respectively.

4.2.4 Flow cytometry

4.2.4.1 Annexin V/Propidium Iodide staining for detection of apoptosis

Cell death quantitation was performed by using FITC-Annexin V Apoptosis Detection Kit I (BD Pharmingen) as per the manufacturer's instructions. At the end of the treatment period, the cells were harvested by trypsinization and washed twice with cold PBS. The cells were then resuspended in Annexin V-binding buffer at a concentration of 1X10^{6} cells/ml. 100 µl of this cell suspension was incubated with 5 µl Annexin-V-FITC and 5 µl Propidium Iodide in dark for 15

minutes at RT. 400 µl Annexin V-binding buffer was then added to these stained cells and vortexed vigorously followed by acquisition on a FACS caliber flow cytometer (FL1 channel: Annexin V-FITC; FL2 channel: PI) and data was analyzed on Cell Quest software (BD Biosciences, USA).

4.2.4.2 Assessment of mitochondrial oxidative stress by MitoSOX Red staining

After the desired treatment period, the cells were harvested by trypsinization and washed twice with PBS. The cells were then incubated with 5 µM MitoSOX Red dye for 10 minutes in incomplete medium at 37^{o}C in a CO_2 incubator followed by washing with PBS. The cells were then resuspended in HBSS and acquisition was performed on FL-2 channel of FACS Caliber flow cytometer and data analysis was performed on Cell Quest software.

4.2.5 Fluorescence microscopy

4.2.5.1 Immunofluorescence

Cells were grown on coverslips and at the end of treatment period, the cells were washed twice with PBS. For visualizing mitochondria, the cells were incubated with 100 nM MitoTracker Red CMXRos dye in incomplete medium (i.e. without serum) for 30 minutes followed by washing with PBS and then fixed with warm 4% (w/v) PFA for 15 minutes at RT. Following PBS washes, the cells were then permeabilized with 0.5% (v/v) Triton X-100 for 5 minutes at RT and again washed twice with PBS. Next, the cells fixed on coverslips were incubated with 5% (w/v) BSA in PBS as a blocking agent for 1 hour at RT. The cells were incubated with appropriate dilutions of the specific primary antibodies (diluted in PBS) either for 1 hour at RT or overnight at 4^{o}C by inverting the coverslips against a drop of the antibody on a parafilm (cell side facing down). Following the washing steps, the cells were incubated with secondary antibodies at suitable dilutions in dark at RT for 1 hour. In case of coimmunofluorescence (dual staining)

experiments, the two primary antibodies used were from two different host species. Incubation with first primary antibody was followed by its corresponding secondary antibody. An intermediate blocking step (which reduces the possibility of signal cross-talk between the two antibodies) follows incubation with a second primary antibody and then appropriate secondary antibody. The cell nuclei were stained with DAPI. Finally, the coverslips were mounted upside down against a drop of Vecta-shield fluorescence anti-quenching mounting medium on acid-washed glass slides and sealed with nailpolish. The slides were stored in dark at $4^{o}C$ until acquisition on a fluorescence microscope.

4.2.5.2 Live-cell imaging

The cells were grown in confocal dishes (live cell chambers). At the end of the desired treatment, the cells were gently washed twice with PBS and then stained with 100 nM MitoTracker Green FM, 100 nM MitoTracker Red CMXRos, 10 µM JC-1 dyes (for 30 minutes each) or 5 µM MitoSOX Red dye (for 10 minutes) in incomplete medium in CO_2 incubator. After incubation with the dyes, the cells were again gently washed with PBS twice and then overlaid with HBSS (without Phenol red). Alternatively, cells stably expressing pBABE-puro mCherry-EGFP-LC3B construct were carefully washed with PBS twice and covered with HBSS. The cells were then observed under a fluorescence confocal microscope. The staining principles for these dyes are explained in detail below.

A) MitoTracker dyes: The cell-permeant MitoTracker probes (which contain a mildly thiol-reactive chloromethyl moiety for labeling mitochondria) passively diffuse across the plasma membrane and accumulate in active mitochondria. Some of the MitoTracker dyes are sequestered and well retained by the mitochondria even after fixation (e.g. MitoTracker Red CMXRos) whereas certain others (such as MitoTracker Green FM) are easily washed out of cells

once the mitochondria experience a loss in membrane potential and therefore cannot be used where cell fixation is required.

B) MitoSOX Red mitochondrial superoxide indicator: MitoSOX Red mitochondrial superoxide indicator is a novel fluorogenic dye for highly selective detection of superoxide in the mitochondria of live cells. MitoSOX Red reagent is live-cell permeant and is rapidly and selectively targeted to the mitochondria. Once in the mitochondria, MitoSOX Red reagent is oxidized by superoxide and exhibits red fluorescence.

C) JC-1 Mitochondrial Membrane Potential Dye: JC-1 is a cationic cell permeable dye which selectively accumulates in the mitochondria and is used to study the mitochondrial membrane potential ($\Delta\Psi m$). Mitochondrial membrane polarization leads to the reversible formation of J-aggregates which accumulate in the mitochondria and causes a shift in the fluorescence emission from 530 nm (corresponding to JC-1 monomers which emit green fluorescence) to 590 nm (corresponding to J-aggregates which emit red-orange fluorescence). Upon a drop in the $\Delta\Psi m$, the J-aggregates dissociate into monomers and diffuse across the cytoplasm.

D) Tandem fluorescence based autophagy reporter assay: Cells were stably transfected with pBABE-puro mCherry-EGFP-LC3B plasmid construct in which mCherry and EGFP are cloned in a tandem arrangement upstream of human LC-3B sequence. The LC-3B protein is therefore expressed in these cells as a fusion protein exhibiting a yellow-orange signal (due to merge of Red and Green) under autophagy-inducing conditions. The EGFP protein is susceptible to the acidic interior of the lysosomes and therefore its fluorescence is quenched when an autophagosome fuses with a lysosome. On the other hand, mCherry is insensitive to acidic interior of the lysosomes and thus retains its fluorescence in an autophagosome as well as in a

fusion compartment (i.e. autolysosome). The cells were cultured in confocal dishes and images were acquired on a fluorescence confocal microscope.

4.2.6 Protein extraction and western blotting

4.2.6.1 Protein extraction from tissues

Human oral tissues were sectioned (10 µm sections) on a cryotome at -20^{o}C and resuspended in Proteo JET mammalian cell lysis reagent containing protease inhibitors and EDTA (EDTA chelates divalent metal ions which serve as cofactors for several proteases). The tissue sections were thoroughly mixed in the lysis buffer by pipetting up and down several times until the tube contents appear clear followed by incubation on ice for 30 minutes. The microcentrifuge tubes were then agitated vigorously on a vortex mixture for 2-3 minutes in a cold room to ensure proper tissue homogenization and placed back on ice for another 5 minutes. The tubes were then centrifuged at 14000 RPM on a cooling centrifuge for 15 minutes at 4^{o}C. The supernatant was then transferred to fresh tubes followed by protein estimation. These tissue lysates were stored at -80^{o}C until used for western blotting.

4.2.6.2 Protein extraction from cultured cells

Cells were harvested from culture plates by trypsinization and washed twice with PBS to remove any traces of culture medium. The cell pellets were resuspended in appropriate volumes of Proteo JET mammalian cell lysis reagent (containing protease inhibitors and EDTA) by vigorous pipeting and placed immediately on ice for 30 minutes. The microcentrifuge tubes were then vigorously agitated on a vortex for 2-3 minutes in a cold room and placed back on ice for another 5 minutes. The tubes were then centrifuged at 14000 RPM on a cooling centrifuge for 15 minutes at 4^{o}C. The supernatant was then transferred to fresh tubes followed by protein estimation. These whole cell lysates were stored at -80^{o}C until used for western blotting.

4.2.6.3 Protein estimation by Bradford assay

This assay is optimized for a microtitre plate. BSA standards were prepared from a BSA stock of 1mg/ml by serial dilutions and 5 µl of each of the serially diluted BSA standards was added to each well in triplicates along with a blank (i.e. no BSA). 1 µl of the cell lysate (i.e. unknown protein sample) was added to each well in triplicates. 100 µl Bradford reagent was added to each well and absorbance was recorded on a microplate reader at 595 nm. The mean absorbance of each standard (blank corrected) was used to draw a scatter plot and a straight line equation was deduced from the trendline. The absorbance of the unknown samples was extrapolated onto the graph and concentrations of the unknown samples were thus derived.

Table 5: Protein estimation by Bradford assay

BSA standard conc. (µg/µl)		**Total amount of protein (µg)**	
0 (Blank)	Add 5 µl of each of the serially diluted BSA standard to each well	0	Add 100 µl Bradford reagent and read at 595 nm on a microplate reader
0.0625		0.3125	
0.125		0.625	
0.25		1.25	
0.5		2.5	
1		5	

Sample preparation for SDS-PAGE: Equal amounts (20 µg) of protein samples were used across all experiments unless otherwise indicated. The desired amount (in microgram) of protein samples was mixed with equal volume (in microlitre) of 2X Laemmli buffer and the total volume

across all the samples was adjusted using 1X Laemmli buffer. These samples were then boiled on a water bath for 5 minutes before being loaded onto SDS PAGE.

4.2.6.4 SDS-Polyacrylamide gel electrophoresis (PAGE)

SDS-PAGE is used to resolve protein samples. The gels are formed by cross linking monomeric acrylamide with N, N'-methylene Bis-Acrylamide and pore size is controlled by modulating the concentrations of acrylamide and Bis-Acrylamide while preparing a gel. The size of these pores decreases as the Bis-Acrylamide: acrylamide ratio increases, therefore resolving gels of different percentage (8% to 15%) were used to properly resolve proteins of different molecular weights.

Table 6: Resolving gel composition

Components (for 10 ml)	**8%**	**10%**	**12%**	**15%**
De-ionized water	4.6 ml	4 ml	3.3 ml	2.3 ml
Acrylamide solution (30%,Acrylamide:Bis-acrylamide=29:1)	2.7 ml	3.3 ml	4 ml	5 ml
Tris (1.5M, pH 8.8)	2.5 ml	2.5 ml	2.5 ml	2.5 ml
SDS (10%)	0.1 ml	0.1 ml	0.1 ml	0.1 ml
APS (10%)	0.1 ml	0.1 ml	0.1 ml	0.1 ml
TEMED	0.008 ml	0.008 ml	0.008 ml	0.008 ml

Table 7: Stacking gel composition

Components (for 10 ml)	**Gel (5%)**
De-ionized water	6.8 ml
Acrylamide solution (30%, Acrylamide : Bis-acrylamide = 29:1)	1.7 ml
Tris (1.5M, pH 8.8)	1.25 ml
SDS (10%)	0.1 ml
APS (10%)	0.1 ml
TEMED	0.008 ml

The boiled protein samples were then loaded into individual wells of the stacking gel and electrophoresed at a constant current of 25 mA for 2-3 hours at RT depending on the resolution required. A pre-stained protein ladder was also run simultaneously in the gel along with protein samples, so as to determine the mobility and molecular weights of the various proteins in the gel.

4.2.6.5 Electroblotting

Proteins that were separated by SDS-PAGE were electro-transferred onto an adsorbent Polyvinylidene difluoride (PVDF) membrane to allow binding of antibodies. Briefly, wet electro-blotting was carried at 18 V overnight (16 hours) or 80 V for 3 hours. Transfer of proteins was visualized using Fast green and destained by washing with distilled water and destainer. Subsequently, the membrane blot was incubated in blocking solution (5% BSA prepared in 1X TBS) for 1 hour at RT on a slow rocker. The blots were then incubated with appropriate concentration of primary antibodies (diluted in 2.5% BSA in 1X TBST) overnight at 4°C or 1 hr at RT on a slow rocker. The blots were then washed three times (20 minutes each)

with 1X TBST followed by incubation with horseradish peroxidase (HRP) conjugated secondary antibody for 1 hour at RT on rocker. The blots were then washed and protein bands were visualized using ECL chemi-luminescence reagent according to the manufacturer's instructions. The X-ray films were developed on the automated developing machine. The protein bands on X-ray films were quantified by densitometric analysis by Image J software (NIH).

4.2.7 Coimmunoprecipitation

The cells were harvested by trypsinization and washed twice with cold PBS. The cells were lysed in ice cold EBC lysis buffer (containing protease inhibitors) with gentle agitation (by pipeting and on a tube rotator but not on a vortex) following incubation on ice for about 30 minutes. The cell lysates were then centrifuged at 14000 RPM in a cooling centrifuge for 15 minutes at 4^{o}C. The supernatants were transferred to fresh microcentrifuge tubes and protein estimation was performed by Bradford assay as described earlier. 1000 µg of total cell lysates were brought to a volume of 1000 µl with EBC lysis buffer and used for individual coimmunoprecipitation reaction. The cell lysates were then incubated with 30 µl preequilibrated Protein G-sepharose bead slurry (1:1 diluted with EBC lysis buffer) for 1 hour at 4^{o}C on a rocking platform followed by centrifugation in a cooling centrifuge at 2000 RPM at 4^{o}C for 2-3 minutes and the "precleared" supernatants were transferred to fresh tubes (a step called as "Preclearing" which eliminates the non-specific protein binding to the beads). These precleared supernatants were then incubated with specific primary antibodies at recommended concentrations overnight at 4^{o}C on a rocking platform. Next day, these cell lysates were incubated with 40 µl preequilibrated protein G-sepharose bead slurry for 3 hours at 4^{o}C on a rocking platform. The immunoprecipitates were recovered by gentle centrifugation at 2000 RPM and 4^{o}C for 5 minutes and were repeatedly washed with ice cold NETN buffer at least 5 times. Finally, the bead pellet

was boiled in 20 µl 2X Laemmli buffer. In the coimmunoprecipitation experiment, an isotype control antibody reaction was also included to rule out any non-specific protein binding to the antibody Fc region. Moreover, 5-10% input (relative to the total amount of initial protein lysates used for coimmunoprecipitation reaction) was included as loading control and to check for the efficiency of pull down.

4.2.8 Cycloheximide chase assay

To determine the half-life of MCL-1 protein, we performed cycloheximide (CHX) chase assay. Cells were exposed to 100 µg/ml cycloheximide and harvested after the indicated time points by trypsinization. Total protein was extracted from the cells followed by protein estimation and western blotting for MCL-1, BCL-2, BCL-XL and actin proteins as described earlier. The levels of individual proteins were determined by densitometric analysis using Image J software relative to actin which serves as a housekeeping control. A graph of percent remaining MCL-1 against time was plotted and half-life of MCL-1 was extrapolated.

4.2.9 Mitochondrial fractionation and cytochrome c release assay

Mitochondria were isolated from cultured cells by using Mitochondria Isolation Kit (Thermo Scientific) by reagent-based method as per manufacturer's instructions. Cell pellets were resuspended in 800 µl reagent A containing protease inhibitors and vortexed at medium speed for 5 seconds followed by incubation on ice for exactly 2 minutes. Then, 10 µl reagent B was added to it and vortexed at maximum speed for 5 seconds and again incubated on ice for 5 minutes. 800 µl reagent C containing protease inhibitors was then added to it and the tube was inverted several times. The tube was centrifuged at 700xg for 10 minutes at 4^{o}C and the supernatant was transferred to a fresh microcentrifuge tube and centrifuged at 12,000xg for 15 minutes at 4^{o}C. Supernatant represents cytosolic fraction whereas pellet contains isolated mitochondria. The

mitochondrial pellet was washed with 500 µl reagent C and again centrifuged at 12,000xg for 15 minutes at 4^{o}C. The supernatant was discarded and the mitochondrial pellet was maintained on ice before downstream processing.

4.2.10 RNA extraction, cDNA synthesis and real time PCR

4.2.10.1 RNA extraction

Total RNA was extracted from cultured cells by using TRIzol reagent which is a monophasic solution of phenol and guanidine isothiocyanate that facilitate the isolation of a variety of RNA species of different molecular sizes. Briefly, cell pellet was resuspended in 1 ml TRIzol reagent by pipeting the cells up and down several times. The cell suspension was then incubated at RT for 5 minutes to permit complete dissociation of the nucleoprotein complex followed by addition of 200 µl chloroform and shaking the tube vigorously for about 15 seconds. The microcentrifuge tubes were then centrifuged at 14000 RPM at 4^{o}C for 15 minutes. The upper aqueous phase which contains RNA was carefully transferred to a fresh microcentrifuge tube and 500 µl 100% Isopropanol was added to it and incubated at RT for 10 minutes followed by centrifugation at 14000 RPM and 4^{o}C for 15 minutes. The supernatant was discarded and RNA pellet was washed with 75% ethanol (w/v in DEPC water). The RNA pellet was air dried for 5-10 minutes, resuspended in 50 µl DEPC water and incubated at 55-60^{o}C. The RNA concentration was estimated by NanoDrop and RNA was stored at -80^{o}C until used for downstream applications.

4.2.10.2 Reverse transcription and cDNA synthesis

cDNA synthesis was performed by High Capacity cDNA Reverse Transcription Kit. The kit components were thawed on ice. The kit components when combined together prepares a 2X reverse transcription (RT) mastermix as below. An equal volume of RNA sample (i.e. 10 µl) was

added to this mastermix and mixed by pipeting up and down twice and placed on ice until ready to load onto the thermal cycler.

Table 8: Reaction mixture for a reverse transcription (RT) reaction

Component	**Volume (µl)**
10X RT Buffer	2
25X dNTP Mix (100 mM)	0.8
10X RT Random Primers	2
MultiScribe Reverse Transcriptase	1
RNase Inhibitor	1
Nuclease-free H_2O	3.2
Total per reaction	10

Table 9: Thermal cycler program for a reverse transcription (RT) reaction

Setting	**Step 1**	**Step 2**	**Step 3**	**Step 4**
Temperature (^oC)	25	37	85	4
Time (Mins.)	10	120	5	∞

4.2.10.3 Quantitative real time PCR

Real-time quantitative PCR was performed by using Power SYBR Green PCR Master Mix on Quant studio 12K Flex Real Time PCR machine (Applied Biosystems).

Table 10: The sequence of the primers used for SYBR Green Real Time PCR

Target gene	Primer sequence	Amplicon size
MCL-1	Forward: 5'-AAGAGGCTGGGATGGGTTTG-3'	150 bp
	Reverse: 5'-CAGCAGCACATTCCTGATGC-3'	
BNIP3	Forward: 5'-CCGGGATGCAGGAGGAGAG-3'	100 bp
	Reverse: 5'-TTATAAATAGAAACCGAGGCTGGAAC-3'	
GAPDH	Forward: 5'-CTCTGCTCCTCCTGTTCGAC-3'	130 bp
	Reverse: 5'-GCGCCCAATACGACCAAATC-3'	

Ct values were determined for MCL-1, BNIP3 and GAPDH by absolute quantitation. The expression of MCL-1 and BNIP3 was represented as $2^{-\Delta Ct}$ relative to GAPDH as housekeeping control.

4.2.11 Immunohistochemistry (IHC)

Ethics approval: The study was reviewed and duly approved by the Institutional Ethics committee (IEC) of the Tata Memorial Centre (TMC) (Project no. 211). Informed consent was obtained from individuals participating in the study.

The tissues were fixed in 10% buffered formalin (v/v in PBS) overnight followed by mounting in Paraffin blocks. The tissue sections (~10 µm) were obtained on silane-coated glass slides. The tissue sections were deparaffinised by passing through several grades of xylene and alcohol before being subjected to blocking of endogenous peroxidase by methanol and H_2O_2 in dark for about 30 minutes at RT. The tissue sections were subsequently washed with PBS and epitope retrieval was performed in Sodium Citrate buffer by microwaving for 5 minutes. The slides were

then allowed to cool and again washed with PBS. The tissue sections were incubated with horse normal serum (for primary antibodies raised in mouse) or goat normal serum (for primary antibodies raised in rabbit) as a blocking agent for 1 hour at RT in a humidified chamber. The blocking agent was then carefully drained off the tissue sections without allowing them to dry. The tissue sections were then incubated with suitably diluted specific primary antibodies either overnight at 4^{o}C or for 1 hour at RT in a humidified chamber. Next day, the tissue sections were washed with 0.1% PBST for 10 minutes followed by washing with PBS. Subsequently, the tissue sections were incubated with appropriately diluted biotin-conjugated secondary antibodies for 1 hour at RT in a humidified chamber. The slides were again washed with PBST and PBS and the tissue sections were incubated with Avidin-Biotin complex (ABC) for 1 hour at RT in a humidified chamber. Following washing steps, the tissue sections were stained with freshly prepared chromogen DAB (3,3′-Diaminobenzidine) and H_2O_2 for sufficient time so as to observe specific staining. The staining was terminated by immersing the slides in deionized water. The tissue sections were next counterstained with Hematoxyline for 30 seconds to 1 minute followed by immersing the slides in tap water. Finally, the tissue sections were again dehydrated by passing through several grades of alcohol and xylene and eventually mounted using a DPX mountant and air dried. The immunostaining was evaluated by counting the percentage of cells expressing the proteins in at least 10-15 different microscopic fields and expressed semiquantitatively as: 0: negative, 1: weak, 2: moderate, 3: intense. The percentage expression was also categorized as: 0: 0-10%, 1: 11-30%, 2: 31-50%, 3: 51-100%. The protein expression was either represented as the percent positivity or as “H score” which is determined by multiplying the staining intensity scores by the percentage expression scores on a scale of 0-9.

4.2.12 *In vivo* studies

Ethics statement: All the experiments related to small animals described throughout this study were conducted in accordance with the ethical standards and according to the declaration of Helsinki, and national and international guidelines. All protocols for the animal studies were reviewed and approved by the Institutional Animal Ethics Committee (IAEC) of Tata Memorial Centre (TMC)-Advanced Centre for Treatment, Research and Education in Cancer (ACTREC) constituted under the guidelines of the Committee for the Purpose of Control and Supervision of Experiments on Animals (CPCSEA), Government of India (Project no. 14/2014).

To assess the *in vivo* antitumor activity of WP1130, we employed xenograft mouse models as described earlier [211, 212]. Briefly, 6-8 weeks old female BALB/C Nude mice were subcutaneously injected in the hind flank with $1X10^6$ cells of SCC029B cell line resuspended in 100 µl incomplete IMDM. The animals were then randomized into 2 groups (Vehicle control and 20mg/kg WP1130) each containing 6 animals. Palpable subcutaneous tumors were observed about 21 days post cell inoculation. WP1130 was formulated as DMSO:Polyethylene Glycol 300 in the proportion of 1:1. The formulated drug was administered to the animals through intraperitoneal injection every alternate day for two consecutive weeks. On the contrary, animals in the vehicle control group were injected with the DMSO:Polyethylene Glycol 300 mixture only. The tumor volume measurements were done using a vernier caliper by the formula: $Length(mm)*[Width(mm)]^2/2$. Tumor volume and weight of the animals was monitored every alternate day for 16-18 days post termination of drug treatment. The animals were sacrificed by CO_2 chamber asphyxiation and vital organs including the tumors were collected. The tumors were sectioned and subjected to IHC for cleaved caspase-3 and MCL-1 proteins. The percentage of cells undergoing apoptosis was determined by TUNEL assay.

We assessed the *in vivo* antitumor efficacy of Obatoclax in xenograft mouse models as described earlier [90]. 6–8 weeks old female BALB/C nude mice were subcutaneously injected with 1×10^6 cells of SCC029B cell line in 100 µl incomplete IMDM medium. The animals were then randomized into 4 groups, containing 6 animals each. Palpable tumors were observed about 21 days post cell inoculation. Each group of animals were intravenously injected (through lateral tail vein) with different doses of Obatoclax (cumulative doses of 1.25 mg/kg, 2.5 mg/kg, 5 mg/kg and a vehicle control group) evenly distributed over a period of consecutive 5 days (i.e. 5 injections). The drug was formulated at the indicated concentrations in 9.6% PEG, 0.4% Tween 20 and 5% dextrose. The tumor volume measurements were done using a vernier caliper by the formula: Length(mm)*[Width(mm)]^2/2. For assessment of any drug associated toxicity, weight of the animals was monitored every alternate day.

4.2.13 TUNEL assay

The percentage of cells undergoing apoptosis in the tumors of the animals was determined by TUNEL assay using *In situ* Apoptosis Detection kit (Takara Bio Inc., Japan) according to the manufacturer's instructions. Briefly, the formalin-fixed paraffin embedded tissue sections were deparaffinized by passing through several grades of xylene and alcohol, followed by proteinase K-mediated epitope retrieval and blocking of endogenous peroxidase. The tissue sections were then incubated with labeling reaction mixture containing TdT enzyme for 90 minutes at 37^{o}C followed by washing with PBS. Finally, the tissue sections were exposed to anti-FITC HRP conjugate for 30 minutes at 37^{o}C and then washed with PBS. The tissue sections were stained with DAB chromogen and counterstained with hematoxyline. The percentage of cells showing specific nuclear brown TUNEL staining was scored as described earlier.

4.2.14 Coimmunoprecipitation coupled with mass spectrometry for identification of MCL-1-interacting proteins

20 mg of total cell lysate of AW8507 cells was subjected to coimmunoprecipitation with anti-MCL-1 antibody as described earlier. As a control reaction, the cell lysate of MCL-1 knockdown AW8507 cells (MCL-1 was knockdown with a pTRIPZ shMCL-1 construct) was also included in the experiment. The immunoprecipitates were resolved on a gradient PAGE (8%-15%) gel and the gel was silver stained. The differential protein bands between the two lanes were compared and the bands specific to MCL-1 immunoprecipitation were excised and subjected to peptide extraction followed by identification by MALDI-MS.

4.2.14.1 Silver staining of the gels

The gel was immersed in fixing solution for 1 hour with gentle agitation and then washed thrice with 50% ethanol for 20 minutes each with continuous shaking. The gel was then treated with pretreatment solution for exactly 1 minute and washed with distilled water for 20 seconds. The gel was soaked in 0.2% $AgNO_3$ solution for 20 minutes and then again washed with distilled water thrice for 20 seconds each. The gel was then soaked in developing solution with gentle agitation till clear protein bands of suitable intensity without background staining are visible. Finally, the gel was washed with distilled water and immersed in fixing solution to stop further development. The silver stained gel was immersed in 10% acetic acid and scanned on the calibrated densitometer GS-800 (Bio-Rad) in an auto scale mode.

4.2.14.2 Peptide extraction from the gel bands

The differential protein bands were excised using a sterile scalpel blade and stored in individual microcentrifuge tubes. Throughout the procedure of gel electrophoresis, peptide extraction and identification, nitrile gloves were worn (to avoid keratin contamination) and unautoclaved pipette

tips and microcentrifuge tubes were used (to avoid interference of polymer contamination during peptide identification). In order to identify and characterize the proteins by MALDI, the gel bands were subjected to trypsin digestion and peptide extraction as reported by Shevchenko et al [213]. The excised gel bands can be stored in 10% acetic acid at 4^{o}C for about 1 month. The gel pieces were washed thrice with fresh distilled water by placing the tubes on a vortex at a moderate speed for 10 minutes each. The gel pieces were destained by immersing in destaining solution for 15 minutes at RT on vortex at moderate speed. The gel pieces were next immersed in gel shrinking solution twice for 10 minutes each on a moderate speed vortex. The gel shrinking solution was removed and 100% Acetonitrile was added to the gel pieces and kept on a table top. The Acetonitrile was completely removed and the gel pieces were vacuum dried in a speedvac at 37^{o}C for about 15 minutes with tube caps open to completely remove the acetonitrile. The gel now appears as a dried mass at the bottom of the tube. Add sufficient volume of Mass Spectrometry grade Trypsin (10 ng/µl w/v in 25 mM Ammonium Bicarbonate) so as to cover the gel piece and incubate at 37^{o}C overnight with gentle agitation. The dried gel now absorbs trypsin and swells. About 40 µl peptide extraction buffer was added to each gel piece and incubated at RT for 30 minutes. The gel pieces again starts to shrink and cleaved peptides comes out. This step was repeated once more and the peptides were transferred to a fresh microcentrifuge tube. These peptides were then subjected to vacuum drying till the tube appears empty. The tubes were then stored at -20^{o}C until the peptides are to be reconstituted for MALDI MS analysis. The peptides were resuspended in reconstitution solution and vortexed for 5 minutes at a moderate speed followed by a centrifugation step to settle down the peptides at the bottom of the tube.

4.2.14.3 Mass spectrometer instrument and calibration

The reconstituted peptides were mixed in equal volume with the matrix (2 µl each) and loaded onto 384 spot plate of MALDI TOF/TOF. Mass calibration was carried out using peptide mixture of five known peptides, spanning mass range of 757-3147 m/z and error was kept to less than 10 ppm. Accelerating voltage of 25 kV was applied to the first TOF tube. The MS data was acquired in an automated manner using a solid state NdYAG laser at 337 nm. The resulting MS data was analysed using Flex analysis-3.0 (Brucker Daltonik, Germany) software and was acquired using Biotools software (Brucker Daltonik, Germany). The MS peak list of the chosen peptides was searched against SwissProt database, using MASCOT search engine for protein ID with precursor tolerance of 100-200 ppm for MS analysis.

4.2.15 Transmission Electron Microscopy (TEM)

The cells were harvested by trypsinization and washed twice with sterile cold PBS without phenol red. The cells were then fixed with 3% (w/v) Glutaraldehyde at 4^{o}C for 2 hours followed by washing twice with 0.1 M Sodium Cacodylate buffer (pH 7.4). The cell pellets were then fixed in 1% (w/v) Osmium tetroxide for 1 hour at 4^{o}C in dark, subjected to dehydration by passing through different grades of alcohol and then embedded with Araldite resin. Ultrathin sections (~60-70 nm) of the cells fixed within the araldite resin were cut on an ultramicrotome (Leica, Germany) and mounted on formvar coated/uncoated copper grids. These sections were stained with 10% Uranyl acetate solution and counterstained with lead citrate. Electron micrographs were captured on a Jeol 100-CXII electron microscope (Jeol, UK) using Olympus camera and iTEM software.

4.2.16 Statistical analysis

Two data sets in an experiment were compared by student's t-test and one-way ANOVA using Graphpad prism software (version 5). The data was represented as mean ± standard error or standard deviation. The difference between mean was considered statistically significant when p value was less than 0.05.

Disease free survival (DFS) was considered as the primary end point for the survival analysis of oral cancer patients. DFS was calculated as the time from the date of the first treatment of the patient to the date of the event (either loco-regional and/or distant metastasis). For analysis of protein expression, median of protein expression was taken as a cut-off to dichotomise the data. The values above the median were considered as high expression and those below the median were considered low expression. The Kaplan–Meier method of Log rank test was used to compare the survival rates between the categories of protein expression.

Chapter 5

Results

5.1 To assess the role of MCL-1-interacting partners that may contribute to its stability in human oral cancers.

5.1.1 To determine the basal levels of BCL-2 family proteins in human oral cancer cell lines

The basal levels of important antiapoptotic (BCL-2, BCL-XL, MCL-1) and proapoptotic (BAK, BAX) members of the BCL-2 family were assessed by western blotting in DOK, AW8507, AW13516 and SCC029B cell lines. DOK expressed low levels of MCL-1 protein as compared to that of AW8507, AW13516 and SCC029B cell lines. Notably, all the cell lines expressed relatively higher levels of at least two of the three predominant antiapoptotic BCL-2 family proteins.

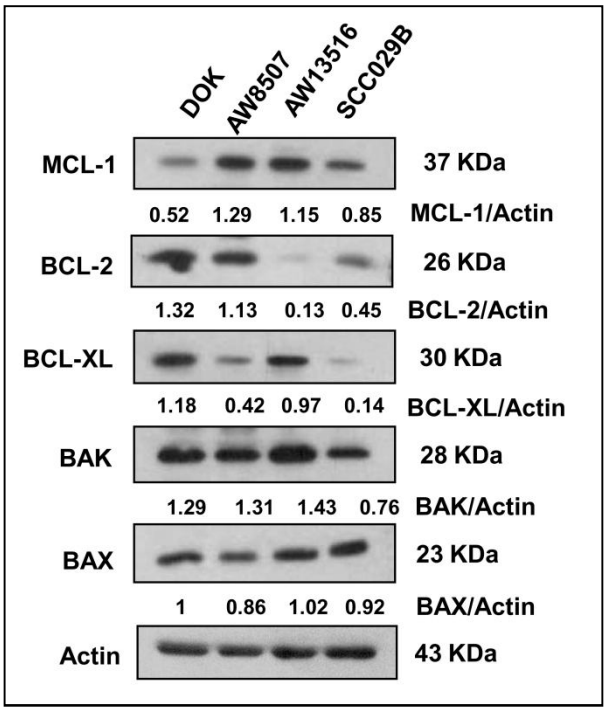

Figure 12: Basal levels of BCL-2 family proteins. Basal level expression of important pro and antiapoptotic BCL-2 family proteins in human oral cancer cells. Actin served as loading control. The relative expression of individual proteins with respect to actin was determined by densitometric analysis.

5.1.2 MCL-1 is rapidly degraded by the ubiquitin-proteasomal pathway

To identify the pathway by which MCL-1 degradation occurs in OSCC cells, AW8507 cells were treated with Cycloheximide (CHX, which blocks *de novo* protein synthesis), Chloroquine (CQ, which inhibits lysosomal activity), Z-VAD-FMK (a pan-caspase inhibitor), E-64d (a cysteine protease inhibitor), MG132 (a proteasome inhibitor) or vehicle control (0.001% DMSO) for 6 hours and the levels of MCL-1 protein were assessed by western blotting. CHX treatment completely abolished the expression of MCL-1, leading to a significant decrease in MCL-1 protein levels whereas, MG132 treatment led to a significant increase in MCL-1 protein levels (Figure 13 A). To further establish that proteasome-mediated destruction is primarily responsible for degradation of MCL-1 protein, AW8507 and SCC029B cells were treated with proteasome inhibitor MG132 and a specific eukaryotic 26S proteasome inhibitor Velcade (Bortezomib). Treatment with MG132 or Velcade leads to a significant increase in MCL-1 protein levels in a dose and time-dependent manner with no changes in the levels of either BCL-2 or BCL-XL proteins (Figure 13 B). When the lysates of MG132 treated AW8507 cells were subjected to immunoprecipitation with anti-MCL-1 antibody, it revealed that the observed accumulation of MCL-1 protein corresponds to its extensive polyubiquitination (Figure 13 C).

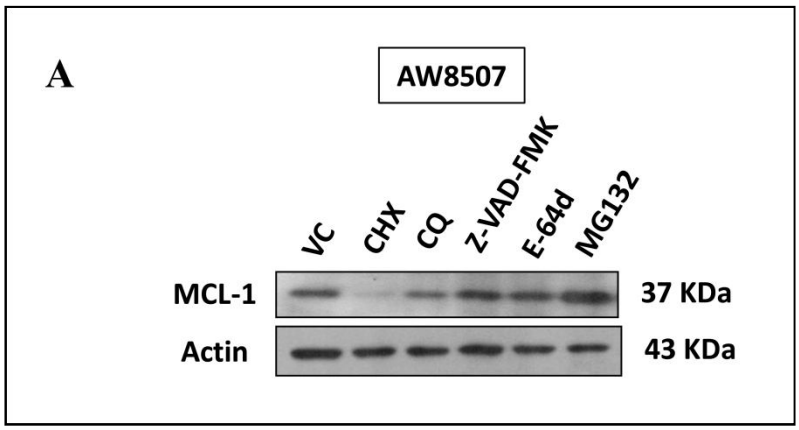

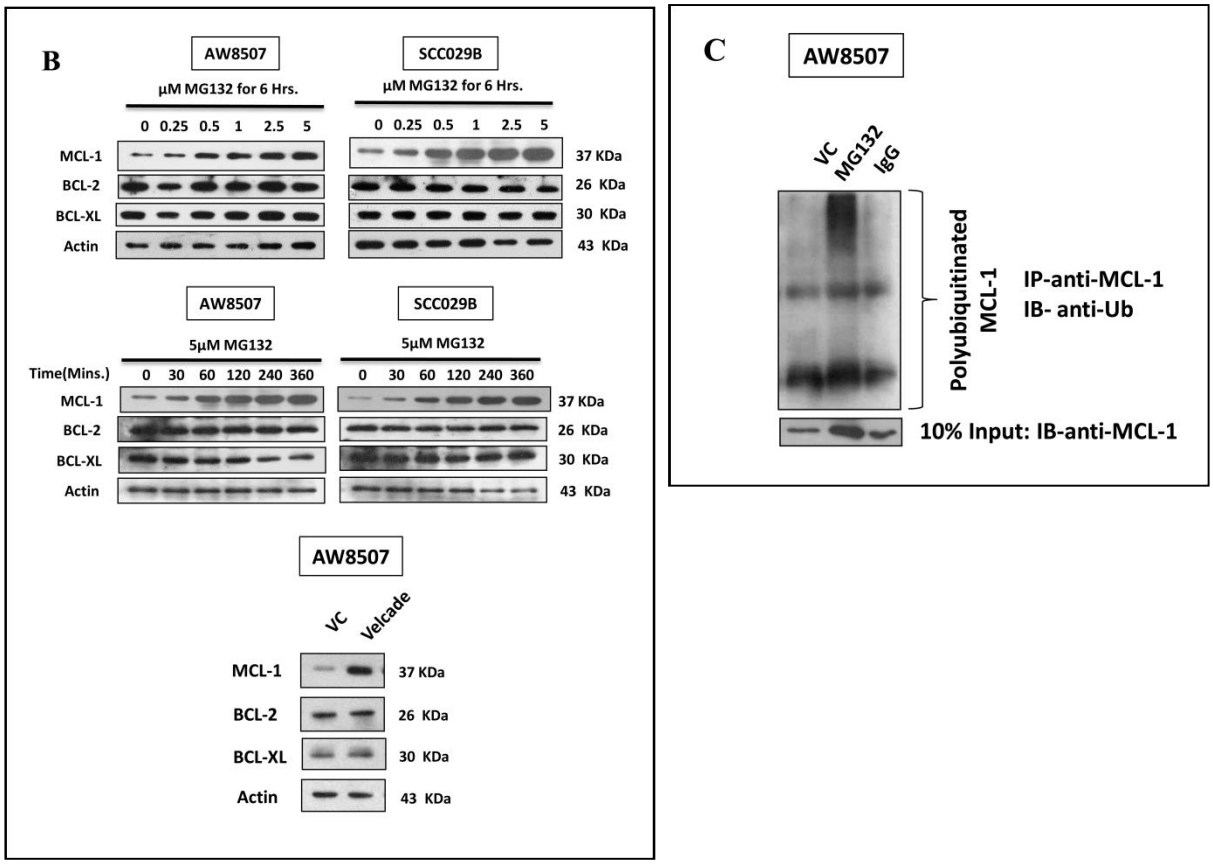

Figure 13: Ubiquitin-dependent proteasomal degradation is the major pathway for MCL-1 turnover. A) AW8507 cells were treated with Cycloheximide (100 µg/ml), Chloroquine (50 µg/ml), Z-VAD-FMK (25 µM), E-64d (10 µg/ml), MG132 (5 µM) or as vehicle control (VC) for 6 hours and the cell lysates were subjected to western blotting for the detection of MCL-1 and actin proteins. **B)** AW8507 and SCC029B cell lines were treated with increasing doses of proteasome inhibitors MG132 or 500 nM Velcade (Bortezomib) for 6 hours or with 5 µM MG132 for the indicated time points. The cell lysates were subjected to western blotting for the detection of MCL-1, BCL-2, BCL-XL and actin proteins. MG132 treatment leads to a dose and time-dependent increase in the levels of MCL-1 but not BCL-2 and BCL-XL. **C)** Anti-MCL-1 immunoprecipitation of MG132 treated lysate of AW8507 cells reveals that this accumulated MCL-1 corresponds to its polyubiquitinated form.

5.1.3 MCL-1 protein has a rapid rate of turnover and a short half-life as compared to BCL-2 and BCL-XL proteins

To determine the half-life of MCL-1 protein in oral cancer cell lines, we performed cycloheximide (CHX) chase assay as described in the methods section. The MCL-1 protein levels diminished completely by about 5 hours after treatment with CHX. However, the levels of BCL-2 and BCL-XL proteins were sustained even upto 12 hours post treatment with CHX. Densitometric analysis revealed that MCL-1 protein has a mean half-life of 150-180 minutes in OSCC cell lines as opposed to the reported half-life of ~60-90 minutes in normal epithelial cells, which indicates its increased stability in oral cancer cells (Figure 14).

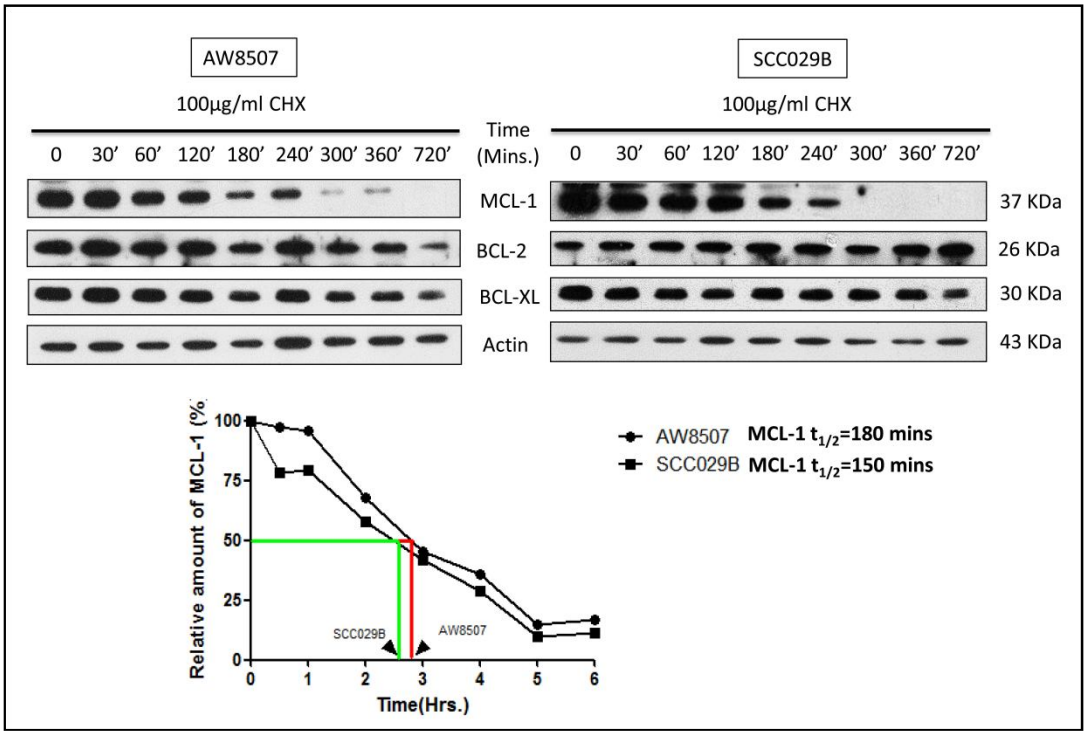

Figure 14: Determination of MCL-1 half-life by cycloheximide chase assay. Cycloheximide chase assay revealed that MCL-1 has a relatively short half-life ($t_{1/2}$=150-180 mins.) as compared to BCL-2 and BCL-XL proteins. The data is represented as mean of 3 independent experiments.

To investigate the role of USP9X in stabilization of MCL-1 protein in oral cancers

5.1.4. MCL-1 protein expression correlates with USP9X expression in oral cell lines and oral tissues

Basal level expression analysis by western blotting revealed that the expression of MCL-1 protein correlates significantly (*p<0.05, r=0.9593) with that of USP9X in OSCC cell lines (Figure 15 A). We also observed high expression of MCL-1 and USP9X proteins in oral tumor samples as compared to the corresponding normal tissues (Figure 15 B).

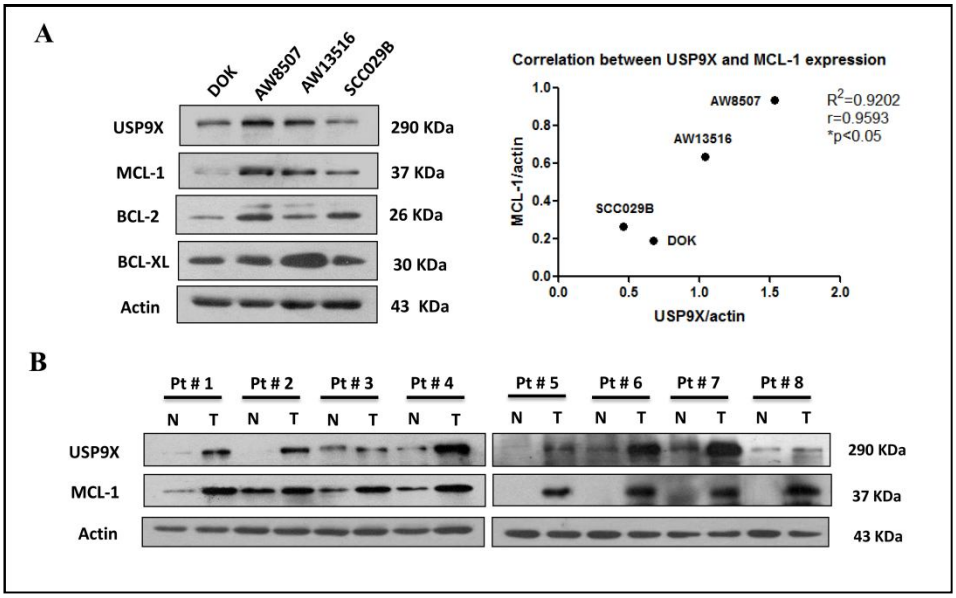

Figure 15: USP9X expression correlates with MCL-1 expression. A) The expression of MCL-1, BCL-2, BCL-XL and USP9X proteins was assessed in four oral cancer cell lines by western blotting. The expression of MCL-1 and USP9X was normalized with actin. The mean normalized expression of MCL-1 and USP9X proteins correlated significantly (r=0.9593, *p<0.05). The data is mean of three independent experiments. **B)** The expression of MCL-1 and USP9X proteins was determined by western blotting in paired normal (N, adjacent normal)-tumor (T) oral tissues of eight representative oral cancer patients. Actin served as the loading control.

5.1.5 USP9X interacts with MCL-1

To investigate the contribution of USP9X in stabilization of MCL-1 protein, we first evaluated their interaction by coimmunofluorescence and coimmunoprecipitation assays which demonstrated their direct physical association (Figure 16 A and B).

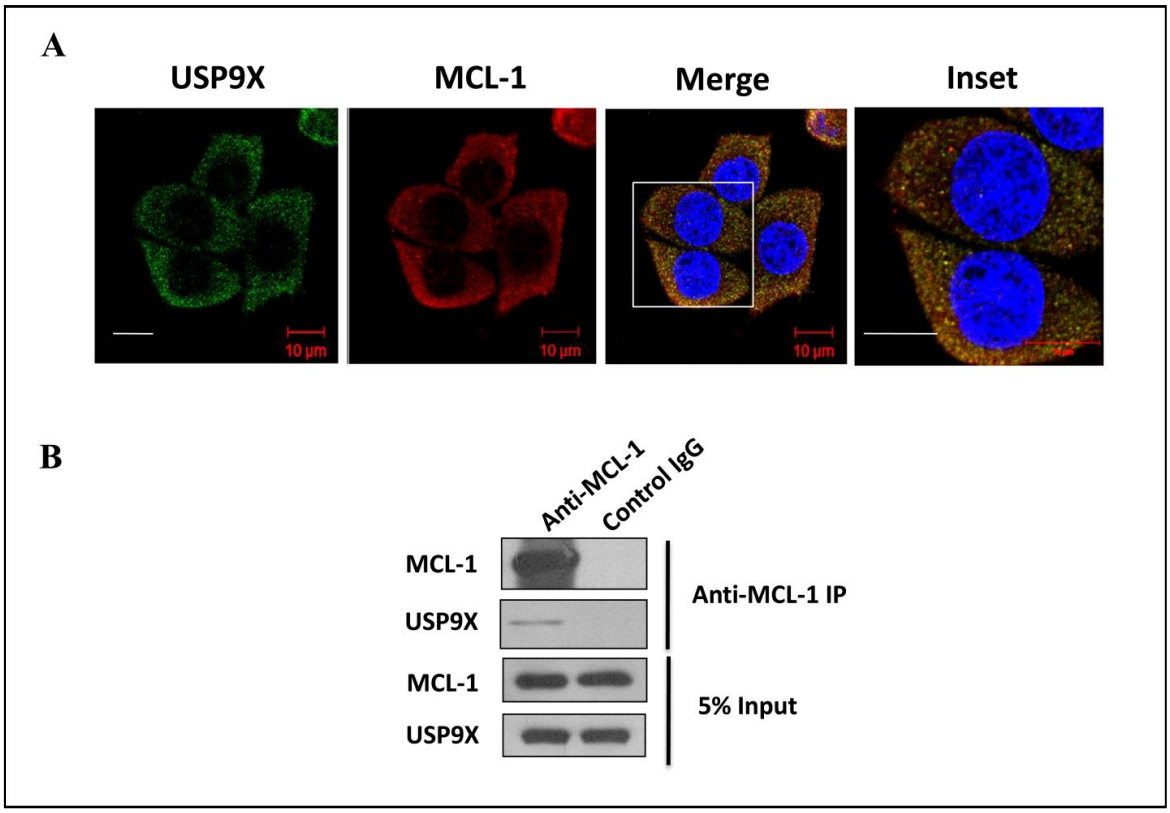

Figure 16: USP9X interacts with MCL-1. A) AW8507 cells were stained with USP9X (Green) and MCL-1 (Red) antibodies. A merge signal (Orange/Yellow) represents colocalization and thus potential interaction between the two proteins. **B)** The lysates of AW8507 cells were subjected to coimmunoprecipitation with anti-MCL-1 antibody. Presence of USP9X in the immunoprecipitate fraction confirms a direct interaction between MCL-1 and USP9X proteins.

5.1.6 Standardization of siRNA transfection and siRNA-mediated USP9X downregulation

For standardization of siRNA transfection, AW8507 cells were transfected with increasing concentrations of USP9X siRNA, Control (Non-targeting/Scrambled) siRNA and siGLO (to assess the transfection efficiency) as discussed in the methods section (Figure 17 A). We observed a significant downregulation of USP9X when the cells were transfected with USP9X siRNA as compared to Control siRNA (Figure 17 B).

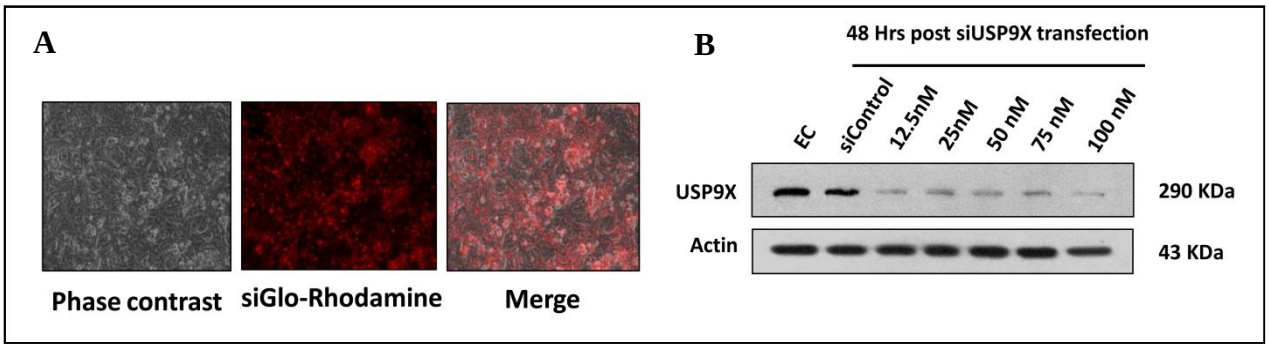

Figure 17: Standardization of siRNA transfection. A) AW8507 cells were transfected with 25 nM siGLO. 24 hours post transfection, the cells were observed under a florescence microscope to assess the efficiency of transfection. We reproducibly obtained a transfection efficiency of 90-95% with OSCC cells. **B)** AW8507 cells were transfected with increasing concentrations of USP9X siRNA (siUSP9X), 50 nM control siRNA (siControl) or left untransfected (Experimental control-EC). The cells were harvested after 48 hours and the cell lysates were subjected to western blotting for the detection of USP9X and actin proteins. The images and blots are representative of three independent experiments.

5.1.7 USP9X downregulation lowers MCL-1 protein levels without affecting transcript expression

USP9X downregulation in AW8507 and SCC029B cells rendered a significant (***p<0.0001) decrease in the levels of MCL-1 protein as compared to siControl transfected cells. There was neither a significant change in the levels of BCL-2 nor BCL-XL proteins (Figure 18 A). MCL-1 transcript levels did not show significant alterations upon siRNA-mediated USP9X depletion (Figure 18 B). Decrease in the expression of MCL-1 protein upon USP9X knockdown was also evident by immunofluorescence microscopy (Figure 18 C).

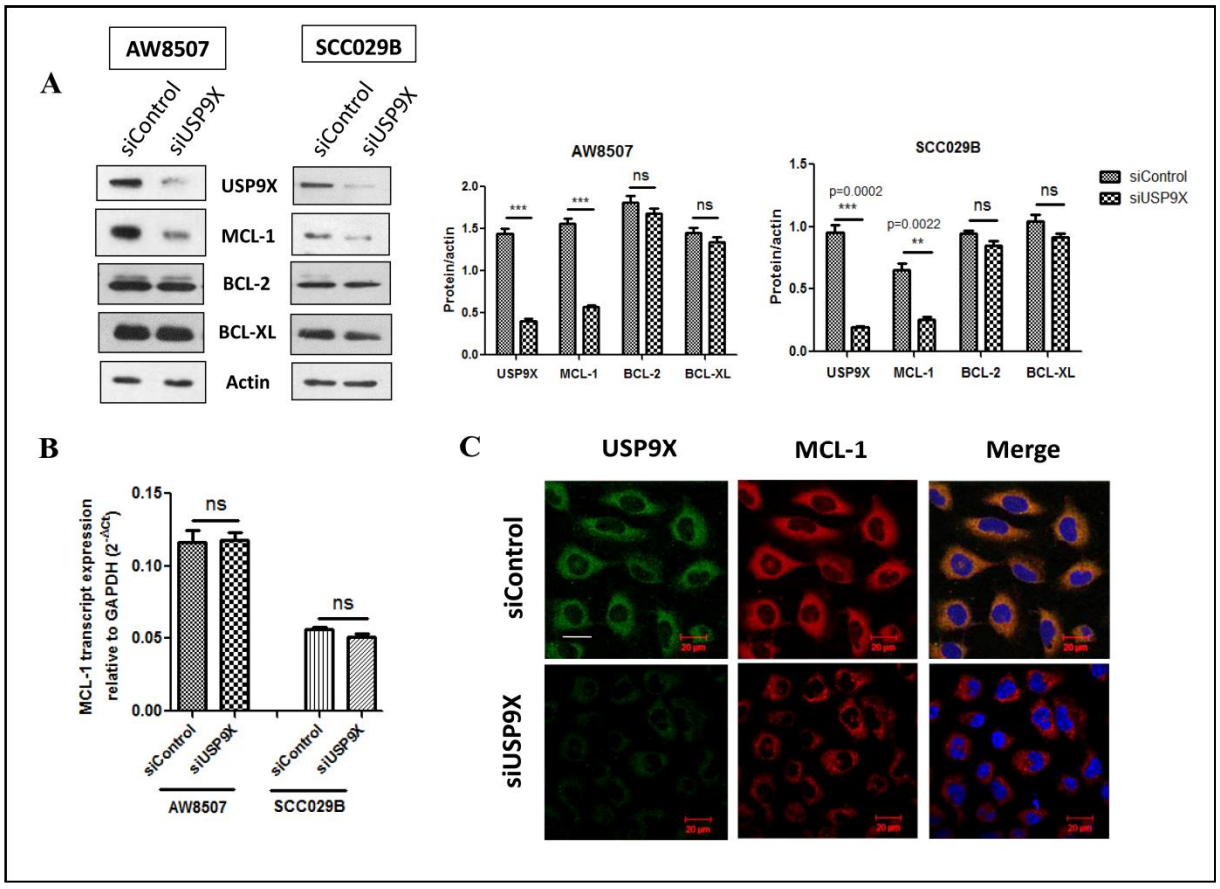

Figure 18: USP9X downregulation lowers MCL-1 protein levels. AW8507 and SCC029B cells were transfected with 50 nM USP9X siRNA (siUSP9X) and 50 nM Control siRNA (siControl). The cells were harvested 48 hours post transfection. **A)** The cell lysates were

subjected to western blotting for the detection of MCL-1, BCL-2, BCL-XL and actin proteins. USP9X downregulation significantly (***p<0.0001) lowered MCL-1 protein levels without significant changes in the levels of either BCL-2 or BCL-XL. The blots are representative of three independent experiments (***p<0.0001, **p<0.001, ns: not significant). **B)** Downregulation of USP9X did not alter the levels of MCL-1 transcript. **C)** AW8507 cells were transfected with indicated siRNA. 48 hours post siRNA transfection, the cells were immunostained for MCL-1 and USP9X (Scale bar: 20 µm).

5.1.8 USP9X downregulation lowers MCL-1 protein levels by increasing its turnover

Cycloheximide chase assay was performed to assess the contribution of USP9X in regulating the turnover rate of MCL-1 protein. As compared to the cells transfected with siControl, downregulation of USP9X by siUSP9X significantly (***p<0.0001) increased the turnover rate of MCL-1 protein in AW8507 cells. It was evident from a significant difference between the mean half-life of MCL-1 protein in cells transfected with siControl (siControl MCL-1 $t_{1/2}$=3 Hours) versus siUSP9X transfected cells (siUSP9X MCL-1 $t_{1/2}$=1.28 Hours) (Figure 19 A). It was associated with an overall increase in the polyubiquitination of MCL-1 protein (Figure 19 B). These observations indicate that USP9X plays an important role in the stabilization of MCL-1 protein by preventing its polyubiquitination.

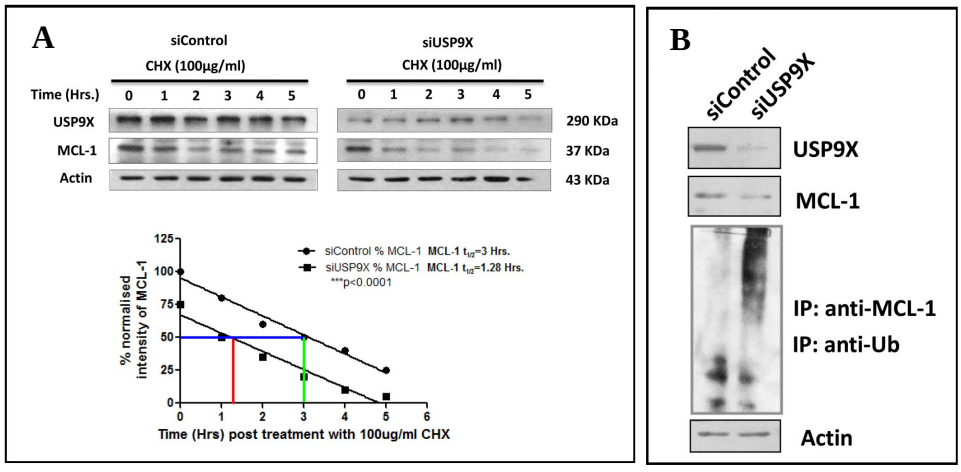

Figure 19: USP9X knockdown increases turnover of MCL-1 protein. A) AW8507 cells were transfected with 50 nM each of siControl or siUSP9X. 48 hours post transfection, the cells were treated with 100 µg/ml CHX and the cells were harvested after the indicated time points. The cell lysates were subjected to western blotting for the detection of USP9X, MCL-1 and actin proteins. The relative expression of MCL-1 protein was determined by densitometric analysis. The data is represented as mean of three independent experiments. **B)** AW8507 cells were transfected with either Control siRNA (siControl) or USP9X siRNA (siUSP9X). 48 hours post transfection, the whole cell lysates were subjected to immunoprecipitation with anti-MCL-1 antibody followed by western blotting for the detection of USP9X, MCL-1, Ubiquitin and actin proteins. The western blots are representative of three independent experiments.

5.1.9 USP9X knockdown increases the radiosensitivity of OSCC cells

Earlier studies from our lab has shown that MCL-1 is a critical radioresistance associated protein in OSCC cells [25]. Further, USP9X overexpression has been demonstrated to be associated with radioresistance through increased stabilization of MCL-1 protein [214]. We therefore evaluated the contribution of deubiquitinase USP9X in conferring radioresistance to OSCC cells. siRNA mediated downregulation of USP9X led to a significant (**p<0.001) reduction in the clonogenic viability of OSCC cells (Figure 20). It is indicative of an important role of USP9X in contributing radioresistance in OSCC cells, possibly by mediating stabilization of MCL-1 protein.

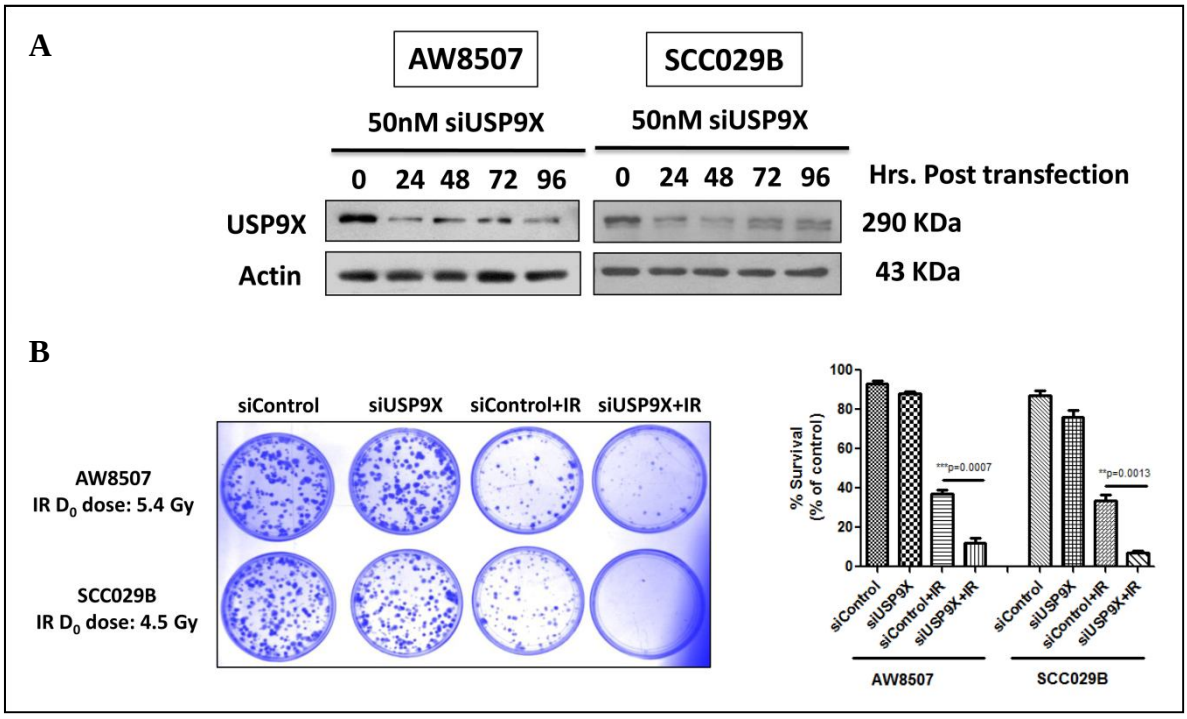

Figure 20: USP9X contributes to radioresistance. A) AW8507 and SCC029B cells were transfected with 50 nM siUSP9X and the cells were harvested at the indicated time points post transfection followed by western blotting for the detection of USP9X and actin proteins. Blots are representative of three independent experiments. **B)** AW8507 and SCC029B cells were

transfected with 50 nM siUSP9X. 48 hours post transfection, the cells were harvested, seeded in 35 mm plates and allowed to grow overnight. Next day, the cells were irradiated with the indicated doses of ionizing radiation (AW8507 cells: D_0 dose = 5.4 Gy, SCC029B cells: D_0 dose = 4.5 Gy; D_0 dose: A dose of radiation which allows survival of 37% cell population) and allowed to grow for further 8-10 days till visible colonies appear. The colonies were scored as described earlier. The image is representative of three experiments. The data is represented as mean ± SEM of three independent experiments.

5.1.10 Deubiquitinase inhibitor WP1130 (Degrasyn) potently induces apoptosis in OSCC cells by causing rapid degradation of MCL-1 protein

We next evaluated the potency of WP1130, a small molecule deubiquitinase inhibitor (Figure 21 A) in OSCC cell lines. WP1130 induced a dose-dependent decrease in the viability of OSCC cells as demonstrated by MTT and clonogenic assays (Figure 21 B, C). WP1130 potently induced apoptotic cell death in OSCC cells evident by PARP and caspase-3 cleavage, flow cytometry and characteristic nuclear fragmentation (Figure 21 D, E, F, G). Notably, the cell death induced by WP1130 in OSCC cells was associated with a rapid depletion of MCL-1 protein levels possibly accounting for its degradation (Figure 21 D).

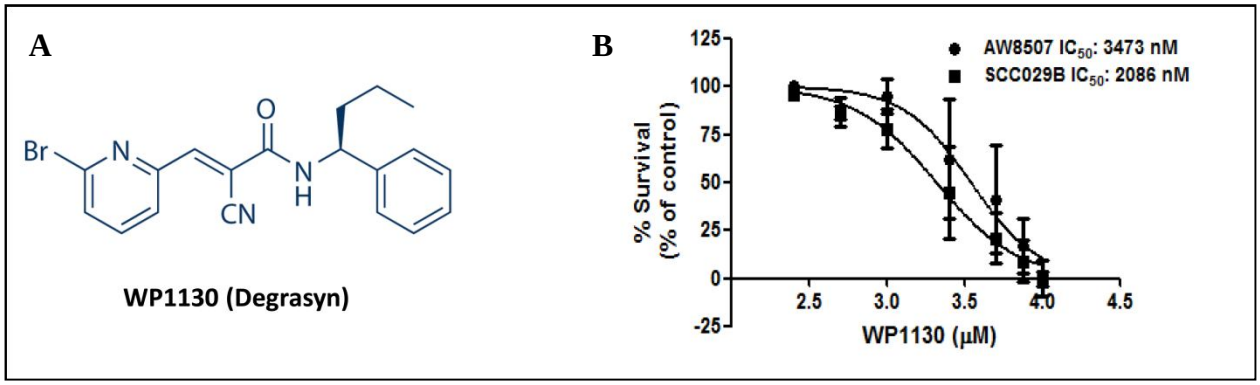

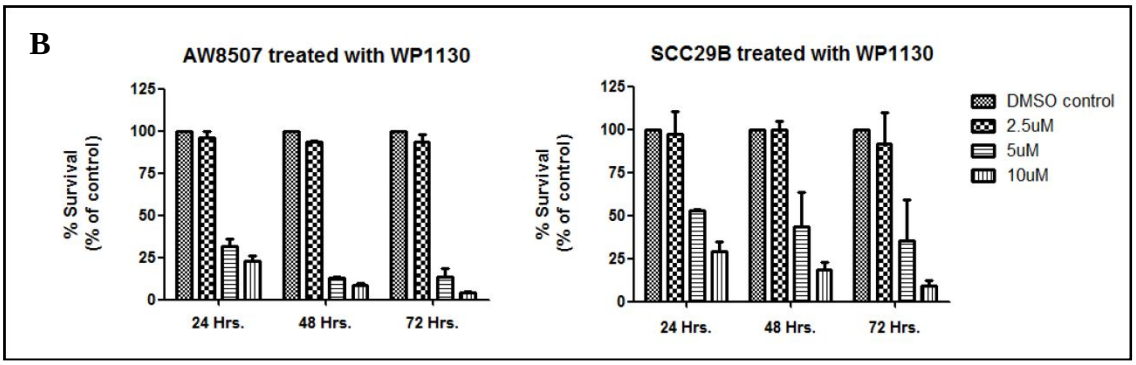
B
AW8507 treated with WP1130
SCC29B treated with WP1130
% Survival (% of control)
125
100
75
50
25
0
24 Hrs.
48 Hrs.
72 Hrs.
DMSO control
2.5uM
5uM
10uM

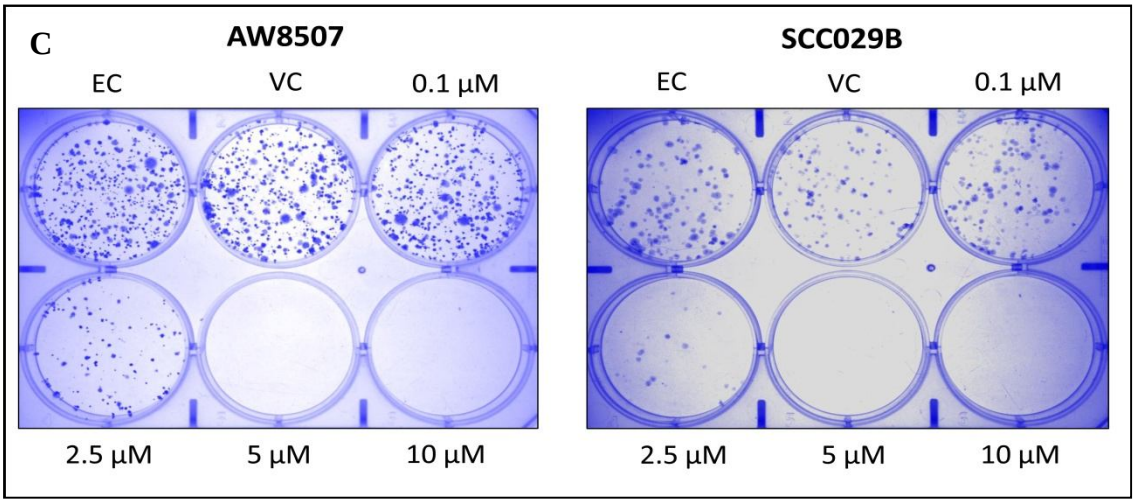
C
AW8507
SCC029B
EC
VC
0.1 µM
2.5 µM
5 µM
10 µM

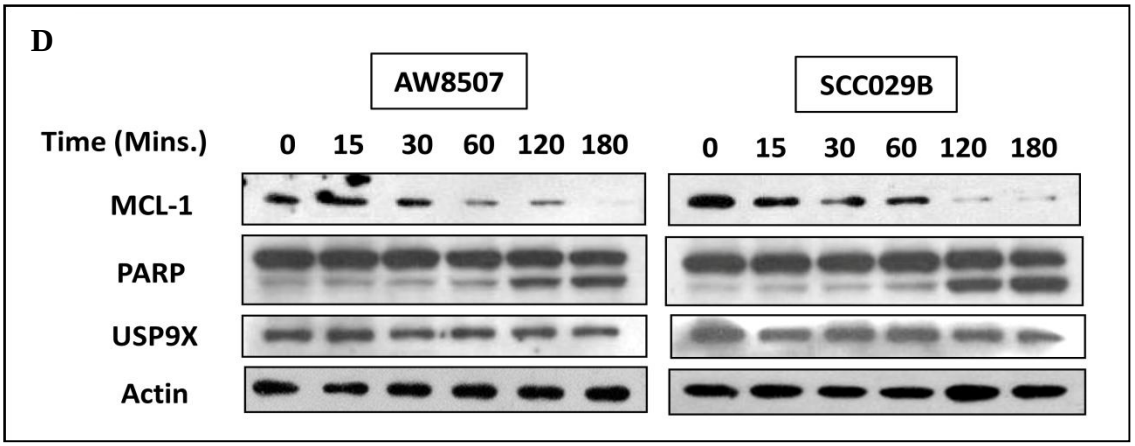
D
AW8507
SCC029B
Time (Mins.)
0 15 30 60 120 180
MCL-1
PARP
USP9X
Actin

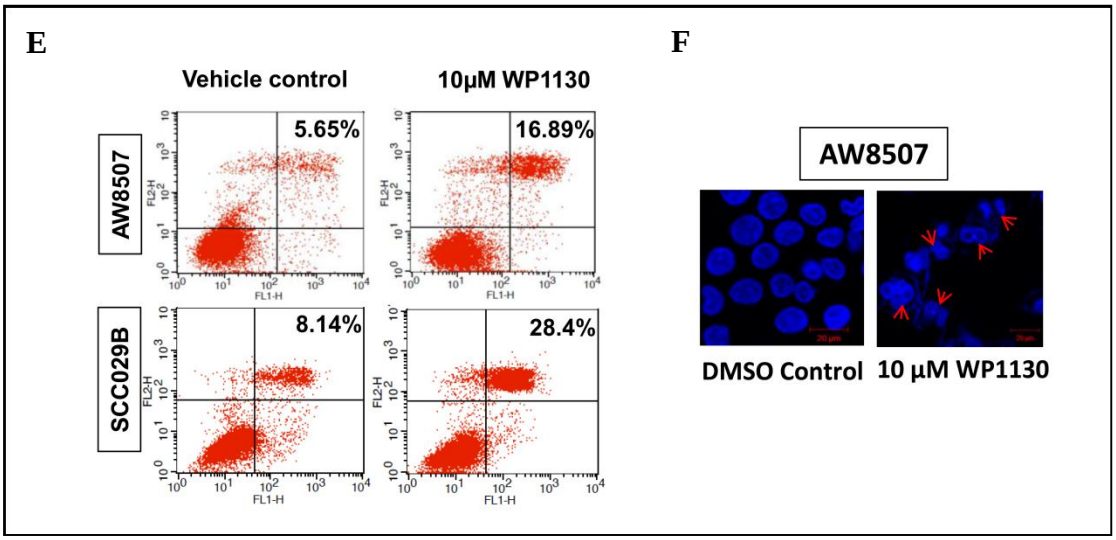
E
Vehicle control
10µM WP1130
AW8507
SCC029B
5.65%
16.89%
8.14%
28.4%
FL2-H
FL1-H
F
AW8507
DMSO Control
10 µM WP1130

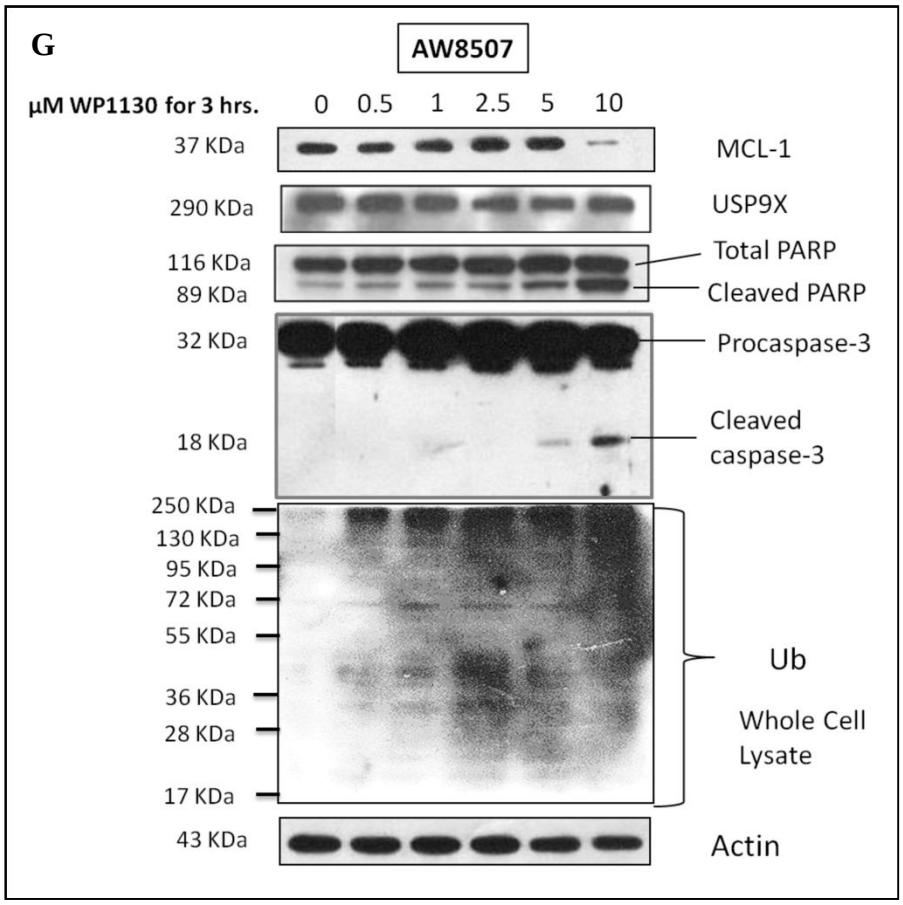

Figure 21: WP1130 potently induces apoptosis in OSCC cells. A) The chemical structure of WP1130 (Degrasyn). **B)** The sensitivity of AW8507 and SCC029B cells to WP1130 was assessed by MTT assay. The cells were treated with indicated concentrations of WP1130 for 24, 48, 72 hours and the cell viability was assessed by MTT assay and expressed as percent viability. **C)** In a clonogenic assay, the cells were exposed to the indicated concentrations of WP1130 for 24 hours or left untreated (EC- Experimental Control or VC-Vehicle control). **D)** The cells were treated with 10 µM WP1130 for 3 hours and the cell lysates were subjected to western blotting for the detection of MCL-1, USP9X, PARP and actin proteins. **E)** AW8507 and SCC029B cells were treated with 10 µM WP1130 for 1 hour and the cells were subjected to apoptosis quantitation by Annexin V/PI staining and flow cytometry. **F)** AW8507 cells were exposed to 10 µM WP1130 for 3 hours and the nuclei were stained with DAPI. Red arrow heads indicates

characteristic fragmented nuclei. **G)** AW8507 cells were exposed to the indicated concentrations of WP1130 for 3 hours and the whole cell lysates were subjected to western blotting for the detection of USP9X, MCL-1, PARP, Caspase-3, actin and ubiquitin. Vehicle control (VC) indicates cells treated with 0.001% DMSO. The blots and images are representative of three independent experiments. The data is represented as mean ± SEM of three independent experiments.

5.1.11 WP1130 treatment triggers rapid accumulation of aggresomes in OSCC cells

WP1130 being a partly selective inhibitor of the deubiquitinases USP9X, USP5, USP14 and UCH37, triggers rapid accumulation of polyubiquitinated (Lys^{48}/Lys^{63}-linked) proteins into juxtanuclear aggresomes [176]. Aggresomes are inclusion bodies marked by p62/SQSTM1 that sequester aggregated proteins which are refractory to proteolysis and are potentially toxic to the cell [215]. The protein aggregates are specifically delivered to the inclusion bodies in a microtubule-dependent dynein-driven process [216]. Treatment of AW8507 cells with WP1130 triggered rapid accumulation of aggresomes which are marked by the punctate cytoplasmic staining of Sequestosome p62/SQSTM1 (Figure 22 A). Electron micrographs also revealed accumulation of aggresomes in WP1130 treated AW8507 cells (Figure 22 B).

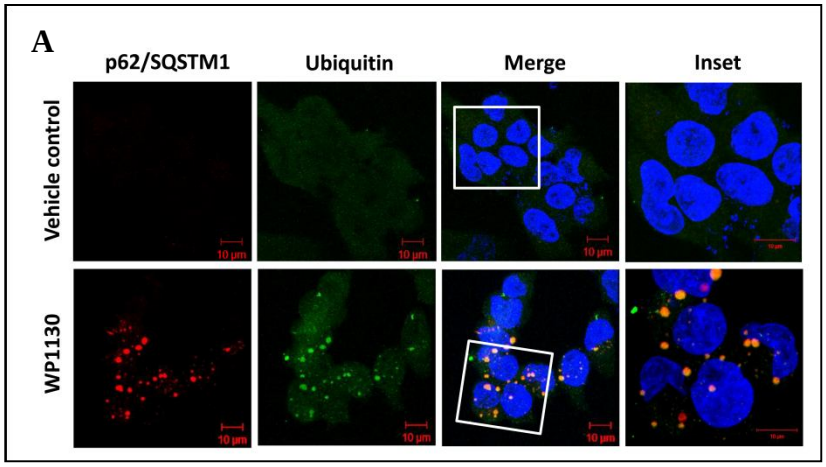

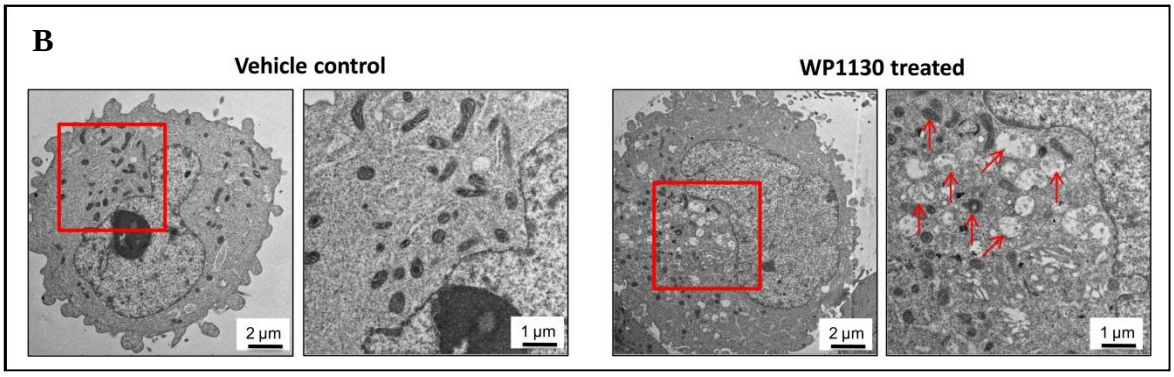

Figure 22: WP1130 triggers aggresome formation. A) AW8507 cells were cultured on coverslip, treated with 10 µM WP1130 for 1 hour and the cells were immunostained with p62/SQSTM1 and ubiquitin antibodies, and DAPI (nucleus). The aggresomes were marked by punctate yellow/orange merge staining of p62/SQSTM1 and Ubiquitin foci (Scale bar: 10 µm). **B)** AW8507 cells were treated with 10 µM WP1130 for 1 hour and the cells were processed for TEM. The cell morphology is evident in the left panel (Scale bar: 2 µm) and the enlarged inset is shown in the right panel (Scale bar: 1 µm). Red arrow heads are indicative of aggresomes. Images are best representatives of two experiments.

5.1.12 *In vivo* efficacy of WP1130 in xenograft mouse models

WP1130 exhibited potent single agent *in vivo* efficacy in xenograft mouse models. The animals which were administered with WP1130 exhibited a significant (*p=0.0242) reduction in the mean tumor volume as compared to the animals in the vehicle control group (Figure 23 A). Moreover, the tumors of WP1130 treated animals exhibited a significant (***p<0.0001) increase in apoptosis indicated by TUNEL and Caspase-3 staining. Notably, the tumors of WP1130 treated animals had significantly (**p=0.0017) lower expression of MCL-1 as opposed to the animals from the vehicle control group (Figure 23 B). These results indicate that WP1130 exhibit *in vivo* antitumor efficacy by triggering apoptosis.

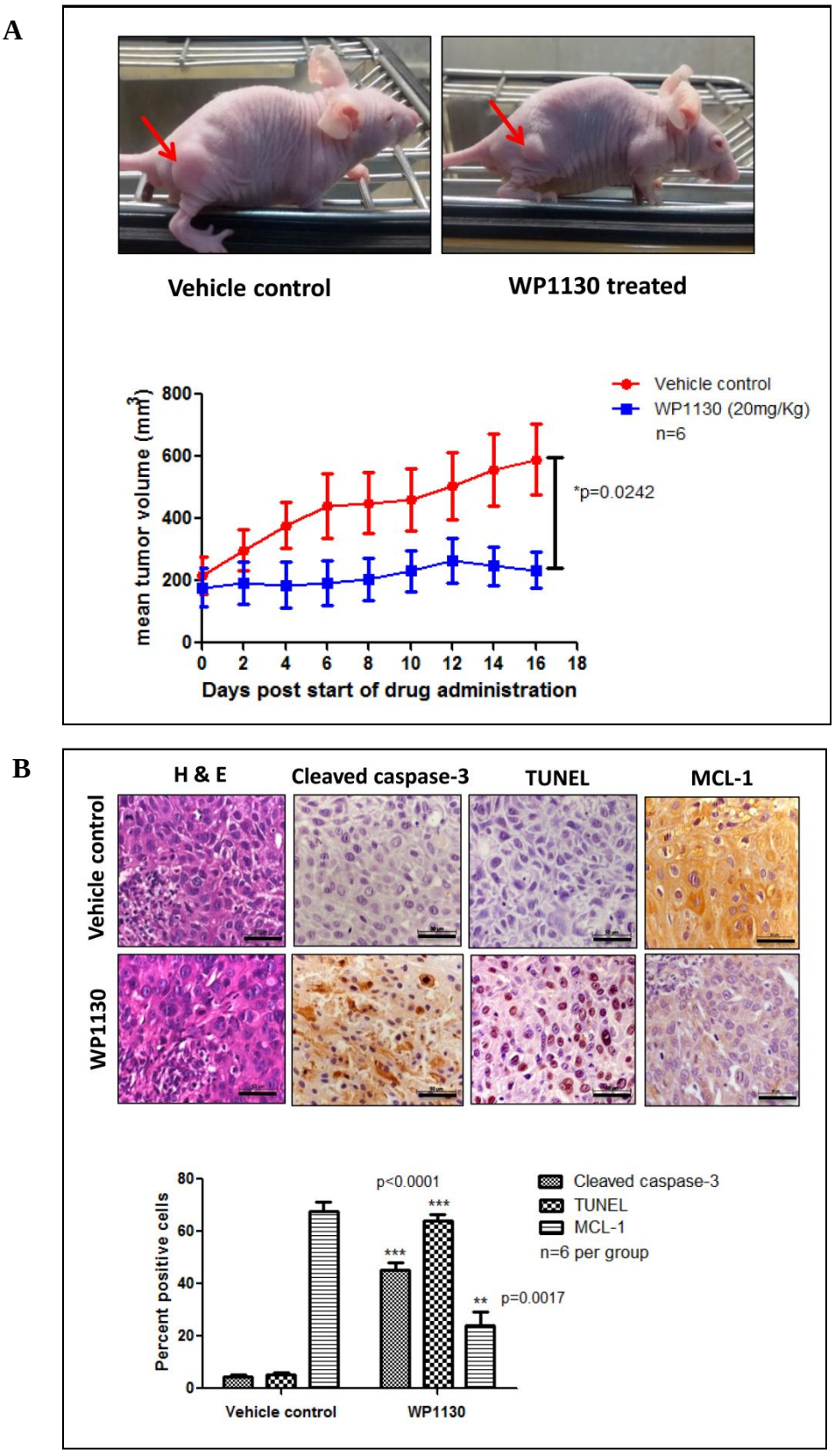

Figure 23: *In vivo* efficacy of WP1130. A) Subcutaneous tumors were established in female BALB/C Nude mice from SCC029B cell line and the animals were randomized into vehicle

control and drug treated group (Six animals per group). Representative images of the animals from either group is shown. The animals administered with WP1130 exhibited a significant (*p=0.0242) reduction in the mean tumor volume as opposed to the vehicle control group. **B)** The tumor tissues of the individual animals were stained for cleaved caspase-3 and MCL-1 by IHC and TUNEL as marker of apoptosis (Scale bar: 50 µm). The data is represented as mean±SEM for 6 animals per group (***p<0.0001).

5.1.13 MCL-1 expression correlates with USP9X expression in different oral histotypes

We evaluated the expression of MCL-1 and USP9X proteins in Normal Oral Mucosa (NOM) (n=50), Oral Potentially Malignant Disorders (OPMD) [which includes Oral Submucous Fibrosis (OSMF, n=25) and Oral Leukoplakia with Epithelial Dysplasia (OL, n=25)] and Oral Squamous Cell Carcinoma (OSCC, n=138) human oral tissue specimens by IHC. The clinicopathological characteristics of the individuals with various oral histotypes are represented in the following tables. The expression of USP9X correlates significantly with MCL-1 in NOM (r=0.3850, **p=0.0058), OSMF (r=0.3954, p=0.0504), OL (r=0.6148, **p=0.0011) and OSCC (r=0.5576, ***p<0.0001) (Figure 24). The expression of USP9X is significantly higher in OPMD and OSCC tissues as compared to NOM consistent with an overexpression of MCL-1 protein (Figure 25).

Table 11: Demographic data for individuals with normal oral mucosa (NOM)

Cases	50
Age	
<50	47 (94%)
>50	03 (06%)
Sex	
Male	30 (60%)
Female	20 (40%)
Site of the tissue taken	
Gingiva	40 (80%)
Frenum	07 (14%)
Buccal mucosa	03 (06%)

Table 12: Clinicopathological characteristics of individuals with OSMF

Cases	25
Age (years)	
<50	00 (0%)
>50	25 (100%)
Sex	
Male	23 (92%)
Female	02 (08%)
Histological differentiation	
Group I (Very early)	03 (12%)
Group II (Early)	10 (40%)
Group III (Moderately advanced)	11 (44%)
Group IV (Advanced)	01 (04%)

Table 13: Clinicopathological characteristics of individuals having Oral Leukoplakia with Epithelial Dysplasia (OL)

Cases	25
Age (Years)	
<50	20 (80%)
>50	05 (20%)
Sex	
Male	20 (80%)
Female	05 (20%)
Site of the lesion	
Buccal mucosa	19 (76%)
Buccal sulcus	01 (04%)
Labial mucosa	05 (20%)
Histological differentiation	
Low risk	14 (56%)
High risk	11 (44%)

Table 14: Clinicopathological parameters of the individuals with oral squamous cell carcinoma (OSCC)

Cases	138
Sex	
Male	111 (80.43%)
Female	27 (19.56%)
Age	
<50	50 (36.23%)
>50	88 (63.76%)
Habits	
Tobacco chewing	61 (44.20%)

Tobacco chewing+Alcohol	16 (11.59%)
Smoking	16 (11.59%)
Smoking+Alcohol	17 (12.31%)
Tobacco chewing+ Smoking	17 (12.31%)
Tobacco chewing+ Smoking+Alcohol	10 (07.24%)
No habits	02 (01.44%)
Site	
Buccal mucosa	76 (55.07%)
Tongue	28 (20.28%)
Alveolus	20 (14.49%)
Gingivobuccal sulcus	05 (03.62%)
Retromolar trigone	03 (02.17%)
Labial mucosa	02 (01.44%)
Lip	04 (02.89%)
Size	
T1	13 (09.42%)
T2	45 (32.60%)
T3	20 (14.49%)
T4	60 (43.47%)
Nodal status	
N0	66 (47.82%)
N1	42 (30.43%)
N2a	20 (14.49%)
N2b	08 (05.79%)
N2c	02 (01.44%)
Histological Differentiation	
Well	41 (29.71%)
Moderate	77 (55.79%)
Poor	16 (11.59%)

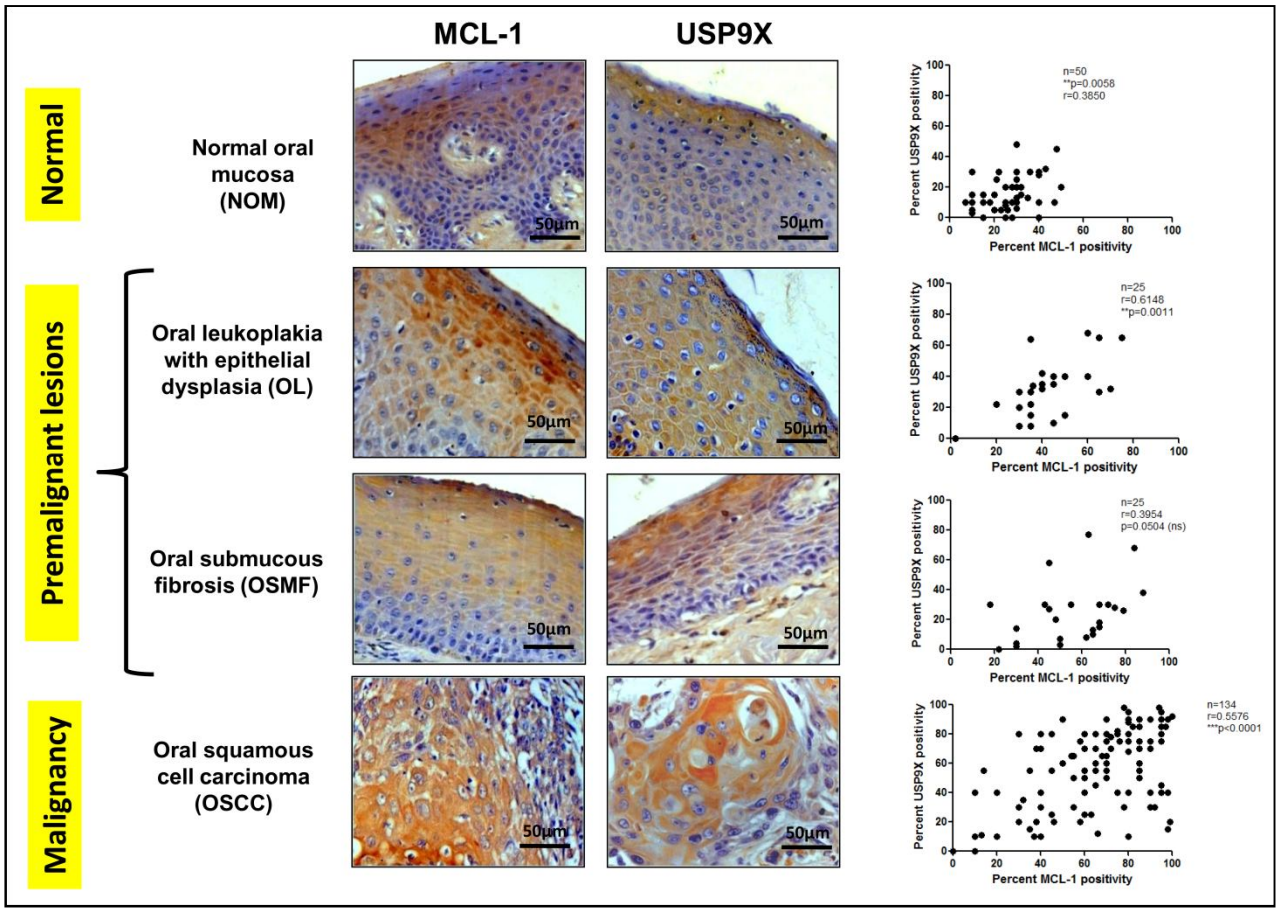

Figure 24: MCL-1 expression correlates with USP9X expression. The expression of MCL-1 and USP9X proteins was assessed by IHC in NOM (n=50), OL (n=25), OSMF (n=25) and OSCC (n=134). The representative images of MCL-1 and USP9X immunohistochemical staining in various histotypes are indicated with their respective correlation analysis on extreme right side (Scale bar: 50 µm). The expression of the individual proteins is represented as percent positivity (r: Pearson correlation coefficient, *p<0.05, **p<0.001, ***p<0.0001).

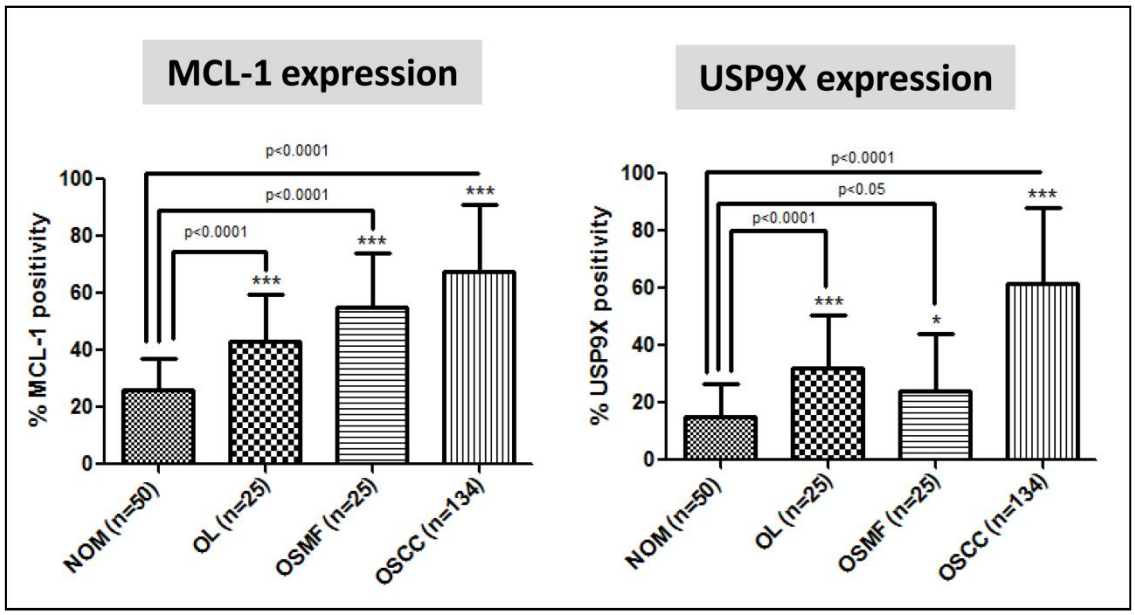

Figure 25: MCL-1 and USP9X proteins are overexpressed in OPMD and OSCC. As described earlier, the expression of MCL-1 and USP9X proteins was assessed by IHC in NOM (n=50), OL (n=25), OSMF (n=25) and OSCC (n=134) tissue samples. The expression of the proteins is represented as percent positivity (*p<0.05, **p<0.001, ***p<0.0001).

5.1.14 High MCL-1 expression correlates with a corresponding high USP9X expression in recurrent oral tumor samples

We further evaluated the expression of MCL-1 and USP9X proteins by IHC in tumor tissues of oral cancer patients showing disease recurrence and those without any evidence of disease relapse. We observed a significantly (*p<0.05) higher expression of both MCL-1 and USP9X proteins in oral cancer patients showing disease recurrence as opposed to the nonrecurrent cases (Figure 26). Moreover, the oral cancer patients showing high MCL-1/USP9X expression exhibited a significantly (*p<0.05) reduced disease free survival as compared to those who expressed relatively lower levels of MCL-1/USP9X (Figure 27).

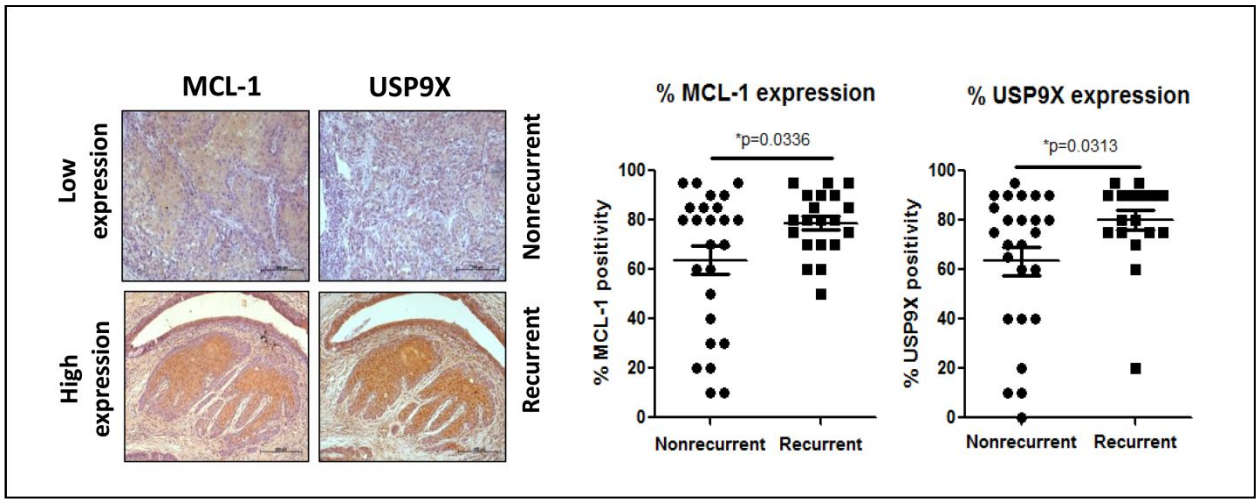

Figure 26: Recurrent oral tumor samples express high levels of MCL-1 and USP9X proteins. Recurrent (n=25) and nonrecurrent (n=20) oral tumor tissues were stained with MCL-1 and USP9X antibodies by IHC. The expression of the two proteins was represented as percent positivity. Representative IHC images of the tumor tissues for the individual proteins demonstrating high and low expression are shown in the left panel.

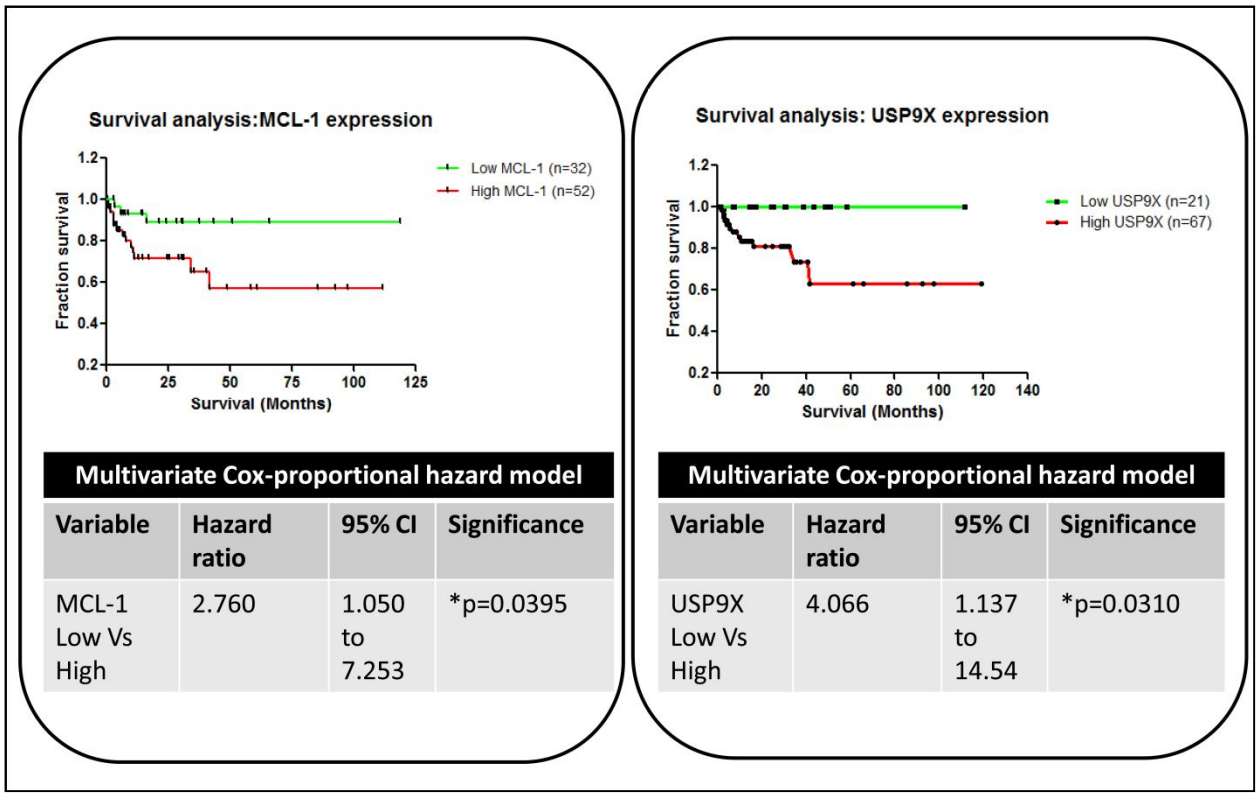

Multivariate Cox-proportional hazard model

Variable	Hazard ratio	95% CI	Significance
MCL-1 Low Vs High	2.760	1.050 to 7.253	*p=0.0395

Multivariate Cox-proportional hazard model

Variable	Hazard ratio	95% CI	Significance
USP9X Low Vs High	4.066	1.137 to 14.54	*p=0.0310

Figure 27: MCL-1 and USP9X serve as important predictor of prognosis in oral cancer patients. The expression of MCL-1 and USP9X was assessed by IHC in oral tumor tissues and was expressed as percent positivity. The high and low cutoff levels of MCL-1 (≥75%) and USP9X (≥50%) were categorized based on their median expression in the present cohort of oral cancer patients and analyzed by Kaplan-Meier survival curves. The multivariate Cox-proportional hazard model are represented below the respective graphs.

To investigate the role of TCTP in stabilization of MCL-1 in oral cancers

5.1.15 To investigate the role of Translationally Controlled Tumor Protein (TCTP) in stabilization of MCL-1 protein

We first assessed the basal level expression of TCTP and MCL-1 proteins in the four oral cell lines DOK, AW8507, AW13516 and SCC029B by western blotting (Figure 28 A). However, we could not find any correlation between MCL-1 and TCTP protein expression in the four cell lines. TCTP was expressed at similar basal levels in the four OSCC cell lines. Next, to directly elucidate the role of TCTP in stabilization of MCL-1 protein, we transfected AW8507 cells with either control siRNA (siControl) or TCTP siRNA (siTCTP). 48 hours post transfection, the cell lysates were subjected to western blotting for the detection TCTP and MCL-1 proteins. However, there was no significant difference between the levels of MCL-1 protein in siControl transfected cells versus siTCTP transfected cells (Figure 28 B). Furthermore, cycloheximide chase assay did not reveal any significant change in the turnover rate of MCL-1 protein (Figure 28 C). All these observations indicate that TCTP may not have a major role in stabilizing MCL-1 protein in OSCC cells.

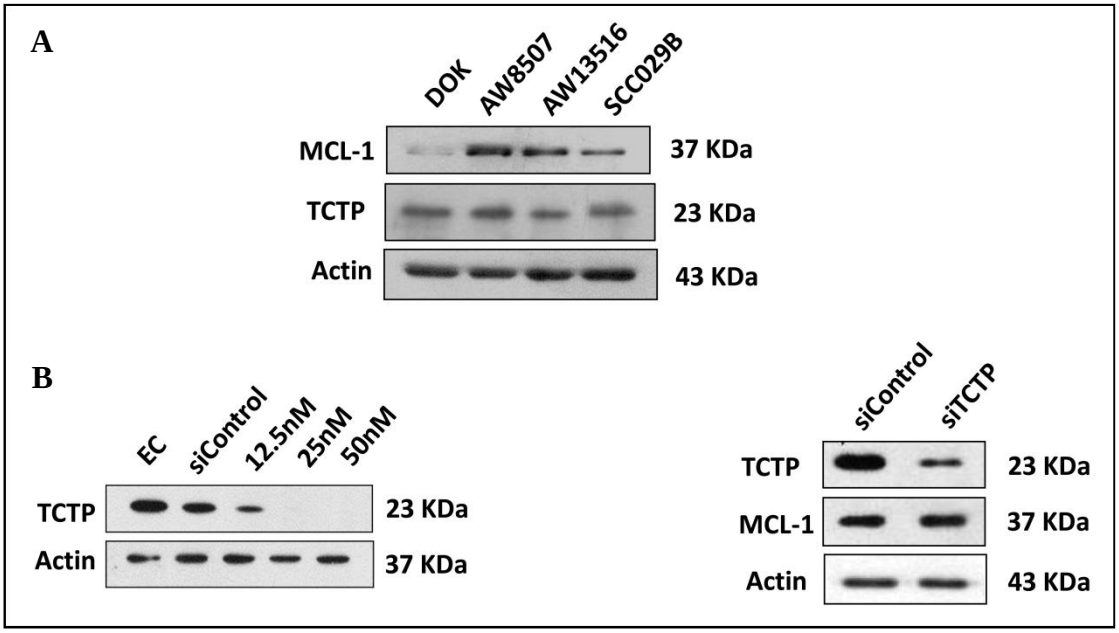

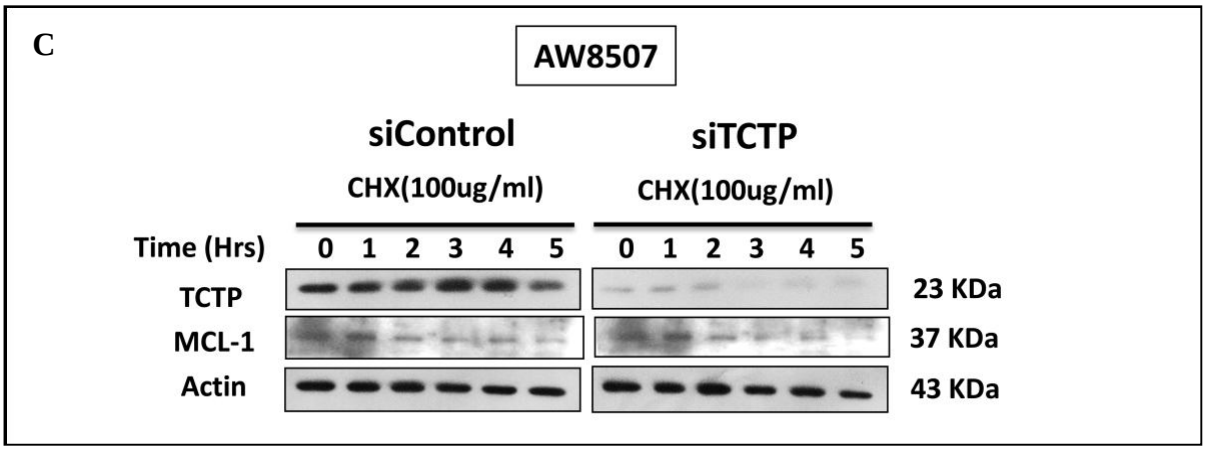

Figure 28: TCTP does not affect stabilization of MCL-1 protein. A) Equal amounts of whole cell lysates of the indicated cell lines were subjected to western blotting for the detection of TCTP, MCL-1 and actin (loading control) proteins. **B)** For TCTP siRNA concentration standardization purpose, AW8507 cells were transfected with increasing concentration of TCTP siRNA along with 50 nM control siRNA (siControl) or left untransfected as Experimental control (EC). Alternatively, the cells were transfected by 50 nM of each of siControl and siTCTP. 48 hours post transfection, the cell lysates were subjected to western blotting for the detection of TCTP, MCL-1 and actin proteins. **C)** AW8507 cells were transfected with siTCTP or siControl. 48 hours post transfection, the cells were treated with 100 µg/ml cycloheximide and the cells were harvested at the indicated time points. The cell lysates were subjected to western blotting for the detection of TCTP, MCL-1 and actin proteins. The western blots are representative of three independent experiments.

5.1.16 MCL-1 and TCTP expression correlates in diverse oral histopathological types

We evaluated the expression of MCL-1 and TCTP proteins in Normal Oral Mucosa (NOM, n=50), Oral Submucous Fibrosis (OSMF, n=25), Oral Leukoplakia with Epithelial Dysplasia (OL, n=25) and Oral Squamous Cell Carcinoma (OSCC, n=50) human oral tissue specimens by IHC. The expression of TCTP correlates significantly with MCL-1 in NOM (r=0.4904, ***p=0.0003), OSMF (r=0.6306, ***p=0.0007), OL (r=0.5323, **p=0.0062) and OSCC (r=0.7997, ***p<0.0001) (Figure 29). The expression of TCTP is significantly higher in OPMD and OSCC tissues as compared to normal oral mucosa consistent with an overexpression of MCL-1 protein (Figure 30).

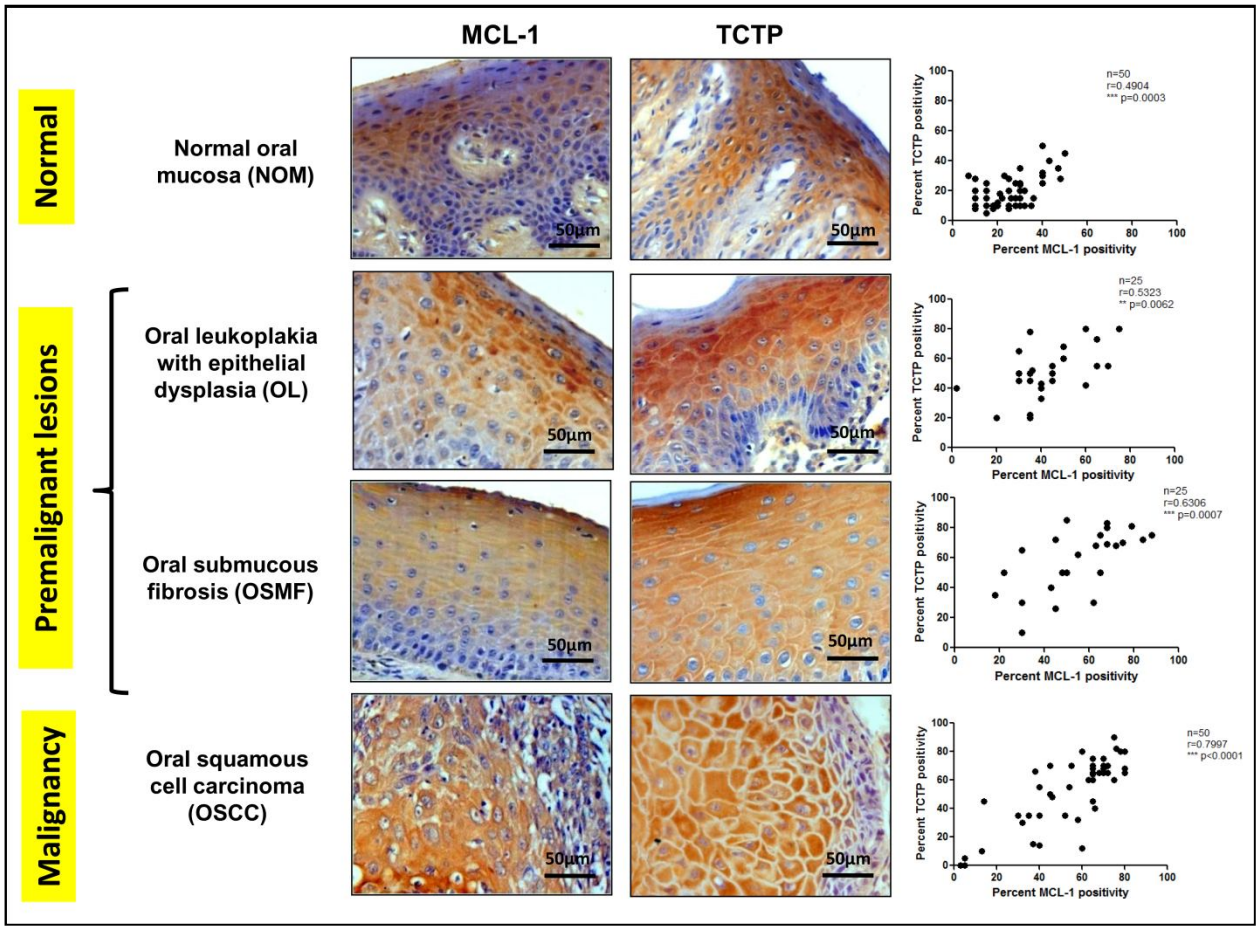

Figure 29: MCL-1 expression correlates with TCTP expression. The expression of MCL-1 and TCTP proteins was assessed by IHC in Normal Oral Mucosa (n=50), Oral Leukoplakia with Epithelial Dysplasia (n=25), Oral Submucous Fibrosis (n=25) and Oral Squamous Cell Carcinoma (n=50) tissues. The representative images of MCL-1 and TCTP immunohistochemical staining in various histotypes are indicated with their respective correlation analysis on extreme right side (Scale bar: 50 µm). The expression of the individual proteins is represented as percent positivity (r: Pearson correlation coefficient, *p<0.05, **p<0.001, ***p<0.0001).

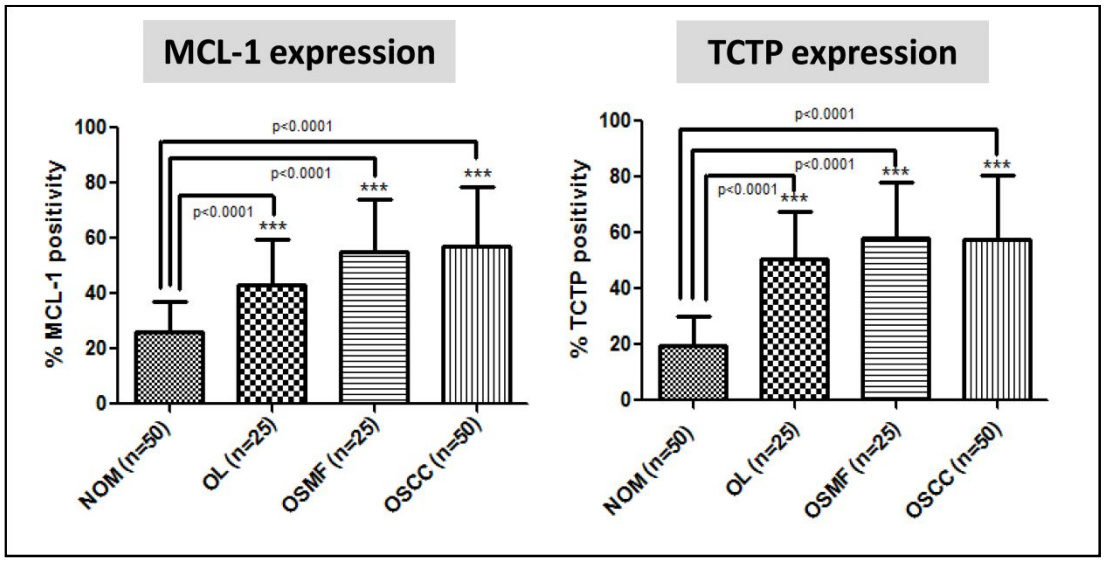

Figure 30: MCL-1 and TCTP proteins are overexpressed in OPMD and OSCC. The expression of MCL-1 and TCTP proteins was assessed by IHC in NOM (n=50), OL (n=25), OSMF (n=25) and OSCC (n=50) tissue samples. The expression of the proteins is represented as percent positivity (*p<0.05, **p<0.001, ***p<0.0001).

To investigate the role of MULE in destabilization of MCL-1 in oral cancers

5.1.17 Evaluation of E3-Ubiquitin Ligase MULE in regulating the stability of MCL-1

The basal level of expression of MCL-1 and MULE proteins was assessed in the four oral cell lines by western blotting. We anticipated an inverse correlation of expression between the two proteins. However, we observed no correlation between them in the cell lines (Figure 31 A). On the other hand, analysis of expression of these proteins by IHC in oral tissues surprisingly revealed a positive correlation in Normal Oral Mucosa (r=0.04645, p=0.7487, ns), Oral Submucous Fibrosis (r=0.5324, **p=0.0062), Oral Leukoplakia with Epithelial Dysplasia (r=0.4681, *p=0.0183) and Oral Squamous Cell Carcinoma (r=0.32, *p=0.0235) (Figure 31 B).

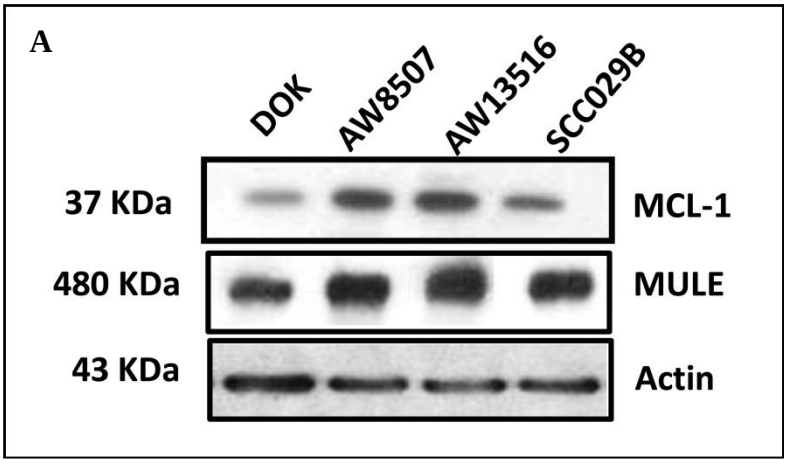

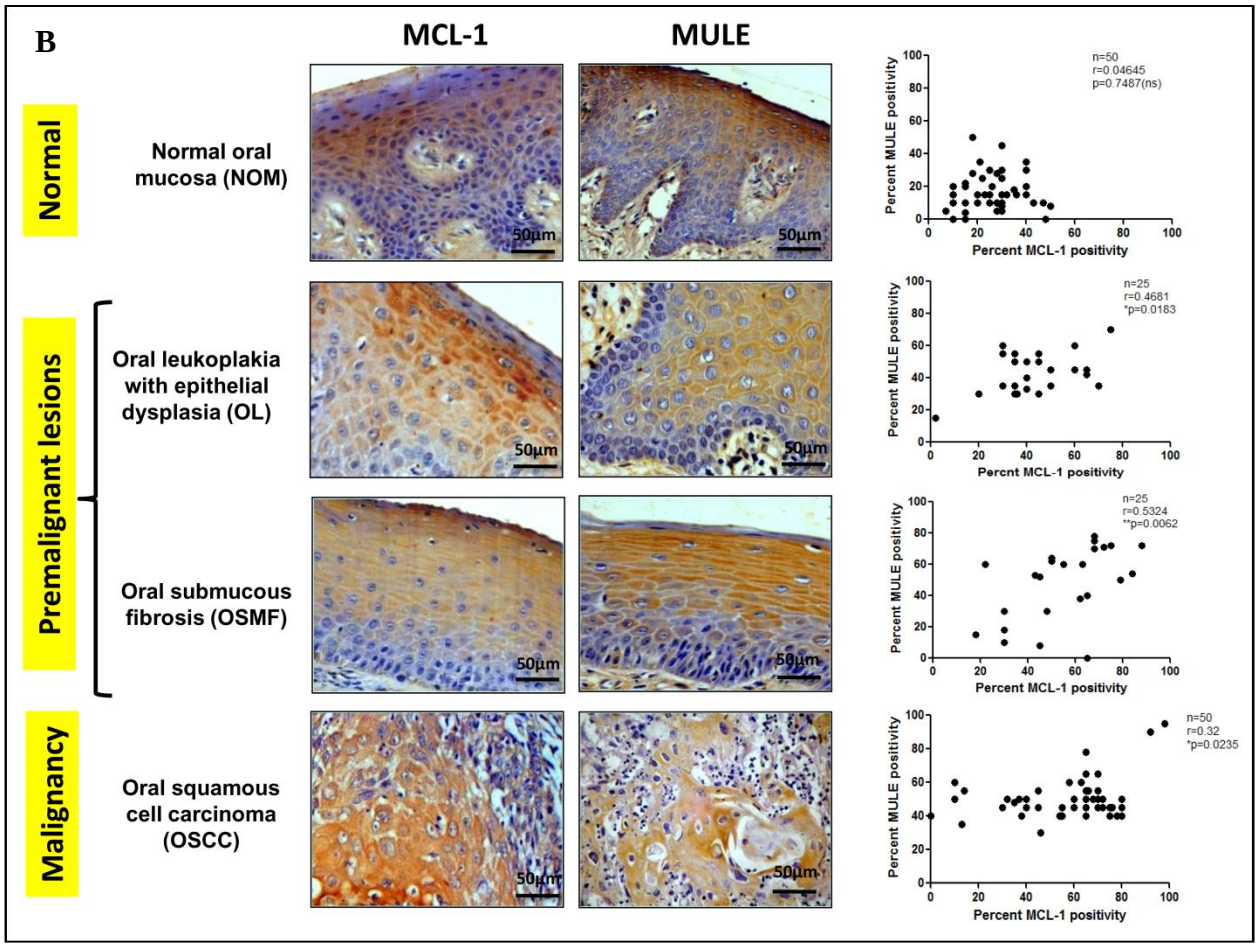
B
MCL-1
MULE
Normal
Normal oral mucosa (NOM)
Premalignant lesions
Oral leukoplakia with epithelial dysplasia (OL)
Oral submucous fibrosis (OSMF)
Malignancy
Oral squamous cell carcinoma (OSCC)
50µm
Percent MULE positivity
Percent MCL-1 positivity
n=50
r=0.04645
p=0.7487(ns)
n=25
r=0.4681
*p=0.0183
n=25
r=0.5324
**p=0.0062
n=50
r=0.32
*p=0.0235

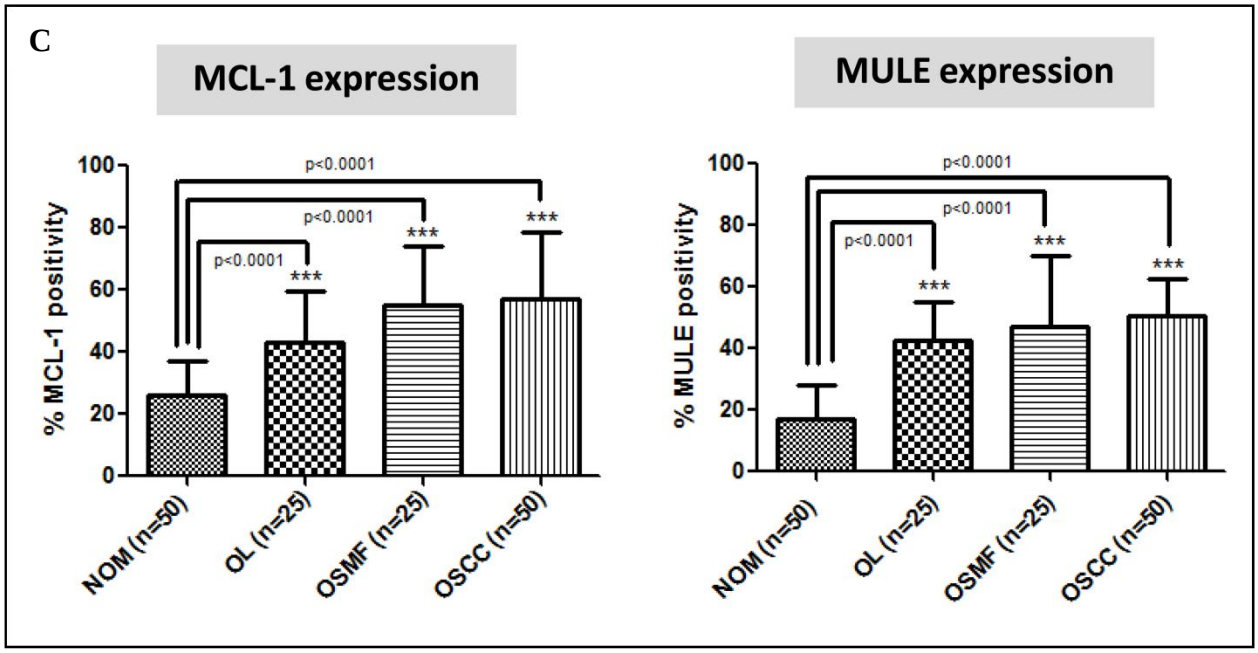
C
MCL-1 expression
MULE expression
% MCL-1 positivity
% MULE positivity
p<0.0001
***
NOM (n=50)
OL (n=25)
OSMF (n=25)
OSCC (n=50)

Figure 31: Analysis of MCL-1 and MULE protein expression in oral cell lines and tissues **A)** The expression of MCL-1 and MULE proteins was analyzed in oral cell lines by western blotting. Actin served as the loading control. **B)** The expression of MCL-1 and MULE proteins was assessed by IHC in Normal Oral Mucosa (n=50), Oral Leukoplakia with Epithelial Dysplasia (n=25), Oral Submucous Fibrosis (n=25) and Oral Squamous Cell Carcinoma (n=50). The representative images of MCL-1 and MULE immunohistochemical staining in various histotypes are indicated with their respective correlation analysis on extreme right side (Scale bar: 50 µm). The expression of the individual proteins is represented as percent positivity (r: Pearson correlation coefficient, *p<0.05, **p<0.001, ***p<0.0001, ns: not significant). **C)** The expression of MCL-1 and MULE is significantly (***p<0.0001) higher in oral potentially malignant disorders and oral tumors as compared to normal oral mucosa.

5.1.18 Identification of novel interacting partners of MCL-1

We employed the approach of endogenous coimmunoprecipitation coupled with Mass Spectrometry to identify novel interacting partner proteins of MCL-1. The silver stained gel from which differential protein bands were excised is indicated in Figure 32B. The MS screen revealed several proteins associated with the regulation of cell cycle, apoptosis and ubiquitin-proteasomal pathway (Table 15).

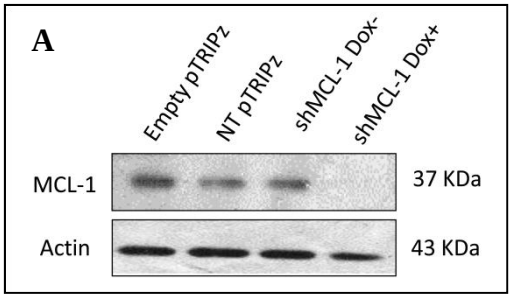

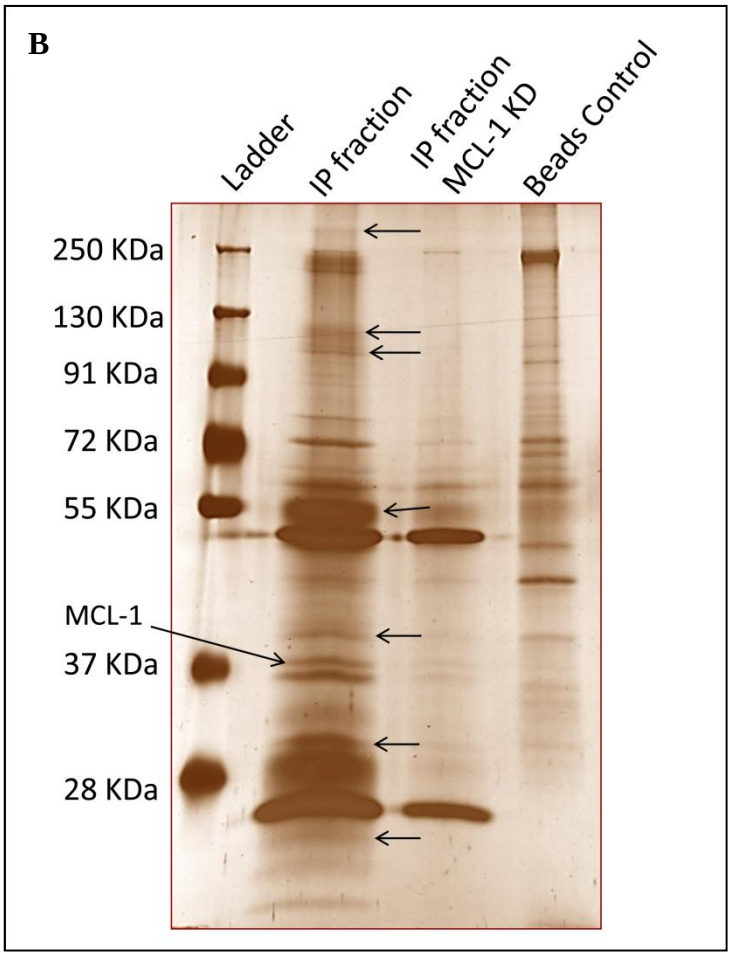

Figure 32: Identification of MCL-1-interacting partners. A) AW8507 cells stably transduced with shRNA cassette against MCL-1 (shMCL-1) in pTRIPZ lentiviral system to downregulate MCL-1 expression. The cells were cultured in a medium containing 10 µg/ml Doxycycline so as to drive the expression of shMCL-1 (Dox+) or else left untreated (Dox+) so that the expression of MCL-1 shRNA doesn't occur. The lysates of cells harboring an empty pTRIPZ and those having a nontargeting shRNA cassette (NT pTRIPZ) is also included as controls. **B)** Silver stained gel from which the differential protein bands (indicated by arrow heads) were excised and eluted for protein identification.

Table 15: Proteins identified through Mass spectrometry screen

Protein	**Mol. mass (KDa)**	**Scores**	**No. of matching peptides**	**Significance/ Function**
NACHT, LRR and PYD domains-containing protein 11 **(NALP11)**	119.9	60	11	NALP11 is an important component of Inflammaosomes (molecular platforms activated in response to infection which triggers proinflammatory cytokines to engage innate immune defenses).
Myc promoter Binding Protein -1 **(MBP-1)**	47.4	92	7	MBP-1 is a truncated form of α-enolase, represses the expression of c-Myc. It upregulate expression of miR-29b which represses MCL-1 expression.
Family with sequence similarity 81, member A **(FAM81A)**	42.4	19	2	Undefined
Ubiquitin-specific peptidase-like protein 1	34.6	22	3	Similar to USP9X, catalyzes removal of polyubiquitin chains from substrate as a deubiquitinase
ER-Golgi Intermediate Compartment 1 **(ERGIC1)**	32.9	22	2	Important in ER to Golgi vesicle-mediated transport
Neuferricin (CYB5D2)	29	21	2	A novel extracellular heme-binding protein
BAX	21	33	3	A multidomain proapoptotic BCL-2 family protein, serve as effector in MOMP
Paraneoplastic Ag-	44.3	18	2	Undefined

like protein 6A				
CASP8 and FADD-like apoptosis regulator **(CFLAR or c-FLIP)**	55.8	31	3	Apoptosis regulator, structurally similar to Caspase-8, but lacks caspase activity and itself cleaved by caspase-8 to generate two peptides
MAP3K12-binding inhibitory protein 1 **(MBIP)**	39.5	21	2	Inhibits the MAP3K12 activity to induce the activation of the JNK/SAPK pathway. It is a component of the ATAC complex, a complex with histone acetyltransferase activity on histones H3 and H4.
Mitotic spindle assembly checkpoint protein **(MAD2A)**	23.6	38	3	Component of the spindle-assembly checkpoint that prevents the onset of anaphase until all chromosomes are properly aligned at the metaphase plate. Required for the execution of the mitotic checkpoint which monitors the process of kinetochore-spindle attachment and inhibits the activity of the anaphase promoting complex by sequestering CDC20 until all chromosomes are aligned at the metaphase plate.
CDK5 regulatory subunit-associated protein 1 **(CDKAL1)**	68.5	24	3	Undefined
Serine/threonine-protein phosphatase 2A regulatory subunit B	58.5	28	3	Roles in Ca^{2+} ion binding, protein binding and bridging, protein phosphatase 2A regulatory activity, regulates Wnt pathway
Tumor protein p63-	30.3	23	2	Undefined

regulated gene 1-like protein **(TPRG1L)**				
PCNA-associated factor **(PAF)**	12	21	2	Acts as a regulator of DNA repair during DNA replication. Following DNA damage, the interaction with PCNA is disrupted, facilitating the interaction between monoubiquitinated PCNA and the translesion DNA synthesis DNA polymerase eta (POLH) at stalled replisomes, facilitating the bypass of replication-fork-blocking lesions. Also acts as a regulator of centrosome number
E3 SUMO-protein ligase NSE2	28.2	23	2	Plays roles in cell division, cellular senescence, double-strand break repair via homologous recombination, positive regulation of mitotic metaphase/anaphase transition, protein sumoylation, telomere maintenance via recombination
MAPK/MAK/MRK overlapping kinase	48.5	19	2	ATP binding, cyclin-dependent protein serine/threonine kinase activity, protein serine/threonine kinase activity
MDM4	55.8	18	2	It is similar to MDM2 and contains a p53 binding domain at the N-terminus and a RING finger domain at the C-terminus. Unlike MDM2 which degrades p53, this protein inhibits p53 by binding its transcriptional activation domain.
26S protease regulatory subunit 4 **(PSMC1)**	49.3	31	3	The 26S protease is involved in the ATP-dependent degradation of ubiquitinated proteins. The regulatory (or ATPase)

				complex confers ATP dependency and substrate specificity to the 26S complex.
CDC27	92.8	24	3	It is a component of the anaphase-promoting complex (APC) which catalyzes the formation of cyclin B-ubiquitin conjugate, which is responsible for the ubiquitin-mediated proteolysis of B-type cyclins. This protein was shown to interact with mitotic checkpoint proteins including Mad2, p55CDC and BUBR1, and it may thus be involved in controlling the timing of mitosis.
E3 ubiquitin-protein ligase RNF144A	34.5	21	2	It accepts ubiquitin from E2 ubiquitin-conjugating enzymes UBE2L3 and UBE2L6 in the form of a thioester and then directly transfers the ubiquitin to targeted substrates. Mediates the ubiquitination and degradation of the DNA damage kinase PRKDC. It is also involved in mediating protein ubiquitination as a posttranslational modification of the proteins.
Mitotic checkpoint serine/threonine-protein kinase BUB1 β	120.7	27	4	It is a serine/threonine-protein kinase which is essential for spindle-assembly checkpoint signaling, for correct chromosome alignment, for the kinetochore localization of PLK1, inhibit the activation of the anaphase promoting complex/cyclosome (APC/C).
Proteasome-associated protein	205.9	26	5	Adapter/scaffolding protein that binds to the 26S proteasome, motor proteins and

ECM29 homolog				other compartment specific proteins. May couple the proteasome to different compartments including endosome, ER and centrosome. May play a role in ERAD and other enhanced proteolyis.

5.2 To assess the *in vitro/in vivo* effects of small molecule inhibitor of MCL-1 on human oral cancer cell lines.

Previous studies from our laboratory demonstrated overexpression of anti-apoptotic members of the BCL-2 family, particularly MCL-1 (Myeloid Cell Leukemia-1) over their pro-apoptotic counterparts in human oral cancers [23]. Subsequent studies from our lab have reported predominant overexpression of antiapoptotic MCL-1 protein in oral cancer tissues versus normal counterparts and its association with therapy resistance and poor prognosis in oral cancer patients [23-26]. MCL-1 is a tightly regulated molecule, has a short half-life and is important for the development and survival of diverse cell types [30]. However, MCL-1 expression is frequently elevated in diverse human malignancies and is associated with therapy resistance. Several mechanisms including increased copy number, chromosomal and epigenetic changes and enhanced stability of MCL-1 protein contributes to its high expression in tumors [33]. Apart from its canonical prosurvival function, role of MCL-1 in mitochondrial homeostasis [92], DNA damage response [97, 98] and autophagy [104] are recently emerging.

All these studies suggests that the antiapoptotic proteins of the BCL-2 family, particularly MCL-1 are promising therapeutic targets in OSCC. Several pan-BCL-2 inhibitors are currently under development. However, therapeutic targeting of MCL-1 protein has largely been hindered by its structural discrepancy from other antiapoptotic BCL-2 family members [90]. But partial functional redundancy allows MCL-1 to substitute BCL-2, BCL-XL and BCL-W for their prosurvival function when they are either inhibited or downregulated. MCL-1 is well known to exhibit resistance to ABT-737 and ABT-263 which potently antagonize BCL-2, BCL-XL and BCL-W [169, 217, 218]. Obatoclax (GX15-070), a BH3 mimetic is capable of inhibiting all the antiapoptotic proteins of the BCL-2 family, and potently inhibit the interaction between MCL-1

and BAK [90]. The potency of Obatoclax has been demonstrated against a variety of human cancer cell lines *in vitro* [90, 180-182] and in several clinical trials against diverse tumor types [183-185]. However, its activity against human oral cancers is rarely explored and largely unknown.

BH3-only proteins and BH3 mimetics are known to induce autophagy by activating multiple pathways [219, 220]. Autophagy has long been regarded as a cytoprotective mechanism deployed by tumor cells under stressful conditions [221]. However, sustained autophagy in response to a prolonged stress may lead to cell death when defective protein and organelle turnover exceeds the processing capacity of the cell [201]. A non-canonical pathway of cell death, Necroptosis has recently been shown to be linked to autophagy which involves a critical role of serine/threonine kinases called Receptor-interacting protein kinases (RIP1K and RIP3K) in a complex called Necrosome [222]. RIP3K further downstream recruits and phosphorylates its substrate Mixed Lineage Kinase Like (MLKL) which is proposed to execute necroptosis by mediating mitochondrial fission, generation of Reactive oxygen species (ROS) in mitochondria and recruitment of Ca^{2+} and Na^{+} ion channels or pore-forming complexes at the plasma membrane [207].

In the present study, therefore we investigate the activity and mechanism of action of Obatoclax (GX15-070) in human oral cancer cell lines.

5.2.1 Obatoclax potently inhibits the clonogenic potential of OSCC cells

We demonstrated the *in vitro* efficacy of Obatoclax against oral cancer cells by clonogenic assay. The plating efficiencies for all the four oral cell lines differed markedly (DOK: 30–40%, AW8507: 60–70%, AW13516: 70–80%, SCC029B: 55–60%). Obatoclax (Figure 33 A) inhibited

the clonogenic potential of these cells in a dose-dependent manner with complete growth inhibition at 200–400 nM concentration (Figure 33 B). The sensitivities of the four cell lines to Obatoclax correlated significantly (*p<0.05, R=0.96) with their MCL-1 protein expression (Figure 33 C). DOK (IC_{50}: 67.5 nM) exhibited highest sensitivity to Obatoclax with complete growth inhibition at about 100 nM concentration (correlates with its relatively lower MCL-1 expression) whereas AW8507 (IC_{50}: 110 nM), AW13516 (IC_{50}: 101 nM) and SCC029B (IC_{50}: 94.5 nM) were relatively less sensitive possibly due to relatively higher MCL-1 expression.

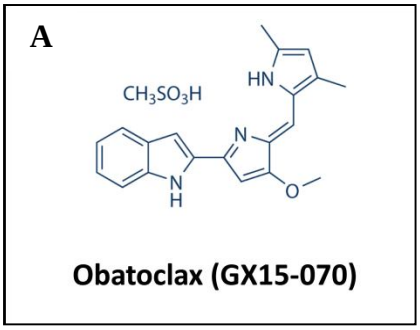

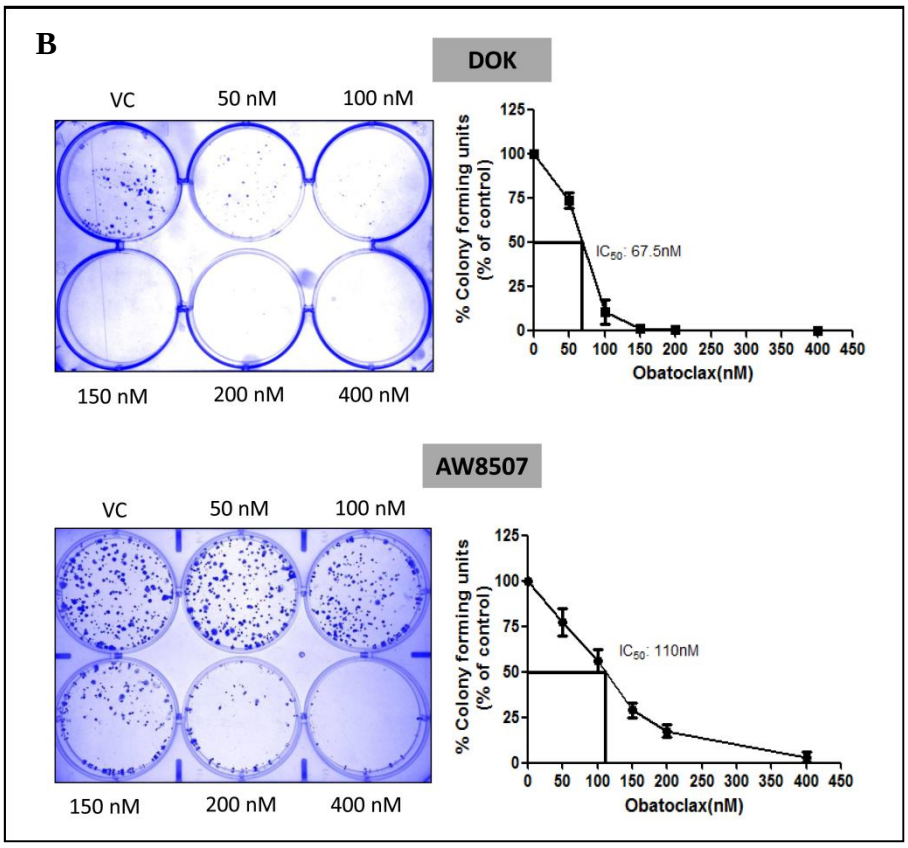

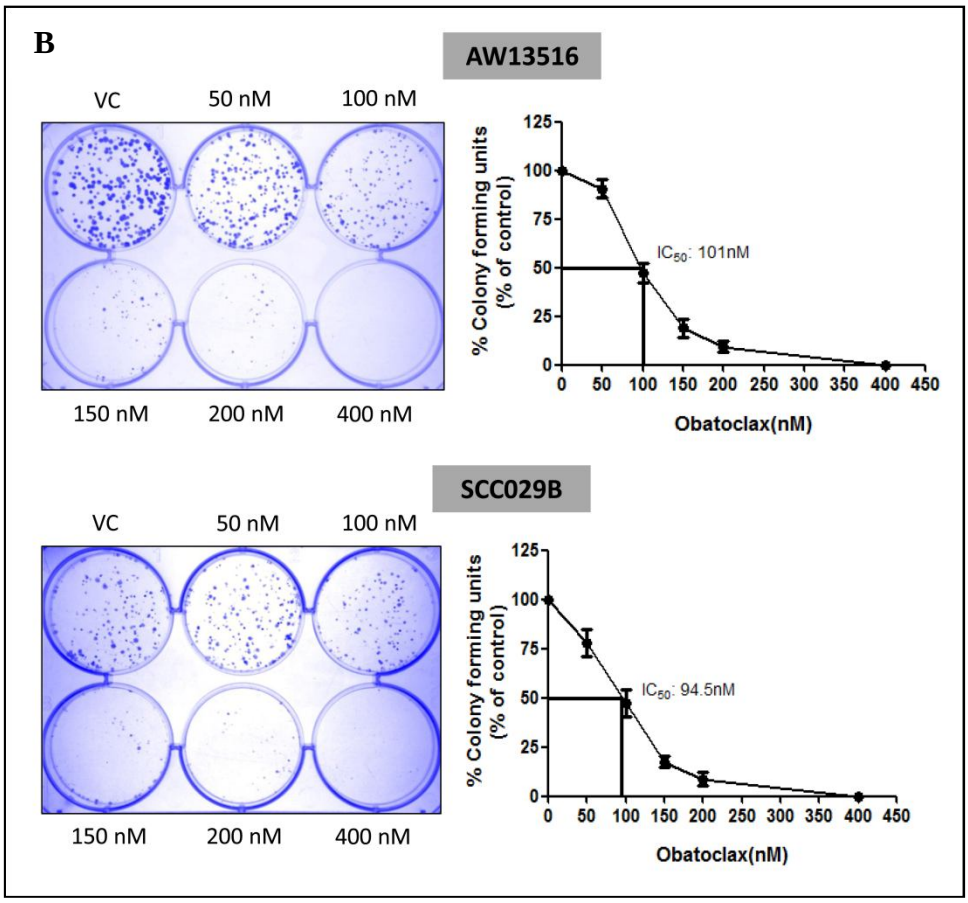
B
AW13516
VC
50 nM
100 nM
150 nM
200 nM
400 nM
% Colony forming units (% of control)
IC50: 101nM
Obatoclax(nM)
SCC029B
VC
50 nM
100 nM
150 nM
200 nM
400 nM
% Colony forming units (% of control)
IC50: 94.5nM
Obatoclax(nM)

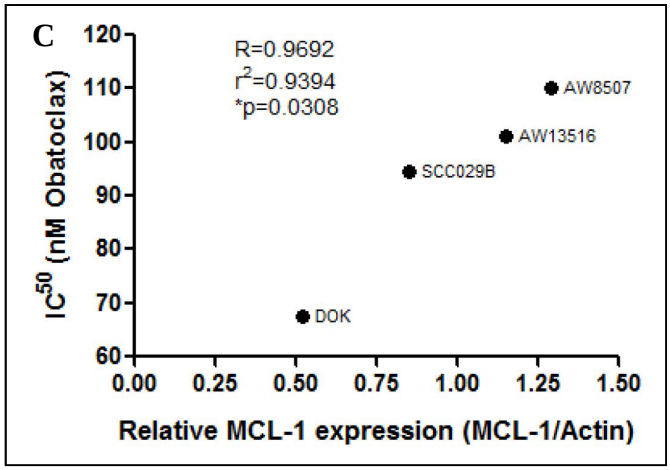
C
R=0.9692
r2=0.9394
*p=0.0308
AW8507
AW13516
SCC029B
DOK
IC50 (nM Obatoclax)
Relative MCL-1 expression (MCL-1/Actin)

Figure 33: Obatoclax potently inhibits the clonogenic potential of oral cancer cells. A) Chemical structure of Obatoclax (GX15-070). **B)** The sensitivity of the four cell lines to Obatoclax was determined by the clonogenic assays. Equal numbers of cells were seeded in a six well plate and exposed to the indicated doses of Obatoclax for 24 hours. The cells were then allowed to grow for further 8-10 days till appearance of visible colonies, which were then fixed, stained and scored. The survival (colony forming units) is expressed as percentage of vehicle controls. Data is represented as mean ± SEM of three independent experiments. **C)** The relative expression of MCL-1 protein was determined by western blotting and densitometric analysis. The sensitivities of the cells to Obatoclax was found to be significantly correlated with their relative MCL-1 expression (*$p<0.05$, $r^2=0.9394$). Data is represented as mean of three independent experiments. The clonogenic assay images are representative of three experiments.

5.2.2 Obatoclax does not alter the expression of BCL-2 family proteins but dissociate MCL-1/BAK interaction and induce BAX translocation to the mitochondria

Obatoclax is shown to induce apoptotic cell death in HNSCC cells by reducing MCL-1 expression [223]. We therefore assessed whether Obatoclax affects the expression of critical members of the BCL-2 family. Exposure of the four cell lines to Obatoclax for 24 hours revealed no significant alterations in the expression of either MCL-1 or other members of the BCL-2 family except for BIM and NOXA proteins, which showed a dose dependent reduction in expression (Figure 34 A). Nevertheless, Obatoclax not only dissociated the constitutive interaction between MCL-1 and BAK in the mitochondrial outer membrane (Figure 34 B) but also induced BAX translocation to the mitochondria (Figure 34 C). Both these events are critical for MOMP. However, despite BAK release from MCL-1 and BAX translocation to the

mitochondria, we could not detect a significant cytochrome c release from mitochondria to the cytosol (Figure 34 C).

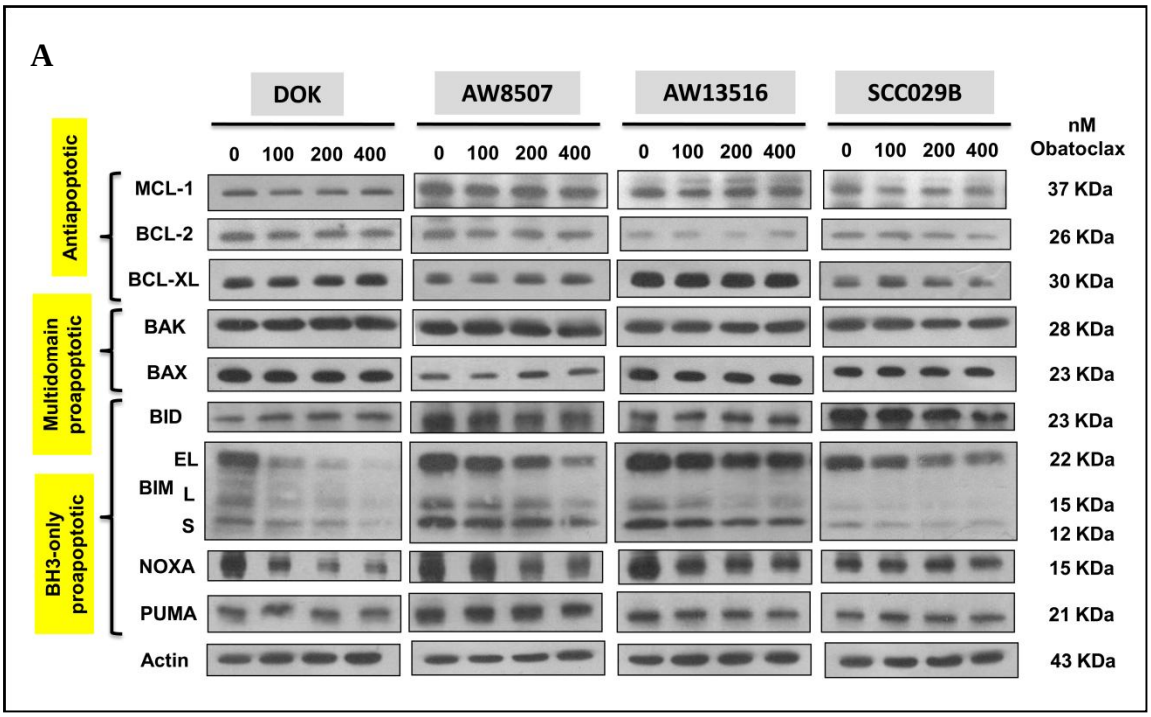

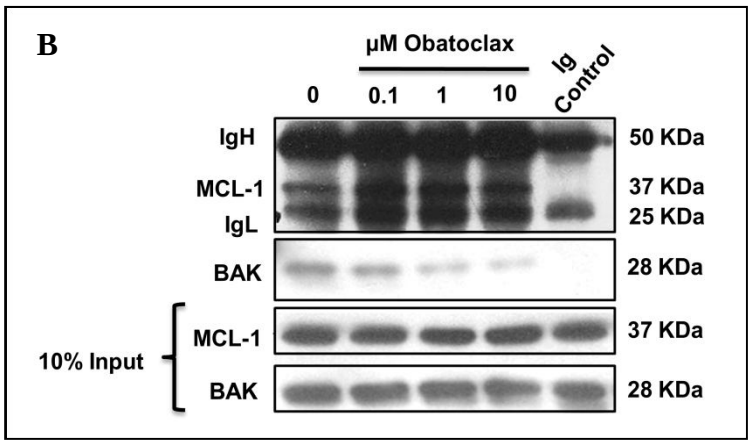

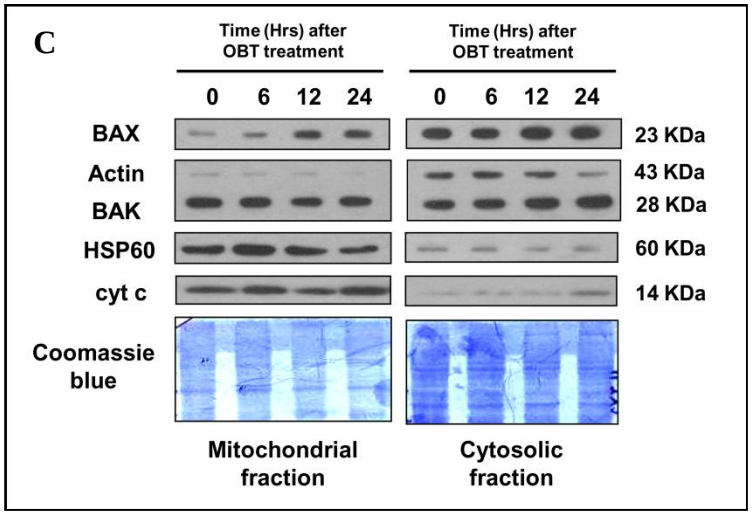

Figure 34: Effect of Obatoclax on the BCL-2 family proteins. A) The cells were exposed to the indicated doses of Obatoclax for 24 hours and equal amounts of whole cell lysates were subjected to immunoblotting for detection of the indicated proteins by western blotting. Actin served as the loading control. The blots are representatives of three independent experiments. **B)** Obatoclax dissociates the interaction between MCL-1 and BAK. SCC029B cells were treated with 0, 0.1, 1 and 10 µM Obatoclax for 6 hours. The cell lysates were then subjected to immunoprecipitation with anti-MCL-1 antibody. The immunoprecipitates were probed with MCL-1 and BAK antibodies in a western blot along with 10% input. **C)** SCC029B cells were treated with 400 nM Obatoclax and harvested at indicated time points. The cells were fractionated into mitochondrial and cytosolic fractions. Equal amounts of mitochondrial and cytosolic fractions were analyzed for BAX, BAK and cytochrome c. Actin and HSP60 served as the loading controls for cytosolic and mitochondrial fractions respectively and to represent the purity of the preparations. BAX levels increased in the mitochondrial fraction in a time dependent manner, indicating increased BAX translocation to the mitochondria. BAK levels however remained unchanged.

5.2.3 Obatoclax triggers caspase-independent cell death in OSCC cells

Obatoclax induced a dose and time-dependent decrease in the viability of OSCC cells as determined by MTT and SRB assays (Figure 35 A and B). To investigate whether Obatoclax mediated cell death via the canonical caspase-dependent pathway, we exposed SCC029B cells to Obatoclax for 0, 24, 48 and 72 hours and assessed caspase activation by western blotting. Absence of caspase-3, caspase-8 and PARP cleavage upon Obatoclax treatment indicates a caspase-independent cell death (Figure 35 C). This was further confirmed by the fact that OSCC

cells exhibited no significant difference in the cell viability when treated with Obatoclax alone or in combination with a pan-caspase inhibitor Z-VAD-FMK (Figure 35 D). Moreover, Obatoclax treated cells showed no signs of nuclear fragmentation (Figure 35 E). Analysis of cell death by flow cytometry revealed no significant increase in annexin V-positive cells in the Obatoclax treated population as compared to vehicle control cells (Figure 35 F). All these observations point towards a caspase-independent, non-apoptotic form of cell death induced by Obatoclax in OSCC cells.

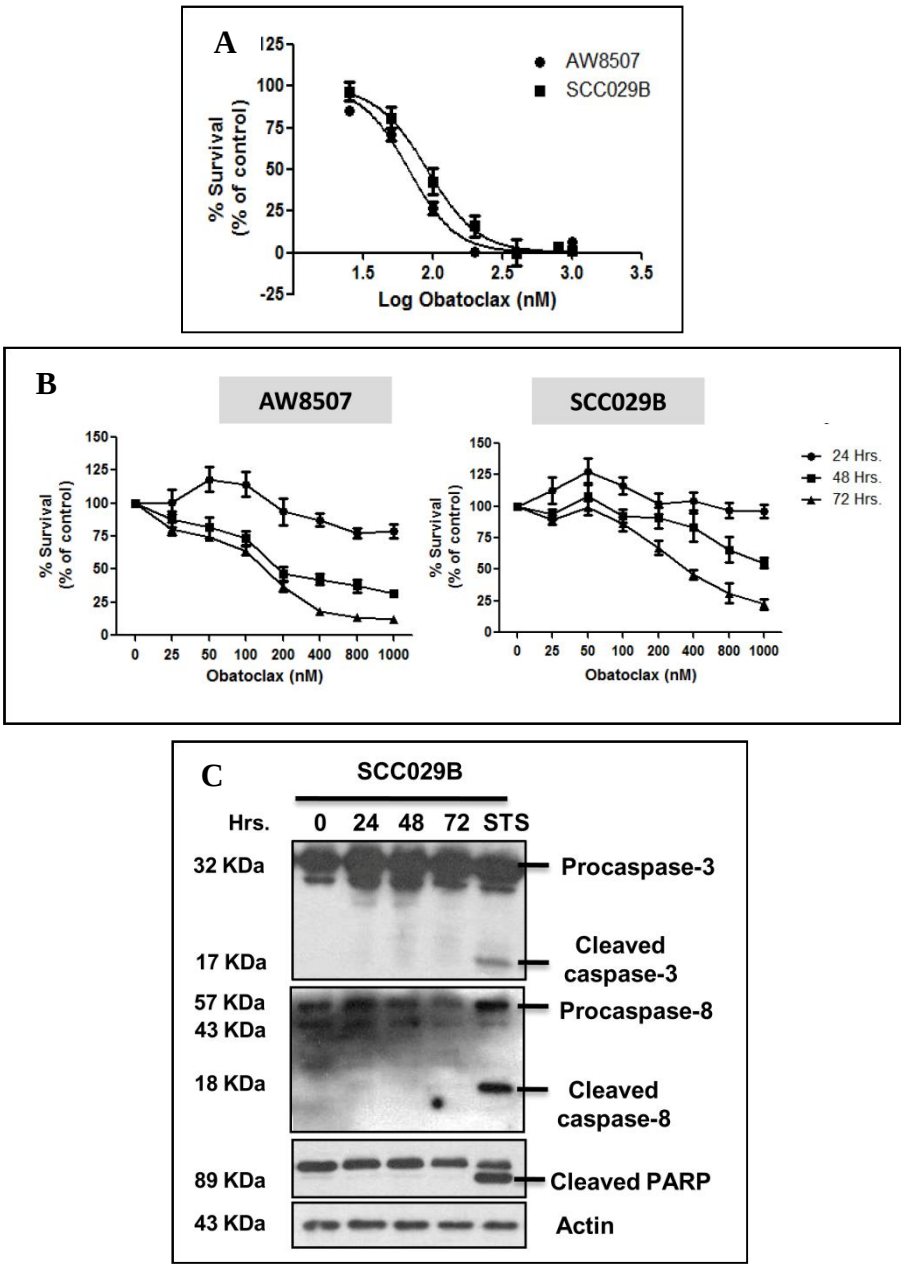

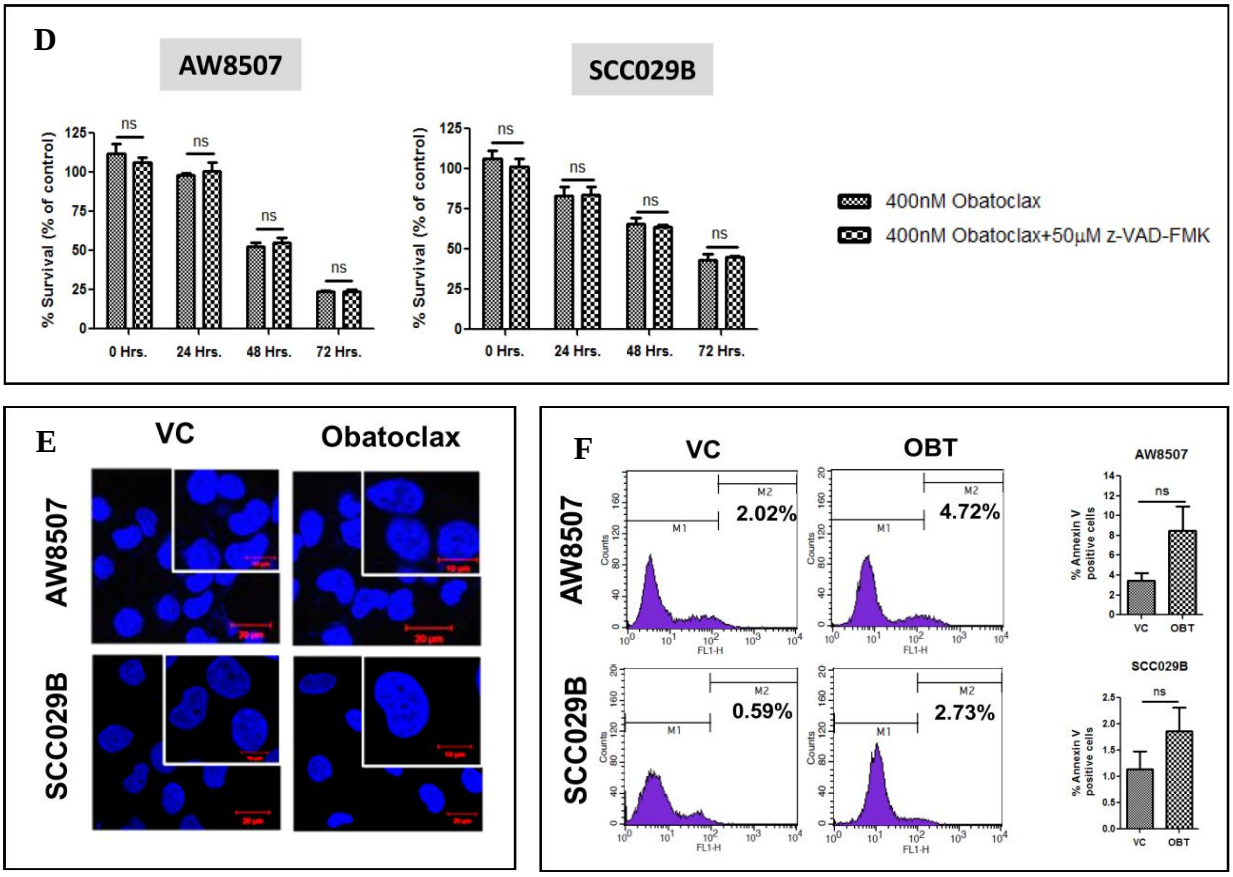

Figure 35: Obatoclax triggers caspase-independent cell death in OSCC cells. A) AW8507 and SCC029B cells were treated with increasing doses of Obatoclax for 72 hours and cell viability was assessed by MTT assay. **B)** The cells were treated with increasing concentrations of Obatoclax for 24, 48 and 72 hours and cytotoxicity was assessed by SRB assay. Cell viability is expressed as percent survival with respect to vehicle control. **C)** SCC029B cells were treated with 400 nM Obatoclax for 0, 24, 48 and 72 hours or 500 nM Staurosporine (STS) for 24 hours. Caspase and PARP cleavage were assessed by western blotting. **D)** The cells were either treated with 400 nM Obatoclax alone or in combination with 50 µM z-VAD-FMK for 24, 48 and 72 hours and cell viability was determined by SRB assay. **E)** The cells were treated with 400 nM Obatoclax for 48 hours and nuclei were stained with DAPI to analyze the nuclear morphology

(Scale bar: 10 µm). **F)** The cells were treated with 400 nM Obatoclax (OBT) for 72 hours or as vehicle control (VC) and the percentage of annexin V positive cells were measured by flow cytometry. Images are representative of three independent experiments. Data is represented as mean ± SEM of three independent experiments; ns indicate not significant.

5.2.4 Obatoclax potently induces autophagy in OSCC cells

ER stress has been implicated in protection of human melanoma cells against the cell death induced by Obatoclax [44]. However, we observed no change in GRP78 (a marker of ER stress) expression, in response to Obatoclax treatment in OSCC cells. BH3-mimetics such as Obatoclax have been shown to induce autophagy in a variety of cancer cells [223-225]. Therefore, we next investigated whether Obatoclax induce autophagy in OSCC cells. Obatoclax-induced autophagy in OSCC cells is evident from the appearance of LC-3BII band (which corresponds to LC-3B lipidation and its incorporation in the autophagosomal membranes). However, there was neither a significant change in Beclin-1 levels nor its subcellular localization. Notably, p62/SQSTM1 protein, a substrate of autophagy showed sustained levels and exhibited a punctate cytoplasmic appearance upon exposure to Obatoclax. The vehicle control cells in contrast, showed a diffuse cytoplasmic staining of p62 (Figure 36 A and B). Autophagy induced by Obatoclax was further quantitated by immunofluorescence microscopy which depicted a significant (***p<0.0001) increase in the appearance of endogenous LC-3B foci in the Obatoclax treated versus control cells (Figure 36 C). Autophagy induced by Obatoclax was also studied in a time course experiment which revealed appearance of numerous LC-3B foci in OSCC cells (Figure 36 D).

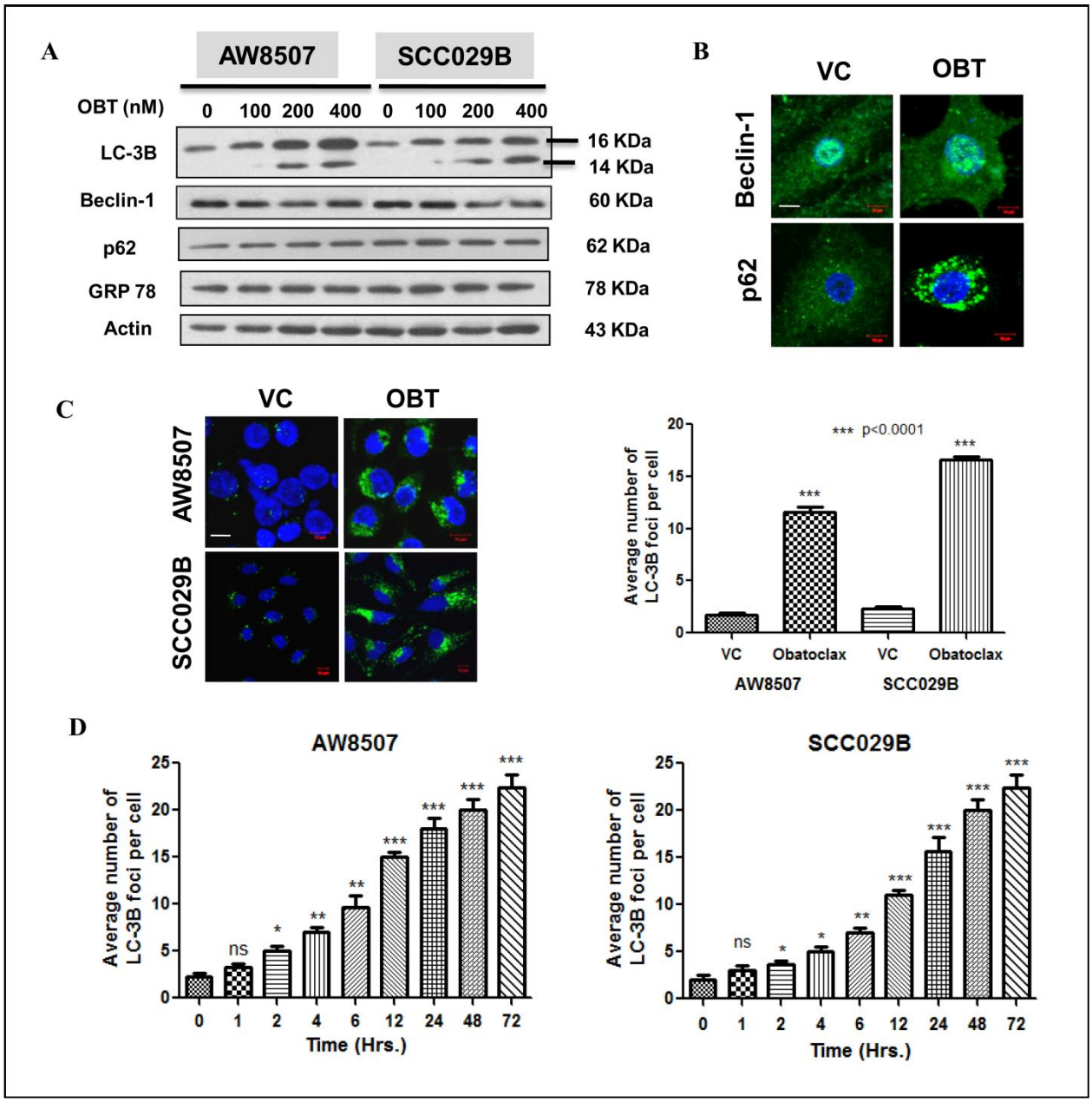

Figure 36: Obatoclax potently induces autophagy in OSCC cells. A) Autophagy induction in OSCC cells is evident from the appearance of LC-3BII band when treated with increasing doses of Obatoclax for 24 hours. Beclin-1, p62 and GRP78 levels did not show significant alterations. **B)** SCC029B cells were either treated as vehicle control (VC) or with 400 nM Obatoclax (OBT) for 24 hours and endogenous Beclin-1 and p62 were detected by immunofluorescence staining

(Scale bar: 10 µm). **C)** Quantitation of autophagy. AW8507 and SCC029B cells were either treated as vehicle control or with 400 nM Obatoclax for 24 hours and endogenous LC-3B was detected by immunostaining. The average number of LC-3B foci were scored in the Obatoclax treated and control cells (Scale bar: 10 µm). **D)** A time course study of autophagy induced by Obatoclax. AW8507 and SCC029B cells were exposed to 400 nM Obatoclax for the indicated time points and average number of LC-3B foci per cell were scored as mentioned above. The data is represented as mean±SEM of three independent experiments. The images are representative of three experiments.

5.2.5 Obatoclax-induced autophagy culminates into cell death

Next, we studied Obatoclax induced autophagy in a time course experiment by LC-3B and p62 immunoblotting. Consistent with the appearance of numerous LC-3B foci in the Obatoclax treated cells, we observed excessive accumulation of LC-3BII and sustained levels of p62 in a time dependent manner. All these observations are suggestive of a defective autophagy (Figure 37 A). To address whether Obatoclax-induced autophagy is death inducing, we downregulated ATG5 (an upstream molecule in the pathway of autophagy critical for the assembly of autophagosomes) by using siRNA and evaluated the Obatoclax-induced autophagy by LC-3BII immunoblotting. ATG5 knockdown significantly reduced the levels of LC-3BII in Obatoclax treated cells (Figure 37 B). Inhibition of autophagy by ATG5 downregulation significantly (**p<0.001) protected both the cell lines from Obatoclax-induced cell death (Figure 37 C). These observations suggest that Obatoclax-induced autophagy ultimately culminates into cell death and is not prosurvival.

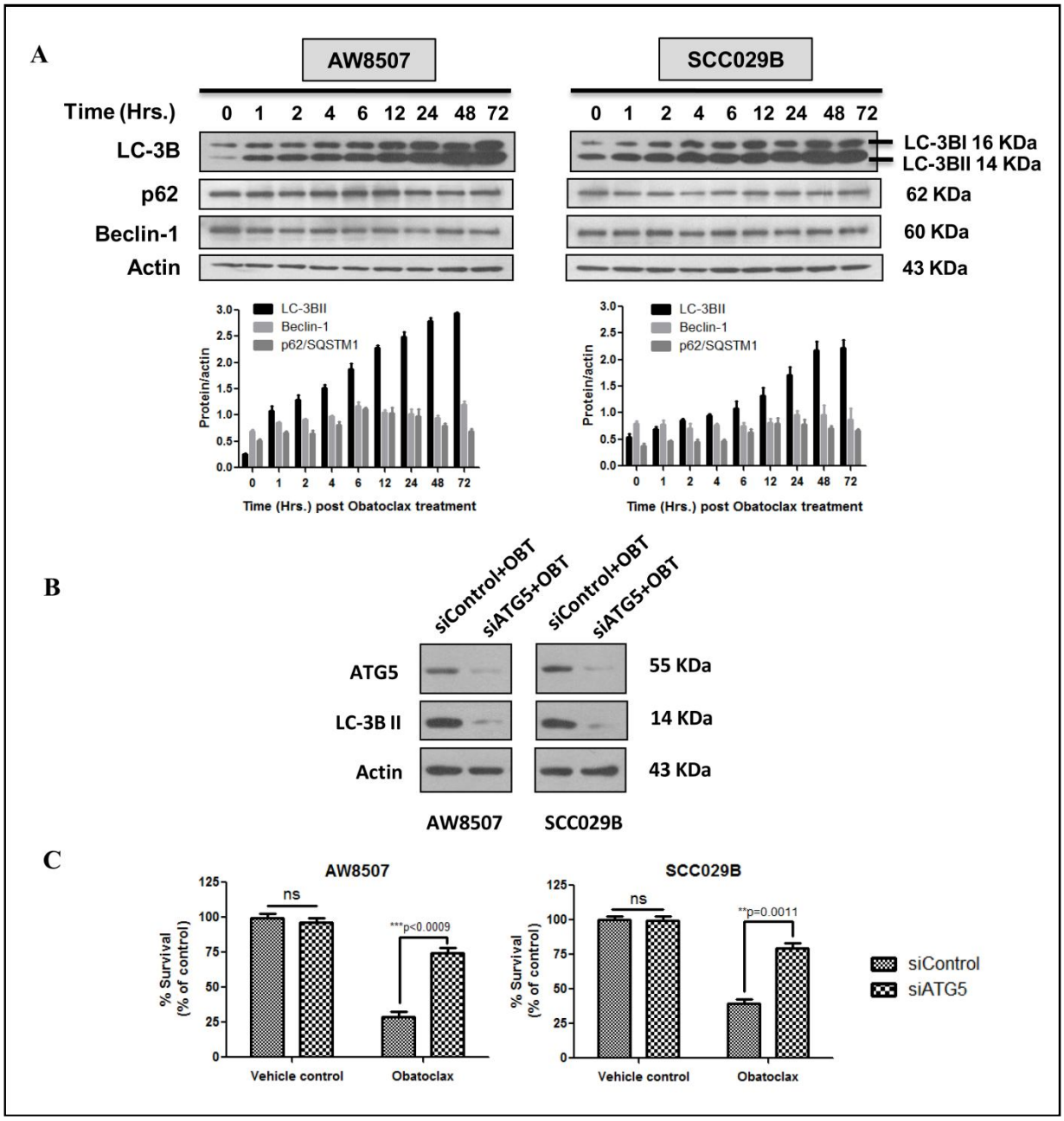

Figure 37: Obatoclax-induced autophagy culminates into cell death. A) A time course study of autophagy induced by Obatoclax revealed bulk accumulation of LC-3BII and sustained levels of p62/SQSTM1. The Beclin-1 levels however did not show significant changes. The

quantitation indicating relative expression of individual proteins obtained by densitometric analysis is represented in the corresponding lowed panels. **B)** AW8507 and SCC029B cells were transfected with 50 nM of either a control/scrambled siRNA (siControl) or siRNA against ATG5 (siATG5). 48 hours post transfection, the cells were treated with 400 nM Obatoclax (OBT) for 24 hours. The levels of LC-3BII were detected by immunoblotting. **C)** The siRNA transfected cells were treated with 400 nM Obatoclax for 72 hours and percent cell viability was determined by SRB assay. Western blots are representative of triplicate experiments. The data is represented as mean±SEM of three independent experiments.

5.2.6 Obatoclax causes a disturbance in autophagic flux leading to a defective autophagy in OSCC cells

To further address whether the excessive accumulation of LC3BII (and the autophagosomes) in response to Obatoclax treatment are a result of their increased formation or reduced clearance of the autophagosomes, we studied the autophagy flux in OSCC cells. We exposed the cells to Chloroquine (50 μM), a lysosomotropic agent, which neutralizes the acidic interior of the lysosomes, thereby inhibiting the activity of lysosomal enzymes and blocking the degradation of the autolysosomal cargo. We observed that Obatoclax and Chloroquine individually induced LC-3BII levels to an equal extent. Whereas, a combination of Obatoclax and Chloroquine induced only a marginal increase (not significant) in LC-3BII levels as compared to either agents alone. These observations indicate that the increased LC-3BII levels in response to Obatoclax treatment are accounted by a block in the terminal degradative phase (Figure 38 A) [226]. By immunofluorescence studies, we confirmed that Obatoclax treatment induces fusion of autophagosomes (LC-3B) with lysosomes (LAMP-1) to form autolysosomes (Figure 38 B). To

further dissect the autophagosome maturation process, we next investigated whether the autolysosomes are functionally competent to degrade the vesicular cargo by tandem fluorescence-tagged LC-3B based reporter [227]. SCC029B cells stably expressing a tandem mCherry/EGFP-LC-3B construct, exhibited yellow-orange (merge of mCherry red and EGFP green) fluorescence upon Obatoclax treatment, indicating functional incompetency of the autolysosomes (The GFP but not mCherry is sensitive to acidic compartment of lysosomes). We observed similar merged yellow-orange fluorescence signal of LC-3B when the cells were exposed to Chloroquine alone or a combination of Obatoclax and Chloroquine indicating a block at the degradation step (Figure 38 C). All these observations together indicate that Obatoclax induced impaired autophagy due to a block in the terminal degradative phase.

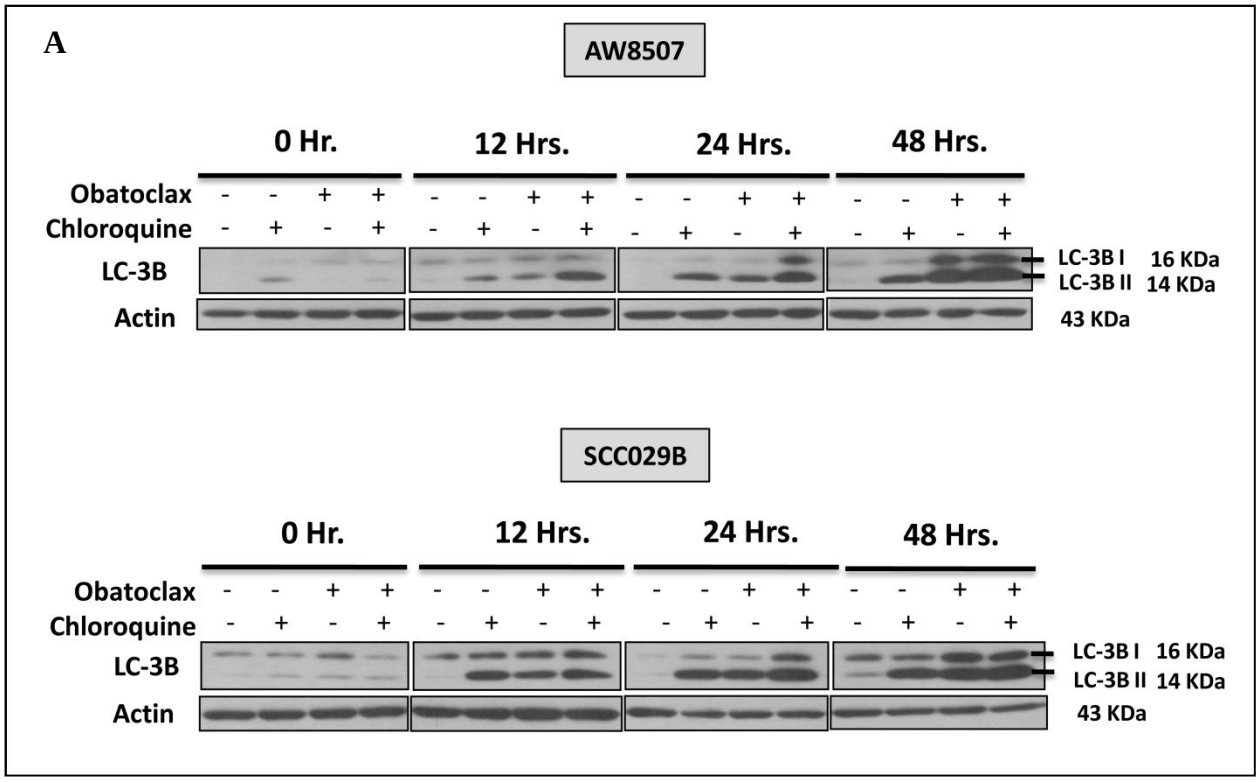

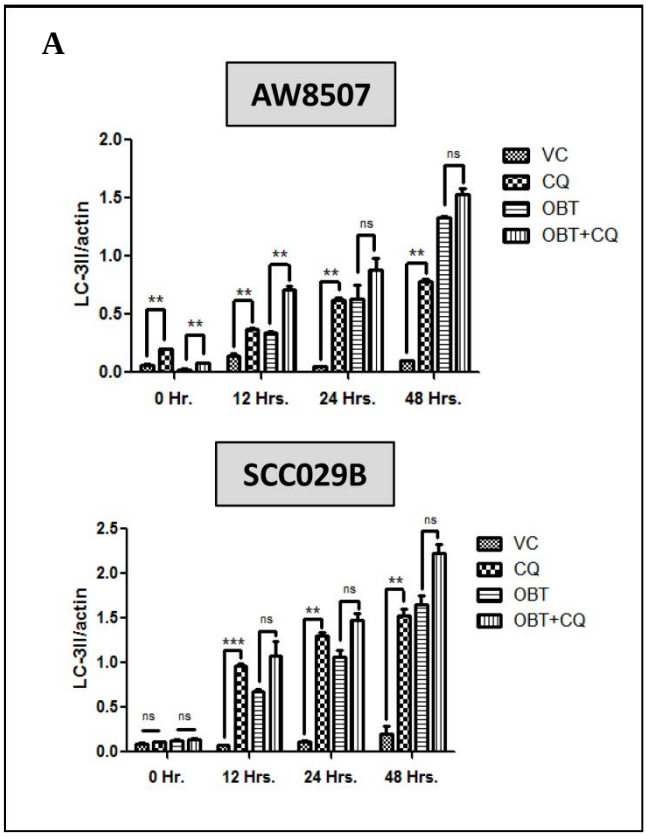
A
AW8507
LC-3II/actin
2.0
1.5
1.0
0.5
0.0
0 Hr.
12 Hrs.
24 Hrs.
48 Hrs.
VC
CQ
OBT
OBT+CQ
SCC029B
2.5

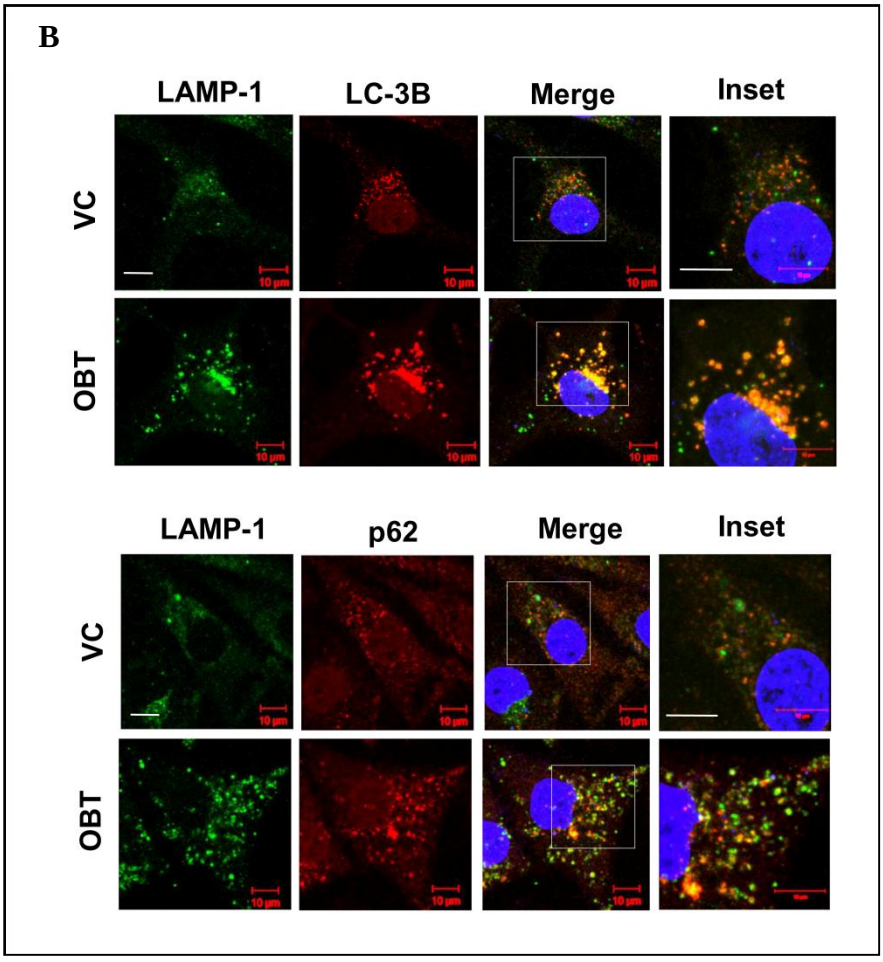
B
LAMP-1
LC-3B
Merge
Inset
VC
OBT
p62

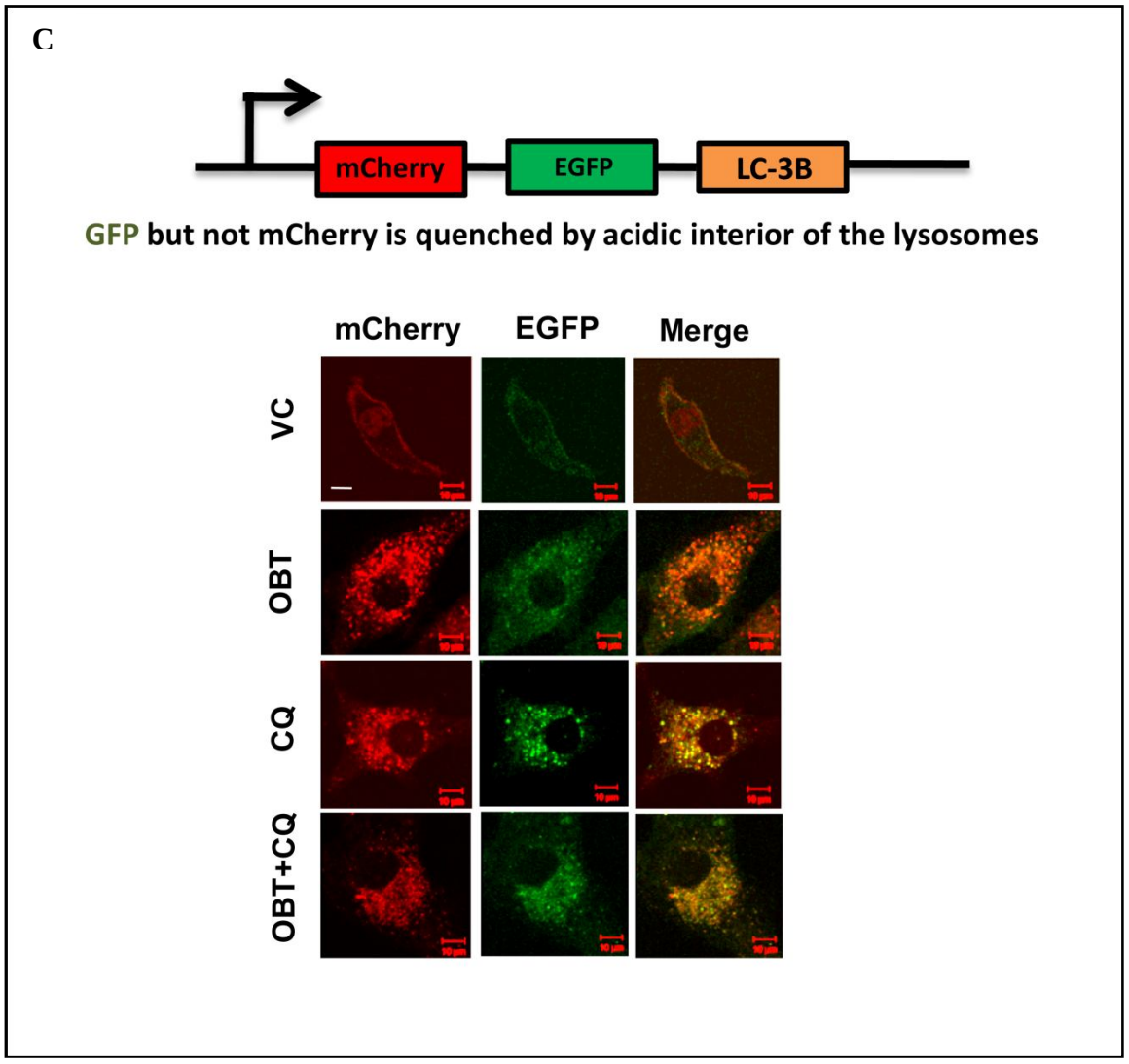

Figure 38: Obatoclax induces a defective autophagy in OSCC cells. A) Time course study of autophagy flux. AW8507 and SCC029B cells were treated with either 50 µM Chloroquine (CQ), 400 nM Obatoclax (OBT), a combination of both or as vehicle control (VC) for the indicated time points and autophagy induction was evaluated by LC-3B immunoblotting. The blots are representative of three independent experiments. The respective densitometric analysis graphs are represented as mean±SEM of three independent experiments (**p<0.01, ***p<0.001).

B) Obatoclax induces fusion of autophagosomes with lysosomes. SCC029B cells were either treated with 400 nM Obatoclax for 48 hours or as vehicle control. Fusion of autophagosomes

(LC-3B: Red) with lysosomes (LAMP-1: Green) appear as yellow-orange dots (due to overlap of red and green) (Scale bar: 10 µm). **C)** Schematic of the pBABE-puro mCherry-EGFP-LC3B construct. SCC029B cells stably expressing the construct were either treated with 50 µM Chloroquine, 400 nM Obatoclax, a combination of both or as vehicle control for 48 hours and the cells were imaged using a fluorescence confocal microscope (Scale bar: 10 µm).

5.2.7 Obatoclax-induced cell death in OSCC cells is mediated by necroptosis

Having shown that Obatoclax induced a caspase-independent, non-apoptotic cell death in OSCC cells, we looked for the cell death pathway linked to autophagy. It has been reported by several groups that defective autophagy in response to a variety of stress stimuli often leads to cell death via necroptosis [203, 228]. We therefore investigated whether necroptosis is involved in the cell death mediated by Obatoclax in OSCC cells. Obatoclax treated cells exhibited appearance of extensive cytoplasmic vacuolation, characteristic of cells under stress (Figure 39 A). Recruitment of RIP1K and RIP3K at the necrosome is an important event during necroptosis. Here we demonstrate that Obatoclax induced the association of p62 with key components of the necrosome RIP1K, RIP3K, and FADD by colocalization and coimmunoprecipitation (Figure 39 B and C). Moreover, treatment with Necrostatin-1 (Nec-1), a RIP1K inhibitor, protected the cells from Obatoclax-induced cell death (Figure 39 D). Obatoclax thus appears to induce cell death in OSCC cells by necroptosis.

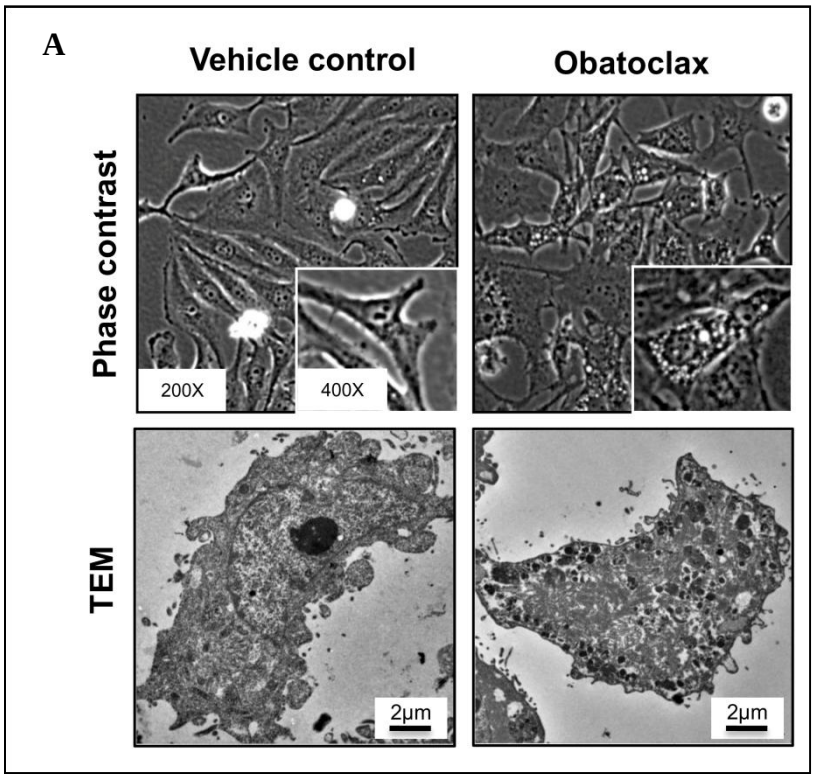
A
Vehicle control
Obatoclax
Phase contrast
200X
400X
TEM
2µm
2µm

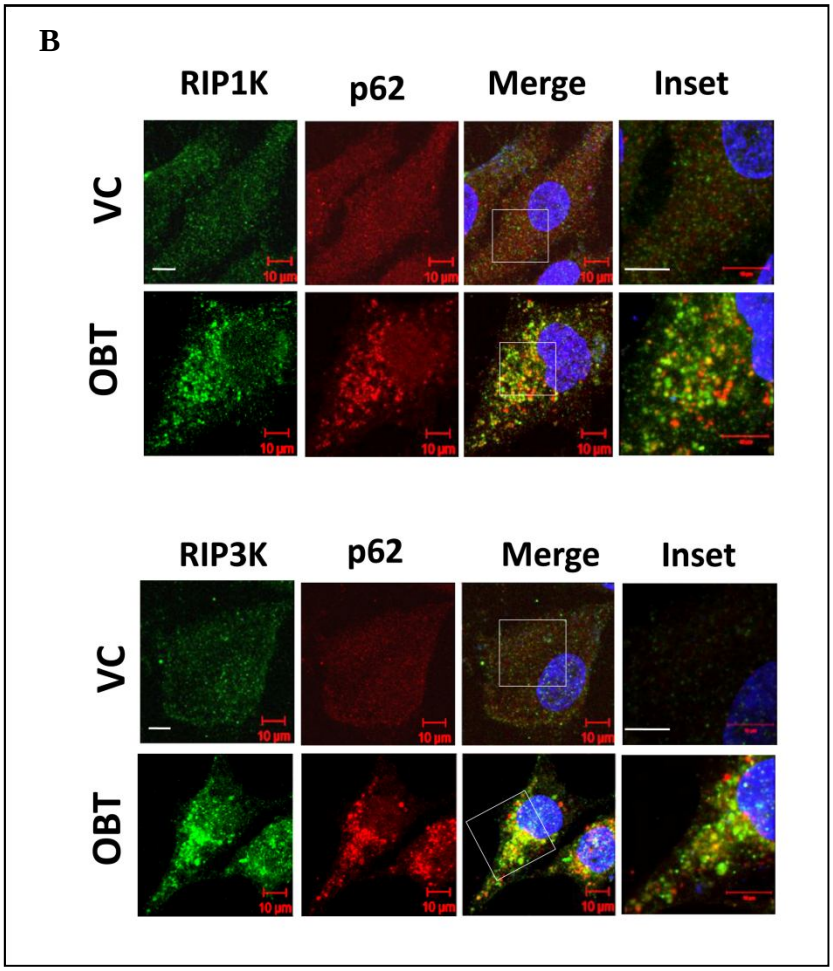
B
RIP1K
p62
Merge
Inset
VC
OBT
RIP3K
p62
Merge
Inset
VC
OBT

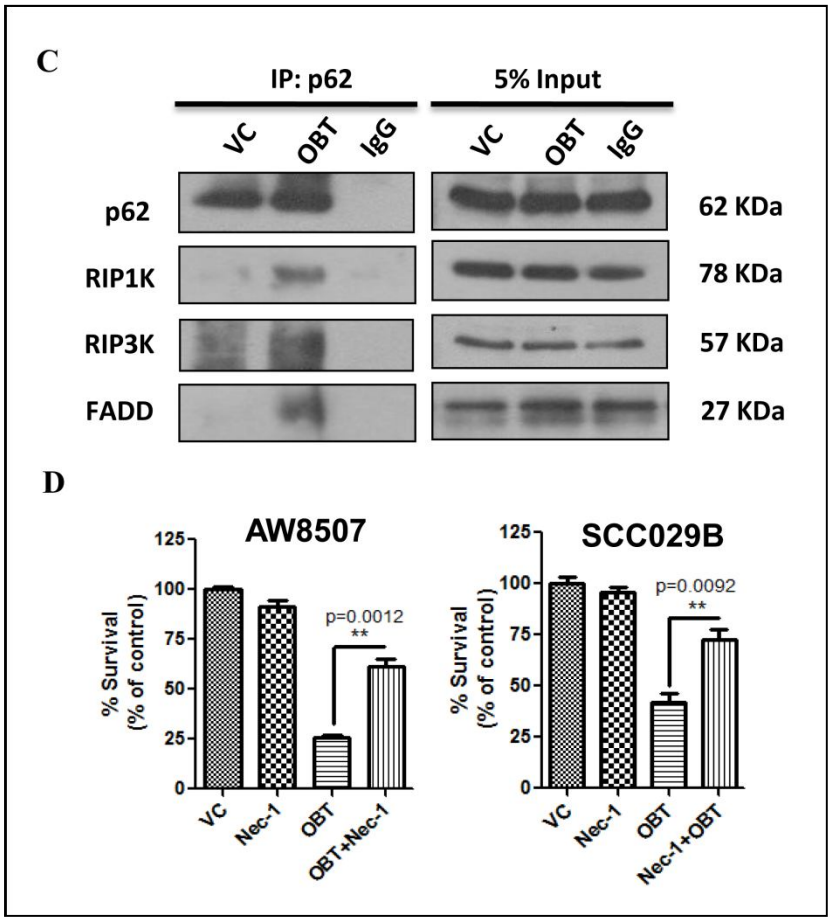

Figure 39: Obatoclax induces necroptosis in OSCC cells. SCC029B cells were either treated as vehicle control (VC) or exposed to 400 nM Obatoclax (OBT) for 48 hours. **A)** The morphology (Phase-contrast microscopy) and ultrastructure (TEM) of control and Obatoclax treated SCC029B cells. **B)** A colocalization of p62 with RIP1K and RIP3K in Obatoclax treated SCC029B cells indicate assembly of necrosomal complexes (Scale bar: 10 µm). **C)** The cell lysates of Obatoclax treated and vehicle control cells were subjected to coimmunoprecipitation using p62 antibody. IgG: Isotype control antibody. The immunoprecipitates were immunoblotted for p62, RIP1K, RIP3K and FADD. **D)** AW8507 and SCC029B cells were treated with 400 nM Obatoclax, 50 µM Necrostatin-1 (Nec-1) or a combination of both for 48 hours and cell viability was quantified by SRB assay. Data is represented as mean±SEM of three independent experiments. Images are representative of three independent experiments.

5.2.8 Obatoclax induces extensive fragmentation of the mitochondrial network

Given the fact that MCL-1 is critical for mitochondrial homeostasis [92] and that putative MCL-1-specific inhibitors induce mitochondrial fragmentation [188], we speculated that Obatoclax could possibly deteriorate the organization of the mitochondrial network through MCL-1 inhibition. Obatoclax caused disruption of the mitochondrial network which involved extensive fragmentation, significant (*$p<0.05$) increase in mitochondrial fission and perinuclear aggregation in a time course study. The aberrations in the mitochondrial network initiated at about 12 hours post Obatoclax treatment and appeared much earlier than the phenotypic changes associated with the cell death (Figure 40 A and B). Necroptosis is believed to execute cell death by inducing mitochondrial stress as one of the principal effector mechanism [206]. To investigate whether Obatoclax induced mitochondrial fragmentation occurs downstream of necroptosis, we treated SCC029B cells with Obatoclax in the presence or absence of RIP1K inhibitor Necrostatin-1 and assessed its effect on the mitochondrial network by HSP60 immunostaining. Blocking RIP1K activity did not prevent mitochondrial fragmentation caused by Obatoclax, indicating that it occurs upstream to and independent of necroptosis (Figure 40 C). Mitochondrial stress has also been implicated as an effector mechanism of autophagy induction. Therefore, to investigate whether the mitochondrial stress induced by Obatoclax is a result of autophagy, we blocked autophagy upstream by knockdown of ATG5. We observed that blocking autophagy did not prevent the mitochondrial fragmentation, indicating that it occurs either independent or upstream of autophagy (Figure 40 D).

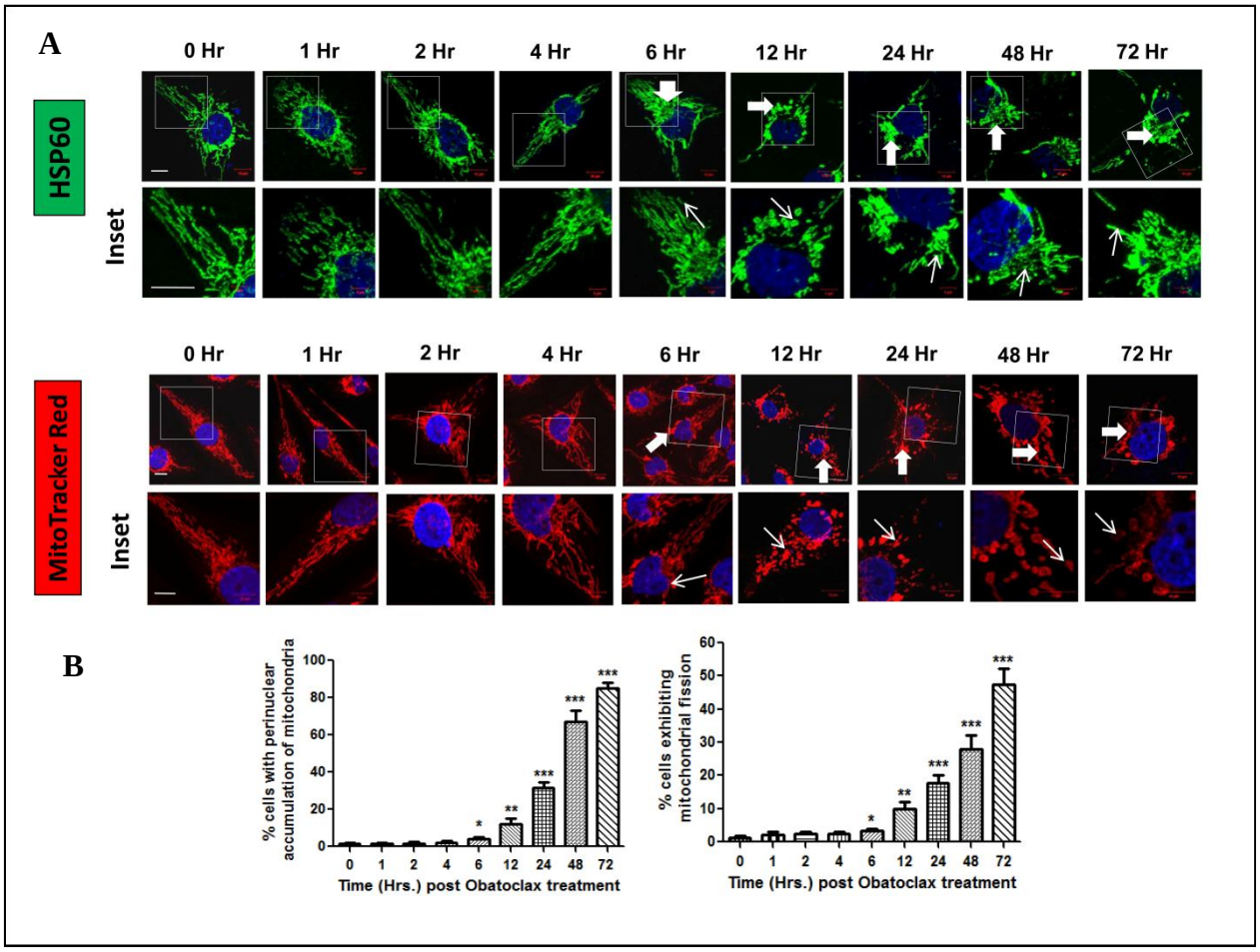
A
0 Hr
1 Hr
2 Hr
4 Hr
6 Hr
12 Hr
24 Hr
48 Hr
72 Hr
HSP60
Inset
MitoTracker Red
Inset
B
% cells with perinuclear accumulation of mitochondria
Time (Hrs.) post Obatoclax treatment
% cells exhibiting mitochondrial fission
Time (Hrs.) post Obatoclax treatment

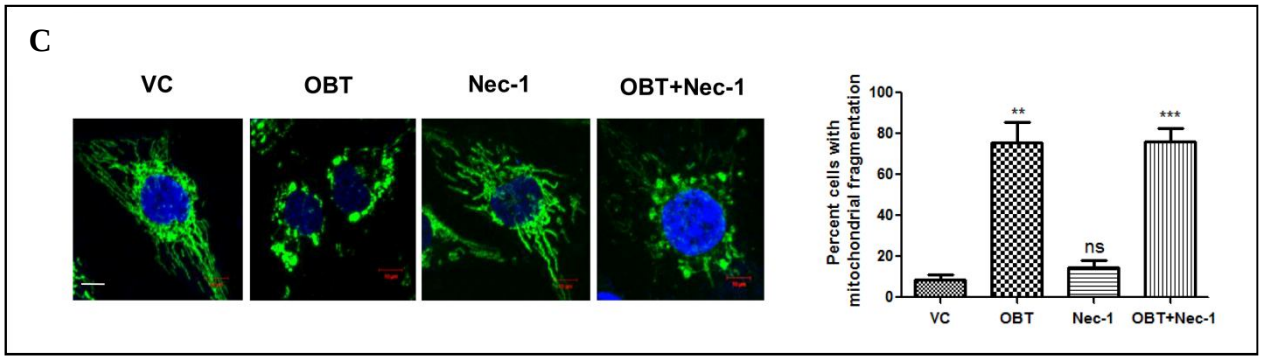
C
VC
OBT
Nec-1
OBT+Nec-1
Percent cells with mitochondrial fragmentation
ns

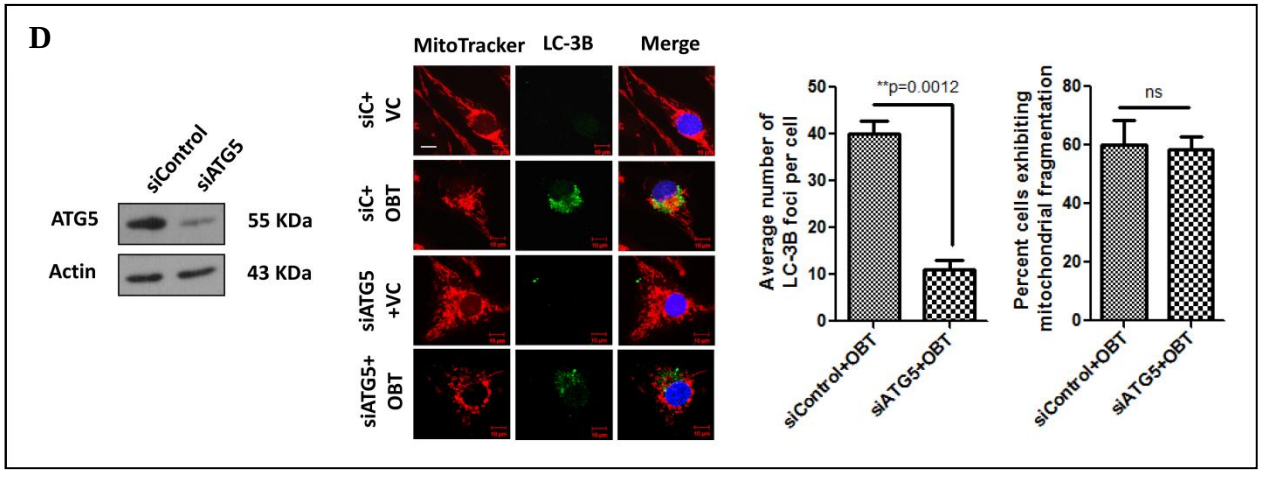
D
siControl
siATG5
ATG5
55 KDa
Actin
43 KDa
MitoTracker
LC-3B
Merge
siC+ VC
siC+ OBT
siATG5 +VC
siATG5+ OBT
Average number of LC-3B foci per cell
**p=0.0012
siControl+OBT
siATG5+OBT
Percent cells exhibiting mitochondrial fragmentation
ns
siControl+OBT
siATG5+OBT

Figure 40: Obatoclax induces mitochondrial fragmentation in OSCC cells. A) SCC029B cells were treated with 400 nM Obatoclax for the indicated time points followed by either immunostaining for HSP60 or staining the cells with MitoTracker Red CMX ROS dye and the nuclei were counterstained with DAPI. The cells were observed under a laser confocal microscope. The mitochondrial morphology is evident in the upper panels. The enlarged images are represented in the corresponding lower panels. **B)** The percentage of cells showing perinuclear aggregation of mitochondria (indicated in the upper panels by thick white arrows) and those showing mitochondrial fragmentation (indicated by thin white arrows in the lower panels) were determined by counting 10 microscopic fields (each containing at least 10–15 cells) per time point. **C)** SCC029B cells were treated with either 400 nM Obatoclax (OBT), 50 µM Necrostatin-1 (Nec-1), a combination of both or as vehicle control (VC) for 48 hours, immunostained for HSP60 and the percentage of cells exhibiting mitochondrial fragmentation was determined as described above. **D)** SCC029B cells were either transfected with 50 nM ATG5 siRNA (siATG5) or control siRNA (siC). 48 hours post transfection, the cells were treated with either 400 nM Obatoclax (OBT) or as vehicle control (VC) for 24 hours. The percentage of cells exhibiting mitochondrial fragmentation and average number of LC-3B foci per cell were scored as described earlier. The data for all experiments is represented as mean±SEM of three independent experiments (ns: not significant, $*p<0.05$, $**p<0.01$, $***p<0.0001$). The images are representative of three independent experiments (Scale bar: 10 µm).

5.2.9 Obatoclax induces mitochondrial oxidative stress and mitochondrial membrane depolarization in OSCC cells

BNIP3 is a BH3-only protein of the BCL-2 family which plays a key role in impairment of the mitochondrial oxidative phosphorylation, reduction in the mitochondrial membrane potential (ΔΨm) and mitophagy under stressful conditions [229]. We therefore analyzed the expression of BNIP3 by real time PCR and observed that Obatoclax induced a significant increase (*p<0.05) in the expression of BNIP3 in SCC029B cells (Figure 41 A). BNIP3 induction during stressful conditions leads to increased mitochondrial oxidative stress. We therefore investigated whether Obatoclax induced ROS accumulation in mitochondria by using MitoSOX Red dye (MitoSOX Red dye specifically accumulates in mitochondria which upon oxidation by superoxide radicals exhibit red fluorescence). Live cell imaging experiment revealed that a significantly (***p<0.0001) higher percentage of Obatoclax treated cells exhibited MitoSOX Red fluorescence as compared to the control cells. This red fluorescence specifically localized to the perinuclear position consistent with the observation that mitochondria under stressful conditions exhibit perinuclear aggregation (Figure 41 B and C). We also noticed a reduction in the fluorescence signal intensity of MitoTracker Green dye in the Obatoclax treated cells possibly because of a drop in ΔΨm. The increased mitochondrial ROS accumulation was also evident by flow cytometry, depicted by an increased proportion of MitoSOX Red positive cells upon Obatoclax treatment (Figure 41 D). BNIP3 induction is also associated with a drop in ΔΨm. We therefore analyzed changes in ΔΨm by using JC-1 dye. As compared to the vehicle control, exposure of SCC029B cells to Obatoclax induced depolarization of the mitochondrial membrane reflected by a significant (***p<0.0001) increase in green to red fluorescence ratio of JC-1 dye. Increase in green fluorescence of JC-1 dye (due to JC-1 monomers) indicates a drop in ΔΨm

whereas increased red fluorescence (due to JC-1 aggregates) corresponds to a stable ΔΨm and thus represents functional mitochondria (Figure 41 E). Finally, we measured a time-dependent decrease in the mitochondrial function upon Obatoclax treatment in OSCC cells by MTT assay (Figure 41 F). All these observations point towards mitochondrial dysfunction upon Obatoclax treatment.

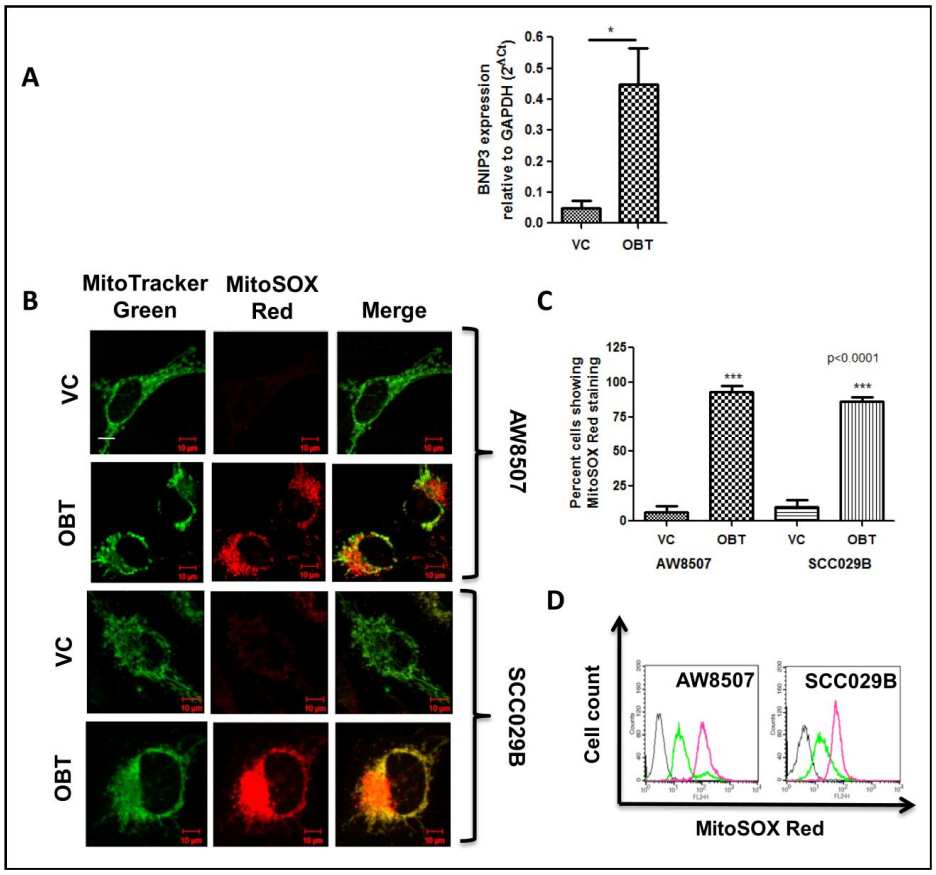

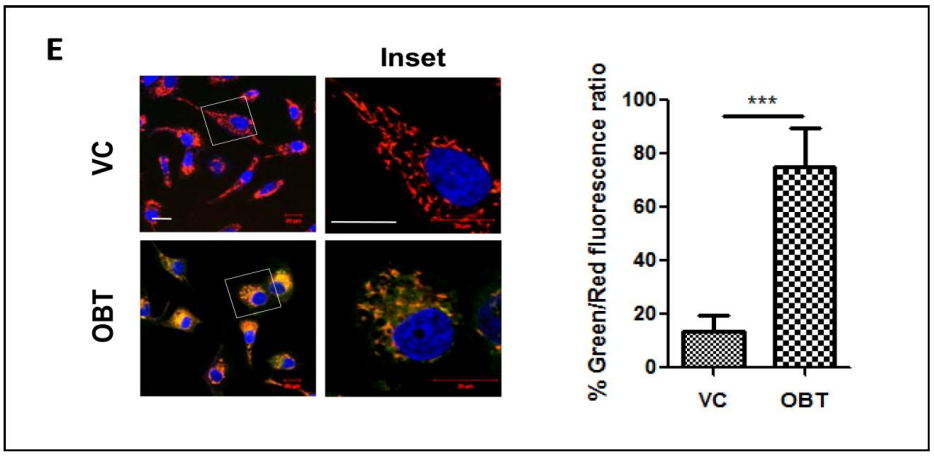

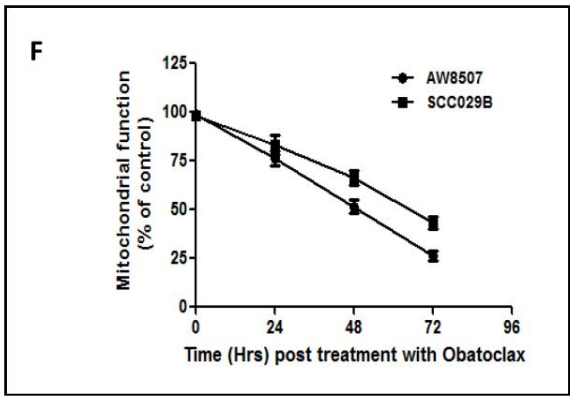

Figure 41: Obatoclax induces oxidative stress and membrane depolarization in the mitochondria of OSCC cells. AW8507 and SCC029B cells were treated with 400 nM Obatoclax (OBT) for 48 hours or as vehicle control (VC). **A)** The expression of BNIP3 was analyzed by real time PCR in SCC029B cells and expressed relative to GAPDH by $2^{-\Delta Ct}$ method. **B)** AW8507 and SCC029B cells grown in confocal dishes were treated with Obatoclax or as vehicle control followed by staining with MitoTracker Green and MitoSOX Red. Images were acquired on a fluorescence confocal microscope (Scale bar: 10 µm). **C)** The percentage of cells exhibiting MitoSOX Red fluorescence was determined by counting 10 different microscopic fields (each containing at least 10–15 cells) per condition. **D)** Following drug treatment, the cells were stained with 5 µM MitoSOX Red dye and the amount of ROS accumulation in mitochondria was measured by flow cytometry on FL2 channel. The gray curve on extreme left indicates unstained cells, the green and pink curves represent vehicle control and Obatoclax treated cells respectively. The histogram plots are representative of three independent experiments. **E)** The Obatoclax treated and vehicle control cells were stained with JC-1 dye and Hoechst dye (stains nuclei). The percent Green/Red fluorescence intensity ratio was quantified by counting 10 different microscopic fields each containing at least 10 cells (Scale bar: 20 µm). Obatoclax induced mitochondrial membrane depolarization is indicated by a significant increase in the green/red fluorescence ratio of JC-1 dye as compared to the control cells. The red

fluorescence was restricted to the mitochondria due to JC-1 aggregates and is indicative of a stable ΔΨm i.e. polarized mitochondria. The green fluorescence was diffused and corresponds to JC-1 monomers and indicates a drop in ΔΨm i.e. depolarized mitochondria. **F)** Mitochondrial dysfunction measured by MTT assay. AW8507 and SCC029B cells were treated with 400 nM Obatoclax for 0, 24, 48 and 72 hours. The amount of reduced formazon dye is represented as percent mitochondrial function. Data is represented as mean ± SEM of three independent experiments.

5.2.10 Obatoclax-induced mitochondrial stress does not culminate into mitophagy

Upregulation of BNIP3 expression in response to stressful conditions often lead to Mitophagy (Selective engulfment of mitochondria) [230, 231]. Moreover, mitophagy has also been linked to necroptosis [232]. We therefore investigated whether Obatoclax-induced mitochondrial stress lead to their selective elimination through mitophagy. Mitophagy leads to a decrease in the mitochondrial mass due to selective elimination of the mitochondria. We therefore measured the functional mitochondrial mass by MitoTracker Green staining followed by flow cytometry. However, we observed no significant decrease in the MitoTracker Green staining intensity upon treatment with Obatoclax. The marginal drop in the MitoTracker Green fluorescence could be attributed to the Obatoclax-induced drop in the Mitochondrial membrane potential (Figure 42 A). Moreover, treatment of SCC029B cells with Obatoclax led to extensive fragmentation of the mitochondrial network. However, these fragmented mitochondria did not colocalize with LC-3B foci i.e. autophagosomes, indicating absence of functional mitophagy (Figure 42 B and C).

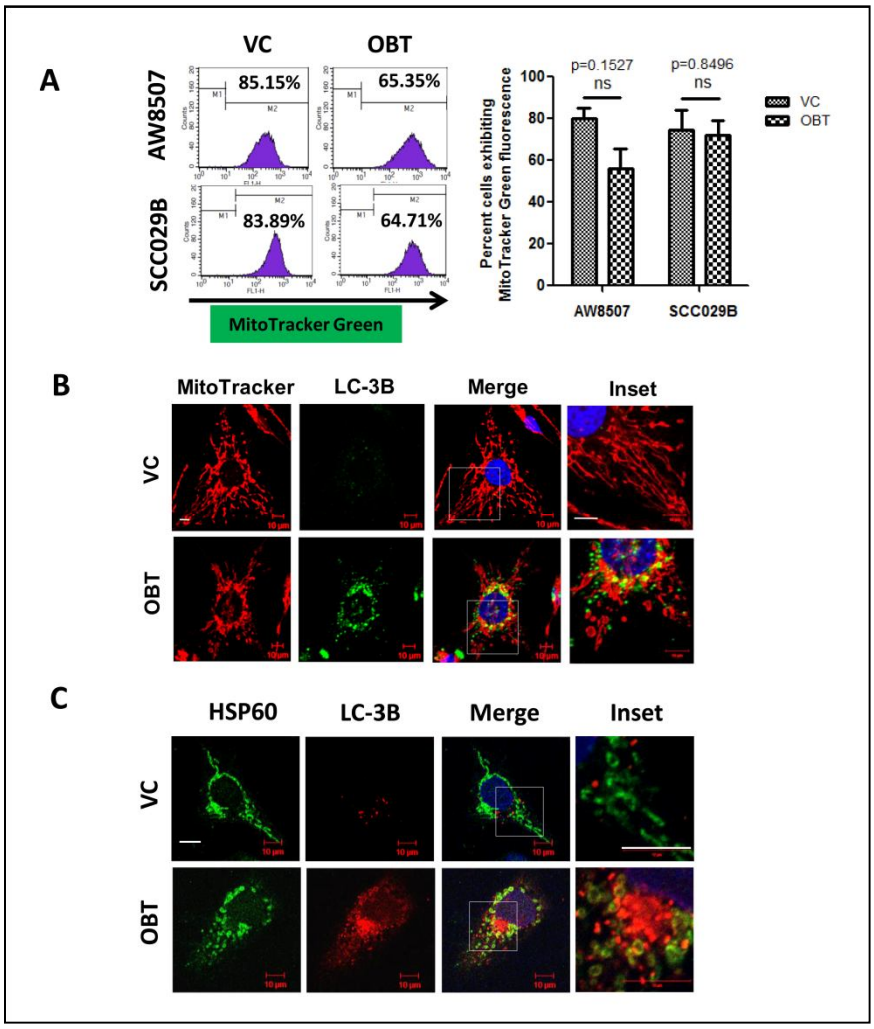

Figure 42: Obatoclax does not induce mitophagy. SCC029B cells were exposed to 400 nM Obatoclax (OBT) for 48 hours or treated as vehicle control (VC). **A)** The cells were stained with MitoTracker Green FM dye followed by acquisition on FL-1 channel of flow cytometer. The percentage of cells exhibiting MitoTracker Green fluorescence was quantified from 3 independent experiments (ns: not significant). **B)** The mitochondria were stained with MitoTracker Red CMXROS dye and endogenous LC-3B foci were immunostained with LC-3B antibody. **C)** The mitochondria (HSP60) and LC-3B foci were immunostained with the respective antibodies. The fragmented mitochondria did not colocalize with LC-3B foci (i.e. autophagosomes) (Scale bar: 10 µm).

5.2.11 MCL-1 downregulation induces mitochondrial stress in SCC029B cells

To investigate the role of MCL-1 in mitochondrial homeostasis, we transiently knocked down MCL-1 by using siRNA in SCC029B cells. SCC029B cells as discussed earlier expressed relatively lower levels of BCL-2 and BCL-XL as compared to MCL-1. MCL- 1 knockdown in these cells resulted in a significant (***p=0.0006) increase in mitochondrial fragmentation (Figure 43 A). We also observed a significant (*p<0.05) increase in the MitoSOX Red staining in siMCL-1 transfected cells as compared to siControl cells (Figure 43 B). Furthermore, MCL-1 downregulation resulted in a significant (*p<0.05) decrease in ΔΨm as compared to the control siRNA transfected cells (Figure 43 C). All these observations indicate a potential role of MCL-1 in maintaining mitochondrial homeostasis in these cells.

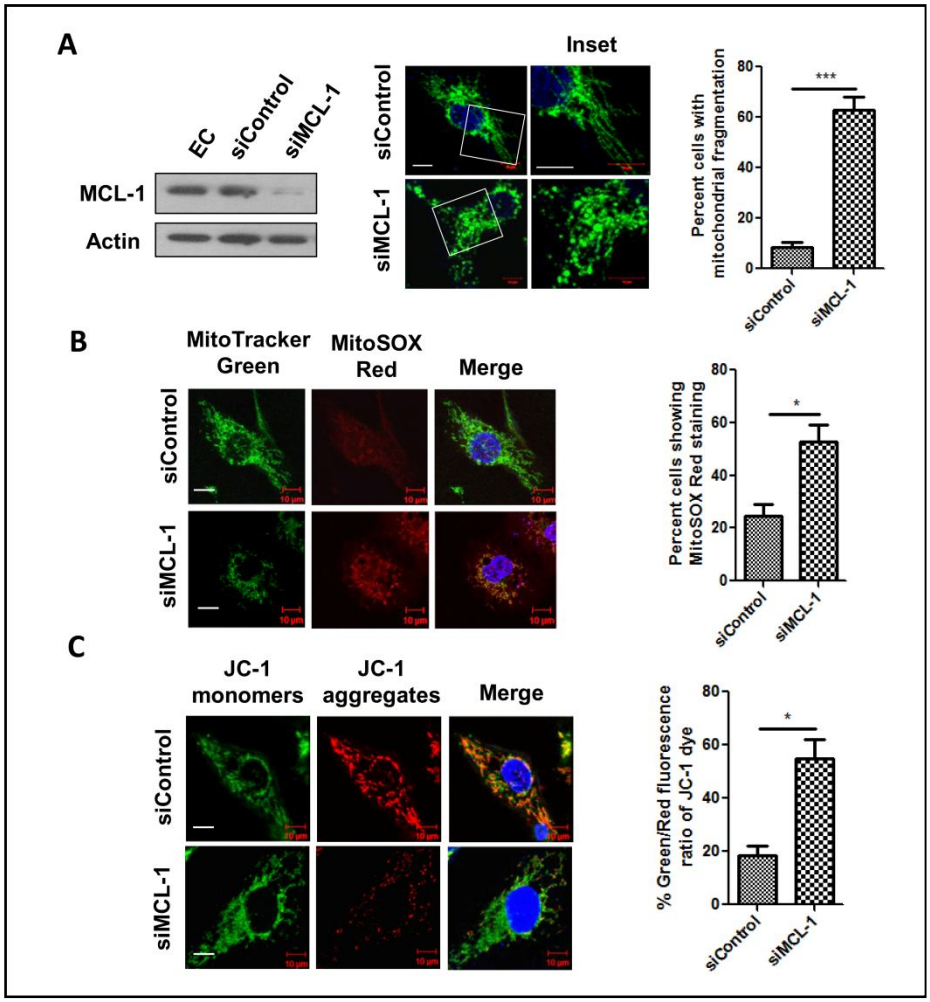

Figure 43: MCL-1 downregulation induces mitochondrial stress in SCC029B cells. SCC029B cells were transfected with 50 nM control siRNA and 50 nM MCL-1 siRNA. 48 hours post transfection, the cells were used for experimental analysis. **A)** The cell lysates were subjected to western blotting for the detection of MCL-1 and β-actin. Alternatively, the siRNA transfected cells were immunostained for HSP60 and observed under a confocal microscope. The percentage of cells showing mitochondrial fragmentation was determined as described earlier. **B)** The siRNA transfected cells were stained with MitoTracker green, MitoSOX Red and Hoechst dyes and observed under a confocal microscope. **C)** The siRNA transfected cells were stained with JC-1 dye and analyzed for change in percent green to red fluorescence intensity ratio of JC-1 dye as discussed earlier. Data is represented as mean±SEM of three independent experiments (Scale bar: 10 μm). Images are representative of three independent experiments.

5.2.12 Ultrastructural changes induced by Obatoclax

Obatoclax induced severe ultrastructural anomalies in OSCC cells. Numerous autophagic vesicles containing electron dense materials, proteinaceous inclusions and degenerating cellular organelles were readily visible throughout the cytoplasm. The autophagic vesicles at various stages of maturation ranging from initiating phagophore, autophagosomes, amphiosomes and autolysosomes were morphologically recognizable. Extensive cytoplasmic vacuolation was also apparent and intact mitochondria were not readily detectable. On the contrary, control cells exhibited numerous mitochondria (with intact inner and outer membranes and distinct cristae) and few cytoplasmic vacuoles (Figure 44).

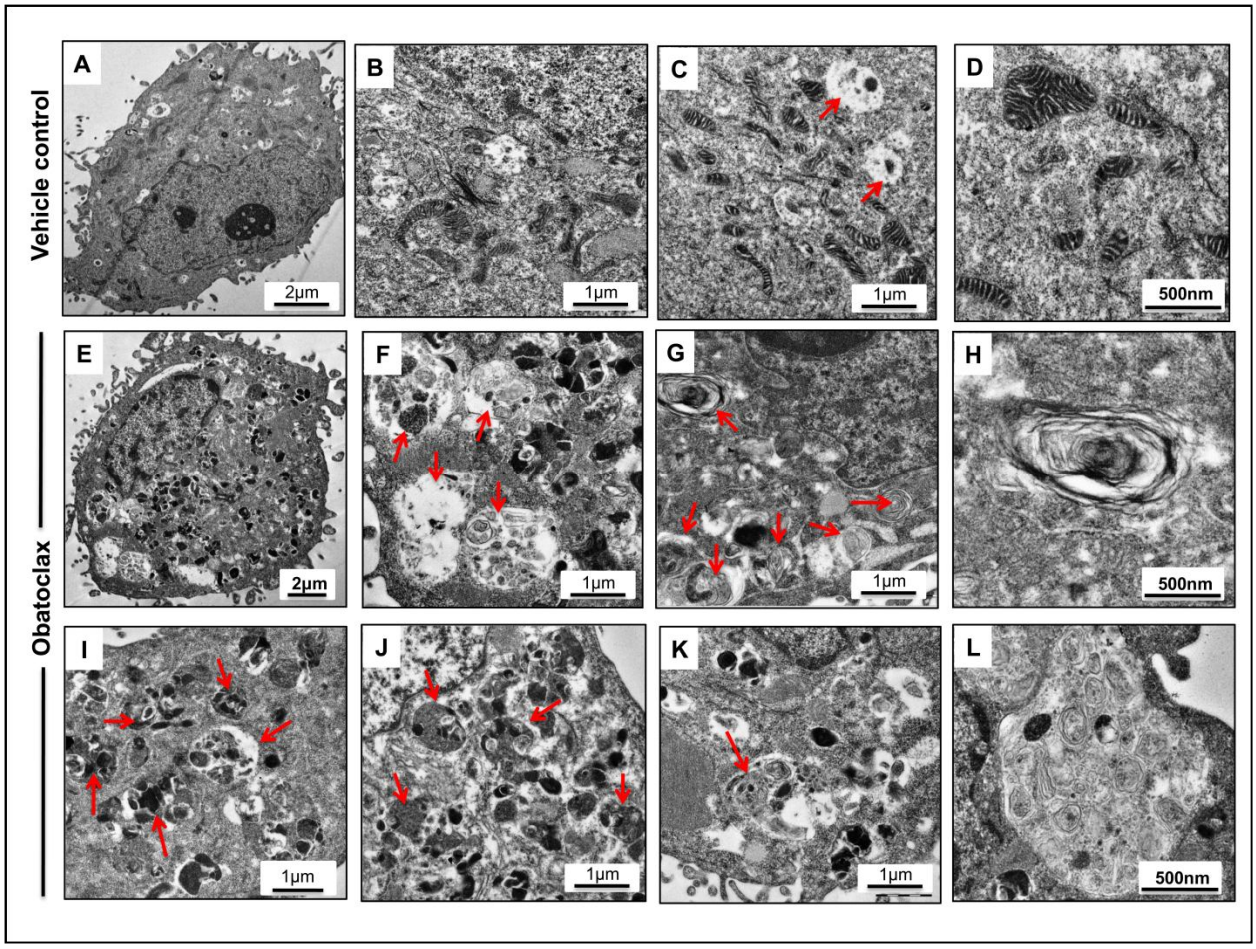

Figure 44: Ultrastructural changes induced by Obatoclax. SCC029B cells when treated with 400 nM Obatoclax for 48 hours induced appearance of numerous autophagic vesicles (Red arrows) containing various cargos. Extensive cytoplasmic vacuolation was apparent with accumulation of electron dense proteinaceous inclusions. Intact mitochondria (those with distinct cristae and internal membranes) were not readily detectable (**E**–**L**). Vehicle control cells on the other hand exhibited significantly less cytoplasmic vacuolation and presence of numerous intact mitochondria with distinct cristae (**A**–**D**).

5.2.13 Obatoclax exhibits potent antitumor activity in xenograft mouse models

Potent single agent antitumor activity of Obatoclax was observed against SCC029B cell line derived subcutaneous tumors in xenograft mouse model. We observed a significant (*p<0.05) reduction in the mean tumor volume (Figure 45 A) without a significant decrease in the weight of the animals (Figure 45 B). The effect was dose dependent with maximal activity observed at the cumulative dose of 5 mg/kg.

A

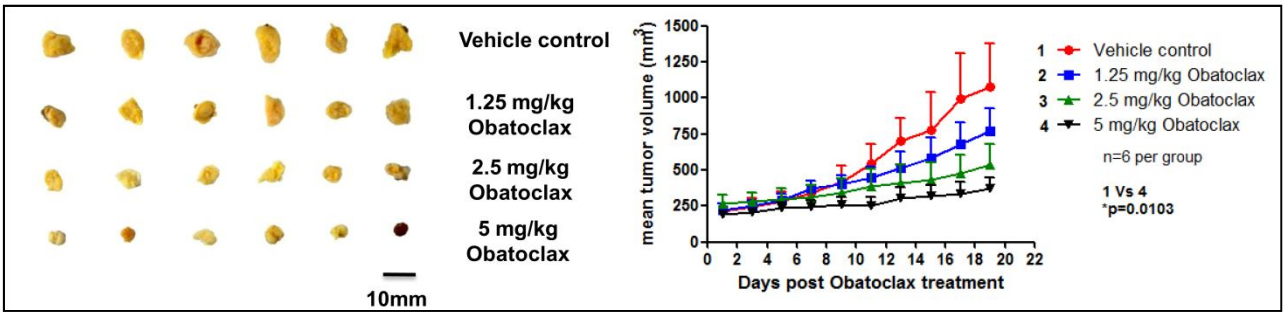

B

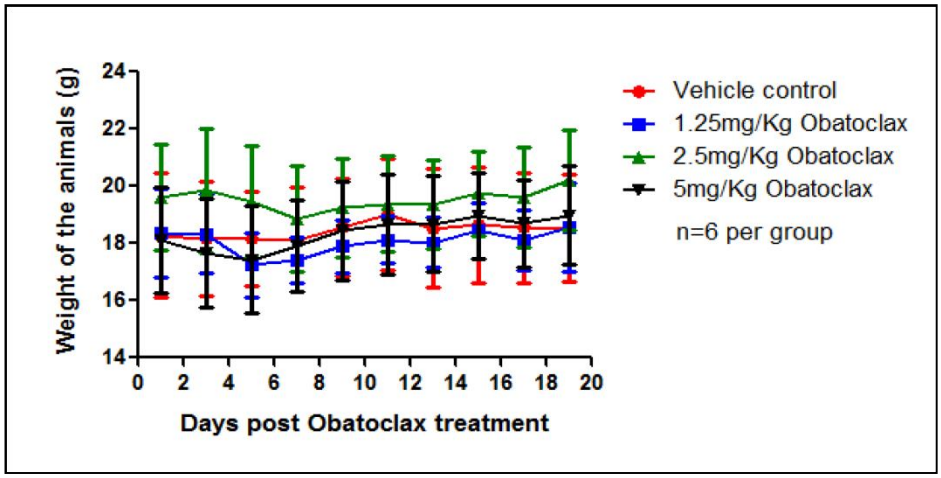

Figure 45: *In vivo* efficacy of Obatoclax. A) Female BALB/C Nude mice bearing subcutaneous tumors derived from SCC029B cell line were administered a cumulative dose of the drug as indicated distributed evenly over a period of five consecutive days. Tumor volumes were measured for a period of 15–20 days post drug administration. The data is expressed as mean+SEM of the mean tumour volumes for each group (six animals per group). **B)** Obatoclax

does not exhibit toxicity in the animals. Weight of the animals was monitored every alternate day post Obatoclax administration upto about 18-20 days. Obatoclax did not exhibit a significant change in the weight of the animals in either a dose or time-dependent manner which is indicative of absence of toxicity in the animals.

5.2.14 Obatoclax exhibits synergism with ionizing radiation to inhibit the clonogenic potential of OSCC cells

Consistent with previous observations from our laboratory that MCL-1 is a critical radioresistance related protein in OSCC cells [23, 25], we sought to test the potency of a combination of Obatoclax with ionizing radiation (IR). From the clonogenic assays, we observed that as compared to radiation alone, the combination treatment significantly (*p<0.05) inhibited the colony formation in the three OSCC cell lines (Figure 46 A). Moreover, we observed a significant growth inhibition when the cells were exposed to a combination of IR and Obatoclax as opposed to radiation alone across a range of IR doses (2 Gy, 4 Gy, 6 Gy, 8 Gy) (Figure 46 B). Obatoclax thus exhibit synergism with radiation treatment to inhibit the clonogenicity of OSCC cells.

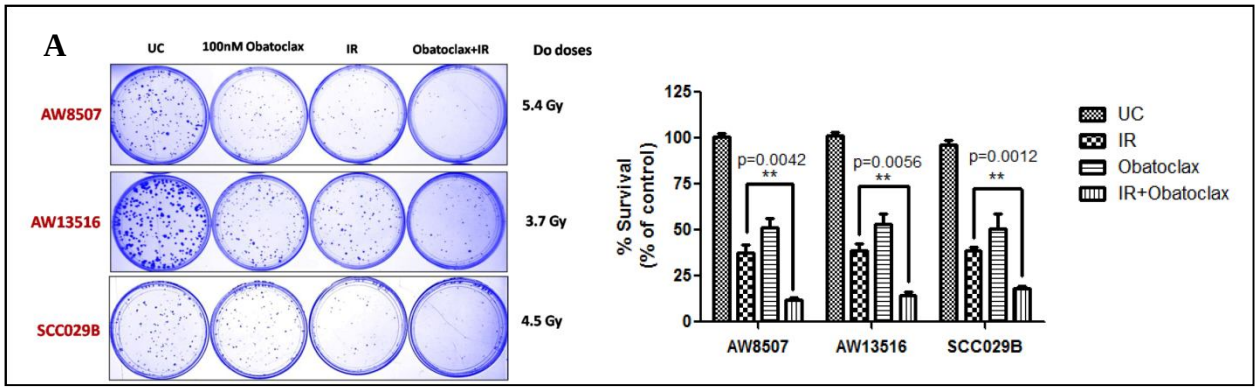

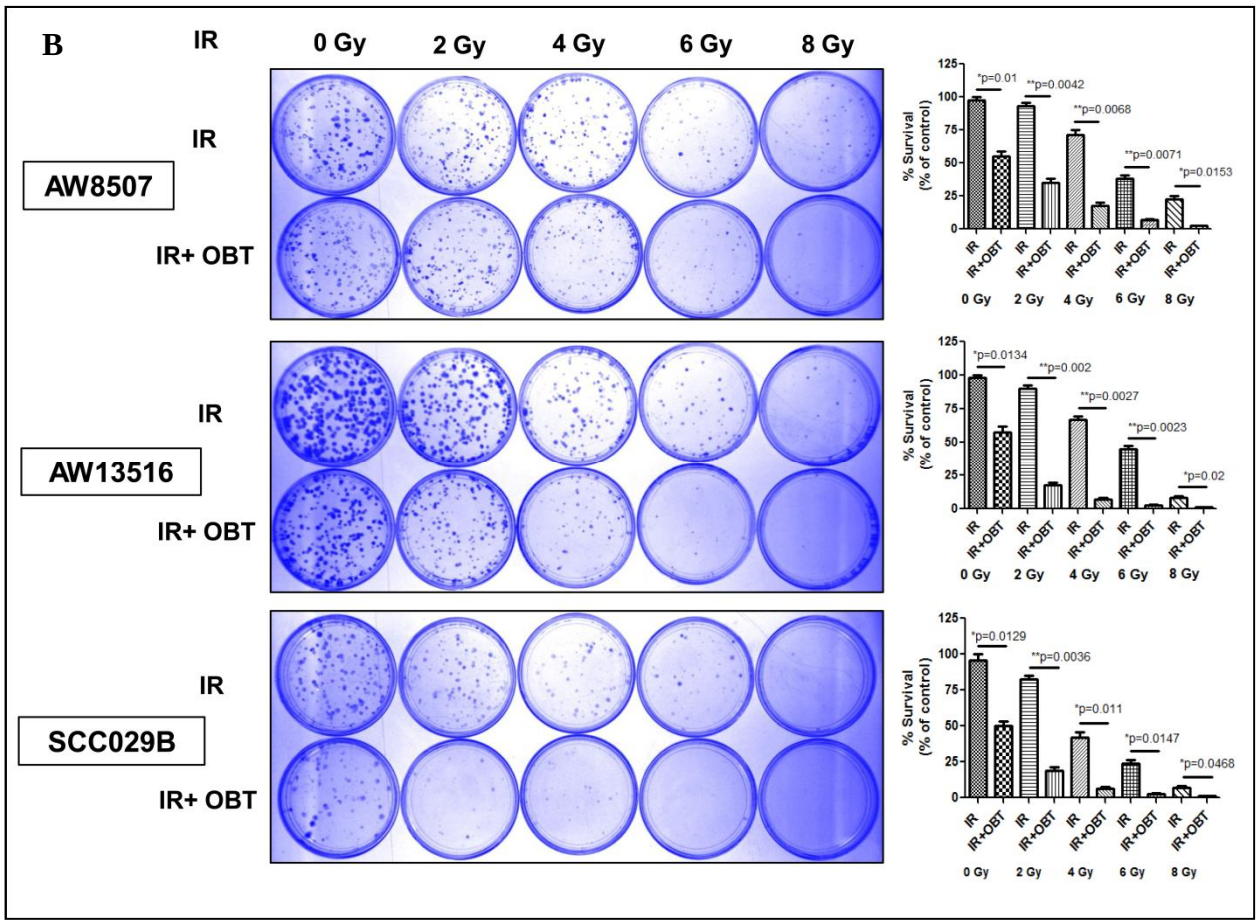

Figure 46: Ionizing radiation treatment exhibits synergism when combined with Obatoclax. **A)** A combination of Obatoclax and ionizing radiation (IR) significantly (**p*<0.05) inhibited the clonogenic potential of OSCC cells as compared to the either treatments alone. **B)** Obatoclax exhibits synergism with ionizing radiation in a dose dependent manner. AW8507, AW13516 and SCC029B cells were treated with different doses of ionizing radiation (0, 2, 4, 6, 8 Gy) with or without 100 nM Obatoclax for 24 hours and the colony forming units were represented as percent viability. Data is represented as mean±SEM of two independent experiments.

Chapter 6
Discussion

Discussion

Oral cancer is the most predominant type of cancer in the Southeast Asia, particularly in India which account for a significantly higher rate of mortality. Tobacco along with other cofactors has been regarded as a major risk factor for the pathogenesis and progression of human oral cancers [3]. Major advances in the Surgery, Radiotherapy and Chemotherapy procedures over the past several decades haven't contributed significantly to improve the life expectancy of oral cancer patients [20]. Therefore, new therapeutic interventions for the better management of oral cancer patients are actively being sought. Identification of novel molecular entities showing aberrant expression in human cancers has enabled their use as prognostic markers and therapeutic targets which paved way for targeted therapies [19]. The BCL-2 family of apoptosis regulators constitutes several such key molecular targets.

Aberrant expression of BCL-2 family proteins, particularly MCL-1 has been implicated in several human cancers including oral cancers [23, 27]. Moreover, MCL-1 overexpression is associated with therapy resistance in oral cancers [24-26] which makes it a potential therapeutic target. Therefore, we carried out the present study to understand the basis of altered regulation of MCL-1 protein which leads to its overexpression. Additionally, we aim at targeting MCL-1 protein with a small molecule inhibitor which will help us assess its therapeutic potential in oral cancers. We discuss here significant findings from the study in following sections.

MCL-1 is unique among the antiapoptotic members of the BCL-2 family in that it has a long unstructured regulatory domain at the N-terminus which contains several polyubiquitination, phosphorylation and caspase cleavage sites responsible for its characteristic short half-life and a rapid rate of turnover [160]. Ubiquitin-dependent proteasomal degradation is therefore believed

to be the principal mode of MCL-1 turnover in mammalian cells [160, 233]. However, several other mechanisms which contribute to MCL-1 degradation exists including Protein kinase Cδ catalytic fragment mediated degradation [234], Granzyme B [235] and Caspase-3 [236] mediated cleavage, and Ubiquitin-independent degradation [237].

Therefore, to ascertain the Ubiquitin-dependent proteasomal mode of MCL-1 degradation in OSCC cell lines, we evaluated the expression of MCL-1 protein when the proteasome activity was inhibited. Blocking the activity of the proteasome with proteasome inhibitors MG132 and Velcade (Bortezomib) caused a significant increase in the levels of MCL-1 protein. This accumulated MCL-1 corresponds to its polyubiquitinated form, indicating that the degradation of MCL-1 protein occurs principally through the ubiquitin-proteasomal pathway in OSCC cells. Cycloheximide chase assay revealed that MCL-1 protein has a relatively rapid rate of turnover (i.e. a short half-life) as compared to BCL-2 and BCL-XL proteins.

6.1 Role of USP9X in stabilization of MCL-1 protein

Deubiquitinase USP9X has recently been shown to interact with MCL-1 protein and stabilize it in tumor cells by catalyzing the removal of Lys^{48}-linked polyubiquitin chains [175]. Hence, in the present study, we evaluated the contribution of USP9X towards stabilizing MCL-1 protein in oral cancer cells.

We observed that, the expression of USP9X and MCL-1 proteins correlates significantly not only in oral cancer cell lines but also in oral tissues. A relatively higher coexpression of MCL-1 and USP9X proteins in tumor samples as opposed to their paired normal counterparts points towards the probable contribution of USP9X in increased stabilization of MCL-1 protein in tumors. Moreover, the expression of MCL-1 and USP9X proteins exhibit a concurrent increase in

histopathological stage-specific manner from normal oral mucosa (Normal) through potentially malignant disorders (Premalignant condition) to oral squamous cell carcinoma (Cancer).

In order to catalyze the removal of polyubiquitin chains from a substrate protein, the deubiquitinase needs to physically associate with the target protein [150]. Therefore, we next demonstrated direct interaction between USP9X and MCL-1 proteins by coimmunoprecipitation and coimmunofluorescence studies. To demonstrate the direct role of USP9X in stabilizing MCL-1 protein in oral cancer cells, we knocked down USP9X by siRNA. Targeted downregulation of USP9X led to a significant decline in MCL-1 protein but not transcript levels, indicating that USP9X does not affect the MCL-1 gene expression but enhances the stability of MCL-1 protein. Further, cycloheximide chase assay revealed that USP9X downregulation significantly increased the turnover rate of MCL-1 protein which was evident from its reduced half-life and increased polyubiquitination. More recently, USP9X has been shown to contribute to the radioresistance in cancer cells by enhancing MCL-1 stabilization [214]. In this context, earlier studies from our lab have shown that MCL-1 protein levels show sustained increase in oral cancer cells upon exposure to ionizing radiation [25]. We also confirmed that targeted downregulation of USP9X significantly increased the radiosensitivity of oral cancer cells. We next investigated whether USP9X can be a predictor of prognosis in OSCC patients. Those oral cancer patients who had a relatively higher expression of MCL-1 and USP9X exhibited a significantly reduced disease free survival as opposed to those having a lower expression. Moreover, those oral cancer patients having disease recurrence showed a relatively higher expression of MCL-1 and USP9X as opposed to those who had no signs of disease relapse. All these observations confirm critical role of USP9X in stabilization of MCL-1 protein in oral cancer cells.

We next evaluated the potential of therapeutic targeting of USP9X by using a small molecule inhibitor WP1130 (Degrasyn) in oral cancer cell lines *in vitro* and *in vivo* [176]. WP1130 induced a dose and time dependent cell death by triggering apoptosis in oral cancer cells. Notably, concomitant with apoptosis, WP1130 triggered rapid degradation of MCL-1 protein. Due to potent inhibition of deubiquitinases, WP1130 caused rapid accumulation of insoluble aggregates of polyubiquitinated proteins in the form of inclusion bodies called as Aggresomes which are marked by p62/SQSTM1 (Sequestosome). Finally, we demonstrate here the potent single-agent *in vivo* antitumor efficacy of WP1130 against oral xenografts. WP1130 alone caused a significant decrease in the mean tumor volume by triggering apoptosis and reducing the expression of MCL-1.

Consistent with our observations, Zhang et al showed that Gemcitabine-mediated disruption of MCL-1/USP9X interaction in solid tumor cell lines is critical for sensitizing them to ABT-737, a BH3-mimetic to which MCL-1 is refractory and thus exhibits resistance to it [238]. Further, USP9X has been demonstrated to contribute to radioresistance in cancer cells by stabilizing MCL-1 protein [214]. Of particular note, a screen for ~90 DUBs encoded by the human genome studied by In-situ Hybridization - Tissue Microarray revealed USP9X to be one of the most significantly dysregulated deubiquitinase in multiple types of solid tumors [239]. Moreover, it has been demonstrated that downregulation or inhibition of USP9X resulted in degradation of MCL-1 and subsequent sensitization of solid tumors (Colon and Lung cancer) to BCL-XL inhibition [240]. More recently, Elgendy et al showed that USP9X not only serve as a deubiquitinase for MCL-1 but also for Beclin-1, thus mediating their stabilization. Interestingly, both Beclin-1 and MCL-1 compete for interaction with USP9X and thereby negatively modulate the stability of each other in a reciprocal manner independent of autophagy [100]. From a

therapeutic view point, small molecule WP1130-mediated inhibition of USP9X potently induced apoptosis in human myeloma and mantle cell lymphoma cell lines by triggering degradation of MCL-1 protein [176]. WP1130-mediated Inhibition of USP9X rapidly induced apoptosis in CML cells by blocking kinase signaling from Bcr-Abl, triggering MCL-1 degradation and aggresomal compartmentalization of Bcr-Abl [241]. All these reports are in accordance with our observations and are suggestive of a pivotal role of USP9X in enhancing the stability of MCL-1 protein and thus contributing to tumorigenesis in oral cancers.

In contrast to its tumor promoting role, USP9X also serves as a tumor suppressor protein in Pancreatic Ductal Adenocarcinoma (PDA) where its loss enhances transformation and protects pancreatic cancer cells from anoikis. Moreover, low USP9X protein expression correlates with poor survival after surgery in PDA patients, and USP9X levels are inversely associated with metastatic burden in advanced disease [242]. Apart from MCL-1, USP9X also serve as a deubiquitinase for Smad4 by removing its inhibitory monoubiquitination and thereby enables Smad4 recycling and re-empowering its competence to mediate TGFβ signaling. Loss of USP9X thus prevents deubiquitination of Smad4 thereby enhancing tumor progression [243]. In yet another observation, USP9X has been reported as one of the most frequently altered genes in Gingivo-buccal oral squamous cell carcinoma (GB-OSCC). However, in contrast to our observations, the authors demonstrate copy number loss and truncating mutations in USP9X consistent with its role as a tumor suppressor protein. The authors did not find any association of altered USP9X expression with mean disease free survival in GB-OSCC patients [244]. The discordance between these observations could possibly be the result of inclusion of a relatively smaller number (n=50) of GB-OSCC patients. Additionally, the data reflects only the nature and extent of genomic alterations derived from exome sequencing specific to GB-OSCC. However,

the expression of USP9X at the transcript or protein level was not confirmed which would be a true indicative of the impact of genomic alteration of USP9X. On the contrary, our present study consisted of a significant number (n=138) of OSCC patients including those with carcinoma of various oral subsites including buccal mucosa, gingiva, tongue, alveolus, and retromolar trigone.

Apart from the above mentioned functions, USP9X is important for a myriad array of normal cellular processes too. It is a stemness associated gene [245] required for polarity and self-renewal of embryonic stem cell-derived neural progenitors [246]. It is also essential for preimplantation mouse embryo development [247]. USP9X negatively modulates mTOR activity and skeletal muscle differentiation [248]. It regulates the activity of AMPK-related kinases NUAK1 and MARK4 by catalyzing the deubiquitination of Lys^{29}/Lys^{33}-linked ubiquitin chains [249]. USP9X also plays a key role in regulating the tight junction assembly by mediating deubiquitination of EFA6, thereby causing a transient increase in its levels at newly forming cell-cell contacts before establishing cell polarity. Loss of cell polarity is a critical event in the metastatic spread of cancer [250].

Our results thus suggest that deubiquitinase USP9X is critical for maintaining the stability of MCL-1 protein in oral cancer cells and that its downregulation or pharmacological inhibition rapidly promotes degradation of MCL-1.

6.2 Role of TCTP in stabilization of MCL-1 protein

Liu et al demonstrated that TCTP interacts with MCL-1 and enhances its stability by interfering with MCL-1's ubiquitin-dependent proteasome degradation pathway [251]. In a contradictory report, however, MCL-1 was demonstrated to serve as a chaperone for fortilin (i.e. TCTP) [252].

Therefore, we investigated the contribution of TCTP in stabilizing MCL-1 protein in human oral cancer cells.

We observed no correlation between the expression of MCL-1 and TCTP proteins in human oral cancer cell lines. Further, siRNA mediated downregulation of TCTP exhibited no change in the levels of MCL-1 protein, indicating that TCTP may not be required for stabilization of MCL-1 protein. However, a strong positive correlation was observed between the expression levels of MCL-1 and TCTP proteins in oral tissues of various histopathological stages. It is suggestive of the fact that both the proteins may perform their antiapoptotic functions independent of each other. Indeed, Graidist et al showed that the two proteins TCTP and MCL-1 serve as antiapoptotic proteins independent of each other [253]. Moreover, TCTP itself serves as an antiapoptotic protein as its ectopic expression protects cells from death signals. Evidently, TCTP protein levels are higher in human tumors and cancer cell lines [158]. TCTP has also been identified as an important gene which is downregulated in a tumor reversion model. Inhibition of TCTP expression by anti-sense cDNA or siRNA results in suppression of malignant phenotype and cellular reorganization [254].

Bommer et al have noted that TCTP often appears as an interacting partner in Yeast two-hybrid screens and therefore careful evaluation and interpretation of its interaction with target proteins is necessary [156]. Most of the reported interactions of TCTP with other proteins including MCL-1 are evident from screening Yeast two-hybrid library. Liu et al reported that the interaction between MCL-1 and TCTP is independent of the BH domains but depends on Lys^{257} residue which lies in a loop region of MCL-1 critical for this interaction. Apart from MCL-1, only A1 is capable of interacting with TCTP which harbors this unique loop [251]. However, subsequently it was demonstrated that BCL-XL through its BH3 domain interacts with N-

terminus domain of TCTP and that it is indispensible for the antiapoptotic function of TCTP [255]. p53 has also been found as a novel interacting partner of TCTP. Overexpression of TCTP promote p53 degradation whereas its depletion stabilizes p53 leading to apoptosis [256]. TCTP also performs several other functions including regulation of cell shape by interacting with actin and microtubule cytoskeleton [257], DNA damage sensing and repair [258], and protecting cells from oxidative stress [259].

All the above reports and our observations thus points towards a prosurvival function of TCTP independent of MCL-1.

6.3 Role of MULE in regulating the stability of MCL-1 protein

MULE being a principal E3-Ubiquitinating ligase for MCL-1 under various physiological conditions, in the present study therefore we investigated the association between MCL-1 and MULE proteins. Evaluation of the expression of MCL-1 and MULE proteins in oral cell lines revealed no correlation between their expressions. Interestingly, in the tissues, MCL-1 and MULE expression showed a positive correlation. It was surprising provided that MULE polyubiquitinates MCL-1 protein leading to its proteasome mediated destruction.

The coexpression of MCL-1 and MULE although surprising, roots from differential interactions of the BH3-only proteins with MCL-1. MULE also contains a well conserved BH3-domain which specifically interacts with MCL-1 but not with BCL-2, BCL-XL or BAX. In healthy cells, MCL-1 is bound to proapoptotic BAK preventing its activation and oligomerization in the OMM. However, upon receiving a cell death trigger, it can be displaced by BH3-only family members (such as BIM, NOXA, PUMA, etc.) promoting BAK activation and allowing MCL-1 to be targeted by MULE for proteasome-dependent degradation [160]. NOXA, a BH3-only

protein is known to control MULE-dependent polyubiquitination of MCL-1. Overexpression of NOXA decreases the interaction between MCL-1 and USP9X whereas it increases the MCL-1-MULE association, leading to its polyubiquitination and proteasomal degradation. Conversely, downregulation of NOXA increases the interaction between MCL-1 and USP9X thereby leading to its stabilization [91]. On the other hand, ectopic expression of another BH3-only protein BIM prevented MCL-1 degradation by dissociating the interaction between MCL-1 and MULE, thereby leading to its stabilization [260]. Overexpression of PUMA, a BH3-only protein similar to BIM enhanced the stability of MCL-1 protein by interacting with it [147]. The differential effects of the two BH3-only proteins BIM and NOXA seem to rely on a discrete C-terminal sequence of the NOXA BH3 domain [260].

Sustained interaction between MCL-1 and MULE therefore appears to be necessary to maintain relatively lower cellular levels of MCL-1 protein. In tumor cells, this interaction may be disrupted to maintain sustained elevated levels of MCL-1. Indeed, Pervin et al demonstrated that although MULE was expressed in breast cancer cells, reduced association between MCL-1 and MULE contributes to increased stability of MCL-1 protein [261]. Furthermore, N-terminal truncation of the newly synthesized MCL-1 protein in the OMM removes a portion that is necessary for its interaction with MULE. The two proteins therefore cannot interact favouring stabilization of MCL-1 [262].

MULE (also known as ARF-BP1) not only polyubiquitinates MCL-1 but also p53, $E3^{Histone}$, and c-myc proteins [263]. MULE conjugates Lys 63-linked polyUb chains to Myc protein which is required for transactivation of multiple genes & induction of cell proliferation [264]**.** MULE is therefore overexpressed in several human tumors and is essential for growth of cancer cell lines but not of normal cell lines [264]. ARF protein serves as a tumor suppressor partly by interacting

with Mdm2 and thereby inhibiting its ability to promote p53 degradation [265]. Alternatively, ARF may sequester Mdm2 in the nucleolus, thereby stabilizing nucleoplasmic forms of p53 [266] or by directly inhibiting the ubiquitin ligase activity of Mdm2 [267]. ARF-BP1 (ARF Binding Protein-1) associates with ARF *in vivo*, thereby inhibiting its tumor suppressor function. ARF-BP1 directly binds and polyubiquitinates p53 in Mdm2-independent manner. Inactivation of endogenous ARF-BP1 is essential for ARF-mediated p53 stabilization [268]. Overexpression of ARF-BP1 may therefore provide a survival advantage to the tumor cells by enhancing p53 degradation. The coexpression of prosurvival proteins ARF-BP1 and MCL-1 thus may contribute to tumor cell survival.

Although MULE appears to be a major E3-ubiquitin ligase for MCL-1, other E3-ubiquitin ligases (includes $SCF^{\beta\text{-}TrCP}$, SCF^{FBW7}, APC/C^{cdc20} and Trim 17) mediate MCL-1 ubiquitination in a context-specific manner. GSK-3 mediated phosphorylation of MCL-1 at the consensus residues Ser^{155}, Ser^{159} and Thr^{163} facilitates its association with $SCF^{\beta\text{-}TrCP}$. β-TrCP mediates polyubiquitination of MCL-1 protein in phosphorylation-dependent manner [233]. Recently, it has been shown that the E3-ubiquitin ligase SCF^{FBW7} also ubiquitinate MCL-1 which is dependent on GSK-3-mediated phosphorylation of MCL-1 protein. The F-box protein FBW7 is a tumor suppressor and is frequently deleted in several human cancers. FBW7 targets Jun, Myc, Cyclin E and notch1 for destruction [269]. During prolonged mitotic arrest, the multi-subunit RING E3 ubiquitin-ligase APC/C^{Cdc20} is involved in MCL-1 degradation which depends on the substrate-recognition co-activator Cdc20 and CDK1/Cyclin B1 mediated phosphorylation of MCL-1 at Thr^{92} [270]. Trim 17 (Tripartite motif containing 17) is a single-protein RING-containing E3 ubiquitin-ligases which is the latest E3-ubiquitin ligase identified for MCL-1 [271].

Several other nonproteasomal modes of MCL-1 destruction also exists, including its cleavage by caspases and granzyme B. Caspase-3 cleaves MCL-1 at Asp^{127} and Asp^{157} during apoptosis and the C-terminal fragments thus generated exhibit proapoptotic activity [236]. Granzyme B cleaves MCL-1 at a site different than caspase-3 and interferes with Bim sequestration by MCL-1 [235]. Stewart et al reported ubiquitin-independent degradation of MCL-1. In a system where MCL-1 mutant was lacking lysine residues required for polyubiquitination, the turnover of mutant MCL-1 was similar to that of the wild type MCL-1. The MCL-1 turnover was found to be unaffected even when E1 ubiquitin activating enzyme was blocked [237].

All the above reports suggest that MCL-1 degradation is tightly regulated by multiple pathways depending on the signalling cues from the surrounding.

6.4 Identification of novel interacting partners of MCL-1

We adopted the approach of endogenous coimmunoprecipitation coupled with MALDI-MS to identify novel MCL-1-binding partner proteins.

Our analysis revealed proteins mainly associated with Ubiquitin-proteasomal pathway, cell cycle, apoptotic pathways and several other uncharacterized proteins. The brief significance of each of these identities is mentioned in the results section. We discuss here a few of the significant hits from the MS screen and their relevance with MCL-1.

Proteins associated with Ubiquitin proteasomal pathway: As discussed in the above sections, the regulation of cellular levels of MCL-1 protein revolves around the Ubiquitin-proteasomal pathway of degradation. In the MS screen, we observed several proteins closely associated with protein ubiquitination and components of the proteasomal complex. It includes Ubiquitin-specific peptidase-like protein 1 (a deubiquitinase), E3 SUMO-protein ligase NSE2, MDM4, 26S

protease regulatory subunit 4, E3 ubiquitin-protein ligase RNF144A and Proteasome-associated protein ECM29 homolog.

Proteins associated with Cell cycle: MCL-1 levels are closely associated with the cell cycle. During normal mitosis, the levels of MCL-1 steadily decreases but the reduction in MCL-1 is insufficient to trigger apoptosis [272]. However, during a prolonged mitotic arrest such as upon exposure to microtubule poisons, the multi-subunit RING E3 ubiquitin-ligase APC/C^{Cdc20} ubiquitinates and targets MCL-1 for degradation. It requires the substrate-recognition co-activator Cdc20 and a prior phosphorylation of MCL-1 at Thr92 by CDK1/cyclin B1 [270]. Therefore, control of MCL-1 instability by APC/C^{Cdc20} constitutes a direct link between the regulation of mitosis and the temporal control of apoptosis [273]. In our MS screen, we have identified several proteins closely related to the cell cycle regulation including Mitotic spindle assembly checkpoint protein MAD2A, CDK5 regulatory subunit-associated protein 1, PCNA-associated factor (PAF), CDC27, and Mitotic checkpoint serine/threonine-protein kinase BUB1 β.

Proteins associated with apoptotic pathways: MCL-1 being a member of the BCL-2 family, is central in regulating the cell fate in response to environmental cues. In the MS screen, we also found a few proteins closely associated with the apoptotic pathways including BAX, CASP8 and FADD-like apoptosis regulator, and Tumor protein p63-regulated gene 1-like protein.

Apart from these proteins, several other interesting hits includes NACHT, LRR and PYD domains-containing protein 11 (NALP11), Alpha enolase/MBP-1, MAP3K12-binding inhibitory protein 1, Serine/threonine-protein phosphatase 2A regulatory subunit B, and MAPK/MAK/MRK overlapping kinase.

Provided the pivotal position of MCL-1 in determining the cell fate, these novel molecular interactions may provide important insights into a more complex regulatory circuit of MCL-1. Further studies are needed to fully understand the significance of these interactions from a tumor cell perspective.

6.5 Efficacy and mode of action of Obatoclax against oral cancer cells

Aberrant expression of antiapoptotic BCL-2 family proteins, particularly MCL-1 has been reported in diverse human cancers including oral cancers [23, 27]. We have earlier demonstrated that the prosurvival MCL-1 protein contributes to therapy resistance and poor prognosis in oral cancers and thus may prove to be a potential therapeutic target in OSCC [24-26]. Hence in the present study, we evaluated the efficacy of a BH3-mimetic pan-BCL-2 inhibitor Obatoclax against human oral cancer cell lines and also elucidated the mechanism of its action.

The four OSCC cell lines used in the present study exhibited high sensitivity to Obatoclax which correlated significantly to their MCL-1 expression. However, Obatoclax-induced growth inhibition was not associated with a reduction in MCL-1 expression primarily because, Obatoclax is a BH3-mimetic which binds with a high affinity to the BH3-domain binding hydrophobic groove on MCL-1 protein and is not known to be associated with inhibition of its expression or mediate its degradation. This observation is in accordance with earlier studies reported in Cholangiocarcinoma cells [182, 274], Pancreatic cancer cells [181], KB carcinoma cells [90] and Breast cancer cells [275]. In contrast, studies by Yazbeck et al demonstrated that sensitivity to Obatoclax has an inverse correlation with MCL-1 expression in HNSCC cells and is associated with a reduction in MCL-1 levels [223]. The discrepancy between these observations may be attributed to the cell type and context specific-dependence of the cells on MCL-1 for survival and the relative expression of other antiapoptotic members of the BCL-2

family. It is noteworthy that, all four OSCC cell lines expressed relatively higher levels of at least two of the three major antiapoptotic proteins (BCL-2, BCL-XL or MCL-1) which imply their dependence on multiple prosurvival proteins of the BCL-2 family for cell viability. Owing to their functional redundancy, tumor cells upregulate the expression of companion prosurvival BCL-2 family proteins in case, one of them is either inhibited or downregulated and therefore neutralization of all of them is necessary to execute apoptotic cascade [217, 218]. Hence the use of a pan-BCL-2 inhibitor like Obatoclax may prove to be an effective therapeutic strategy.

In the present study, the growth inhibition induced by Obatoclax in OSCC cells was not associated with significant alterations in the expression of the BCL-2 family proteins except BIM and NOXA, whose levels were found to be reduced post Obatoclax treatment. Interestingly, NOXA and BIM downregulation partially protected H23 lung cancer cells from cell death induced due to MCL-1 knockdown [276]. A similar prosurvival response may probably be actuated in oral cancer cells in response to Obatoclax-mediated MCL-1 inhibition. Moreover, NOXA is a negative regulator whereas BIM is a positive regulator of MCL-1 protein stability [91, 260]. Therefore, BH3-only proteins are tightly regulated at the transcriptional and post-translational level in response to different stress stimuli [75]. Both BIM and NOXA are also predicted to compete with Beclin-1 for interaction with MCL-1 and thereby regulate autophagy [275, 277, 278]. The regulation of expression of these BH3-only proapoptotic proteins therefore appears to be context and cell-type specific.

Recently, Wroblewski et al has shown that Obatoclax induces unfolded protein response (UPR) in human melanoma cells which leads to MCL-1 upregulation, thereby preventing cell death [279]. UPR is characterized by increased GRP78 (Bip) expression, a principal chaperone in the

ER. However, in our studies, GRP78 expression remains unaltered in OSCC cells upon exposure to Obatoclax, indicating that Obatoclax may not induce ER stress in these cells.

Obatoclax is reported to execute cell death via both caspase-dependent as well as caspase-independent pathways in a variety of cell types [181, 225]. In our studies, we observed that Obatoclax induced a caspase-independent, non-apoptotic cell death in OSCC cells. It is consistent with the observation that although Obatoclax dissociated the MCL-1-BAK interaction and induced BAX translocation to the mitochondria, there was no cytochrome c release. It is in accordance with observations made by Smoot et al in cholangiocarcinoma cells [182]

Several studies have shown that Obatoclax potently induces autophagy in a variety of cancer cells [223-225]. Our present study also demonstrates autophagy induction in OSCC cells upon Obatoclax treatment which is evident from excessive accumulation of LC-3BII. BCL-2, BCL-XL and MCL-1 are known to bind Beclin-1 and thereby inhibit Beclin-1-mediated autophagy. Like BIM and NOXA, BH3 mimetics have been predicted to competitively disrupt this interaction and thereby induce autophagy [219, 280]. However, we neither found significant alterations in Beclin-1 levels nor its altered subcellular localization pattern upon Obatoclax treatment in OSCC cells. McCoy et al have demonstrated Beclin-1-indpependent autophagy induction by Obatoclax in non-small-cell lung carcinoma cells [225]. Blocking autophagy by ATG5 knockdown significantly protected OSCC cells from Obatoclax-induced cell death, indicating that Obatoclax-induced autophagy leads to cell death and is not prosurvival. Obatoclax caused a disturbed autophagy flux which account for the bulk accumulation of LC-3BII and sustained levels of p62/SQSTM1 protein in OSCC cells (p62 is regarded as a substrate of autophagy which serves as a linker between polyubiquitinated cargo and LC-3BII on the autophagosomal membrane). A late-stage block in the autophagosome maturation process led to

defective autophagy. More recently, Stamelos et al have shown that Obatoclax accumulates in the lysosomes, mediates their alkalinization causing a block in the terminal degradative phase leading to a defective autophagy [281].

Having shown that Obatoclax induced a caspase-independent, non-apoptotic form of cell death in OSCC cells, we then investigated the cell death pathway linked to impaired autophagy. Here, we demonstrate that Obatoclax induced the interaction of p62 with RIP1K, RIP3K and FADD which are key components of the necrosome (A necrosome is a molecular platform similar to apoptosome). Moreover, RIP1K inhibition by Necrostatin-1 protected the OSCC cells from Obatoclax-induced cell death. Our data thus suggests that Obatoclax mediates cell death in OSCC cells via autophagy-dependent necroptosis.

Our studies also revealed that Obatoclax perturbed the normal tubular architecture of the mitochondria and induced extensive fragmentation of the mitochondrial network. This corresponds to increased mitochondrial fission and perinuclear aggregation. Initially it was believed that abrogation of the mitochondrial network, increased mitochondrial membrane permeability, mitochondrial ROS accumulation and mitochondrial dysfunction are one of the several effector mechanisms of Necroptosis [222, 282]. However, recent studies argue the involvement of mitochondrial fission and mitochondrial ROS during necroptotic cell death [283, 284]. Our data also suggests that mitochondrial fragmentation in response to Obatoclax treatment occurs either independent or upstream of autophagy induction and necroptosis.

Under stressful conditions, BNIP3 expression is induced which causes reduced energy output, increased accumulation of mitochondrial ROS and a drop in $\Delta\Psi m$ which mark the mitochondria as damaged and dysfunctional [229, 277]. On the same lines, we observed a significant increase

in the expression of BNIP3 upon Obatoclax treatment. In accordance with the downstream effects of BNIP3 induction, we demonstrated a significant increase in the mitochondrial oxidative stress, compromised integrity of the mitochondrial membrane as indicated by a reduced ΔΨm (i.e. depolarized mitochondria) and a time-dependent decrease in mitochondrial function in these cells upon Obatoclax treatment. All the above characteristic events possibly mark the mitochondria as damaged and dysfunctional.

Besides its canonical prosurvival function, MCL-1 protein is critical for the organization and physiological functions of mitochondria [92]. MCL-1's critical involvement in mitochondrial dynamics has also been recently highlighted by Morciano et al [93]. Owing to its key role in mitochondrial homeostasis, MCL-1 is proposed to empower mitochondrial physiology in normal as well as tumor cells [94]. Since MCL-1 is overexpressed in oral cancer cells and serves as an important prosurvival protein, we probed into its critical involvement in the maintenance of mitochondrial homeostasis in OSCC cells. In the present study, we evaluated and compared the effect of Obatoclax-mediated MCL-1 inhibition (without a significant change in MCL-1 levels) with that of siRNA-mediated MCL-1 downregulation in context of mitochondrial architecture and physiology. MCL-1 downregulation in these cells led to extensive mitochondrial fragmentation, increased mitochondrial oxidative stress and a reduced mitochondrial membrane potential. These aberrations in the mitochondrial architecture and physiology were identical to those induced by Obatoclax treatment, thus highlighting the potential contribution of MCL- 1 to the normal mitochondrial organization and function. Perciavalle et al provided evidence for contribution of MCL-1 to mitochondrial physiology. Apart from the antiapoptotic form of MCL-1 which localizes to the OMM, an amino-terminally truncated form of MCL-1 (contains intact carboxyl-terminus domain which harbors the BH3 domain binding hydrophobic groove where

Obatoclax is predicted to bind) localizes to the mitochondrial matrix, plays a critical role in maintaining normal architecture, physiology, homeostasis, bioenergetics and fusion of the mitochondria [92]. Interestingly, putative MCL-1-specific BH3 mimetics such as BI97C1 and BI112D1 have also been shown to induce mitochondrial fragmentation, generation of ROS in mitochondria and inhibition of mitochondrial fusion independent of apoptosis and without affecting MCL-1 levels. In the same paper, the authors demonstrate extensive mitochondrial fragmentation upon siRNA-mediated MCL-1 depletion in H23 lung cancer cells [188]. We therefore speculate that Obatoclax-mediated MCL-1 antagonization may significantly contribute to the abolishment of mitochondrial structure and function.

We also demonstrate the single agent efficacy of Obatoclax in xenograft mouse model. Obatoclax exhibited dose-dependent tumor regression in oral xenografts without detectable animal toxicity or weight loss. Moreover, consistent with our prior observation that MCL-1 is a critical radioresistance related protein in OSCC cells [25], Obatoclax exhibited synergism with ionizing radiation as opposed to the either treatments alone. The radiosensitizing effect of Obatoclax observed in the present study suggests that oral cancer patients may benefit from the combined therapeutic regimens including Obatoclax.

In summary, our studies indicate that Obatoclax which targets the prosurvival members of the BCL-2 family, particularly MCL-1, induces autophagy in OSCC cells leading to a caspase-independent, nonapoptotic form of cell death called necroptosis. These events are associated with extensive mitochondrial stress and dysfunction, are upstream to necroptosis and primarily attributed to Obatoclax-mediated MCL-1 antagonization (Figure 47).

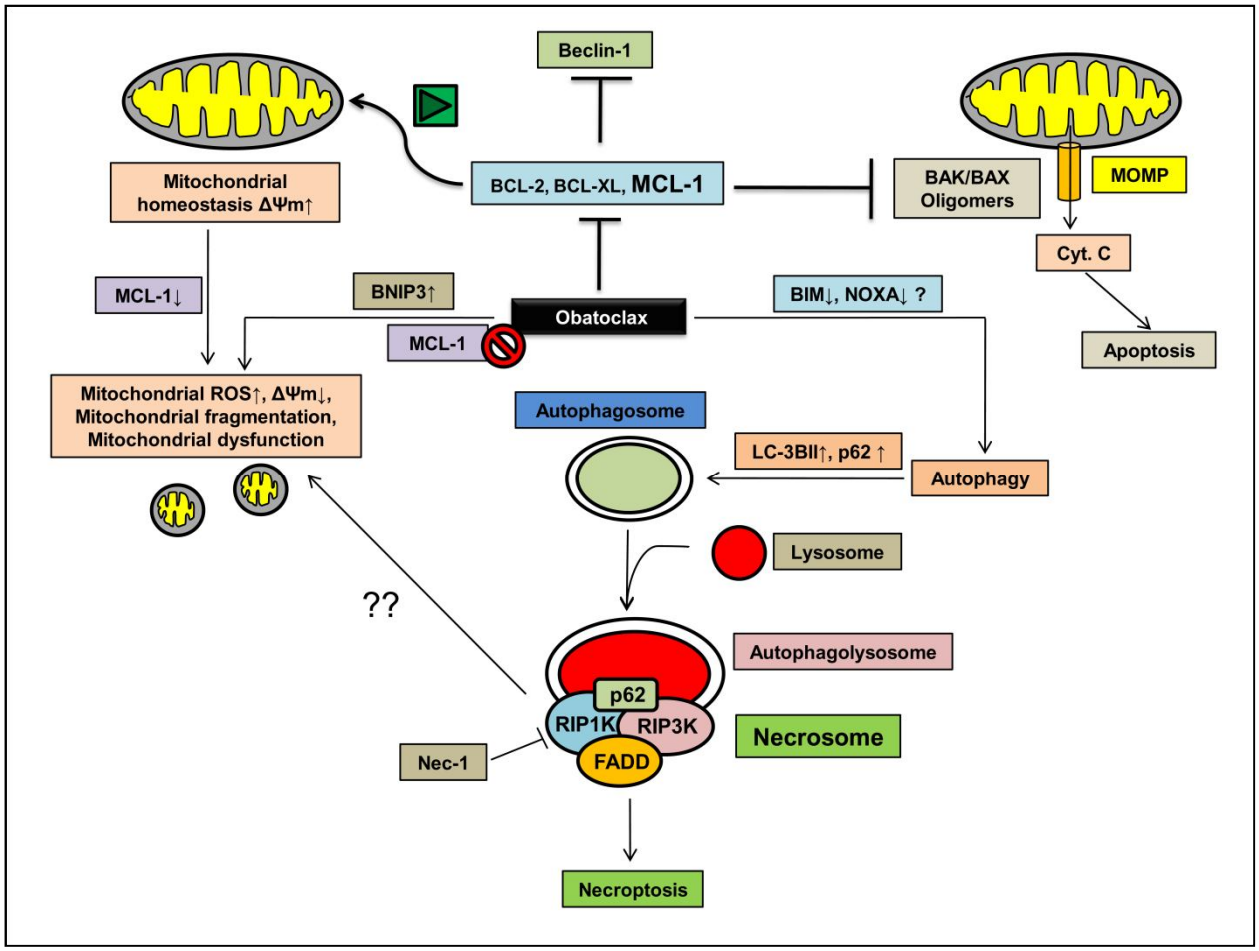

Figure 47: The proposed mode of Obatoclax action. Obatoclax potently induces autophagy in OSCC cells. However, a late-stage block in the degradation step of autophagy leads to assembly of key proteins of the necrosome such as RIP1K, RIP3K and FADD at the autophagosomes along with p62/SQSTM1 in a complex called necrosome. Necroptosis is associated with extensive mitochondrial fragmentation, induction of BNIP3 expression which potentiates ROS accumulation in the mitochondria, reduced mitochondrial membrane potential leading to mitochondrial dysfunction. Alternatively, whether or not MCL-1 inhibition mediated by Obatoclax at least partly contributes to the impaired mitochondrial homeostasis needs to be evaluated.

Chapter 7
Summary and Conclusions

The aim of the present study was to identify the altered regulatory mechanisms responsible for the observed overexpression of antiapoptotic MCL-1 protein in human oral cancers and to evaluate the efficacy of a small molecule inhibitor of MCL-1 against human oral cancer cell lines from a therapeutic point of view.

The key findings from the study are as follows:

- Ubiquitin-dependent proteasomal degradation is the principal mode of MCL-1 turnover in oral cancer cells. Cycloheximide chase assay revealed that MCL-1 protein has a relatively short half-life and a rapid rate of turnover as compared to other antiapoptotic members (BCL-2 and BCL-XL).
- Expression of the deubiquitinase USP9X correlates significantly to the MCL-1 protein levels in oral cancer cell lines and oral tissues. Of note, the expression of MCL-1 and USP9X proteins is significantly higher in tumor as compared to adjacent normal tissues.
- Direct interaction between MCL-1 and USP9X proteins was confirmed by coimmunoprecipitation and coimmunofluorescence studies. siRNA mediated depletion of USP9X led to the downregulation of MCL-1 protein by increasing its turnover rate, indicating key role of USP9X in enhancing MCL-1 protein stability. USP9X downregulation also sensitized oral cancer cells to ionizing radiation, thus highlighting its key role in resistance to radiation treatment.
- USP9X and MCL-1 expression exhibited significant correlation in oral tissues of different histopathological stages. The coexpression of the two proteins showed a gradual increase from normal oral mucosa through potentially malignant conditions to OSCC. Further, the relative expression of the two proteins was significantly higher in OSCC patients having disease relapse as opposed to those showing no evidence of disease recurrence. Moreover, the OSCC patients

having a relatively higher expression of USP9X exhibited an overall reduced disease free survival.

- A small molecule deubiquitinase inhibitor WP1130 potently induced apoptosis in oral cancer cells by triggering rapid degradation of MCL-1 and accumulation of aggresomes. It also exhibited potent *in vivo* antitumor efficacy against oral xenograft by inducing apoptosis, associated with reduced expression of MCL-1.
- To the best of our knowledge, this is the first study which deduced the association of MCL-1 with USP9X in human oral cancers. Provided the key role of deubiquitinase USP9X in promoting MCL-1 protein stability, the study warrants great therapeutic implications in the management of human oral cancers.
- We also investigated the role of a small ubiquitously expressed protein TCTP in promoting the stability of MCL-1 in oral cancer cells. However, TCTP does not appear to be important for MCL-1 stability. Nevertheless, MCL-1 expression correlated significantly with TCTP expression in oral tissues but not cell lines. It is probably due to the fact that TCTP itself serve as an antiapoptotic protein independent of MCL-1 and it performs a variety of important cellular functions which gives tumor cell a survival advantage.
- MULE is an E3 ubiquitin ligase which interacts with MCL-1, polyubiquitinate it and promotes its degradation. We therefore evaluated the status of MULE in oral cell lines and tissues. However, to our surprise, MCL-1 and MULE exhibited a positive correlation instead of the anticipated negative correlation. A plausible explanation for this observation lies in the fact that MULE also targets p53 for degradation independent of MDM2. Moreover, there could be a reduced association between MCL-1 and MULE. As MULE harbors a BH3 domain, the BH3-

only proteins BIM and NOXA may regulate the interaction between MCL-1 and MULE, thereby regulating MCL-1 stability.

- This is the first of its kind of a study which evaluated the association between MCL-1 and non-BCL-2 family proteins (USP9X, TCTP, MULE which directly interact with MCL-1 and regulate its stability by interfering with its ubiquitin-proteasomal pathway of degradation) in human tissues.
- We also aimed at identifying novel interacting partners of MCL-1 by coimmunoprecipitation coupled with Mass Spectrometry. The MS screen revealed several proteins belonging to the ubiquitin proteasomal pathway, Cell cycle regulatory circuits, Apoptosis pathway proteins and certain previously uncharacterized candidate proteins. These new interacting proteins and the significance of their interactions with MCL-1 await further investigation.
- We also evaluated the efficacy of a small molecule MCL-1 antagonist Obatoclax against oral cancer cell lines and investigated the mechanism of its action. Obatoclax induced a dose and time dependent reduction in the viability of oral cancer cells. The sensitivity of these cell lines correlated with their MCL-1 expression but was not associated with changes in the expression of BCL-2 family proteins.
- Although Obatoclax induced dissociation of MCL-1/BAK interaction within the OMM and translocation of BAX to OMM, we could not detect a significant efflux of cytochrome c from mitochondria to the cytosol. Consequently, Obatoclax induced a caspase-independent cell death in OSCC cell lines primarily associated with autophagy induction. Obatoclax induced a defective autophagy in OSCC cells evident from a disturbed autophagy flux ultimately leading to cell death by necroptosis. Necroptosis was evident by assembly of key components of the necrosome (RIP1K, RIP3K and FADD) at the autophagosomal membranes along with p62/SQSTM1.

- Obatoclax also triggxqered extensive mitochondrial fragmentation, increased mitochondrial oxidative stress, reduced mitochondrial membrane potential and lowered mitochondrial energy output but no evidence of mitophagy. These events coincided with mitochondrial aberrations observed upon downregulation of MCL-1 in SCC029B cells, confirming a key role of MCL-1 in mitochondrial physiology.
- We further confirmed potent *in vivo* antitumor efficacy of Obatoclax against oral cancer xenografts. We also demonstrated synergism of Obatoclax with ionizing radiation in inhibiting the clonogenic viability of oral cancer cells *in vitro*. To the best of our knowledge, it is the first study demonstrating the efficacy and mechanism of action of Obatoclax against human oral cancer cell lines.
- Our present study thus provides insights into the mechanisms underlying MCL-1 overexpression in human oral cancers and also presents therapeutic opportunities for the use of MCL-1 antagonists such as Obatoclax for the better management of oral cancer patients in the clinics.

Chapter 8

References

References:

1. Scully C and Bagan J. Oral squamous cell carcinoma overview. Oral oncology. 2009; 45(4):301-308.

2. Shah JP and Gil Z. Current concepts in management of oral cancer–surgery. Oral oncology. 2009; 45(4):394-401.

3. Dikshit R, Gupta PC, Ramasundarahettige C, Gajalakshmi V, Aleksandrowicz L, Badwe R, Kumar R, Roy S, Suraweera W and Bray F. Cancer mortality in India: a nationally representative survey. The Lancet. 2012; 379(9828):1807-1816.

4. Kumar M, Nanavati R, Modi TG and Dobariya C. Oral cancer: Etiology and risk factors: A review. Journal of cancer research and therapeutics. 2016; 12(2):458-463.

5. Herrero R, Castellsagué X, Pawlita M, Lissowska J, Kee F, Balaram P, Rajkumar T, Sridhar H, Rose B and Pintos J. Human papillomavirus and oral cancer: the International Agency for Research on Cancer multicenter study. Journal of the National Cancer Institute. 2003; 95(23):1772-1783.

6. D'Souza G, Kreimer AR, Viscidi R, Pawlita M, Fakhry C, Koch WM, Westra WH and Gillison ML. Case–control study of human papillomavirus and oropharyngeal cancer. New England Journal of Medicine. 2007; 356(19):1944-1956.

7. Mehrotra R and Yadav S. Oral squamous cell carcinoma: etiology, pathogenesis and prognostic value of genomic alterations. Indian J Cancer. 2006; 43(2):60-66.

8. Warnakulasuriya S. Global epidemiology of oral and oropharyngeal cancer. Oral Oncol. 2009; 45(4-5):309-316.

9. Feller L and Lemmer J. Oral Squamous Cell Carcinoma: Epidemiology, Clinical Presentation and Treatment. Journal of Cancer Therapy. 2012; 3(4).

10. Notani PN. Global variation in cancer incidence and mortality. Current Science-Bangalore. 2001; 81(5):465-474.

11. Mehrotra R and Yadav S. Oral squamous cell carcinoma: etiology, pathogenesis and prognostic value of genomic alterations. Indian journal of cancer. 2006; 43(2):60.

12. Omura K. Current status of oral cancer treatment strategies: surgical treatments for oral squamous cell carcinoma. International journal of clinical oncology. 2014; 19(3):423-430.

13. Braakhuis BJ, Bloemena E, Leemans CR and Brakenhoff RH. Molecular analysis of surgical margins in head and neck cancer: more than a marginal issue. Oral oncology. 2010; 46(7):485-491.

14. Bessell A, Glenny AM, Furness S, Clarkson JE, Oliver R, Conway DI, Macluskey M, Pavitt S, Sloan P and Worthington HV. Interventions for the treatment of oral and oropharyngeal cancers: surgical treatment. The Cochrane Library. 2011.

15. Carrillo MM, Martín IT, Lara IM, de Almodóvar Rivera JMR and Ávila RDM. Selective use of postoperative neck radiotherapy in oral cavity and oropharynx cancer: a prospective clinical study. Radiation Oncology. 2013; 8(1):1.

16. Bucci B, Misiti S, Cannizzaro A, Marchese R, Raza GH, Miceli R, Stigliano A, Amendola D, Monti O and Biancolella M. Fractionated ionizing radiation exposure induces apoptosis through caspase-3 activation and reactive oxygen species generation. Anticancer research. 2006; 26(6B):4549-4557.

17. Ishigami T, Uzawa K, Higo M, Nomura H, Saito K, Kato Y, Nakashima D, Shiiba M, Bukawa H and Yokoe H. Genes and molecular pathways related to radioresistance of oral squamous cell carcinoma cells. International journal of cancer. 2007; 120(10):2262-2270.

18. Specenier PM and Vermorken JB. Current concepts for the management of head and neck cancer: chemotherapy. Oral oncology. 2009; 45(4):409-415.

19. Lorch JH, Posner MR, Wirth LJ and Haddad RI. Seeking alternative biological therapies: The future of targeted molecular treatment. Oral oncology. 2009; 45(4):447-453.

20. Lee K, Veness M, Pearl-Larson T and Morgan G. Role of combined modality treatment of buccal mucosa squamous cell carcinoma. Australian dental journal. 2005; 50(2):108-113.

21. Massano J, Regateiro FS, Januário G and Ferreira A. Oral squamous cell carcinoma: review of prognostic and predictive factors. Oral Surgery, Oral Medicine, Oral Pathology, Oral Radiology, and Endodontology. 2006; 102(1):67-76.

22. Barbellido SA, Trapero JC, Sánchez JC, García MAP, Castaño NE and Martínez AB. Gene therapy in the management of oral cancer: review of the literature. Med Oral Patol Oral Cir Bucal. 2008; 13(1):E15-21.

23. Mallick S, Patil R, Gyanchandani R, Pawar S, Palve V, Kannan S, Pathak K, Choudhary M and Teni T. Human oral cancers have altered expression of Bcl-2 family members and increased expression of the anti-apoptotic splice variant of Mcl-1. The Journal of pathology. 2009; 217(3):398-407.

24. Mallick S, Agarwal J, Kannan S, Pawar S, Kane S and Teni T. PCNA and anti-apoptotic Mcl-1 proteins predict disease-free survival in oral cancer patients treated with definitive radiotherapy. Oral oncology. 2010; 46(9):688-693.

25. Palve VC and Teni TR. Association of anti-apoptotic Mcl-1L isoform expression with radioresistance of oral squamous carcinoma cells. Radiat Oncol. 2012; 7:135-145.

26. Palve V, Mallick S, Ghaisas G, Kannan S and Teni T. Overexpression of Mcl-1L Splice Variant Is Associated with Poor Prognosis and Chemoresistance in Oral Cancers. PloS one. 2014; 9(11):e111927.

27. Placzek W, Wei J, Kitada S, Zhai D, Reed J and Pellecchia M. A survey of the anti-apoptotic Bcl-2 subfamily expression in cancer types provides a platform to predict the efficacy of Bcl-2 antagonists in cancer therapy. Cell death & disease. 2010; 1(5):e40.

28. Akgul C. Mcl-1 is a potential therapeutic target in multiple types of cancer. Cellular and molecular life sciences. 2009; 66(8):1326-1336.

29. Gores GJ and Kaufmann SH. Selectively targeting Mcl-1 for the treatment of acute myelogenous leukemia and solid tumors. Genes & development. 2012; 26(4):305-311.

30. Thomas LW, Lam C and Edwards SW. Mcl-1; the molecular regulation of protein function. FEBS Lett. 2010; 584(14):2981-2989.

31. Hogarty MD. Mcl1 becomes ubiquitin-ous: new opportunities to antagonize a pro-survival protein. Cell research. 2010; 20(4):391.

32. Yang-Yen H-F. Mcl-1: a highly regulated cell death and survival controller. Journal of biomedical science. 2006; 13(2):201-204.

33. Ertel F, Nguyen M, Roulston A and Shore GC. Programming cancer cells for high expression levels of Mcl1. EMBO Rep. 2013.

34. Van der Waal I. Potentially malignant disorders of the oral and oropharyngeal mucosa; terminology, classification and present concepts of management. Oral oncology. 2009; 45(4):317-323.

35. Carvalho AL, Pintos J, Schlecht NF, Oliveira BV, Fava AS, Curado MP, Kowalski LP and Franco EL. Predictive factors for diagnosis of advanced-stage squamous cell carcinoma of the head and neck. Archives of Otolaryngology–Head & Neck Surgery. 2002; 128(3):313-318.

36. Petti S. Lifestyle risk factors for oral cancer. Oral oncology. 2009; 45(4):340-350.

37. Musto DF. The mystery of addiction. The Lancet. 1999; 354:SIV1.

38. Mackay J and Eriksen MP. (2002). The tobacco atlas: World Health Organization).

39. Mehta FS, Gupta P, Daftary D, Pindborg J and Choksi S. An epidemiologic study of oral cancer and precancerous conditions among 101,761 villagers in Maharashtra, India. International Journal of Cancer. 1972; 10(1):134-141.

40. Warnakulasuriya K, Johnson N, Linklater K and Bell J. Cancer of mouth, pharynx and nasopharynx in Asian and Chinese immigrants resident in Thames regions. Oral Oncology. 1999; 35(5):471-475.

41. Scully C, Field J and Tanzawa H. Genetic aberrations in oral or head and neck squamous cell carcinoma (SCCHN): 1. Carcinogen metabolism, DNA repair and cell cycle control. Oral oncology. 2000; 36(3):256-263.

42. Pickwell SM, Schimelpfening S and Palinkas LA. 'Betelmania'. Betel quid chewing by Cambodian women in the United States and its potential health effects. Western Journal of Medicine. 1994; 160(4):326.

43. IARC Working Group on the Evaluation of Carcinogenic Risks to Humans WHO, International Agency for Research on Cancer. (2004). Betel-quid and areca-nut chewing and some areca-nut-derived nitrosamines: IARC).

44. Subapriya R, Thangavelu A, Mathavan B, Ramachandran CR and Nagini S. Assessment of risk factors for oral squamous cell carcinoma in Chidambaram, Southern India: a case–control study. European journal of cancer prevention. 2007; 16(3):251-256.

45. Seitz HK and Stickel F. Molecular mechanisms of alcohol-mediated carcinogenesis. Nature Reviews Cancer. 2007; 7(8):599-612.

46. Jaegerstad M and Skog K. Genotoxicity of heat-processed foods. Mutation Research/Fundamental and Molecular Mechanisms of Mutagenesis. 2005; 574(1):156-172.

47. Marmot M, Atinmo T, Byers T, Chen J, Hirohata T, Jackson A, James W, Kolonel L, Kumanyika S and Leitzmann C. Food, nutrition, physical activity, and the prevention of cancer: a global perspective. 2007.

48. Nomura A, Ziegler RG, Stemmermann GN, Chyou P-H and Craft NE. Serum micronutrients and upper aerodigestive tract cancer. Cancer Epidemiology Biomarkers & Prevention. 1997; 6(6):407-412.

49. Westra WH. The changing face of head and neck cancer in the 21st century: the impact of HPV on the epidemiology and pathology of oral cancer. Head and neck pathology. 2009; 3(1):78-81.

50. Dayyani F, Etzel CJ, Liu M, Ho C-H, Lippman SM and Tsao AS. Meta-analysis of the impact of human papillomavirus (HPV) on cancer risk and overall survival in head and neck squamous cell carcinomas (HNSCC). Head & neck oncology. 2010; 2(1):1.

51. Shillitoe EJ. The role of viruses in squamous cell carcinoma of the oropharyngeal mucosa. Oral oncology. 2009; 45(4):351-355.

52. Maden C, Beckmann AM, Thomas DB, McKnight B, Sherman KJ, Ashley RL, Corey L and Daling JR. Human papillomaviruses, herpes simplex viruses, and the risk of oral cancer in men. American journal of epidemiology. 1992; 135(10):1093-1102.

53. Regezi JA, Sciubba JJ and Jordan RC. (2016). Oral pathology: clinical pathologic correlations: Elsevier Health Sciences).

54. Talamini R, Vaccarella S, Barbone F, Tavani A, La Vecchia C, Herrero R, Muñoz N and Franceschi S. Oral hygiene, dentition, sexual habits and risk of oral cancer. British journal of cancer. 2000; 83(9):1238.

55. Meurman JH. Infectious and dietary risk factors of oral cancer. Oral oncology. 2010; 46(6):411-413.

56. Jeggo P and Lavin MF. Cellular radiosensitivity: how much better do we understand it? International journal of radiation biology. 2009; 85(12):1061-1081.

57. Steel G. The dose rate effect: brachytherapy and targeted radiotherapy. Basic clinical radiobiology London: Arnold. 2002:192-204.

58. Mazeron R, Tao Y, Lusinchi A and Bourhis J. Current concepts of management in radiotherapy for head and neck squamous-cell cancer. Oral oncology. 2009; 45(4):402-408.

59. Forastiere AA and Burtness BA. Epidermal growth factor receptor inhibition in head and neck cancer—more insights, but more questions. Journal of clinical oncology. 2007; 25(16):2152-2155.

60. Grothey A, Voigt W, Schöber C, Müller T, Dempke W and Schmoll H. The role of insulin-like growth factor I and its receptor in cell growth, transformation, apoptosis, and chemoresistance in solid tumors. Journal of cancer research and clinical oncology. 1999; 125(3-4):166-173.

61. Kerr JF, Wyllie AH and Currie AR. Apoptosis: a basic biological phenomenon with wide-ranging implications in tissue kinetics. British journal of cancer. 1972; 26(4):239.

62. Wong RS. Apoptosis in cancer: from pathogenesis to treatment. Journal of Experimental & Clinical Cancer Research. 2011; 30(1):1.

63. Hanahan D and Weinberg RA. Hallmarks of cancer: the next generation. cell. 2011; 144(5):646-674.

64. Herr I and Debatin K-M. Cellular stress response and apoptosis in cancer therapy. Blood. 2001; 98(9):2603-2614.

65. Kerr JF, Winterford CM and Harmon BV. Apoptosis. Its significance in cancer and cancer therapy. Cancer. 1994; 73(8):2013-2026.

66. Fulda S and Debatin K. Extrinsic versus intrinsic apoptosis pathways in anticancer chemotherapy. Oncogene. 2006; 25(34):4798-4811.

67. Richard J. Youle AS. The BCL-2 protein family: opposing activities that mediate cell death. nature reviews molecular cell biology. 2008; 9:47-59.

68. Ghobrial IM, Witzig TE and Adjei AA. Targeting apoptosis pathways in cancer therapy. CA: a cancer journal for clinicians. 2005; 55(3):178-194.

69. Von Ahsen O, Waterhouse N, Kuwana T, Newmeyer D and Green D. Theharmless' release of cytochrome c. Cell death and differentiation. 2000; 7:1192-1199.

70. Riedl SJ and Salvesen GS. The apoptosome: signalling platform of cell death. Nature reviews Molecular cell biology. 2007; 8(5):405-413.

71. Adams J and Cory S. The Bcl-2 apoptotic switch in cancer development and therapy. Oncogene. 2007; 26(9):1324-1337.

72. Chipuk JE and Green DR. Do inducers of apoptosis trigger caspase-independent cell death? Nature Reviews Molecular Cell Biology. 2005; 6(3):268-275.

73. Chipuk J, Bouchier-Hayes L and Green D. Mitochondrial outer membrane permeabilization during apoptosis: the innocent bystander scenario. Cell Death Differ. 2006; 13(8):1396-1402.

74. Gélinas C and White E. BH3-only proteins in control: specificity regulates MCL-1 and BAK-mediated apoptosis. Genes & development. 2005; 19(11):1263-1268.

75. Puthalakath H and Strasser A. Keeping killers on a tight leash: transcriptional and post-translational control of the pro-apoptotic activity of BH3-only proteins. Cell death and differentiation. 2002; 9(5):505-512.

76. Kozopas KM, Yang T, Buchan HL, Zhou P and Craig RW. MCL1, a gene expressed in programmed myeloid cell differentiation, has sequence similarity to BCL2. P Natl Acad Sci. 1993; 90(8):3516-3520.

77. Craig RW, Jabs EW, Zhou P, Kozopas KM, Hawkins AL, Rochelle JM, Seldin MF and Griffins CA. Human and mouse chromosomal mapping of the Myeloid cell leukemia-1 gene: MCL1 maps to human chromosome 1q21, a region that is frequently altered in preneoplastic and neoplastic disease. Genomics. 1994; 23(2):457-463.

78. Yang T, Kozopas KM and Craig RW. The intracellular distribution and pattern of expression of Mcl-1 overlap with, but are not identical to, those of Bcl-2. J Cell Biol. 1995; 128(6):1173-1184.

79. Michels J, O'Neill JW, Dallman CL, Mouzakiti A, Habens F, Brimmell M, Zhang KY, Craig RW, Marcusson EG and Johnson PW. Mcl-1 is required for Akata6 B-lymphoma cell

survival and is converted to a cell death molecule by efficient caspase-mediated cleavage. Oncogene. 2004; 23(28):4818-4827.

80. Maurer U, Charvet C, Wagman AS, Dejardin E and Green DR. Glycogen synthase kinase-3 regulates mitochondrial outer membrane permeabilization and apoptosis by destabilization of MCL-1. Mol Cell. 2006; 21(6):749-760.

81. Rinkenberger JL, Horning S, Klocke B, Roth K and Korsmeyer SJ. Mcl-1 deficiency results in peri-implantation embryonic lethality. Gene Dev. 2000; 14(1):23-27.

82. Opferman JT, Iwasaki H, Ong CC, Suh H, Mizuno Si, Akashi K and Korsmeyer SJ. Obligate role of anti-apoptotic MCL-1 in the survival of hematopoietic stem cells. Science. 2005; 307(5712):1101-1104.

83. Opferman JT, Letai A, Beard C, Sorcinelli MD, Ong CC and Korsmeyer SJ. Development and maintenance of B and T lymphocytes requires antiapoptotic MCL-1. Nature. 2003; 426(6967):671-676.

84. Derenne S, Monia B, Dean NM, Taylor JK, Rapp M-J, Harousseau J-L, Bataille R and Amiot M. Antisense strategy shows that Mcl-1 rather than Bcl-2 or Bcl-xL is an essential survival protein of human myeloma cells. Blood. 2002; 100(1):194-199.

85. Zhou P, Qian L, Kozopas KM and Craig RW. Mcl-1, a Bcl-2 family member, delays the death of hematopoietic cells under a variety of apoptosis-inducing conditions. Blood. 1997; 89(2):630-643.

86. Jiang CC, Lucas K, Avery-Kiejda KA, Wade M, Thorne RF, Allen J, Hersey P and Zhang XD. Up-regulation of Mcl-1 is critical for survival of human melanoma cells upon endoplasmic reticulum stress. Cancer Res. 2008; 68(16):6708-6717.

87. Adams JM. Ways of dying: multiple pathways to apoptosis. Gene Dev. 2003; 17(20):2481-2495.

88. Cuconati A, Mukherjee C, Perez D and White E. DNA damage response and MCL-1 destruction initiate apoptosis in adenovirus-infected cells. Gene Dev. 2003; 17(23):2922-2932.

89. Willis SN, Chen L, Dewson G, Wei A, Naik E, Fletcher JI, Adams JM and Huang DC. Proapoptotic Bak is sequestered by Mcl-1 and Bcl-xL, but not Bcl-2, until displaced by BH3-only proteins. Gene Dev. 2005; 19(11):1294-1305.

90. Nguyen M, Marcellus RC, Roulston A, Watson M, Serfass L, Madiraju SM, Goulet D, Viallet J, Bélec L and Billot X. Small molecule obatoclax (GX15-070) antagonizes MCL-1 and overcomes MCL-1-mediated resistance to apoptosis. Proceedings of the National Academy of Sciences. 2007; 104(49):19512-19517.

91. Gomez-Bougie P, Ménoret E, Juin P, Dousset C, Pellat-Deceunynck C and Amiot M. Noxa controls Mule-dependent Mcl-1 ubiquitination through the regulation of the Mcl-1/USP9X interaction. Biochemical and biophysical research communications. 2011; 413(3):460-464.

92. Perciavalle RM, Stewart DP, Koss B, Lynch J, Milasta S, Bathina M, Temirov J, Cleland MM, Pelletier S and Schuetz JD. Anti-apoptotic MCL-1 localizes to the mitochondrial matrix and couples mitochondrial fusion to respiration. Nature cell biology. 2012; 14(6):575-583.

93. Morciano G, Giorgi C, Balestra D, Marchi S, Perrone D, Pinotti M and Pinton P. Mcl-1 involvement in mitochondrial dynamics is associated with apoptotic cell death. Molecular biology of the cell. 2016; 27(1):20-34.

94. Perciavalle RM and Opferman JT. Delving deeper: MCL-1's contributions to normal and cancer biology. Trends in cell biology. 2013; 23(1):22-29.

95. Skvara H, Thallinger C, Wacheck V, Monia BP, Pehamberger H, Jansen B and Selzer E. Mcl-1 blocks radiation-induced apoptosis and inhibits clonogenic cell death. Anticancer Res. 2005; 25(4):2697-2703.

96. Guoan X, Hanning W, Kaiyun C and Hao L. Adenovirus-mediated siRNA targeting Mcl-1 gene increases radiosensitivity of pancreatic carcinoma cells in vitro and in vivo. Surgery. 2010; 147(4):553-561.

97. Jamil S, Mojtabavi S, Hojabrpour P, Cheah S and Duronio V. An essential role for MCL-1 in ATR-mediated CHK1 phosphorylation. Mol Biol Cell. 2008; 19(8):3212-3220.

98. Jamil S, Stoica C, Hackett TL and Duronio V. MCL-1 localizes to sites of DNA damage and regulates DNA damage response. Cell Cycle. 2010; 9(14):2915-2927.

99. Levine B and Kroemer G. Autophagy in the pathogenesis of disease. Cell. 2008; 132(1):27-42.

100. Elgendy M, Ciro M, Abdel-Aziz AK, Belmonte G, Dal Zuffo R, Mercurio C, Miracco C, Lanfrancone L, Foiani M and Minucci S. Beclin 1 restrains tumorigenesis through Mcl-1 destabilization in an autophagy-independent reciprocal manner. Nature communications. 2014; 5.

101. Levine B, Sinha SC and Kroemer G. Bcl-2 family members: dual regulators of apoptosis and autophagy. Autophagy. 2008; 4(5):600-606.

102. Germain M, Nguyen AP, Le Grand JN, Arbour N, Vanderluit JL, Park DS, Opferman JT and Slack RS. MCL-1 is a stress sensor that regulates autophagy in a developmentally regulated manner. The EMBO journal. 2011; 30(2):395-407.

103. Germain M and Slack RS. MCL-1 regulates the balance between autophagy and apoptosis. Autophagy. 2011; 7(5):549-551.

104. Thomas RL, Roberts DJ, Kubli DA, Lee Y, Quinsay MN, Owens JB, Fischer KM, Sussman MA, Miyamoto S and Gustafsson ÅB. Loss of MCL-1 leads to impaired autophagy and rapid development of heart failure. Genes & development. 2013; 27(12):1365-1377.

105. Franziska Ertel MN, Anne Roulston & Gordon C. Shore. Programming cancer cells for high expression levels of Mcl1. European Molecular Biology Orgnization. 2013.

106. Craig RW JE, Zhou P, Kozopas KM, Hawkins AL, Rochelle JM, Seldin MF, Griffin CA. Human and mouse chromosomal mapping of the myeloid cell leukemia-1 gene: MCL1 maps to human chromosome 1q21, a region that is frequently altered in preneoplastic and neoplastic disease. Genomics. 1994; 23(2):457-463.

107. Beroukhim R, Mermel CH, Porter D, Wei G, Raychaudhuri S, Donovan J, Barretina J, Boehm JS, Dobson J and Urashima M. The landscape of somatic copy-number alteration across human cancers. Nature. 2010; 463(7283):899-905.

108. Moshynska O, Sankaran K, Pahwa P and Saxena A. Prognostic significance of a short sequence insertion in the MCL-1 promoter in chronic lymphocytic leukemia. J Natl Cancer I. 2004; 96(9):673-682.

109. Kitada S and Reed JC. MCL-1 promoter insertions dial-up aggressiveness of chronic leukemia. J Natl Cancer I. 2004; 96(9):642-643.

110. Wei G, Margolin AA, Haery L, Brown E, Cucolo L, Julian B, Shehata S, Kung AL, Beroukhim R and Golub TR. Chemical Genomics Identifies Small-Molecule MCL1 Repressors and BCL-xL as a Predictor of MCL1 Dependency. Cancer cell. 2012; 21(4):547-562.

111. Liu H MY, Cole SM, Zander C, Chen KH, Karras J, Pope RM. Serine phosphorylation of STAT3 is essential for Mcl-1 expression and macrophage survival. Blood. 2003; 102(1):344-352.

112. Isomoto H KS, Werneburg NW, Bronk SF, Guicciardi ME, Frank DA, Gores GJ. Interleukin 6 upregulates myeloid cell leukemia-1 expression through a STAT3 pathway in cholangiocarcinoma cells. Hepatology 2005; 42(6):1329-1338.

113. Wang JM CJ, Chen W, Kuo ML, Yen JJ, Yang-Yen HF. The antiapoptotic gene mcl-1 is upregulated by the phosphatidylinositol 3-kinase/Akt signalling pathway through a transcription factor complex containing CREB. Mol Cell Biol. 1999; 19(9):6195-6206.

114. Townsend KJ TJ, Traupman MA, Eastman A, Craig RW. Expression of the antiapoptotic MCL1 gene product is regulated by a mitogen activated protein kinase-mediated pathway triggered through microtubule disruption and protein kinase C. Oncogene. 1998; 17(10):1223-1234.

115. Aichberger KJ, Mayerhofer M, Krauth M-T, Skvara H, Florian S, Sonneck K, Akgul C, Derdak S, Pickl WF and Wacheck V. Identification of Mcl-1 as a BCR/ABL-dependent target in chronic myeloid leukemia (CML): evidence for cooperative antileukemic effects of imatinib and mcl-1 antisense oligonucleotides. Blood. 2005; 105(8):3303-3311.

116. Wang J-M, Lai M-Z and Yang-Yen H-F. Interleukin-3 stimulation of mcl-1 gene transcription involves activation of the PU. 1 transcription factor through a p38 mitogen-activated protein kinase-dependent pathway. Molecular and cellular biology. 2003; 23(6):1896-1909.

117. Piret J-P, Minet E, Cosse J-P, Ninane N, Debacq C, Raes M and Michiels C. Hypoxia-inducible factor-1-dependent overexpression of myeloid cell factor-1 protects hypoxic cells against tert-butyl hydroperoxide-induced apoptosis. Journal of Biological Chemistry. 2005; 280(10):9336-9344.

118. Dong L, Jiang C, Thorne R, Croft A, Yang F, Liu H, de Bock C, Hersey P and Zhang X. Ets-1 mediates upregulation of Mcl-1 downstream of XBP-1 in human melanoma cells upon ER stress. Oncogene. 2011; 30(34):3716-3726.

119. Jiang CC, Lucas K, Avery-Kiejda KA, Wade M, Thorne RF, Allen J, Hersey P and Zhang XD. Up-regulation of Mcl-1 is critical for survival of human melanoma cells upon endoplasmic reticulum stress. Cancer Research. 2008; 68(16):6708-6717.

120. Croxton R MY, Song L, Haura EB, Cress WD. Direct repression of the Mcl-1 promoter by E2F1. Oncogene. 2002; 21(9):1359-1369.

121. Puzianowska-Kuznicka MPaM. p53-dependent repression of the human MCL-1 gene encoding an anti-apoptotic member of the BCL-2 family: the role of Sp1 and of basic transcription factor binding sites in the MCL-1 promoter. Biol Chem. 2008; 389:383-393.

122. Moulding DA, Akgul C, Derouet M, White MR and Edwards SW. BCL-2 family expression in human neutrophils during delayed and accelerated apoptosis. Journal of leukocyte biology. 2001; 70(5):783-792.

123. Mott JL, Kobayashi S, Bronk SF and Gores GJ. mir-29 regulates Mcl-1 protein expression and apoptosis. Oncogene. 2007; 26(42):6133-6140.

124. Crawford M BK, Yu L, Wu X, Nuovo GJ, Marsh CB, Otterson GA, Nana-Sinkam SP. MicroRNA 133B targets pro-survival molecules MCL-1 and BCL2L2 in lung cancer. Biochem Biophys Res Commun. 2009; 388(3):483-489.

125. Li RY, Chen LC, Zhang HY, Du WZ, Feng Y, Wang HB, Wen JQ, Liu X, Li XF and Sun Y. MiR-139 Inhibits Mcl-1 Expression and Potentiates TMZ-Induced Apoptosis in Glioma. CNS neuroscience & therapeutics. 2013.

126. Subramaniam D, Natarajan G, Ramalingam S, Ramachandran I, May R, Queimado L, Houchen CW and Anant S. Translation inhibition during cell cycle arrest and apoptosis: Mcl-1 is a novel target for RNA binding protein CUGBP2. American Journal of Physiology-Gastrointestinal and Liver Physiology. 2008; 294(4):G1025-G1032.

127. Bingle CD, Craig RW, Swales BM, Singleton V, Zhou P and Whyte MK. Exon skipping in Mcl-1 results in a bcl-2 homology domain 3 only gene product that promotes cell death. Journal of Biological Chemistry. 2000; 275(29):22136-22146.

128. Bae J, Leo CP, Hsu SY and Hsueh AJ. MCL-1S, a splicing variant of the antiapoptotic BCL-2 family member MCL-1, encodes a proapoptotic protein possessing only the BH3 domain. Journal of Biological Chemistry. 2000; 275(33):25255-25261.

129. Kim J-H, Sim S-H, Ha H-J, Ko J-J, Lee K and Bae J. MCL-1ES, a novel variant of MCL-1, associates with MCL-1L and induces mitochondrial cell death. FEBS letters. 2009; 583(17):2758-2764.

130. Ding Q HL, Yang JY, Xia W, Wei Y, Liao Y, Chang CJ, Yang Y, Lai CC, Lee DF, Yen CJ, Chen YJ, Hsu JM, Kuo HP, Lin CY, Tsai FJ, Li LY, Tsai CH, Hung MC. Down-regulation of myeloid cell leukemia-1 through inhibiting Erk/Pin 1 pathway by sorafenib facilitates chemosensitization in breast cancer. Cancer Res 2008; 68(15):6109-6117.

131. Kodama Y TK, Miura K, Schnabl B, Osawa Y, Brenner D. Antiapoptotic effect of c-Jun N-terminal kinase-1 through Mcl-1 stabilization in TNF-induced hepatocyte apoptosis. Gastroenterology 2009; 136(4):1423–1434.

132. Ding Q HX, Hsu JM, Xia W, Chen CT, Li LY, Lee DF, Liu JC, Zhong Q, Wang X, Hung MC. Degradation of Mcl-1 by beta-TrCP mediates glycogen synthase kinase 3-induced tumor suppression and chemosensitization. Mol Cell Biol. 2007; 27(11):4006-4017.

133. Morel C, Carlson SM, White FM and Davis RJ. Mcl-1 integrates the opposing actions of signaling pathways that mediate survival and apoptosis. Molecular and cellular biology. 2009; 29(14):3845-3852.

134. Inoshita S, Takeda K, Hatai T, Terada Y, Sano M, Hata J, Umezawa A and Ichijo H. Phosphorylation and inactivation of myeloid cell leukemia 1 by JNK in response to oxidative stress. Journal of Biological Chemistry. 2002; 277(46):43730-43734.

135. Sitailo LA, Tibudan SS and Denning MF. The protein kinase Cδ catalytic fragment targets Mcl-1 for degradation to trigger apoptosis. Journal of Biological Chemistry. 2006; 281(40):29703-29710.

136. Zhong Q, Gao, W., Du, F. and Wang, X. . Mule/ARFBP1, a BH3-only E3 ubiquitin ligase, catalyzes the polyubiquitination of Mcl-1 and regulates apoptosis. Cell. 2005; 121:1085–1095.

137. Warr MR, Acoca S, Liu Z, Germain M, Watson M, Blanchette M, Wing SS and Shore GC. BH3-ligand regulates access of MCL-1 to its E3 ligase. FEBS letters. 2005; 579(25):5603-5608.

138. Inuzuka H SS, Onoyama I, Gao D, Tseng A, Maser RS, Zhai B, Wan L, Gutierrez A, Lau AW, Xiao Y, Christie AL, Aster J, Settleman J, Gygi SP, Kung AL, Look T, Nakayama KI, DePinho RA, Wei W. SCFFBW7 regulates cellular apoptosis by targeting MCL1 for ubiquitylation and destruction. Nature. 2011; 471(7336):104-109.

139. Harley ME, Allan LA, Sanderson HS and Clarke PR. Phosphorylation of Mcl-1 by CDK1–cyclin B1 initiates its Cdc20-dependent destruction during mitotic arrest. The EMBO journal. 2010; 29(14):2407-2420.

140. Xu S, Peng G, Wang Y, Fang S and Karbowski M. The AAA-ATPase p97 is essential for outer mitochondrial membrane protein turnover. Molecular Biology of the Cell. 2011; 22(3):291-300.

141. Weng C, Li Y, Xu D, Shi Y and Tang H. Specific cleavage of Mcl-1 by caspase-3 in tumor necrosis factor-related apoptosis-inducing ligand (TRAIL)-induced apoptosis in Jurkat leukemia T cells. Journal of Biological Chemistry. 2005; 280(11):10491-10500.

142. Han J, Goldstein LA, Gastman BR, Froelich CJ, Yin X-M and Rabinowich H. Degradation of Mcl-1 by Granzyme B Implications for Bim-mediated mitochondrial apoptotic events. Journal of Biological Chemistry. 2004; 279(21):22020-22029.

143. Stewart DP, Koss B, Bathina M, Perciavalle RM, Bisanz K and Opferman JT. Ubiquitin-independent degradation of antiapoptotic MCL-1. Molecular and cellular biology. 2010; 30(12):3099-3110.

144. De Biasio A, Vrana JA, Zhou P, Qian L, Bieszczad CK, Braley KE, Domina AM, Weintraub SJ, Neveu JM and Lane WS. N-terminal truncation of antiapoptotic MCL1, but not G2/M-induced phosphorylation, is associated with stabilization and abundant expression in tumor cells. Journal of Biological Chemistry. 2007; 282(33):23919-23936.

145. Warr MR MJ, Nguyen M, Lemaire-Ewing S, Baardsnes J, Sun KL, Malina A, Young JC, Jeyaraju DV, O'Connor-McCourt M, Pellegrini L, Pelletier J, Shore GC:. Mitochondrion-dependent N-terminal Processing of Outer Membrane Mcl-1 Protein Removes an Essential Mule/Lasu1Protein-binding Site. Journal of Biological Chemistry. 2011; 286(28):25098-25107.

146. Germain M and Duronio V. The N terminus of the anti-apoptotic BCL-2 homologue MCL-1 regulates its localization and function. Journal of Biological Chemistry. 2007; 282(44):32233-32242.

147. Mei Y, Du W, Yang Y and Wu M. Puma*Mcl-1 interaction is not sufficient to prevent rapid degradation of Mcl-1. Oncogene. 2005; 24(48):7224-7237.

148. Warr MR, Acoca S, Liu Z, Germain M, Watson M, Blanchette M, Wing SS and Shore GC. BH3-ligand regulates access of MCL-1 to its E3 ligase. FEBS Lett. 2005; 579(25):5603-5608.

149. Pickart CM. Mechanisms underlying ubiquitination. Annual review of biochemistry. 2001; 70(1):503-533.

150. Komander D, Clague MJ and Urbé S. Breaking the chains: structure and function of the deubiquitinases. Nature reviews Molecular cell biology. 2009; 10(8):550-563.

151. Wilkinson KD. DUBs at a glance. J Cell Sci. 2009; 122(14):2325-2329.

152. Sacco JJ, Coulson JM, Clague MJ and Urbé S. Emerging roles of deubiquitinases in cancer-associated pathways. IUBMB life. 2010; 62(2):140-157.

153. Hussain S, Zhang Y and Galardy P. DUBs and cancer: the role of deubiquitinating enzymes as oncogenes, non-oncogenes and tumor suppressors. Cell cycle. 2009; 8(11):1688-1697.

154. Nicholson B, Marblestone JG, Butt TR and Mattern MR. Deubiquitinating enzymes as novel anticancer targets. 2007.

155. Schwickart M, Huang X, Lill JR, Liu J, Ferrando R, French DM, Maecker H, O'Rourke K, Bazan F and Eastham-Anderson J. Deubiquitinase USP9X stabilizes MCL1 and promotes tumour cell survival. Nature. 2010; 463(7277):103-107.

156. Bommer U-A and Thiele B-J. The translationally controlled tumour protein (TCTP). The international journal of biochemistry & cell biology. 2004; 36(3):379-385.

157. Liu H, Peng H-W, Cheng Y-S, Yuan HS and Yang-Yen H-F. Stabilization and enhancement of the antiapoptotic activity of mcl-1 by TCTP. Molecular and cellular biology. 2005; 25(8):3117-3126.

158. Li F, Zhang D and Fujise K. Characterization of fortilin, a novel antiapoptotic protein. Journal of Biological Chemistry. 2001; 276(50):47542-47549.

159. Tuynder M SL, Prieur S, Besse S, Fiucci G, Amson R, Telerman A. Biological models and genes of tumor reversion: cellular reprogramming through tpt1/TCTP and SIAH-1. Proc Natl Acad Sci USA. 2002; 99(23):14976-14981.

160. Zhong Q, Gao W, Du F and Wang X. Mule/ARF-BP1, a BH3-only E3 ubiquitin ligase, catalyzes the polyubiquitination of Mcl-1 and regulates apoptosis. Cell. 2005; 121(7):1085-1095.

161. Sieghart W, Losert D, Strommer S, Cejka D, Schmid K, Rasoul-Rockenschaub S, Bodingbauer M, Crevenna R, Monia BP and Peck-Radosavljevic M. Mcl-1 overexpression in hepatocellular carcinoma: a potential target for antisense therapy. Journal of hepatology. 2006; 44(1):151-157.

162. Krajewska M, Krajewski S, Epstein JI, Shabaik A, Sauvageot J, Song K, Kitada S and Reed JC. Immunohistochemical analysis of bcl-2, bax, bcl-X, and mcl-1 expression in prostate cancers. The American journal of pathology. 1996; 148(5):1567.

163. Miyamoto Y, Hosotani R, Wada M, Lee J-U, Koshiba T, Fujimoto K, Tsuji S, Nakajima S, Kato M and Shimada Y. Immunohistochemical analysis of Bcl-2, Bax, Bcl-X, and Mcl-1 expression in pancreatic cancers. Oncology. 1999; 56(1):73-82.

164. Derenne S, Monia B, Dean NM, Taylor JK, Rapp MJ, Harousseau JL, Bataille R and Amiot M. Antisense strategy shows that Mcl-1 rather than Bcl-2 or Bcl-xL is an essential survival protein of human myeloma cells. Blood. 2002; 100(1):194-199.

165. Cho-Vega JH, Rassidakis GZ, Admirand JH, Oyarzo M, Ramalingam P, Paraguya A, McDonnell TJ, Amin HM and Medeiros LJ. MCL-1 expression in B-cell non-Hodgkin's lymphomas. Human pathology. 2004; 35(9):1095-1100.

166. Schulze-Bergkamen H, Ehrenberg R, Hickmann L, Vick B, Urbanik T, Schimanski CC, Berger MR, Schad A, Weber A and Heeger S. Bcl-xL and Myeloid cell leukaemia-1 contribute to apoptosis resistance of colorectal cancer cells. World J Gastroentero. 2008; 14(24):3829.

167. Thallinger C, Wolschek MF, Maierhofer H, Skvara H, Pehamberger H, Monia BP, Jansen B, Wacheck V and Selzer E. Mcl-1 Is a Novel Therapeutic Target for Human Sarcoma Synergistic Inhibition of Human Sarcoma Xenotransplants by a Combination of Mcl-1 Antisense Oligonucleotides with Low-Dose Cyclophosphamide. Clinical cancer research. 2004; 10(12):4185-4191.

168. Chetoui N, Sylla K, Gagnon Houde JV, Alcaide Loridan C, Charron D, Al Daccak R and Aoudjit F. Down-regulation of Mcl-1 by small interfering RNA sensitizes resistant melanoma cells to fas-mediated apoptosis. Mol Cancer Res. 2008; 6(1):42-52.

169. Chen S, Dai Y, Harada H, Dent P and Grant S. Mcl-1 down-regulation potentiates ABT-737 lethality by cooperatively inducing Bak activation and Bax translocation. Cancer research. 2007; 67(2):782-791.

170. Xu H and Krystal GW. Actinomycin D decreases Mcl-1 expression and acts synergistically with ABT-737 against small cell lung cancer cell lines. Clin Cancer Res. 2010; 16(17):4392-4400.

171. Raje N, Kumar S, Hideshima T, Roccaro A, Ishitsuka K, Yasui H, Shiraishi N, Chauhan D, Munshi NC and Green SR. Seliciclib (CYC202 or R-roscovitine), a small-molecule cyclin-

dependent kinase inhibitor, mediates activity via down-regulation of Mcl-1 in multiple myeloma. Blood. 2005; 106(3):1042-1047.

172. Huber S, Oelsner M, Decker T, zum Büschenfelde CM, Wagner M, Lutzny G, Kuhnt T, Schmidt B, Oostendorp R and Peschel C. Sorafenib induces cell death in chronic lymphocytic leukemia by translational downregulation of Mcl-1. Leukemia. 2011; 25(5):838-847.

173. Ma Y, Cress WD and Haura EB. Flavopiridol-induced Apoptosis Is Mediated through Up-Regulation of E2F1 and Repression of Mcl-11. Mol Cancer Ther. 2003; 2(1):73-81.

174. Müller A, Zang C, Chumduri C, Dörken B, Daniel PT and Scholz CW. Concurrent inhibition of PI3K and mTORC1/mTORC2 overcomes resistance to rapamycin induced apoptosis by down-regulation of Mcl-1 in mantle cell lymphoma. Int J Cancer. 2013.

175. Schwickart M, Huang X, Lill JR, Liu J, Ferrando R, French DM, Maecker H, O'Rourke K, Bazan F and Eastham-Anderson J. Deubiquitinase USP9X stabilizes MCL1 and promotes tumour cell survival. Nature. 2009; 463(7277):103-107.

176. Kapuria V, Peterson LF, Fang D, Bornmann WG, Talpaz M and Donato NJ. Deubiquitinase inhibition by small-molecule WP1130 triggers aggresome formation and tumor cell apoptosis. Cancer Res. 2010; 70(22):9265-9276.

177. Oltersdorf T, Elmore SW, Shoemaker AR, Armstrong RC, Augeri DJ, Belli BA, Bruncko M, Deckwerth TL, Dinges J and Hajduk PJ. An inhibitor of Bcl-2 family proteins induces regression of solid tumours. Nature. 2005; 435(7042):677-681.

178. Walensky LD. From mitochondrial biology to magic bullet: navitoclax disarms BCL-2 in chronic lymphocytic leukemia. J Clin Oncol. 2012; 30(5):554-557.

179. Lee EF, Czabotar PE, Van Delft MF, Michalak EM, Boyle MJ, Willis SN, Puthalakath H, Bouillet P, Colman PM and Huang DC. A novel BH3 ligand that selectively targets Mcl-1 reveals that apoptosis can proceed without Mcl-1 degradation. J Cell Biol. 2008; 180(2):341-355.

180. Rahmani M, Aust MM, Attkisson E, Williams DC, Ferreira-Gonzalez A and Grant S. Inhibition of Bcl-2 antiapoptotic members by obatoclax potently enhances sorafenib-induced apoptosis in human myeloid leukemia cells through a Bim-dependent process. Blood. 2012; 119(25):6089-6098.

181. Huang S, Okumura K and Sinicrope FA. BH3 mimetic obatoclax enhances TRAIL-mediated apoptosis in human pancreatic cancer cells. Clinical Cancer Research. 2009; 15(1):150-159.

182. Smoot RL, Blechacz BR, Werneburg NW, Bronk SF, Sinicrope FA, Sirica AE and Gores GJ. A Bax-mediated mechanism for obatoclax-induced apoptosis of cholangiocarcinoma cells. Cancer research. 2010; 70(5):1960-1969.

183. O'Brien SM, Claxton DF, Crump M, Faderl S, Kipps T, Keating MJ, Viallet J and Cheson BD. Phase I study of obatoclax mesylate (GX15-070), a small molecule pan–Bcl-2 family antagonist, in patients with advanced chronic lymphocytic leukemia. Blood. 2009; 113(2):299-305.

184. Schimmer AD, O'Brien S, Kantarjian H, Brandwein J, Cheson BD, Minden MD, Yee K, Ravandi F, Giles F and Schuh A. A phase I study of the pan bcl-2 family inhibitor obatoclax mesylate in patients with advanced hematologic malignancies. Clinical cancer research. 2008; 14(24):8295-8301.

185. Parikh SA, Kantarjian H, Schimmer A, Walsh W, Asatiani E, El-Shami K, Winton E and Verstovsek S. Phase II study of obatoclax mesylate (GX15-070), a small-molecule BCL-2 family

antagonist, for patients with myelofibrosis. Clinical Lymphoma Myeloma and Leukemia. 2010; 10(4):285-289.

186. Zhang Z, Song T, Zhang T, Gao J, Wu G, An L and Du G. A novel BH3 mimetic S1 potently induces Bax/Bak-dependent apoptosis by targeting both Bcl-2 and Mcl-1. Int J Cancer. 2011; 128(7):1724-1735.

187. Dash R, Azab B, Quinn BA, Shen X, Wang XY, Das SK, Rahmani M, Wei J, Hedvat M and Dent P. Apogossypol derivative BI-97C1 (Sabutoclax) targeting Mcl-1 sensitizes prostate cancer cells to mda-7/IL-24–mediated toxicity. P Natl Acad Sci. 2011; 108(21):8785-8790.

188. Varadarajan S, Butterworth M, Wei J, Pellecchia M, Dinsdale D and Cohen GM. Sabutoclax (BI97C1) and BI112D1, Putative Inhibitors of MCL-1, Induce Mitochondrial Fragmentation Either Upstream of or Independent of Apoptosis. Neoplasia. 2013; 15(5):568.

189. Maji S, Samal SK, Pattanaik L, Panda S, Quinn BA, Das SK, Sarkar D, Pellecchia M, Fisher PB and Dash R. Mcl-1 is an important therapeutic target for oral squamous cell carcinomas. Oncotarget. 2015; 6(18):16623.

190. Jackson RS, Placzek W, Fernandez A, Ziaee S, Chu C-Y, Wei J, Stebbins J, Kitada S, Fritz G and Reed JC. Sabutoclax, a Mcl-1 antagonist, inhibits tumorigenesis in transgenic mouse and human xenograft models of prostate cancer. Neoplasia. 2012; 14(7):656-IN624.

191. Doi K, Li R, Sung SS, Wu H, Liu Y, Manieri W, Krishnegowda G, Awwad A, Dewey A and Liu X. Discovery of marinopyrrole A (maritoclax) as a selective Mcl-1 antagonist that overcomes ABT-737 resistance by binding to and targeting Mcl-1 for proteasomal degradation. J Biol Chem. 2012; 287(13):10224-10235.

192. Rabinowitz JD and White E. Autophagy and metabolism. Science. 2010; 330(6009):1344-1348.

193. Klionsky DJ and Emr SD. Autophagy as a regulated pathway of cellular degradation. Science. 2000; 290(5497):1717-1721.

194. Debnath J, Baehrecke EH and Kroemer G. Does autophagy contribute to cell death? Autophagy. 2005; 1(2):66-74.

195. Fulda S. Autophagy and cell death. Autophagy. 2012; 8(8):1250-1251.

196. Kroemer G and Levine B. Autophagic cell death: the story of a misnomer. Nature reviews Molecular cell biology. 2008; 9(12):1004-1010.

197. Huang J and Klionsky DJ. Autophagy and human disease. Cell cycle. 2007; 6(15):1837-1849.

198. Choi AM, Ryter SW and Levine B. Autophagy in human health and disease. New England Journal of Medicine. 2013; 368(7):651-662.

199. Shintani T and Klionsky DJ. Autophagy in health and disease: a double-edged sword. Science. 2004; 306(5698):990-995.

200. Chen S, Rehman SK, Zhang W, Wen A, Yao L and Zhang J. Autophagy is a therapeutic target in anticancer drug resistance. Biochimica et Biophysica Acta (BBA)-Reviews on Cancer. 2010; 1806(2):220-229.

201. Yang ZJ, Chee CE, Huang S and Sinicrope FA. The role of autophagy in cancer: therapeutic implications. Molecular cancer therapeutics. 2011; 10(9):1533-1541.

202. Rosenfeldt MT and Ryan KM. The role of autophagy in tumour development and cancer therapy. Expert reviews in molecular medicine. 2009; 11:e36.

203. Bonapace L, Bornhauser BC, Schmitz M, Cario G, Ziegler U, Niggli FK, Schäfer BW, Schrappe M, Stanulla M and Bourquin J-P. Induction of autophagy-dependent necroptosis is

required for childhood acute lymphoblastic leukemia cells to overcome glucocorticoid resistance. The Journal of clinical investigation. 2010; 120(4):1310.

204. Kharaziha P, Chioureas D, Baltatzis G, Fonseca P, Björklund BZ, Grandér D, Egevad L, Nilsson S and Panaretakis T. Sorafenib-induced defective autophagy promotes cell death by necroptosis. prostate. 2015; 4:6.

205. Linkermann A and Green DR. Necroptosis. New England Journal of Medicine. 2014; 370(5):455-465.

206. Christofferson DE and Yuan J. Necroptosis as an alternative form of programmed cell death. Current opinion in cell biology. 2010; 22(2):263-268.

207. Pasparakis M and Vandenabeele P. Necroptosis and its role in inflammation. Nature. 2015; 517(7534):311-320.

208. Chang SE, Foster S, Betts D and Marnock WE. DOK, a cell line established from human dysplastic oral mucosa, shows a partially transformed non-malignant phenotype. International journal of cancer. 1992; 52(6):896-902.

209. Tatake RJ, Rajaram N, Damle R, Balsara B, Bhisey A and Gangal SG. Establishment and characterization of four new squamous cell carcinoma cell lines derived from oral tumors. Journal of cancer research and clinical oncology. 1990; 116(2):179-186.

210. Martin CL, Reshmi SC, Ried T, Gottberg W, Wilson JW, Reddy JK, Khanna P, Johnson JT, Myers EN and Gollin SM. Chromosomal imbalances in oral squamous cell carcinoma: examination of 31 cell lines and review of the literature. Oral oncology. 2008; 44(4):369-382.

211. Bartholomeusz G, Talpaz M, Bornmann W, Kong L-Y and Donato NJ. Degrasyn activates proteasomal-dependent degradation of c-Myc. Cancer research. 2007; 67(8):3912-3918.

212. Bartholomeusz GA, Talpaz M, Kapuria V, Kong LY, Wang S, Estrov Z, Priebe W, Wu J and Donato NJ. Activation of a novel Bcr/Abl destruction pathway by WP1130 induces apoptosis of chronic myelogenous leukemia cells. Blood. 2007; 109(8):3470-3478.

213. Shevchenko A, Tomas H, Havli J, Olsen JV and Mann M. In-gel digestion for mass spectrometric characterization of proteins and proteomes. Nature protocols. 2006; 1(6):2856-2860.

214. Trivigno D, Essmann F, Huber SM and Rudner J. Deubiquitinase USP9x confers radioresistance through stabilization of Mcl-1. Neoplasia. 2012; 14(10):893-IN894.

215. Seibenhener ML, Geetha T and Wooten MW. Sequestosome 1/p62–more than just a scaffold. FEBS letters. 2007; 581(2):175-179.

216. Kopito RR. Aggresomes, inclusion bodies and protein aggregation. Trends in cell biology. 2000; 10(12):524-530.

217. Yecies D, Carlson NE, Deng J and Letai A. Acquired resistance to ABT-737 in lymphoma cells that up-regulate MCL-1 and BFL-1. Blood. 2010; 115(16):3304-3313.

218. van Delft MF, Wei AH, Mason KD, Vandenberg CJ, Chen L, Czabotar PE, Willis SN, Scott CL, Day CL and Cory S. The BH3 mimetic ABT-737 targets selective Bcl-2 proteins and efficiently induces apoptosis via Bak/Bax if Mcl-1 is neutralized. Cancer cell. 2006; 10(5):389-399.

219. Maiuri MC, Criollo A, Tasdemir E, Vicencio JM, Tajeddine N, Hickman JA, Geneste O and Kroemer G. BH3-only proteins and BH3 mimetics induce autophagy by competitively disrupting the interaction between Beclin 1 and Bcl-2/Bcl-XL. Autophagy. 2007; 3(4):374-376.

220. Malik S, Orhon I, Morselli E, Criollo A, Shen S, Marino G, BenYounes A, Benit P, Rustin P and Maiuri M. BH3 mimetics activate multiple pro-autophagic pathways. Oncogene. 2011; 30(37):3918-3929.

221. Moreau K, Luo S and Rubinsztein DC. Cytoprotective roles for autophagy. Current opinion in cell biology. 2010; 22(2):206-211.

222. Vandenabeele P, Galluzzi L, Berghe TV and Kroemer G. Molecular mechanisms of necroptosis: an ordered cellular explosion. Nature reviews Molecular cell biology. 2010; 11(10):700-714.

223. Yazbeck VY, Li C, Grandis JR, Zang Y and Johnson DE. Single-agent obatoclax (GX15-070) potently induces apoptosis and pro-survival autophagy in head and neck squamous cell carcinoma cells. Oral oncology. 2014; 50(2):120-127.

224. Basit F, Cristofanon S and Fulda S. Obatoclax (GX15-070) triggers necroptosis by promoting the assembly of the necrosome on autophagosomal membranes. Cell Death & Differentiation. 2013; 20(9):1161-1173.

225. F McCoy JH, N McTavish, I Paul, C Barnes, B O'Hagan, K Odrzywol, J Murray, D Longley, G McKerr and DA Fennell. Obatoclax induces Atg7-dependent autophagy independent of beclin-1 and BAX/BAK. Cell Death and Disease. 2010; 1(108):1-13.

226. Mizushima N and Yoshimori T. How to interpret LC3 immunoblotting. Autophagy. 2007; 3(6):542-545.

227. Kimura S, Noda T and Yoshimori T. Dissection of the autophagosome maturation process by a novel reporter protein, tandem fluorescent-tagged LC3. Autophagy. 2007; 3(5):452-460.

228. Kharaziha P, Chioureas D, Baltatzis G, Fonseca P, Rodriguez P, Gogvadze V, Lennartsson L, Björklund A-C, Zhivotovsky B and Grandér D. Sorafenib-induced defective autophagy promotes cell death by necroptosis. Oncotarget. 2015; 6(35):37066.

229. Burton TR and Gibson SB. The role of Bcl-2 family member BNIP3 in cell death and disease: NIPping at the heels of cell death. Cell Death & Differentiation. 2009; 16(4):515-523.

230. Lemasters JJ. Selective mitochondrial autophagy, or mitophagy, as a targeted defense against oxidative stress, mitochondrial dysfunction, and aging. Rejuvenation research. 2005; 8(1):3-5.

231. Thomas RL, Kubli DA and Gustafsson ÅB. Bnip3-mediated defects in oxidative phosphorylation promote mitophagy. Autophagy. 2011; 7(7):775-777.

232. Mizumura K, Cloonan SM, Nakahira K, Bhashyam AR, Cervo M, Kitada T, Glass K, Owen CA, Mahmood A and Washko GR. Mitophagy-dependent necroptosis contributes to the pathogenesis of COPD. The Journal of clinical investigation. 2014; 124(9):3987.

233. Ding Q, He X, Hsu JM, Xia W, Chen CT, Li LY, Lee DF, Liu JC, Zhong Q and Wang X. Degradation of Mcl-1 by β-TrCP mediates glycogen synthase kinase 3-induced tumor suppression and chemosensitization. Mol Cell Biol. 2007; 27(11):4006-4017.

234. Sitailo LA, Tibudan SS and Denning MF. The protein kinase Cδ catalytic fragment targets Mcl-1 for degradation to trigger apoptosis. J Biol Chem. 2006; 281(40):29703-29710.

235. Han J, Goldstein LA, Gastman BR, Froelich CJ, Yin XM and Rabinowich H. Degradation of Mcl-1 by Granzyme B Implications for Bim-mediated mitochondrial apoptotic events. J Biol Chem. 2004; 279(21):22020-22029.

236. Weng C, Li Y, Xu D, Shi Y and Tang H. Specific cleavage of Mcl-1 by caspase-3 in tumor necrosis factor-related apoptosis-inducing ligand (TRAIL)-induced apoptosis in Jurkat leukemia T cells. J Biol Chem. 2005; 280(11):10491-10500.

237. Stewart DP, Koss B, Bathina M, Perciavalle RM, Bisanz K and Opferman JT. Ubiquitin-independent degradation of antiapoptotic MCL-1. Mol Cell Biol. 2010; 30(12):3099-3110.

238. Zhang C, Cai T-y, Zhu H, Yang L-q, Jiang H, Dong X-w, Hu Y-z, Lin N-m, He Q-j and Yang B. Synergistic antitumor activity of gemcitabine and ABT-737 in vitro and in vivo through disrupting the interaction of USP9X and Mcl-1. Molecular cancer therapeutics. 2011; 10(7):1264-1275.

239. Luise C, Capra M, Donzelli M, Mazzarol G, Jodice MG, Nuciforo P, Viale G, Di Fiore PP and Confalonieri S. An atlas of altered expression of deubiquitinating enzymes in human cancer. PloS one. 2011; 6(1):e15891.

240. Peddaboina C, Jupiter D, Fletcher S, Yap JL, Rai A, Tobin RP, Jiang W, Rascoe P, Rogers MKN and Smythe WR. The downregulation of Mcl-1 via USP9X inhibition sensitizes solid tumors to Bcl-xl inhibition. BMC cancer. 2012; 12(1):541.

241. Sun H, Kapuria V, Peterson LF, Fang D, Bornmann WG, Bartholomeusz G, Talpaz M and Donato NJ. Bcr-Abl ubiquitination and Usp9x inhibition block kinase signaling and promote CML cell apoptosis. Blood. 2011; 117(11):3151-3162.

242. Pérez-Mancera PA, Rust AG, van der Weyden L, Kristiansen G, Li A, Sarver AL, Silverstein KA, Grützmann R, Aust D and Rümmele P. The deubiquitinase USP9X suppresses pancreatic ductal adenocarcinoma. Nature. 2012; 486(7402):266-270.

243. Dupont S, Mamidi A, Cordenonsi M, Montagner M, Zacchigna L, Adorno M, Martello G, Stinchfield MJ, Soligo S and Morsut L. FAM/USP9x, a deubiquitinating enzyme essential for TGFβ signaling, controls Smad4 monoubiquitination. Cell. 2009; 136(1):123-135.

244. of the International IPT and Consortium CG. Mutational landscape of gingivo-buccal oral squamous cell carcinoma reveals new recurrently-mutated genes and molecular subgroups. Nature communications. 2013; 4.

245. Ivanova NB, Dimos JT, Schaniel C, Hackney JA, Moore KA and Lemischka IR. A stem cell molecular signature. Science. 2002; 298(5593):601-604.

246. Jolly LA, Taylor V and Wood SA. USP9X enhances the polarity and self-renewal of embryonic stem cell-derived neural progenitors. Molecular biology of the cell. 2009; 20(7):2015-2029.

247. Pantaleon M, Kanai-Azuma M, Mattick JS, Kaibuchi K, Kaye PL and Wood SA. FAM deubiquitylating enzyme is essential for preimplantation mouse embryo development. Mechanisms of development. 2001; 109(2):151-160.

248. Agrawal P, Chen Y-T, Schilling B, Gibson BW and Hughes RE. Ubiquitin-specific peptidase 9, X-linked (USP9X) modulates activity of mammalian target of rapamycin (mTOR). Journal of Biological Chemistry. 2012; 287(25):21164-21175.

249. Al-Hakim AK, Zagorska A, Chapman L, Deak M, Peggie M and Alessi DR. Control of AMPK-related kinases by USP9X and atypical Lys29/Lys33-linked polyubiquitin chains. Biochemical Journal. 2008; 411(2):249-260.

250. Théard D, Labarrade F, Partisani M, Milanini J, Sakagami H, Fon EA, Wood SA, Franco M and Luton F. USP9x-mediated deubiquitination of EFA6 regulates de novo tight junction assembly. The EMBO journal. 2010; 29(9):1499-1509.

251. Liu H, Peng HW, Cheng YS, Yuan HS and Yang Yen HF. Stabilization and enhancement of the antiapoptotic activity of mcl-1 by TCTP. Mol Cell Biol. 2005; 25(8):3117-3126.

252. Zhang D, Li F, Weidner D, Mnjoyan ZH and Fujise K. Physical and functional interaction between myeloid cell leukemia 1 protein (MCL1) and Fortilin The potential role of MCL1 as a fortilin chaperone. Journal of Biological Chemistry. 2002; 277(40):37430-37438.

253. Graidist P, Phongdara A and Fujise K. Antiapoptotic protein partners fortilin and MCL1 independently protect cells from 5-fluorouracil-induced cytotoxicity. Journal of Biological Chemistry. 2004; 279(39):40868-40875.

254. Tuynder M, Susini L, Prieur S, Besse S, Fiucci G, Amson R and Telerman A. Biological models and genes of tumor reversion: cellular reprogramming through tpt1/TCTP and SIAH-1. Proceedings of the National Academy of Sciences. 2002; 99(23):14976-14981.

255. Yang Y, Yang F, Xiong Z, Yan Y, Wang X, Nishino M, Mirkovic D, Nguyen J, Wang H and Yang X-F. An N-terminal region of translationally controlled tumor protein is required for its antiapoptotic activity. Oncogene. 2005; 24(30):4778-4788.

256. Rho SB, Lee JH, Park MS, Byun H-J, Kang S, Seo S-S, Kim J-Y and Park S-Y. Anti-apoptotic protein TCTP controls the stability of the tumor suppressor p53. FEBS letters. 2011; 585(1):29-35.

257. Bazile F, Pascal A, Arnal I, Le Clainche C, Chesnel F and Kubiak JZ. Complex relationship between TCTP, microtubules and actin microfilaments regulates cell shape in normal and cancer cells. Carcinogenesis. 2009:bgp022.

258. Zhang J, de Toledo SM, Pandey BN, Guo G, Pain D, Li H and Azzam EI. Role of the translationally controlled tumor protein in DNA damage sensing and repair. Proceedings of the National Academy of Sciences. 2012; 109(16):E926-E933.

259. Lucibello M, Gambacurta A, Zonfrillo M, Pierimarchi P, Serafino A, Rasi G, Rubartelli A and Garaci E. TCTP is a critical survival factor that protects cancer cells from oxidative stress-induced cell-death. Experimental cell research. 2011; 317(17):2479-2489.

260. Czabotar PE, Lee EF, van Delft MF, Day CL, Smith BJ, Huang DC, Fairlie WD, Hinds MG and Colman PM. Structural insights into the degradation of Mcl-1 induced by BH3 domains. Proceedings of the National Academy of Sciences. 2007; 104(15):6217-6222.

261. Pervin S, Tran A, Tran L, Urman R, Braga M, Chaudhuri G and Singh R. Reduced association of anti-apoptotic protein Mcl-1 with E3 ligase Mule increases the stability of Mcl-1 in breast cancer cells. British journal of cancer. 2011; 105(3):428-437.

262. Warr MR, Mills JR, Nguyen M, Lemaire-Ewing S, Baardsnes J, Sun KL, Malina A, Young JC, Jeyaraju DV and O'Connor-McCourt M. Mitochondrion-dependent N-terminal processing of outer membrane Mcl-1 protein removes an essential Mule/Lasu1 protein-binding site. J Biol Chem. 2011; 286(28):25098-25107.

263. Opferman J. Unraveling MCL-1 degradation. Cell Death & Differentiation. 2006; 13(8).

264. Adhikary S, Marinoni F, Hock A, Hulleman E, Popov N, Beier R, Bernard S, Quarto M, Capra M and Goettig S. The ubiquitin ligase HectH9 regulates transcriptional activation by Myc and is essential for tumor cell proliferation. Cell. 2005; 123(3):409-421.

265. Zhang Y, Xiong Y and Yarbrough WG. ARF promotes MDM2 degradation and stabilizes p53: ARF-INK4a locus deletion impairs both the Rb and p53 tumor suppression pathways. Cell. 1998; 92(6):725-734.

266. Weber JD, Taylor LJ, Roussel MF, Sherr CJ and Bar-Sagi D. Nucleolar Arf sequesters Mdm2 and activates p53. Nature cell biology. 1999; 1(1):20-26.

267. Midgley CA, Desterro JM, Saville MK, Howard S, Sparks A, Hay RT and Lane DP. An N-terminal p14ARF peptide blocks Mdm2-dependent ubiquitination in vitro and can activate p53 in vivo. Oncogene. 2000; 19(19):2312-2323.

268. Chen D, Kon N, Li M, Zhang W, Qin J and Gu W. ARF-BP1/Mule is a critical mediator of the ARF tumor suppressor. Cell. 2005; 121(7):1071-1083.

269. Inuzuka H, Shaik S, Onoyama I, Gao D, Tseng A, Maser RS, Zhai B, Wan L, Gutierrez A and Lau AW. SCFFBW7 regulates cellular apoptosis by targeting MCL1 for ubiquitylation and destruction. Nature. 2011; 471(7336):104-109.

270. Harley ME, Allan LA, Sanderson HS and Clarke PR. Phosphorylation of Mcl-1 by CDK1–cyclin B1 initiates its Cdc20-dependent destruction during mitotic arrest. EMBO J. 2010; 29(14):2407-2420.

271. Magiera M, Mora S, Mojsa B, Robbins I, Lassot I and Desagher S. Trim17-mediated ubiquitination and degradation of Mcl-1 initiate apoptosis in neurons. Cell Death & Differentiation. 2013; 20(2):281-292.

272. Mojsa B, Lassot I and Desagher S. Mcl-1 ubiquitination: unique regulation of an essential survival protein. Cells. 2014; 3(2):418-437.

273. Millman SE and Pagano M. MCL1 meets its end during mitotic arrest. EMBO reports. 2011; 12(5):384-385.

274. Mott JL, Bronk SF, Mesa RA, Kaufmann SH and Gores GJ. BH3-only protein mimetic obatoclax sensitizes cholangiocarcinoma cells to Apo2L/TRAIL-induced apoptosis. Mol Cancer Ther. 2008; 7(8):2339-2347.

275. Tang Y, Hamed HA, Cruickshanks N, Fisher PB, Grant S and Dent P. Obatoclax and lapatinib interact to induce toxic autophagy through NOXA. Molecular pharmacology. 2012; 81(4):527-540.

276. Zhang H, Guttikonda S, Roberts L, Uziel T, Semizarov D, Elmore S, Leverson J and Lam L. Mcl-1 is critical for survival in a subgroup of non-small-cell lung cancer cell lines. Oncogene. 2011; 30(16):1963-1968.

277. Luo S, Garcia-Arencibia M, Zhao R, Puri C, Toh PP, Sadiq O and Rubinsztein DC. Bim inhibits autophagy by recruiting Beclin 1 to microtubules. Molecular cell. 2012; 47(3):359-370.

278. Luo S and Rubinsztein DC. BCL2L11/BIM: a novel molecular link between autophagy and apoptosis. Autophagy. 2013; 9(1):104-105.

279. Wroblewski D, Jiang CC, Croft A, Farrelly ML, Zhang XD and Hersey P. OBATOCLAX and ABT-737 induce ER stress responses in human melanoma cells that limit induction of apoptosis. PloS one. 2013; 8(12):e84073.

280. Pattingre S, Tassa A, Qu X, Garuti R, Liang XH, Mizushima N, Packer M, Schneider MD and Levine B. Bcl-2 antiapoptotic proteins inhibit Beclin 1-dependent autophagy. Cell. 2005; 122(6):927-939.

281. Stamelos VA, Fisher N, Bamrah H, Voisey C, Price JC, Farrell WE, Redman CW and Richardson A. The BH3 Mimetic Obatoclax Accumulates in Lysosomes and Causes Their Alkalinization. PloS one. 2016; 11(3):e0150696.

282. Nakagawa T, Shimizu S, Watanabe T, Yamaguchi O, Otsu K, Yamagata H, Inohara H, Kubo T and Tsujimoto Y. Cyclophilin D-dependent mitochondrial permeability transition regulates some necrotic but not apoptotic cell death. Nature. 2005; 434(7033):652-658.

283. Tait SW, Oberst A, Quarato G, Milasta S, Haller M, Wang R, Karvela M, Ichim G, Yatim N and Albert ML. Widespread mitochondrial depletion via mitophagy does not compromise necroptosis. Cell reports. 2013; 5(4):878-885.

284. Murphy JM, Czabotar PE, Hildebrand JM, Lucet IS, Zhang J-G, Alvarez-Diaz S, Lewis R, Lalaoui N, Metcalf D and Webb AI. The pseudokinase MLKL mediates necroptosis via a molecular switch mechanism. Immunity. 2013; 39(3):443-453.

Chapter 9
Appendix

Appendix 1

1. 1X Phosphate Buffered Saline (PBS)

NaCl	137 mM
Na_2HPO_4	10 mM
NaH_2PO_4	10 mM
pH	7.4

2. 1X Phosphate Buffered Saline containing Tween 20 (PBST)

Add 0.1% (v/v) Tween 20 to 1X PBS to prepare 1X PBST

3. EBC lysis buffer

Tris Base	50 mM
NaCl	150 mM
EDTA	1 mM
NP-40	0.5%
pH	7.4

4. NETN buffer

Tris Base	20 mM
NaCl	100 mM
EDTA	1 mM
NP-40	0.5%
pH	7.4

5. 10X Electrophoresis buffer for SDS PAGE

Tris Base	30 g
Glycine	144 g
SDS	10 g
Distilled Water	Make up the volume to 1000 ml

6. Transfer/Electroblotting buffer

Tris Base	9 g
Glycine	39.5 g
Methanol	600 ml
10% SDS	1 ml
Distilled Water	Make up the volume to 3000 ml

7. 1X Tris Buffered Saline (TBS)

Tris Base	50 mM
NaCl	150 mM
pH	7.4

8. 1X Tris Buffered Saline containing Tween 20 (TBST)

Add 0.1% (v/v) Tween 20 to 1X TBS to prepare 1X TBST

9. Stripping Buffer

β-Mercaptoethanol	1.63 g
10% SDS	40 ml
1M Tris	12.5 ml
Distilled Water	Make up the volume to 200 ml

10. 10X Sodium Citrate Buffer

Tri Sodium Citrate	2.94 g
pH	5.8-6
Distilled Water	Make up the volume to 1000 ml

11. Destaining/fixing solution

50% (v/v) Methanol

10% (v/v) Glacial Acetic Acid

12. 2X Gel loading dye

1 M Tris (pH 6.8)	0.625 ml
β-Mercaptoethanol (add fresh)	0.5 ml
Glycerol	1 ml
SDS	0.23 g
1% Bromophenol Blue	0.5 ml
Distilled Water	Make up the volume to 10 ml

13. Fast Green staining solution

Fast Green stain powder	0.1 g
10% (v/v) Glacial Acetic Acid	100 ml

14. Coomassie Blue staining solution

CBB R-250	0.05 g
Methanol	50 ml
Glacial Acetic Acid	10 ml
Distilled Water	Make up the volume to 100 ml

15. Pretreatment solution

$Na_2S_2O_3$	0.02 g
Distilled Water	Make up the volume to 100 ml

16. Silver nitrate solution

$AgNO_3$	0.2 g
Formaldehyde	75 µl
Distilled Water	Make up the volume to 100 ml

17. Developer solution

Na_2CO_3	6 g
Pretreatment solution	2 ml
Formaldehyde	50 µl
Distilled Water	Make up the volume to 100 ml

18. Destaining solution for MALDI-MS

$K_3[Fe(CN)_6]$	1%
$Na_2S_2O_3$	1.58%

Mix the two solutions in 1:1 proportion.

19. Gel shrinking solution for MALDI-MS

Acetonitrile	100%
Ammonium Bicarbonate	25 mM

Mix the two solutions in 1:1 proportion

20. Peptide extraction buffer for MALDI-MS

Acetonitrile	50%
Trifluoro Acetic Acid	0.1%

21. Peptide reconstitution solution for MALDI-MS

Trifluoro Acetic Acid	0.1%
Acetonitrile	10%

Chapter 10
Publication

BH3 mimetic Obatoclax (GX15-070) mediates mitochondrial stress predominantly via MCL-1 inhibition and induces autophagy-dependent necroptosis in human oral cancer cells

Prasad Sulkshane[1], **Tanuja Teni**[1]

[1]Teni Lab, Advanced Centre for Treatment, Research and Education in Cancer (ACTREC), Tata Memorial Centre (TMC), Kharghar, Navi Mumbai-410210, Maharashtra, India

Correspondence to: Tanuja Teni, **email:** tteni@actrec.gov.in

Keywords: *MCL-1, Obatoclax, autophagy, necroptosis, mitochondria*

Received: *December 26, 2015* ***Accepted:*** *July 23, 2016* ***Published:*** *August 05, 2016*

ABSTRACT

We have previously reported overexpression of antiapoptotic MCL-1 protein in human oral cancers and its association with therapy resistance and poor prognosis, implying it to be a potential therapeutic target. Hence, we investigated the efficacy and mechanism of action of Obatoclax, a BH3 mimetic pan BCL-2 inhibitor in human oral cancer cell lines. All cell lines exhibited high sensitivity to Obatoclax with complete clonogenic inhibition at 200–400 nM concentration which correlated with their MCL-1 expression. Mechanistic insights revealed that Obatoclax induced a caspase-independent cell death primarily by induction of a defective autophagy. Suppression of autophagy by ATG5 downregulation significantly blocked Obatoclax-induced cell death. Further, Obatoclax induced interaction of p62 with key components of the necrosome RIP1K and RIP3K. Necrostatin-1 mediated inhibition of RIP1K significantly protected the cells from Obatoclax induced cell death. Moreover, Obatoclax caused extensive mitochondrial stress leading to their dysfunction. Interestingly, MCL-1 downregulation alone caused mitochondrial stress, highlighting its importance for mitochondrial homeostasis. We also demonstrated *in vivo* efficacy of Obatoclax against oral cancer xenografts and its synergism with ionizing radiation *in vitro*. Our studies thus suggest that Obatoclax induces autophagy-dependent necroptosis in oral cancer cells and holds a great promise in the improved management of oral cancer patients.

INTRODUCTION

Oral squamous cell carcinoma (OSCC) is one of the most common cancers in Indian males and comprises 30–40% of all malignancies. Although it is primarily attributed to tobacco chewing habit, smoking and alcohol consumption [1], its association with Human Papilloma Virus (HPV) is recently emerging [2]. Indeed, a nationally representative survey revealed that, tobacco-related cancers account for about 42% male and 18% female cancer deaths across India [3]. About 40% OSCC patients die from loco-regional disease while 24% develop distant metastases [4]. However, despite major improvements in cancer therapeutics, the 5-year survival rate of OSCC patients has not shown a significant improvement over the past several years [5]. Hence, there is an urgent need to identify more effective therapeutic agents for the better management of OSCC.

p53 regulates the intrinsic pathway of apoptosis by modulating the expression and activities of BCL-2 (B cell lymphoma-2) family proteins [6–8]. The role of tobacco and HPV in inactivation of p53 is well documented [9, 10]. About 46% of oral cancer patients in India harbor inactivated p53 [10]. Apoptotic dysregulation is believed to be one of the key underlying reason for the progression of OSCC [11]. BCL-2 and BCL-XL overexpression correlates with therapy resistance and poor prognosis in OSCC [12–15]. We have previously reported overexpression of anti-apoptotic members of the BCL-2 family, particularly MCL-1 (Myeloid Cell Leukemia-1) over their pro-apoptotic counterparts in human oral cancers [16]. We also demonstrated predominant overexpression

of antiapoptotic MCL-1 protein in oral cancer tissues versus normal and its association with therapy resistance and poor prognosis in oral cancer patients [16–19]. MCL-1 is a tightly regulated molecule, has a short half-life and is important for the development and survival of diverse cell types [20]. However, MCL-1 expression is frequently elevated in diverse human malignancies and is associated with therapy resistance. Several mechanisms including increased copy number, chromosomal and epigenetic changes and enhanced stability of MCL-1 protein contribute to its high expression in tumors [21]. Apart from its canonical prosurvival function, role of MCL-1 in mitochondrial homeostasis [22], DNA damage response [23, 24] and autophagy [25] are recently emerging.

All these studies suggests that the antiapoptotic proteins of the BCL-2 family, particularly MCL-1 are promising therapeutic targets in OSCC. Several pan-BCL-2 inhibitors are currently under development. However, therapeutic targeting of MCL-1 protein has largely been hindered by its structural discrepancy from other antiapoptotic BCL-2 family members [26]. But partial functional redundancy allows MCL-1 to substitute BCL-2, BCL-XL and BCL-W for their prosurvival function when they are inhibited or downregulated. MCL-1 is well known to exhibit resistance to ABT-737 and ABT-263 which potently antagonize BCL-2, BCL-XL and BCL-W [27–29]. Obatoclax (GX15-070), a BH3 mimetic is capable of inhibiting all the antiapoptotic proteins of the BCL-2 family, and potently inhibit the interaction between MCL-1 and BAK [26]. The potency of Obatoclax has been demonstrated against a variety of human cancer cell lines *in vitro* [26, 30–32] and in several clinical trials against diverse tumor types [33–35]. However, its activity against human oral cancers is rarely explored and largely unknown.

BH3-only proteins and BH3 mimetics are known to induce autophagy by activating multiple pathways [36, 37]. Autophagy has long been regarded as a cytoprotective mechanism deployed by tumor cells under stressful conditions [38]. However, sustained autophagy in response to a prolonged stress may lead to cell death when defective protein and organelle turnover exceeds the processing capacity of the cell [39]. A non-canonical pathway of cell death, Necroptosis has recently been shown to be linked to autophagy which involves a critical role of serine/threonine kinases called Receptor-interacting protein kinases (RIP1K and RIP3K) in a complex called Necrosome [40]. RIP3K further downstream recruits and phosphorylates its substrate Mixed Lineage Kinase Like (MLKL) which is proposed to execute necroptosis by mediating mitochondrial fission, generation of Reactive oxygen species (ROS) in mitochondria and recruitment of Ca^{2+} and Na^{+} ion channels or pore-forming complexes at the plasma membrane [41].

The present study demonstrates that Obatoclax mediates a caspase-independent, autophagy-dependent necroptosis in oral cancer cells associated with extensive mitochondrial stress. A late-stage block in autophagy leads to the association of p62 protein with RIP1K, RIP3K and FADD which triggers cell death by necroptosis. We also demonstrate the single agent *in vivo* efficacy of Obatoclax in xenograft mouse model. Additionally, we show the synergistic effect of Obatoclax with ionizing radiation treatment on oral cancer cells.

RESULTS

Obatoclax potently inhibits the clonogenicity of oral squamous carcinoma cells

We demonstrated the efficacy of Obatoclax against four oral cancer cell lines (DOK, AW8507, AW13516, SCC029B). The basal levels of important pro and antiapoptotic BCL-2 family proteins were assessed by western blotting (Figure 1A). DOK expressed low levels of MCL-1 protein as compared to that of AW8507, AW13516 and SCC029B cell lines. Notably, all the cell lines expressed relatively higher levels of at least two of the three predominant antiapoptotic BCL-2 family proteins. We then performed the *in vitro* clonogenic assays. The plating efficiencies for all the four cell lines differed markedly (DOK: 30–40%, AW8507: 60–70%, AW13516: 70–80%, SCC029B: 55–60%). Obatoclax (Figure 1B) inhibited the clonogenic potential of these cells in a dose-dependent manner with complete growth inhibition at 200–400 nM concentration (Figure 1C). The sensitivities of the four cell lines to Obatoclax correlated significantly ($p < 0.05$, $R = 0.96$) with their MCL-1 expression which is in agreement with previous reports [32, 42]. DOK (IC_{50}: 67.5 nM) exhibited highest sensitivity to Obatoclax with complete growth inhibition at about 100 nM concentration (correlates with its relatively lower MCL-1 expression) whereas AW8507 (IC_{50}: 110 nM), AW13516 (IC_{50}: 101 nM) and SCC029B (IC_{50}: 94.5 nM) were relatively less sensitive possibly due to relatively higher MCL-1 expression. Obatoclax is shown to induce cell death in head and neck squamous carcinoma cells (HNSCC) by reducing MCL-1 expression [43]. We therefore assessed whether Obatoclax affects the expression of critical proteins of the BCL-2 family. Exposure of the four cell lines to Obatoclax for 24 hours revealed no significant alterations in the expression of either MCL-1 (Figure 1D) or other members of the BCL-2 family except for BIM and NOXA proteins, which showed a dose dependent reduction in expression (Supplementary Figure S1). Nevertheless, Obatoclax not only dissociated the constitutive interaction between MCL-1 and BAK in the mitochondrial outer membrane (Supplementary Figure S2A) but also induced BAX translocation to the mitochondria. Both these events are critical for Mitochondrial Outer Membrane Permeabilization (MOMP). However, we were not able to detect a significant cytochrome c release from the mitochondria to the cytosol (Supplementary Figure S2B).

Obatoclax mediates caspase-independent cell death in OSCC cells

Obatoclax induced a dose and time dependent decrease in the viability of OSCC cells as determined by MTT and SRB assay (Figure 2A and 2B). To investigate whether Obatoclax mediated cell death via the canonical caspase-dependent pathway, we exposed SCC029B cells to Obatoclax for 0, 24, 48 and 72 hours and assessed caspase activation by western blotting. Absence of caspase-3, caspase-8 and PARP cleavage upon Obatoclax treatment indicate a caspase-independent cell death (Figure 2C). This was further supported by the fact that OSCC cells exhibited no significant difference in the cell viability when treated with Obatoclax alone or in combination with a pan-caspase inhibitor Z-VAD-FMK (Figure 2D). Obatoclax treated cells showed no signs of nuclear fragmentation, characteristic of cells undergoing apoptotic cell death (Figure 2E). Analysis of cell death by flow cytometry revealed no significant increase in annexin V-positive cells in the Obatoclax treated population as compared to vehicle control cells (Figure 2F). All these observations point towards a caspase-independent, non-apoptotic form of cell death induced by Obatoclax in OSCC cells.

Obatoclax induces autophagy in OSCC cells

Endoplasmic Reticulum (ER) stress has been implicated in protection of human melanoma cells against the cell death induced by Obatoclax [44]. However, we observed no change in GRP78 (a marker of ER stress) expression, in response to Obatoclax treatment in OSCC cells. It has been shown that Obatoclax induces autophagy in a variety of cancer cells. Therefore, we next investigated whether Obatoclax induced autophagy in OSCC cells. Obatoclax induced autophagy in OSCC cells is evident from the appearance of LC-3BII band (which corresponds to LC-3B lipidation and its incorporation in the autophagosomal membranes). However, there was neither a significant change in Beclin-1 levels nor

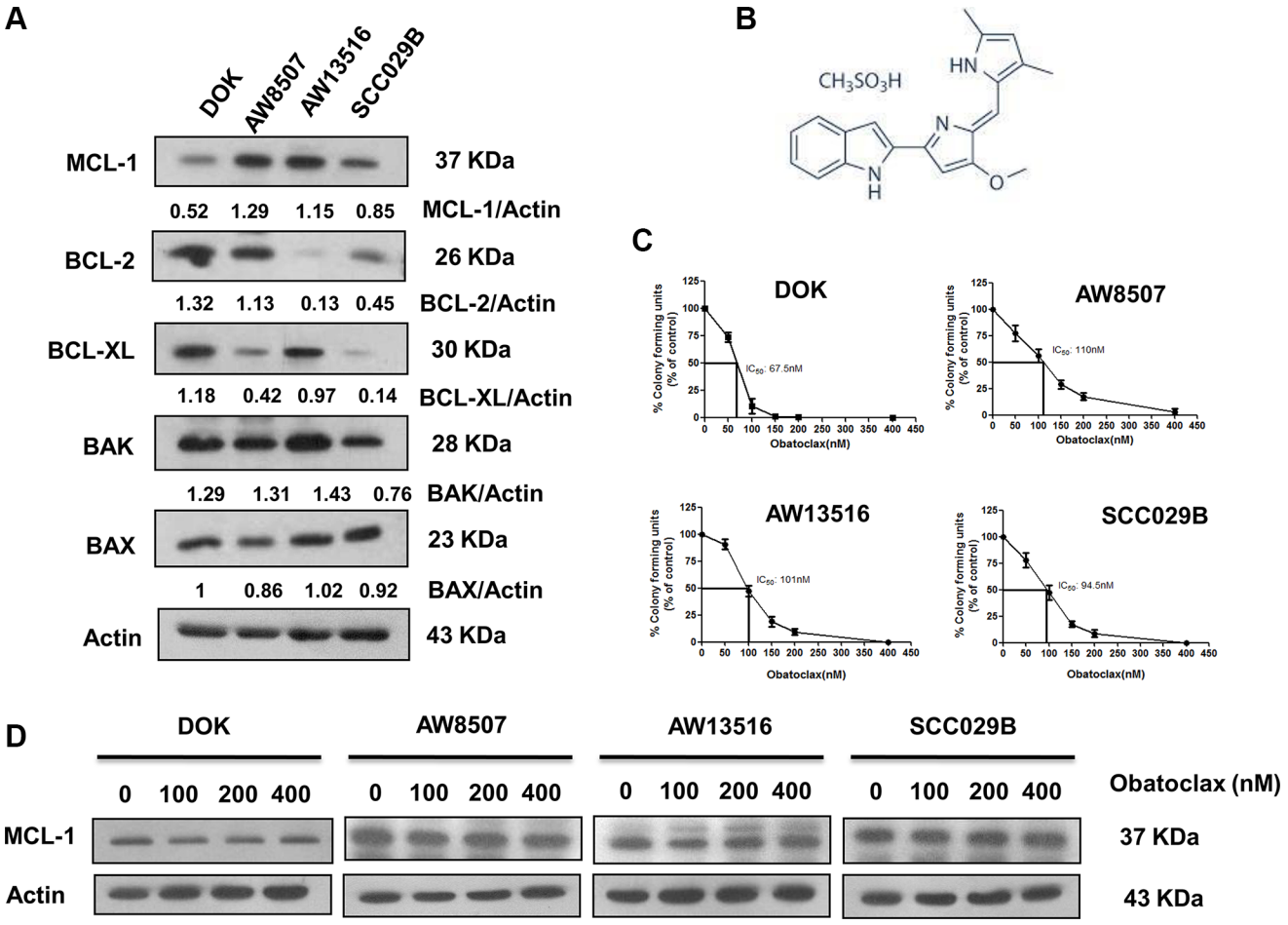

Figure 1: Obatoclax potently inhibits the clonogenic potential of oral cancer cells. (**A**) Basal level expression of important pro and antiapoptotic BCL-2 family proteins in human oral cancer cells. β-actin served as loading control. (**B**) Chemical structure of Obatoclax. (**C**) Sensitivity of the four cell lines to Obatoclax was determined by the clonogenic assays. The survival (colony forming units) is expressed as percentage of vehicle controls. Data is represented as mean ± SEM of three independent experiments. (**D**) Effect of Obatoclax treatment on MCL-1 expression in the four OSCC cell lines. Images shown are representatives of triplicate experiments.

its subcellular localization. Notably, p62/SQSTM1 protein, a substrate of autophagy showed sustained levels and exhibited a punctate cytoplasmic appearance upon exposure to Obatoclax. The vehicle control cells in contrast, showed a diffuse cytoplasmic staining of p62 (Figure 3A and 3B). Autophagy induced by Obatoclax was further quantitated by immunofluorescence microscopy which depicted a significant ($p < 0.0001$) increase in the appearance of endogenous LC-3B foci in the Obatoclax treated versus control cells (Figure 3C). Autophagy induced by Obatoclax was also studied in a time course experiment which revealed appearance of numerous LC-3B foci in OSCC cells (Figure 3D).

Obatoclax induced autophagy culminates into cell death

We then studied Obatoclax induced autophagy in a time course experiment by LC-3B and p62 immunoblotting. Consistent with the appearance of numerous LC-3B foci in the Obatoclax treated cells, we observed excessive accumulation of LC-3BII and sustained levels of p62 in a time dependent manner. All these observations are suggestive of a defective autophagy (Figure 4A). To address whether the Obatoclax induced autophagy is death inducing, we downregulated ATG5 by using siRNA and evaluated the Obatoclax-induced

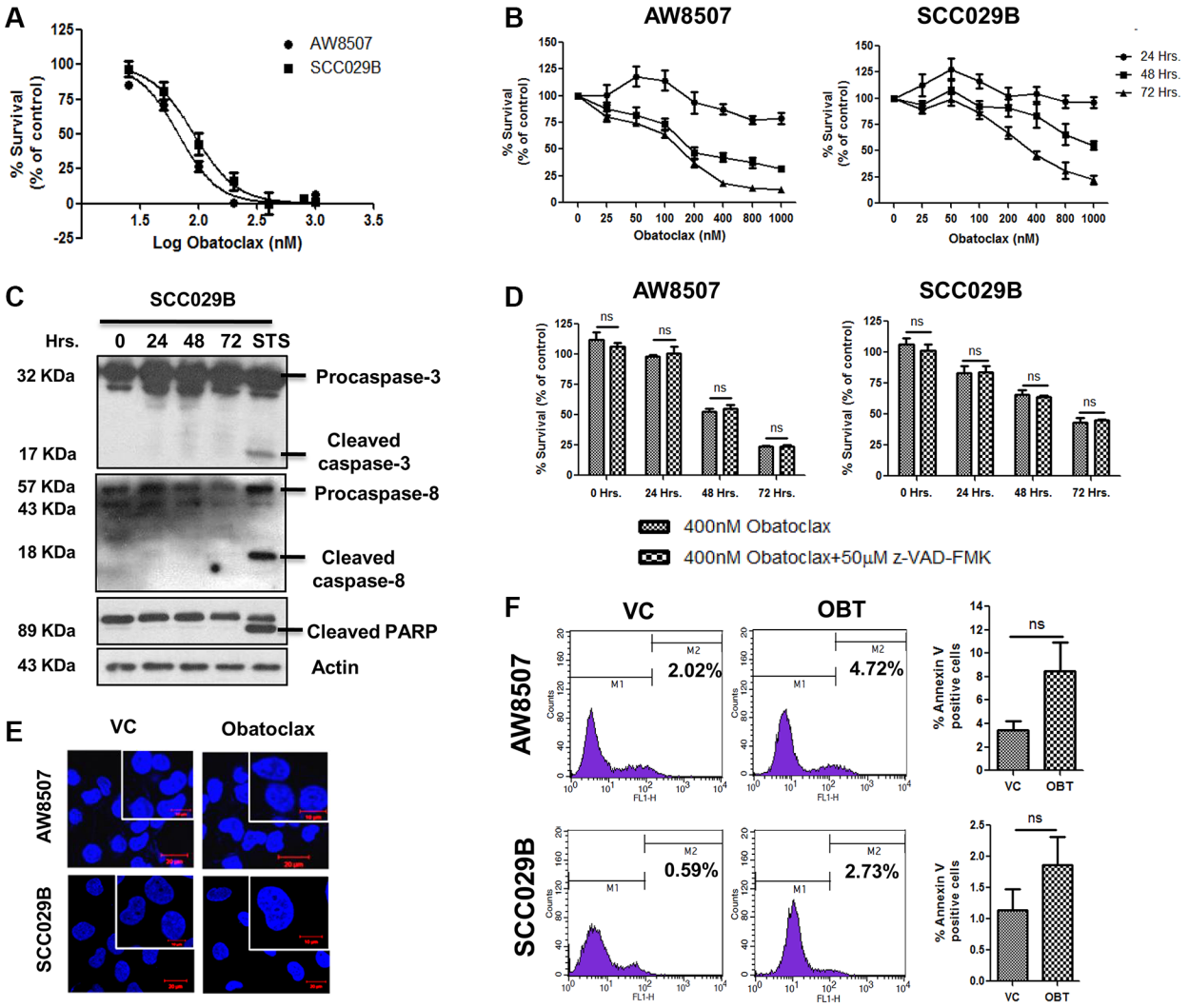

Figure 2: Obatoclax induces a caspase-independent cell death in OSCC cells. (**A**) AW8507 and SCC029B cells were treated with increasing doses of Obatoclax for 72 hours and cell viability was assessed by MTT assay. (**B**) The cells were treated with increasing concentrations of Obatoclax for 24, 48 and 72 hours and cytotoxicity was assessed by SRB assay. Cell viability is expressed as percent survival with respect to vehicle control. (**C**) SCC029B cells were treated with 400 nM Obatoclax for 0, 24, 48 and 72 hours or 500 nM Staurosporine (STS) for 24 hours. Caspase and PARP cleavage were assessed by western blotting. (**D**) The cells were either treated with 400 nM Obatoclax alone or in combination with 50 μM z-VAD-FMK for 24, 48 and 72 hours and cell viability was determined by SRB assay. (**E**) The cells were treated with 400 nM Obatoclax for 48 hours and nuclei were stained with DAPI to analyze the nuclear morphology (Scale bar: 10 μm). (**F**) The cells were treated with 400 nM Obatoclax (OBT) for 72 hours or as vehicle control (VC) and the percentage of annexin V positive cells were measured by flow cytometry. Images are representative of three independent experiments. Data is represented as mean ± SEM of three independent experiments; ns indicate not significant.

autophagy by LC-3BII immunoblotting. ATG5 knockdown significantly reduced the levels of LC-3BII in Obatoclax treated AW8507 and SCC029B cells (Figure 4B). Inhibition of autophagy by ATG5 downregulation significantly ($p < 0.001$) protected both the cell lines from Obatoclax-induced cell death (Figure 4C). These observations suggest that Obatoclax induced autophagy ultimately culminates into cell death.

Obatoclax causes a disturbance in autophagic flux leading to a defective autophagy in OSCC cells

To further address whether the excessive accumulation of LC3BII (and the autophagosomes) in response to Obatoclax treatment are a result of their increased formation or reduced clearance of the autophagosomes, we studied the autophagy flux in OSCC cells. We exposed the cells to Chloroquine (50 μM), a lysosomotropic agent, which neutralizes the acidic interior of the lysosomes, thereby inhibiting the activity of lysosomal enzymes and blocking the degradation of the autolysosomal cargo. We observed that Obatoclax and Chloroquine individually induced LC-3BII levels to an equal extent. Whereas, a combination of Obatoclax and Chloroquine induced only a marginal increase (not significant) in LC-3BII levels as compared to either agents alone. These observations indicate that the increased LC-3BII levels in response to Obatoclax treatment are accounted by a block in the terminal degradative phase (Figure 5A) [45]. By immunofluorescence studies, we confirmed that Obatoclax treatment induces fusion of autophagosomes (LC-3B) with lysosomes (LAMP-1) to form autolysosomes (Figure 5B). To further dissect the

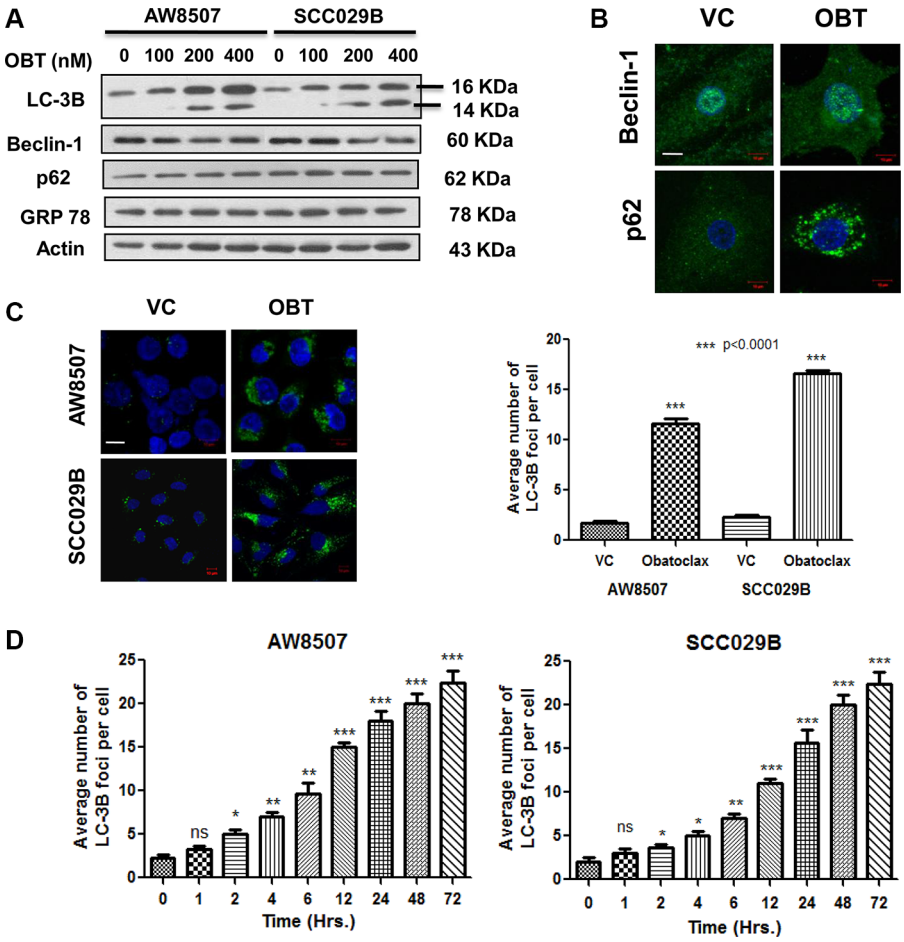

Figure 3: Obatoclax induces autophagy in OSCC cells. (**A**) Autophagy induction in OSCC cells is evident from appearance of LC-3BII band when treated with increasing doses of Obatoclax for 24 hours. Beclin-1, p62 and GRP78 levels did not show significant alterations. (**B**) SCC029B cells were either treated as vehicle control (VC) or with 400 nM Obatoclax (OBT) for 24 hours and endogenous Beclin-1 and p62 were detected by immunofluorescence staining (Scale bar: 10 μm). (**C**) Quantitation of autophagy. AW8507 and SCC029B cells were either treated as vehicle control or with 400 nM Obatoclax for 24 hours and endogenous LC-3B was detected by immunostaining. The average number of LC-3B foci were scored in the Obatoclax treated and control cells (Scale bar: 10 μm). (**D**) A time course study of autophagy induced by Obatoclax. AW8507 and SCC029B cells were exposed to 400 nM Obatoclax for different time points and the average number of LC-3B foci per cell were detected as mentioned above. The data is represented as mean ± SEM of three independent experiments. The images are representative of three independent trials.

autophagosome maturation process, we next investigated whether the autolysosomes are functionally competent to degrade the vesicular cargo by tandem fluorescent-tagged LC-3B based reporter [46]. SCC029B cells stably expressing a tandem mCherry/EGFP-LC-3B construct, exhibited yellow-orange (merge of mCherry red and EGFP green) fluorescence upon Obatoclax treatment, indicating functional incompetency of the autolysosomes (The GFP but not mCherry signal is sensitive to acidic compartment of lysosomes). We observed similar merged yellow-orange fluorescence signal of LC-3B when the cells were exposed to Chloroquine alone or a combination of Obatoclax and Chloroquine indicating a block at the degradation step (Figure 5C). All these observations together indicate that Obatoclax induced impaired autophagy due to a block in the terminal degradative phase.

Obatoclax induced cell death in OSCC cells is mediated by necroptosis

Having shown that Obatoclax induced a caspase-independent, non-apoptotic cell death in OSCC cells, we looked for the cell death pathway linked to autophagy. It has been reported by several groups that defective autophagy in response to a variety of stress stimuli often leads to cell death via necroptosis [47, 48]. We therefore investigated whether necroptosis is involved in the cell death mediated by Obatoclax in OSCC cells. Obatoclax treated cells exhibited appearance of extensive cytoplasmic vacuolation, characteristic of cells under stress (Figure 6A). Recruitment of RIP1K and RIP3K at the necrosome is an important event during necroptosis. Here we demonstrate that Obatoclax induced the

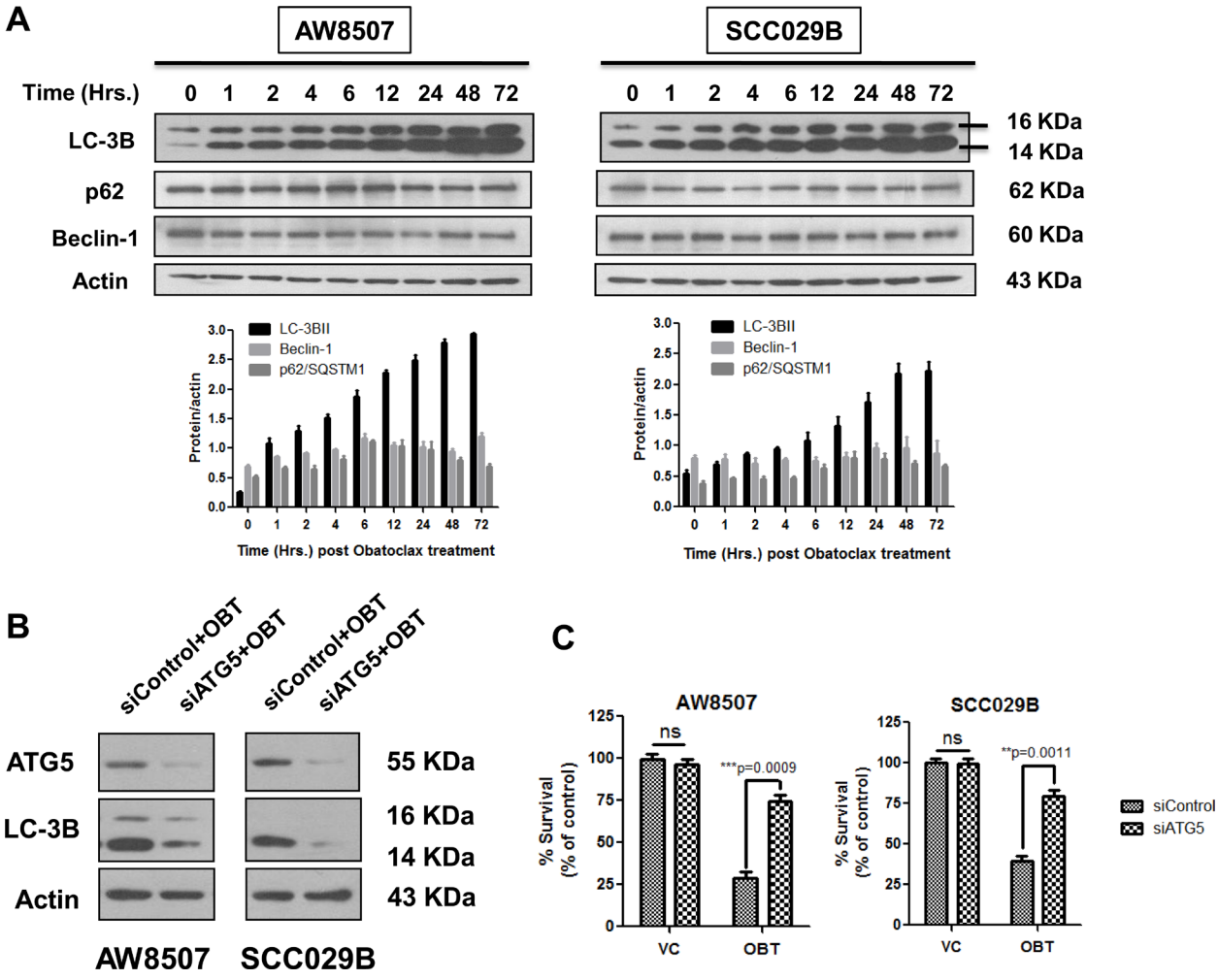

Figure 4: Obatoclax induced autophagy leads to cell death. (**A**) A time course study of autophagy induced by Obatoclax revealed bulk accumulation of LC-3BII and sustained levels of p62/SQSTM1. The Beclin-1 levels however did not show significant changes. (**B**) AW8507 and SCC029B cells were transfected with either a control/scrambled siRNA (siControl) or siRNA against ATG5 (siATG5) and treated with 400 nM Obatoclax (OBT) for 24 hours. The levels of LC-3BII were detected by immunoblotting. (**C**) The siRNA transfected cells were treated with 400 nM Obatoclax for 72 hours and percent cell viability was determined by SRB assay. Western blots are representative of triplicate experiments. The data is represented as mean ± SEM of three independent experiments.

association of p62 with the components of the necrosome RIP1K, RIP3K, and FADD by colocalization and coimmunoprecipitation (Figure 6B and 6C). Moreover, treatment with Necrostatin-1 (Nec-1), a RIP1K inhibitor, partially protected the cells from Obatoclax-induced cell death (Figure 6D). Obatoclax thus appears to induce cell death in OSCC cells by necroptosis.

Obatoclax induced extensive fragmentation of the mitochondrial network

Given the fact that MCL-1 is critical for mitochondrial homeostasis [22] and that putative MCL-1-specific inhibitors induce mitochondrial fragmentation [49], we speculated that Obatoclax could possibly deteriorate the organization of the mitochondrial network through MCL-1 inhibition. Obatoclax caused disruption of the mitochondrial network which involved extensive fragmentation, significant ($p < 0.05$) increase in mitochondrial fission and perinuclear aggregation in a time course study. The aberrations in the mitochondrial network initiated at about 12 hours post Obatoclax treatment and appeared much earlier than the phenotypic changes associated with the cell death (Figure 7A and 7B). Necroptosis is believed to execute cell death by inducing mitochondrial stress as one of the principal effector mechanism [50]. To investigate whether Obatoclax induced mitochondrial fragmentation occurs downstream of necroptosis, we treated SCC029B cells with Obatoclax in the presence or absence of RIP1K inhibitor Necrostatin-1 and assessed its effect on the mitochondrial network by HSP60 immunostaining. Mitochondrial fragmentation was evident even when RIP1K activity was inhibited, indicating that it occurs upstream to and independent of necroptosis (Figure 7C).

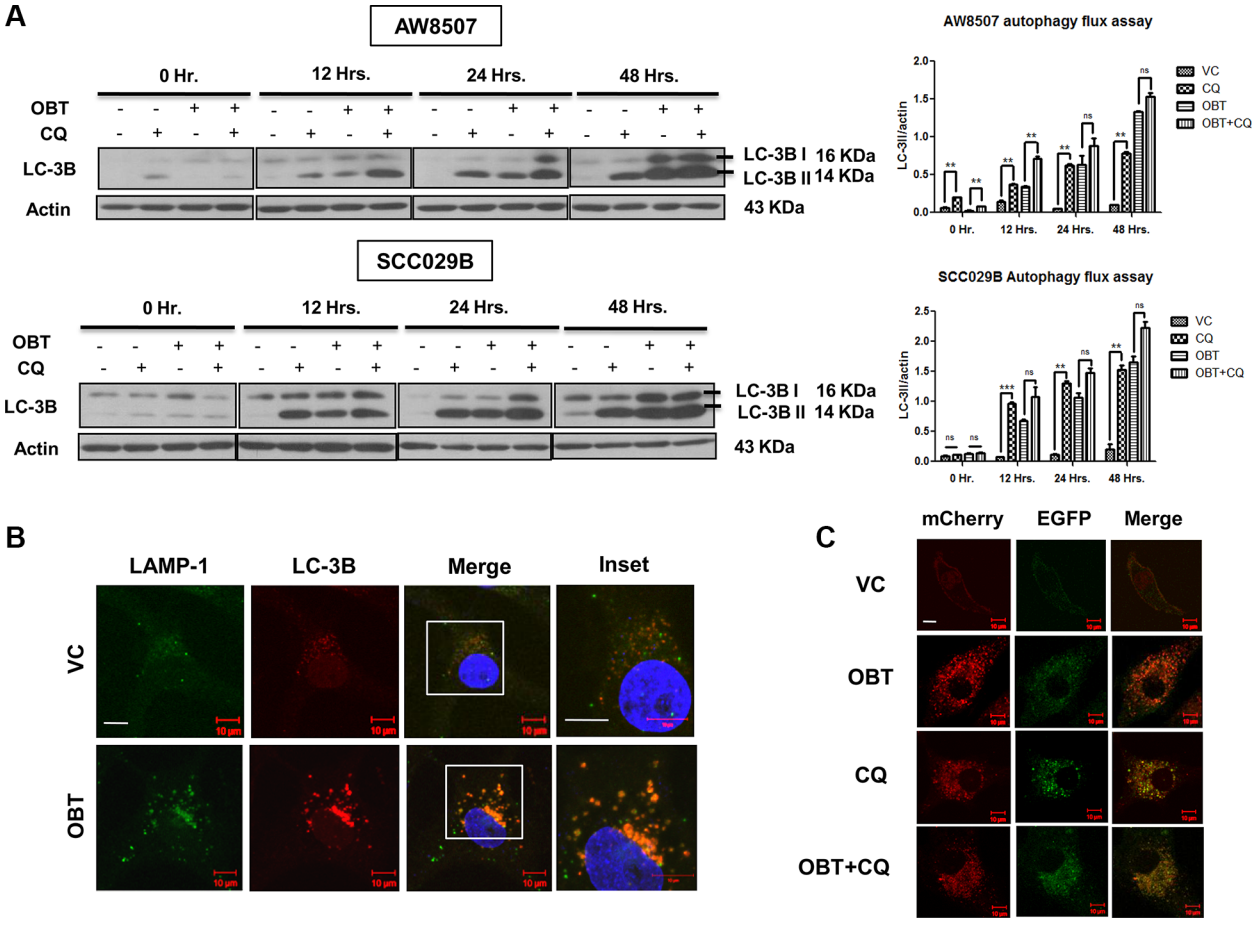

Figure 5: Obatoclax induces a defective autophagy in OSCC cells. (**A**) Time course study of autophagy flux. AW8507 and SCC029B cells were treated with either 50 μM Chloroquine (CQ), 400 nM Obatoclax (OBT), a combination of both or as vehicle control (VC) for 0, 12, 24, 48 hours and autophagy induction was evaluated by LC-3B immunoblotting. The blots are representative of three independent experiments. The respective densitometric analysis graphs are represented as mean ± SEM of three independent experiments (**$p < 0.01$, ***$p < 0.001$). (**B**) Obatoclax induces fusion of autophagosomes with lysosomes. SCC029B cells were either treated with 400 nM Obatoclax for 48 hours or as vehicle control. Fusion of autophagosomes (LC-3B: Red) with lysosomes (LAMP-1: Green) appear as yellow-orange dots (due to overlap of red and green) (Scale bar: 10 μm). (**C**) SCC029B cells stably expressing pBABE-puro mCherry-EGFP-LC3B construct were either treated with 50 μM Chloroquine, 400 nM Obatoclax, a combination of both or as vehicle control for 48 hours and the cells were imaged using a fluorescence confocal microscope (Scale bar: 10 μm).

Obatoclax induces mitochondrial oxidative stress and mitochondrial membrane depolarization in OSCC cells

BNIP3 (BCL-2-Nineteen kilodalton interacting protein 3) is a BH3 only protein of the BCL-2 family which plays a key role in impairment of the mitochondrial oxidative phosphorylation, reduction in the mitochondrial membrane potential (ΔΨm) and mitophagy under stressful conditions [51]. We therefore analyzed the expression of BNIP3 by real time PCR and observed that Obatoclax induced a significant increase ($p < 0.05$) in the expression of BNIP3 in SCC029B cells (Figure 8A). BNIP3 induction during stressful conditions leads to increased mitochondrial oxidative stress. We therefore investigated whether Obatoclax induced ROS (Reactive Oxygen Species) accumulation in mitochondria by using MitoSOX Red dye (MitoSOX Red dye specifically accumulates in mitochondria which upon oxidation by superoxide radicals exhibit red fluorescence). Live cell imaging experiment revealed that a significantly ($p < 0.0001$) higher percentage of Obatoclax treated cells exhibited MitoSOX Red fluorescence as compared to the control cells. This red fluorescence specifically localized to the perinuclear position consistent with the observation that mitochondria under stressful conditions exhibit perinuclear aggregation (Figure 8B and 8C). We also noticed a reduction in the fluorescence signal intensity of MitoTracker Green dye in the Obatoclax treated cells possibly because of a drop in ΔΨm. The increased ROS accumulation is also evident by flow cytometry, depicted by an increased proportion of MitoSOX Red positive cells upon Obatoclax treatment (Figure 8D). BNIP3 induction is also associated with a drop in ΔΨm. We therefore analyzed changes in ΔΨm by using JC-1 dye. As compared to the vehicle control, exposure of SCC029B cells to Obatoclax

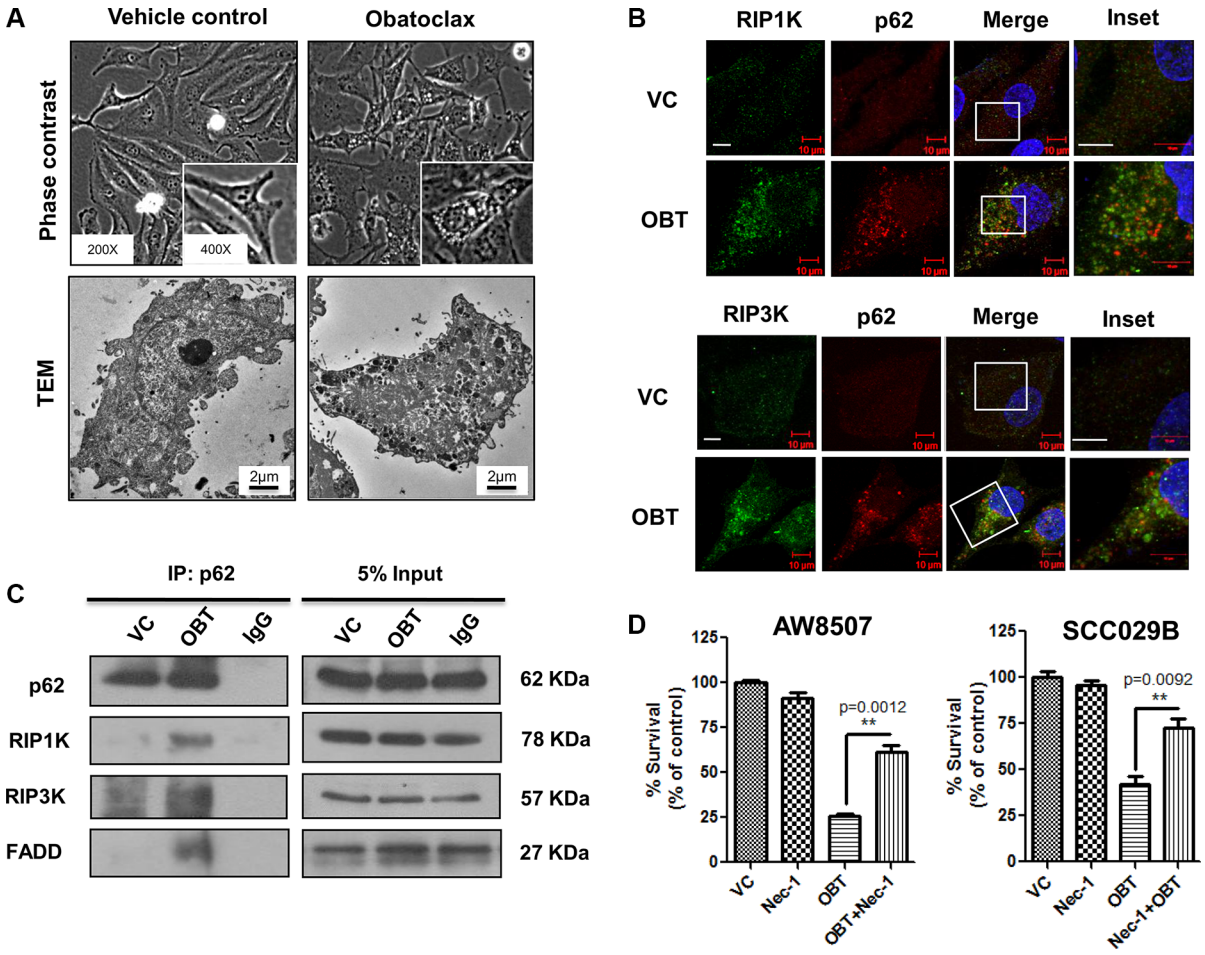

Figure 6: Obatoclax induces necroptosis in OSCC cells. SCC029B cells were either treated as vehicle control (VC) or exposed to 400 nM Obatoclax (OBT) for 48 hours. (**A**) The morphology and ultrastructure of control and Obatoclax treated SCC029B cells. (**B**) A colocalization of p62 with RIP1K and RIP3K in Obatoclax treated SCC029B cells indicate assembly of necrosomal complexes (Scale bar: 10 μm). (**C**) The Obatoclax treated and vehicle control cell lysates were subjected to coimmunoprecipitation using p62 antibody. IgG: Isotype control antibody. (**D**) AW8507 and SCC029B cells were treated with 400 nM Obatoclax, 50 μM Necrostatin-1 (Nec-1) or a combination of both for 48 hours and cell viability was quantified by SRB assay. Data is represented as mean ± SEM of three independent experiments. Images are representative of three independent experiments.

induced depolarization of the mitochondrial membrane reflected by a significant ($p < 0.0001$) increase in green to red fluorescence ratio of JC-1 dye. Increase in green fluorescence of JC-1 dye (due to JC-1 monomers) indicates a drop in ΔΨm whereas increased red fluorescence (due to JC-1 aggregates) corresponds to a stable ΔΨm and thus represents functional mitochondria (Figure 8E). Finally, we measured a time-dependent decrease in mitochondrial function upon Obatoclax treatment in OSCC cells by MTT assay (Figure 8F). All these observations point towards mitochondrial dysfunction upon Obatoclax treatment.

MCL-1 downregulation induces mitochondrial stress in SCC029B cells

To investigate the role of MCL-1 in mitochondrial homeostasis, we transiently knocked down MCL-1 by using siRNA in SCC029B cells. SCC029B cells as discussed earlier expressed relatively lower levels of BCL-2 and BCL-XL as compared to MCL-1. MCL-1 knockdown in these cells resulted in a significant ($p = 0.0006$) increase in mitochondrial fragmentation (Figure 9A). We also observed a significant ($p < 0.05$) increase in the MitoSOX Red staining in siMCL-1 transfected cells as compared to siControl cells (Figure 9B). Furthermore, MCL-1 downregulation resulted in a significant ($p < 0.05$) decrease in ΔΨm as compared to the control siRNA transfected cells (Figure 9C). All these observations indicate a potential role of MCL-1 in maintaining mitochondrial homeostasis in these cells.

Ultrastructural changes induced by Obatoclax

Obatoclax induced severe ultrastructural anomalies in OSCC cells. Numerous autophagic vesicles containing electron dense materials, protein inclusions and degenerating cellular organelles were readily visible throughout the cytoplasm. The autophagic vesicles at various stages of maturation ranging from initiating phagophore, autophagosomes, amphiosomes and autolysosomes were morphologically recognizable. Extensive cytoplasmic vacuolation was also apparent and intact mitochondria were not readily detectable. On the contrary, control cells exhibited numerous

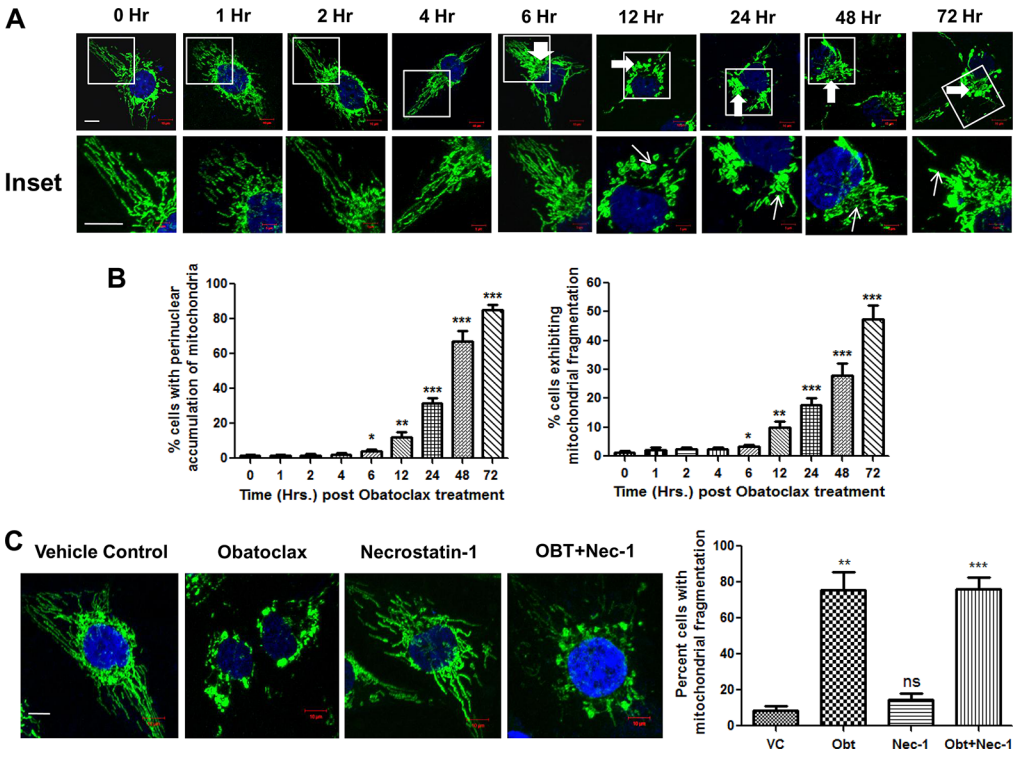

Figure 7: Obatoclax induces mitochondrial fragmentation in OSCC cells. (**A**) SCC029B cells were treated with 400 nM Obatoclax for different time points followed by immunostaining for HSP60 and the nuclei were counterstained with DAPI. The cells were observed under a laser confocal microscope. The mitochondrial morphology is evident in the upper panels. The enlarged images are represented in the corresponding lower panels. (**B**) The percentage of cells showing perinuclear aggregation of mitochondria (indicated in the upper panels by thick white arrows) and those showing mitochondrial fragmentation (indicated by thin white arrows in the lower panels) were determined by counting 10 microscopic fields (each containing at least 10–15 cells) per time point. (**C**) SCC029B cells were treated with either 400 nM Obatoclax (OBT), 50 μM Necrostatin-1 (Nec-1), a combination of both or as vehicle control (VC) for 48 hours, immunostained for HSP60 and the percentage of cells exhibiting mitochondrial fragmentation was determined as described above. The data for all experiments is represented as mean ± SEM of three independent experiments (ns: not significant, *$p < 0.05$, **$p < 0.01$, ***$p < 0.0001$). The images are representative of three independent experiments (Scale bar: 10 μm).

mitochondria (with intact inner and outer membranes and distinct cristae) and few cytoplasmic vacuoles (Figure 10).

Obatoclax exhibits potent antitumor activity in xenograft mouse models

Potent single agent antitumor activity of Obatoclax was observed against SCC029B cell line derived subcutaneous tumors in xenograft mouse model. We observed a significant ($p < 0.05$) reduction in the mean tumor volume without a significant decrease in the weight of the animals (Supplementary Figure S3). The effect was dose dependent with maximal activity observed at the cumulative dose of 5 mg/kg (Figure 11A).

Obatoclax exhibits synergism with ionizing radiation to inhibit the clonogenic potential of OSCC cells

Consistent with our previous finding that MCL-1 is an important radioresistance related factor in OSCC cells [17, 18], we sought to test the potency of a combination of Obatoclax with ionizing radiation (IR). From the clonogenic assays, we observed that as compared to radiation alone, the combination treatment significantly ($p < 0.05$) inhibited the colony formation in the three OSCC cell lines (Figure 11B). Moreover, we observed a significant growth inhibition when the cells were exposed to a combination of IR and Obatoclax as opposed to radiation alone across a range of IR doses (2 Gy, 4 Gy,

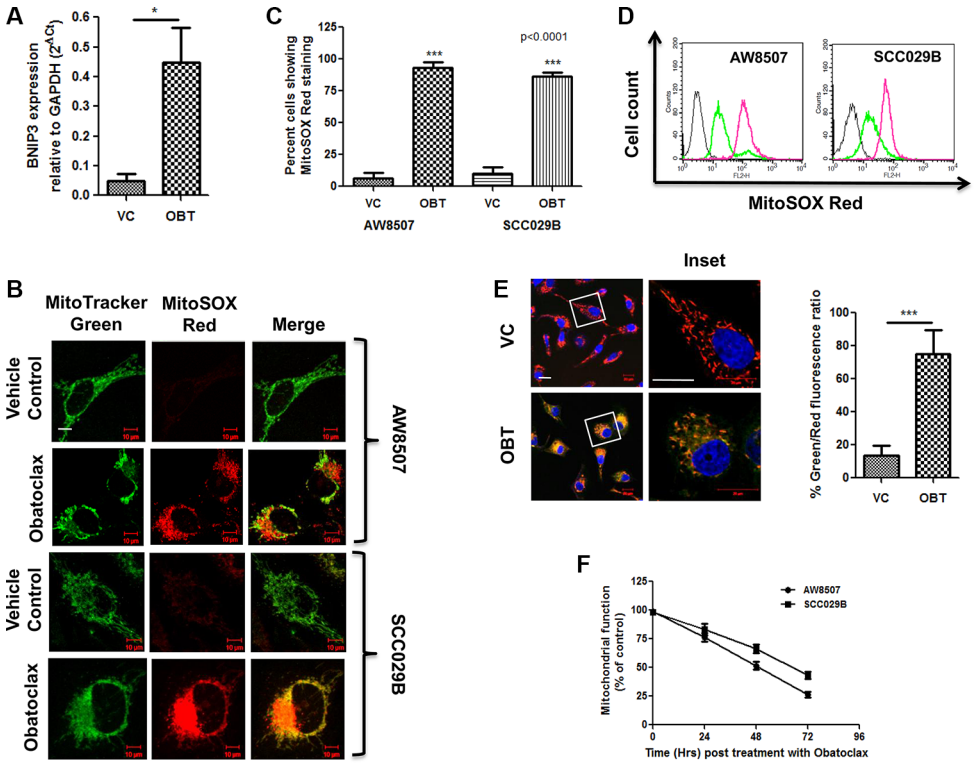

Figure 8: Obatoclax induces oxidative stress and membrane depolarization in the mitochondria of OSCC cells. AW8507 and SCC029B cells were treated with 400 nM Obatoclax (OBT) for 48 hours or as vehicle control (VC). (**A**) The expression of BNIP3 was analyzed by real time PCR in SCC029B cells and expressed relative to GAPDH by $2^{-\Delta Ct}$ method. (**B**) AW8507 and SCC029B cells grown in confocal dishes were treated with Obatoclax or as vehicle control followed by staining with MitoTracker Green and MitoSOX Red. Images were acquired on a fluorescence confocal microscope (Scale bar: 10 μm). (**C**) The percentage of cells exhibiting MitoSOX Red fluorescence was determined by counting 10 different microscopic fields (each containing at least 10–15 cells) per condition. (**D**) Followed by drug treatment, the cells were stained with 5 μM MitoSOX Red dye and the amount of ROS accumulation in mitochondria was measured by flow cytometry on FL2 channel. The gray curve on extreme left indicate unstained cells, the green and pink curves represent vehicle control and Obatoclax treated cells respectively. The histogram plots are representative of three independent experiments. (**E**) The Obatoclax treated or vehicle control cells were stained with JC-1 dye and Hoechst dye. The percent Green/Red fluorescence intensity ratio was quantified by counting 10 different microscopic fields each containing at least 10 cells (Scale bar: 20 μm). Obatoclax induced mitochondrial membrane depolarization is indicated by a significant increase in the green/red fluorescence ratio of JC-1 dye as compared to the control cells. The red fluorescence was restricted to the mitochondria due to JC-1 aggregates and is indicative of a stable ΔΨm i.e. polarized mitochondria. The green fluorescence was diffused and corresponds to JC-1 monomers and indicates a drop in ΔΨm i.e. depolarized mitochondria. (**F**) Mitochondrial dysfunction measured by MTT assay. AW8507 and SCC029B cells were treated with 400 nM Obatoclax for 0, 24, 48 and 72 hours. The amount of reduced formazon dye is represented as percent mitochondrial function. Data is represented as mean ± SEM of three independent experiments.

6 Gy, 8 Gy) (Supplementary Figure S4). Obatoclax thus exhibit synergism with radiation treatment to inhibit the clonogenicity of OSCC cells.

DISCUSSION

Aberrant expression of antiapoptotic BCL-2 family proteins, particularly MCL-1 has been reported in diverse human cancers including oral cancers [16, 52]. We have earlier demonstrated that the prosurvival MCL-1 protein contributes to therapy resistance and poor prognosis in oral cancers and thus may prove to be a potential therapeutic target in OSCC [15, 17–19]. Hence in the present study, we evaluated the efficacy of a BH3-mimetic pan-BCL-2 inhibitor Obatoclax against human oral cancer cell lines and also elucidated the mechanism of its action.

The four OSCC cell lines used in the present study exhibited high sensitivity to Obatoclax which correlated significantly to their MCL-1 expression. However, Obatoclax induced growth inhibition was not associated with a reduction in MCL-1 expression primarily because, Obatoclax is a BH3-mimetic which binds with a high affinity to the BH3-domain binding hydrophobic groove on MCL-1 protein and is not known to be associated with inhibition of its expression or mediate its degradation. This observation is in accordance with earlier studies reported in Cholangiocarcinoma cells [32, 53], Pancreatic cancer cells [31], KB carcinoma cells [26] and Breast cancer cells [42]. In contrast, studies by Yazbeck et al. demonstrated that sensitivity to Obatoclax has an inverse correlation with MCL-1 expression in HNSCC cells and is associated with a reduction in MCL-1 levels [43]. The discrepancy between these observations may be attributed to the cell type and context specific-dependence of the cells on MCL-1 for survival and the relative expression of other antiapoptotic members of the BCL-2 family. It is noteworthy that, all four OSCC cell lines expressed relatively higher levels of at least two of the three major antiapoptotic proteins (BCL-2, BCL-XL or MCL-1) which imply their dependence on multiple prosurvival proteins of the BCL-2 family for cell viability. Owing to their functional redundancy, tumor cells upregulate the expression of companion prosurvival BCL-2 family proteins in case, one of them is either inhibited or

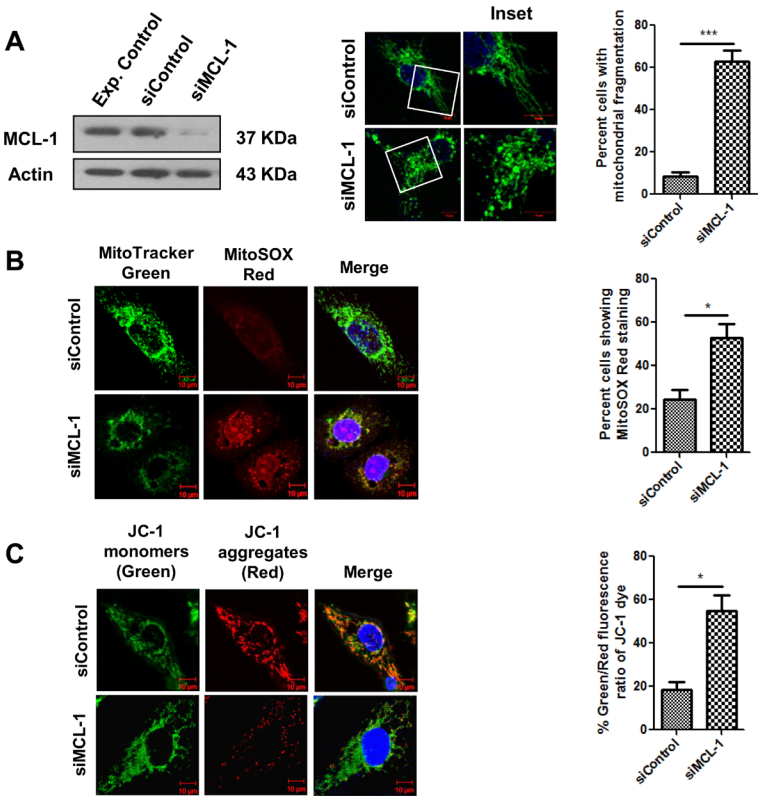

Figure 9: MCL-1 downregulation induces mitochondrial stress in SCC029B cells. SCC029B cells were transfected with 50 nM control siRNA and 50 nM MCL-1 siRNA. 48 hours post transfection, cells were used for experimental analysis. (**A**) The cell lysates were subjected to western blotting for MCL-1 and β-actin. Alternatively, the siRNA transfected cells were immunostained for HSP60 and observed under a confocal microscope. The percentage of cells showing mitochondrial fragmentation was determined as described earlier. (**B**) The siRNA transfected cells were stained with MitoTracker green, MitoSOX Red and Hoechst dyes and observed under a confocal microscope. (**C**) The siRNA transfected cells were stained with JC-1 dye and analyzed for change in percent green to red fluorescence intensity ratio of JC-1 dye as discussed earlier. Data is represented as mean ± SEM of three independent experiments (Scale bar: 10 μm). Images are representative of three independent experiments.

downregulated and therefore neutralization of all of them is necessary to execute apoptotic cascade [27, 28]. Hence the use of a pan-BCL-2 inhibitor like Obatoclax may prove to be an effective therapeutic strategy. In the present study, the growth inhibition induced by Obatoclax in OSCC cells was not associated with significant alterations in the expression of the BCL-2 family proteins except BIM and NOXA, whose levels were found to be reduced post Obatoclax treatment. Interestingly, NOXA and BIM downregulation partially protected H23 lung cancer cells from cell death induced due to MCL-1 knockdown [54] which probably explains why their expression is reduced upon Obatoclax mediated MCL-1 inhibition. Both BIM and NOXA are predicted to compete with Beclin-1 for interaction with MCL-1 and thereby regulate autophagy [42, 55, 56]. The regulation of expression of these BH3-only proapoptotic proteins therefore appears to be context and cell-type specific.

Recently, Wroblewski et al. has shown that Obatoclax induces unfolded protein response (UPR) in human melanoma cells which leads to MCL-1 upregulation, thereby preventing cell death [44]. UPR is characterized by increased GRP78 (Bip) expression, a principal chaperone in the endoplasmic reticulum (ER). However, in our studies, GRP78 expression remains unaltered in OSCC cells upon exposure to Obatoclax, indicating that Obatoclax may not induce ER stress in these cells. Obatoclax is reported to execute cell death via both caspase-dependent as well as caspase-independent pathways in a variety of cell types [31, 57]. In our studies, we observed that Obatoclax induced a caspase-independent, non-apoptotic cell death in OSCC cells.

Several studies have shown that Obatoclax potently induces autophagy in a variety of cancer cells [43, 57, 58]. Our present study also demonstrates autophagy induction in OSCC cells by Obatoclax which is evident from excessive accumulation of LC-3BII. BCL-2, BCL-XL and MCL-1 are known to bind Beclin-1 and thereby inhibit Beclin-1-mediated autophagy. Like BIM and NOXA, BH3 mimetics have been predicted to competitively disrupt this interaction and thereby mediate autophagy [36, 59]. However, we neither found significant alterations in Beclin-1 levels nor its altered subcellular localization pattern upon Obatoclax treatment in OSCC cells. McCoy et al. have demonstrated Beclin-1-indpependent autophagy induction by Obatoclax in non-small-cell lung carcinoma cells [57]. Blocking

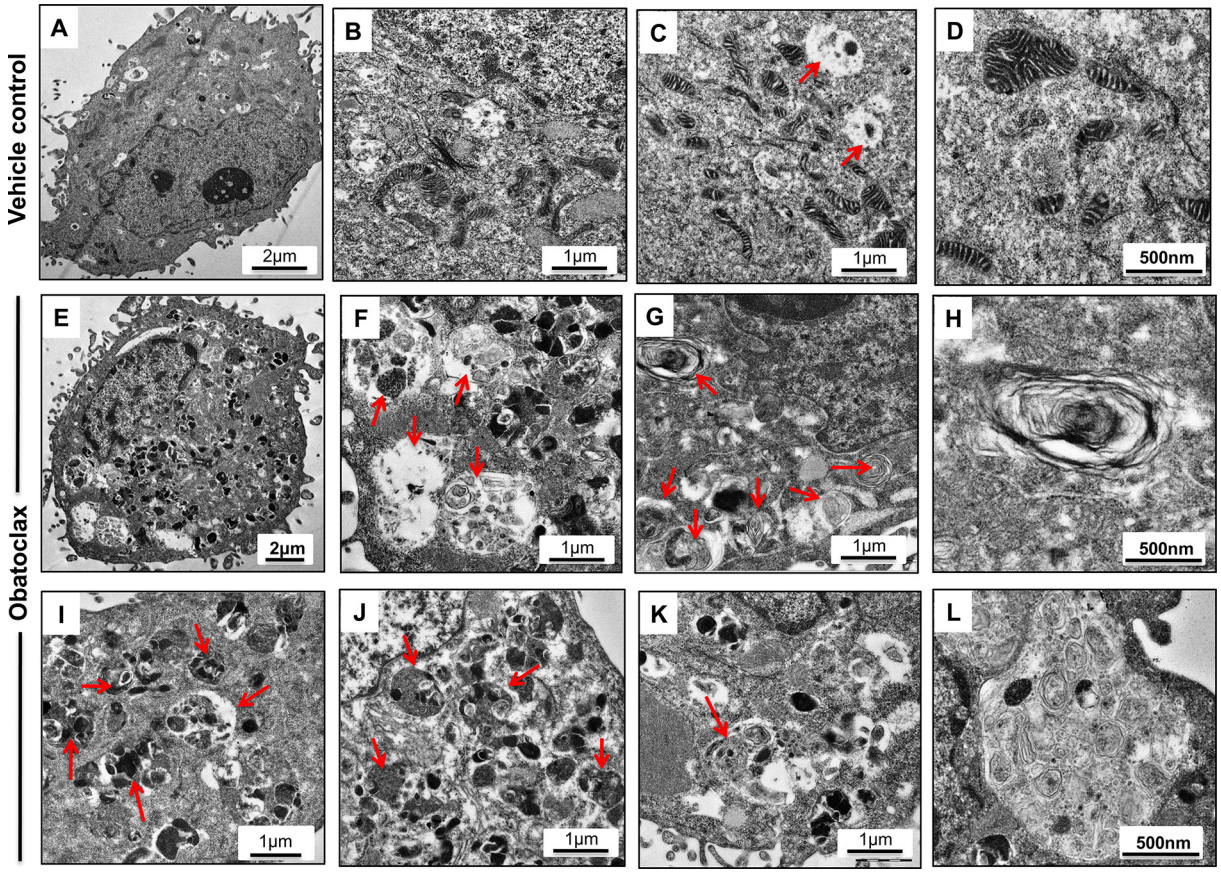

Figure 10: Ultrastructural changes induced by Obatoclax. SCC029B cells when treated with 400 nM Obatoclax for 48 hours induced appearance of numerous autophagic vesicles (Red arrows) containing various cargos. Extensive cytoplasmic vacuolation was apparent with accumulation of electron dense proteinaceous inclusions. Intact mitochondria (those with distinct cristae and internal membranes) were not readily detectable (**E**–**L**). Vehicle control cells on the other hand exhibited significantly less cytoplasmic vacuolation and presence of numerous intact mitochondria with distinct cristae (**A**–**D**).

autophagy by ATG5 knockdown significantly protected the OSCC cells from Obatoclax-induced cell death, indicating that Obatoclax-induced autophagy leads to cell death and is not prosurvival. Obatoclax caused a disturbed autophagy flux which account for the bulk accumulation of LC-3BII and sustained levels of p62 protein (p62 is regarded as a substrate of autophagy which serves as a linker between polyubiquitinated cargo and LC-3BII on the autophagosomal membrane) in OSCC cells. A late-stage block in the autophagosome maturation process led to defective autophagy. More recently, Stamelos et al. have shown that Obatoclax accumulates in the lysosomes, mediates their alkalinization causing a block in the terminal degradative phase leading to a defective autophagy [60].

Having shown that Obatoclax induced a caspase-independent, non-apoptotic form of cell death in OSCC cells, we then investigated whether impaired autophagy culminates into cell death by necroptosis. Here, we demonstrate that Obatoclax induced the interaction of p62 with RIP1K, RIP3K and FADD, key components of the necrosome. Moreover, RIP1K inhibition by necrostatin-1 protected the OSCC cells from Obatoclax induced cell death. Our data thus suggests that Obatoclax mediates cell death in OSCC cells via autophagy-dependent necroptosis.

Our studies reveal that Obatoclax perturbed the normal tubular architecture of the mitochondria and induced extensive fragmentation of the mitochondrial network. This corresponds to increased mitochondrial fission and perinuclear aggregation. Initially it was believed that abrogation of the mitochondrial network, increased mitochondrial membrane permeability, mitochondrial ROS accumulation and mitochondrial dysfunction are one of the several effector mechanisms of Necroptosis [40, 61]. However, recent studies argue the involvement of mitochondrial fission and mitochondrial ROS during necroptotic cell death [62, 63]. Our data also suggests that mitochondrial fragmentation in response to Obatoclax treatment occurs independent of RIP1K activation and upstream of necroptosis.

Under stressful conditions, BNIP3 expression is induced which causes reduced energy output, increased accumulation of mitochondrial ROS and a drop in ΔΨm which mark the mitochondria as damaged and dysfunctional [51, 55]. On the same lines, we observed a significant increase in the expression of BNIP3 upon Obatoclax treatment. In accordance with the downstream effects of BNIP3 induction, we demonstrated a significant increase in the mitochondrial oxidative stress, compromised integrity of the mitochondrial membrane as indicated by a reduced ΔΨm (i.e. depolarized mitochondria) and a time-dependent decrease in mitochondrial function in these cells upon Obatoclax treatment. All the above characteristic events possibly mark the mitochondria as damaged and dysfunctional.

Besides its canonical prosurvival function, MCL-1 protein is critical for the organization and physiological functions of mitochondria [22]. Since MCL-1 is overexpressed in oral cancer cells and serve as an important prosurvival protein, we probed into its critical involvement in the maintenance of mitochondrial homeostasis in OSCC cells. In the present study, we evaluated and compared the effect of Obatoclax mediated MCL-1 inhibition (without a significant change in MCL-1 levels) with that of siRNA-mediated

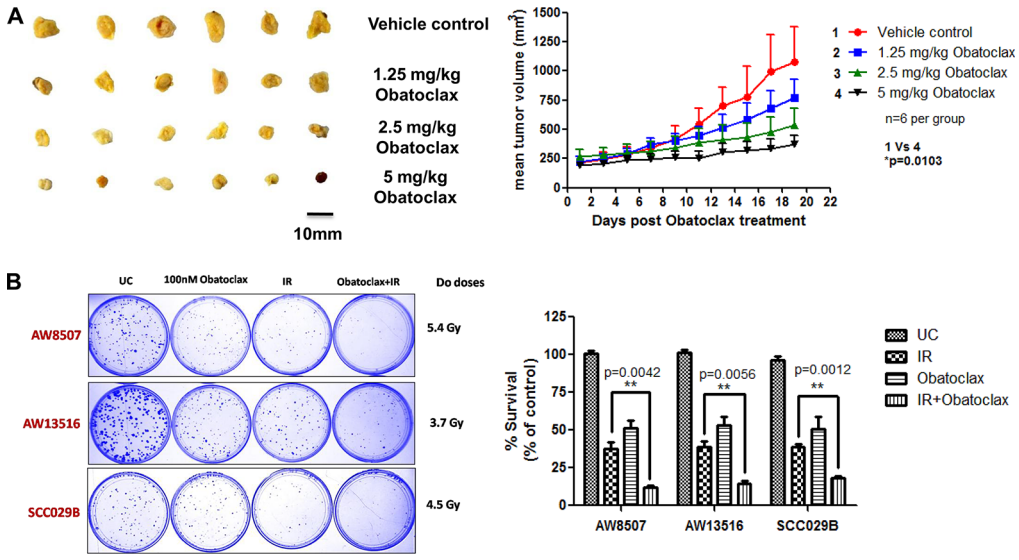

Figure 11: (**A**) *In vivo* efficacy of Obatoclax. BALB/C Nude mice bearing subcutaneous tumors derived from SCC029B cell line were administered a cumulative dose of the drug as indicated distributed evenly over a period of five consecutive days. Tumor volumes were measured for a period of 15–20 days post drug administration. The data is expressed as mean + SEM of the mean tumour volumes for each group (six animals per group). (**B**) Ionizing radiation treatment exhibits synergism when combined with Obatoclax. A combination of Obatoclax and ionizing radiation (IR) significantly ($p < 0.05$) inhibited the clonogenic potential of OSCC cells as compared to the either treatments alone.

MCL-1 downregulation in context of mitochondrial architecture and physiology. MCL-1 downregulation in these cells led to extensive mitochondrial fragmentation, increased mitochondrial oxidative stress and a reduced mitochondrial membrane potential. These aberrations in the mitochondrial architecture and physiology were identical to those induced by Obatoclax treatment, thus highlighting the potential contribution of MCL-1 to normal mitochondrial organization and function. Perciavalle et al. provided evidence for contribution of MCL-1 to mitochondrial physiology. Apart from the antiapoptotic form of MCL-1 which localizes to the mitochondrial outer membrane, an amino-terminally truncated form of MCL-1 (contains intact carboxyl-terminus domain which harbors the BH3 domain binding hydrophobic groove where Obatoclax is predicted to bind) which localizes to the mitochondrial matrix plays a critical role in maintaining normal architecture, physiology, homeostasis, bioenergetics and fusion of the mitochondria [22]. Interestingly, putative MCL-1 specific BH3 mimetics such as BI97C1 and BI112D1 have also been shown to induce mitochondrial fragmentation, generation of ROS in mitochondria and inhibition of mitochondrial fusion independent of apoptosis and without affecting MCL-1 levels. In the same paper, the authors demonstrate extensive mitochondrial fragmentation upon siRNA mediated MCL-1 depletion in H23 lung cancer cells [49]. We therefore speculate that Obatoclax mediated MCL-1 antagonization may significantly contribute to the abolishment of mitochondrial structure and function.

We also demonstrate the single agent efficacy of Obatoclax in xenograft mouse model. Obatoclax exhibited dose dependent tumor regression in OSCC cell line derived subcutaneous tumors without detectable animal toxicity or weight loss. Moreover, consistent with our prior observation that MCL-1 is a critical radioresistance related factor in OSCC cells [18], Obatoclax exhibited a significant clonogenic inhibition in combination with ionizing radiation as opposed to the either treatments alone. The radiosensitizing effect of Obatoclax observed in the present study suggests that oral cancer patients may benefit from the combined therapeutic regimens including Obatoclax.

In summary, our studies indicate that Obatoclax which targets the prosurvival members of the BCL-2 family, specifically MCL-1, induces autophagy in OSCC cells leading to a caspase-independent, nonapoptotic form of cell death called necroptosis. These events are associated with extensive mitochondrial stress and dysfunction, are upstream to necroptosis and primarily attributed to Obatoclax mediated MCL-1 antagonization (Figure 12).

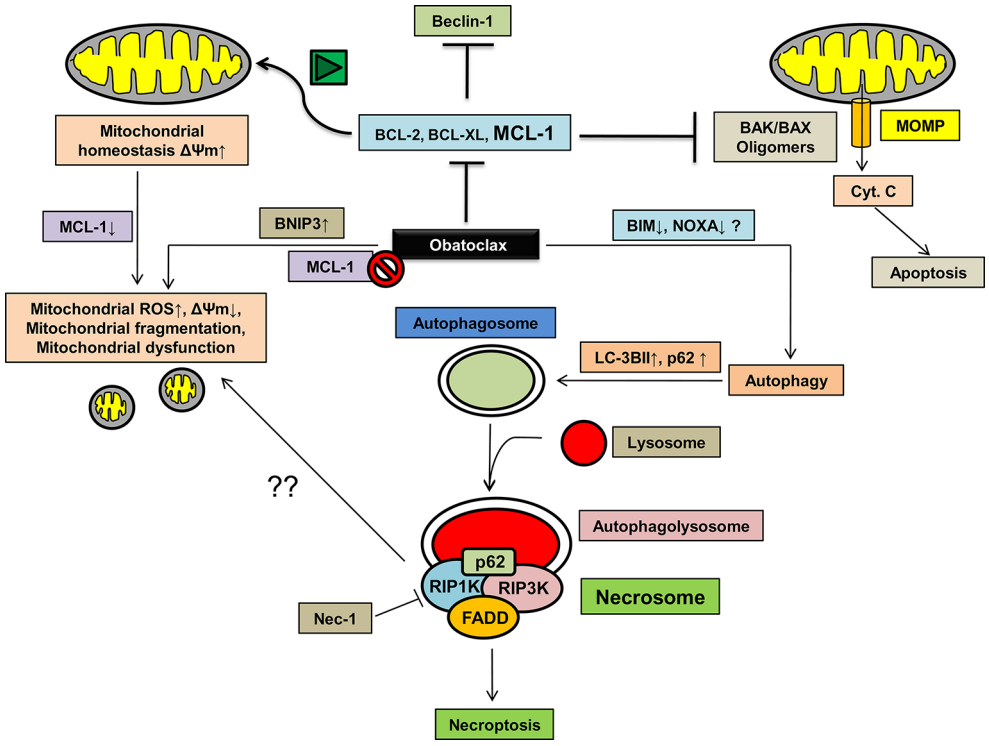

Figure 12: The proposed mode of Obatoclax action. Obatoclax potently induces autophagy in OSCC cells. However, a late-stage block in the degradation step of autophagy leads to assembly of key proteins of the necrosome such as RIP1K, RIP3K and FADD at the autophagosomes along with p62/SQSTM1 in a complex called necrosome. Necroptosis is associated with extensive mitochondrial fragmentation, an induction of BNIP3 expression which potentiates ROS accumulation in the mitochondria, reduced mitochondrial membrane potential leading to mitochondrial dysfunction. Alternatively, whether or not MCL-1 inhibition mediated by Obatoclax at least partly contributes to the impaired mitochondrial homeostasis needs to be evaluated.

Although surgery remains the primary treatment modality for oral cancers, a multimodal approach including postoperative radiotherapy or chemotherapy (5-fluorouracil, platinum based drugs) is administered for advanced-stage disease [64]. However, we and others have reported the association of MCL-1 overexpression with resistance to radiation and cisplatin in oral cancers [18, 19]. Our studies also provide evidence for a synergistic combination of ionizing radiation and Obatoclax for the treatment of oral cancers. Although phase I clinical trials have demonstrated robust single-agent activity of Obatoclax in patients with advanced CLL [33] and small cell lung cancer [65], these were associated with neurotoxicity. Phase II clinical trials however, have not shown significant efficacy and were restricted by dose-limiting toxicity which includes thrombocytopenia, anemia, neutropenia, fatigue and ataxia [35]. Nevertheless, rational combination of treatments, systematic planning of therapeutic regimens and evaluation of molecular determinants of therapeutic outcomes may enhance the potency of Obatoclax.

We thus propose its potential application in the clinics for the better management of oral cancers.

MATERIALS AND METHODS

Cell culture

Four human oral cell lines derived from different oral subsites were used in the study. DOK (Dysplastic oral keratinocyte) derived from tongue epithelium [66] was cultured in DMEM (Gibco, USA) supplemented with 5 μg/ml hydrocortisone and 10% fetal bovine serum (Gibco). AW13516 and AW8507 cell lines were derived from poorly differentiated squamous cell carcinoma and epidermoid carcinoma of the tongue respectively [67]. UPCI:SCC029B cell line was derived from poorly differentiated squamous cell carcinoma of buccal mucosa [68]. AW8507, AW13516 and SCC029B cells were cultured in IMDM (Gibco) containing 10% fetal bovine serum. All the cell lines were authenticated by short tandem repeat (STR) profiling of 21 markers.

Reagents and antibodies

Inhibitors, reagents and constructs

Obatoclax Mesylate (GX15-070) (Selleck chemicals, Texas, USA) was resuspended in DMSO to prepare a stock solution of 20 mM, aliquoted and stored at –20°C. It was brought to the desired working concentration by appropriately diluting in culture medium. 0.001% DMSO was used as vehicle control across all experiments. The pan-caspase inhibitor Z-VAD-FMK (Abcam, Cambridge, UK), Chloroquine and Necrostatin-1 (Calbiochem, USA) were used at 50 μM concentration. MTT reagent was dissolved in phosphate buffered saline (PBS) to a final concentration of 5 mg/ml. Changes in the mitochondrial network architecture were studied by using MitoTracker Green, MitoTracker Red CMXRos and MitoSOX Red dyes (Molecular probes, Invitrogen, USA). DAPI (4′,6-diamidino-2-phenylindole) or Hoechst 33342 (BD Biosciences, New Jersey, USA) were used to visualize nuclei. All standard chemicals were purchased from Sigma unless otherwise indicated. pBABE-puro mCherry-EGFP-LC3B construct was a gift from Jayanta Debnath (Addgene plasmid #22418). Control/Scrambled siRNA, siGLO, siRNA against human MCL-1 and ATG5 were obtained from Dharmacon (CO, USA). siRNA transfections were performed using Lipofectamine 2000 reagent (Invitrogen) according to the manufacturer's instructions.

Antibodies

Primary antibodies against MCL-1 (sc-20679, sc-819), BCL-2 (sc-492), BAK (sc-832), NOXA (sc-26917), BID (sc-6538), Beclin-1 (sc-11427) and Actin (sc-1616R) were obtained from Santa Cruz Biotechnology (Texas, USA). Antibodies for p62 (#5114), HSP60 (#12165), BIM (#2933), BCL-XL (#2764), ATG5 (#12994), RIP1K (#4926) and RIP3K (#13526) were obtained from Cell Signaling technologies (Massachusetts, USA). Antibodies for PUMA (ab9643) and LC-3B (ab51520) were purchased from Abcam, and BAX (A3533) antibody from Dako (Denmark). For immunofluorescence, Alexa fluor 488, and Alexa fluor 568 secondary antibodies were used (Molecular probes).

Colony formation assays

Briefly, cells were seeded in a 6-well plate (Nunc, Denmark) in duplicate and allowed to grow overnight followed by exposure to a range of Obatoclax concentrations for 24 hours. After the treatment, the drug containing medium was replaced with fresh growth medium and the cells were allowed to grow for further 10 days till appearance of visible colonies. The colonies were fixed and stained with Crystal Violet (Hi-Media Laboratories, India) and scored manually.

Clonogenic assays to assess radiosensitivities in combination with Obatoclax

Exponentially growing cells were seeded in 35 mm plates and allowed to grow for 24 hours. Next day, the cells were irradiated (γ-irradiation on a ^{60}Co source) with their respective D_0 doses (previously determined by standard clonogenic assays [18]). Immediately after irradiation, the cells were exposed to 100 nM Obatoclax for 24 hours. After treatment, the drug containing medium was replaced with fresh growth medium and the cells

were allowed to grow for further 8–10 days until visible colonies appeared in the control plate. The colonies were stained and scored as described earlier.

Protein extraction and western blotting

The cells were harvested and lysed in cell lysis buffer (50 mM Tris pH 7.4, 150 mM NaCl, 0.5% NP-40) containing protease inhibitors (Fermentas, Canada). The cell lysates were incubated on ice for 30 minutes followed by centrifugation and the supernatants were subjected to protein estimation by Bradford assay (BioRad, USA). Equal amounts of proteins were resolved on SDS-PAGE and electroblotted onto PVDF membranes (Pall Technologies, USA). The membranes were blocked in 5% bovine serum albumin (BSA) in tris buffered saline (TBS) for 1 hour and then incubated with primary antibodies overnight at 4°C. Next day, the membranes were washed and incubated with secondary antibody at room temperature for 1 hour followed by washing. The proteins were visualized using enhanced chemiluminiscence kit (GE Healthcare, UK). Densitometric analysis was performed using the image J software (NIH, Bethesda, MD). β-actin served as the loading control. Mitochondrial fractionation from the cells was performed by using Mitochondria isolation kit (#89874, Thermo Scientific, IL, USA) according to manufacturer's instructions.

Coimmunoprecipitation

The cells were harvested and lysed in EBC lysis buffer (50 mM Tris pH 7.4, 150 mM NaCl, 1 mM EDTA, 0.5% NP-40) containing protease inhibitors followed by centrifugation. The supernatants were precleared with protein G-sepharose beads (GE, UK) and subjected to overnight incubation with appropriate antibody at 4°C on a rocking platform. Next day, these cell lysates were incubated with protein G-sepharose bead slurry for 3 hours. The immunoprecipitates were recovered by gentle centrifugation, boiled in laemmli buffer and subjected to immunoblotting.

RNA extraction, cDNA synthesis and real time PCR

Total RNA was extracted from cells by using TRIZol reagent (Invitrogen) according to manufacturer's instructions. 500 ng of total RNA was converted to cDNA by High Capacity cDNA synthesis kit (Applied Biosystems). The primers used for BNIP3 and GAPDH were as reported earlier [69]. Real Time PCR was performed on ABI QuantStudio 12 K Flex Sequence detection system (Applied Biosystems) using SYBR Green mastermix (Applied Biosystems). The results were analyzed by relative quantitation and expressed as $2^{-\Delta Ct}$.

Flow cytometry

Measurement of ROS accumulation in mitochondria

The mitochondrial ROS accumulation was assessed by staining the cells with 5 μM MitoSOX Red for 10 minutes at 37°C in dark followed by acquisition on FL-2 channel of FACS caliber flow cytometer (Becton Dickinson, USA) and data was analyzed on Cell Quest software (BD Biosciences).

Annexin V-FITC staining

After the drug treatment, the cells were harvested by trypsinization, washed twice with PBS and resuspended in Annexin V binding buffer (BD Biosciences) and incubated with Annexin V-FITC antibody (BD Biosciences) in dark for 15 minutes at room temperature followed by acquisition on FL-1 channel of FACS caliber flow cytometer and data was analyzed on Cell Quest software.

Immunofluorescence and confocal microscopy

For live cell imaging, cells were cultured in confocal dishes and stained with 100 nM MitoTracker Green, 5 μM MitoSOX Red or 10 μM JC-1 dyes. For immunofluorescence staining, cells growing on coverslips were fixed with 4% paraformaldehyde followed by permeabilization with 0.5% triton X-100. Blocking was done in 5% BSA for 1 hour. The cells were then incubated with primary antibodies for 1 hour at room temperature followed by detection with appropriate secondary antibodies with 1 hour incubation at room temperature in dark. Nuclei were counterstained with DAPI. The coverslips were mounted with Vecta-shield (Vector laboratories, UK) on glass slides, sealed with nail polish and observed under a laser confocal microscope (LSM 510 Metaconfocal, Zeiss, Germany).

Cell viability assays

MTT assay

Cells growing in the exponential phase were harvested by trypsinization and 2000 cells per well were seeded in 96-well plates (Nunc) and allowed to grow overnight. Next day, the medium was removed and the cells were treated with indicated concentrations of Obatoclax for the specified time points. At the end of the treatment period, 20 μl MTT was added to each well and the plates were again incubated in CO_2 incubator for 4 hours. The formazon crystals were dissolved by addition of DMSO and absorbance was recorded on a microplate reader (Spectrostar nano, BMG Labtech, Germany) at 540 nm with a reference wavelength of 690 nm.

Sulforhodamine B (SRB) assay

After the specified time point of drug treatment, the cells in 96 well plates were fixed with 30% Trichloroacetic acid (TCA) for 1 hour at 4°C followed by washing with water. The plates were then air dried and stained with SRB dye (0.05% w/v) for 30 minutes at room temperature. Excess dye was washed off by repeated washing with 1% acetic acid (v/v) and the plates were again air dried. Finally, the protein-bound dye was solubilized by addition of 10 mM Tris (pH 10) and absorbance was recorded at 540 nm with a reference wavelength of 690 nm on a microplate reader.

Assessment of mitochondrial membrane potential (ΔΨm)

To study the effect of Obatoclax on the mitochondrial membrane potential (ΔΨm), we employed JC-1 dye (eBiosciences, San Diego, CA, USA) which is a cationic cell permeable dye and selectively accumulates in mitochondria in a potential dependent manner. Mitochondrial membrane polarization leads to the reversible formation of J-aggregates which causes a shift in the fluorescence emission from 530 nm (corresponding to JC-1 monomers which emits green fluorescence) to 590 nm (corresponding to J-aggregates which emits red-orange fluorescence). Cells growing in confocal dishes were incubated with 10 µM JC-1 dye for 30 minutes. The cells were then washed with PBS, replenished with fresh medium and observed under a fluorescence microscope.

Transmission electron microscopy

Briefly, the cells were harvested by trypsinization and fixed with 3% glutaraldehyde at 4°C for 3–4 hours followed by washing with 0.1 M sodium cacodylate buffer. The cell pellets were then fixed in Osmium tetroxide for 1 hour at 4°C in dark, subjected to dehydration by passing through different grades of alcohol and then mounted with Araldite resin. The ultrathin sections (~60–70 nm) were mounted on formvar coated copper grids. These sections were stained with uranyl acetate solution and counterstained with lead citrate. Electron micrographs were captured on a Jeol 100-CXII electron microscope (Jeol, UK) using Olympus camera and iTEM software.

In vivo studies

Ethics statement

Investigation has been conducted in accordance with the ethical standards and according to the declaration of Helsinki and national and international guidelines. The study has been approved by the Institutional Animal Ethics Committee (IAEC) of Tata Memorial Centre (TMC)-Advanced Centre for Treatment, Research and Education in Cancer (ACTREC). To assess the *in vivo* antitumor activity of Obatoclax, we employed xenograft mouse model as described earlier [26]. Briefly, 6–8 weeks old female BALB/C nude mice were subcutaneously injected with 1×10^6 SCC029B cells in 100 µl IMDM medium. The animals were then randomized into 4 groups, containing 6 animals each. Tumors were observed about 21 days post cell inoculation. Each group of animals were intravenously injected (through lateral tail vein) with different doses of Obatoclax (cumulative doses of 1.25 mg/kg, 2.5 mg/kg, 5 mg/kg and a vehicle control group) evenly distributed over a period of 5 days (i.e. 5 injections). The drug was formulated at the indicated concentrations in 9.6% PEG, 0.4% Tween 20 and 5% dextrose. The tumor volume measurements were done using a vernier caliper every alternate day by the formula: Length (mm) * [Width (mm)]^2/2. For assessment of any drug associated toxicity, weight of the animals was monitored every alternate day.

Statistical analysis

All the statistical analyses were performed using GraphPad Prism software (version 5.01). Two data sets in an experiment were compared by a two-tailed unpaired student's *t* test. The data is represented as mean ± Standard error mean (SEM). The difference between mean was considered significant when $p < 0.05$.

ACKNOWLEDGMENTS AND FUNDING

We are thankful to Prof. Sussane Gollin-University of Pittsburgh, PA and Dr. Ken Parkinson, Queen Mary's School of Medicine & Dentistry, UK for their kind gift of oral cell lines. We would also like to thank Miss. Priyanka Rajput, Miss. Harshada Sulkshane, Mr. Aniket Kamble for assistance with western blotting and Mr. Vivek Teli for his help with animal experimentation. Mr. Prasad Sulkshane is a fellow of Department of Biotechnology, Government of India.

CONFLICTS OF INTEREST

The authors declare that no competing interest exists.

REFERENCES

1. Tandle A, Sanghvi V, Saranath D. Determination of p53 genotypes in oral cancer patients from India. Brit J Cancer. 2001; 84.
2. Herrero R, Castellsagué X, Pawlita M, Lissowska J, Kee F, Balaram P, Rajkumar T, Sridhar H, Rose B, Pintos J. Human papillomavirus and oral cancer: the International Agency for Research on Cancer multicenter study. J Natl Cancer I. 2003; 95:1772–1783.

3. Dikshit R, Gupta PC, Ramasundarahettige C, Gajalakshmi V, Aleksandrowicz L, Badwe R, Kumar R, Roy S, Suraweera W, Bray F. Cancer mortality in India: a nationally representative survey. The Lancet. 2012; 379:1807–1816.

4. Notani PN. Global variation in cancer incidence and mortality. Curr Sci India. 2001; 81:465–474.

5. Lee K, Veness M, Pearl, Larson T, Morgan G. Role of combined modality treatment of buccal mucosa squamous cell carcinoma. Aust Dent J. 2005; 50:108–113.

6. Miyashita T, Krajewski S, Krajewska M, Wang HG, Lin H, Liebermann DA, Hoffman B, Reed JC. Tumor suppressor p53 is a regulator of bcl-2 and bax gene expression *in vitro* and *in vivo*. Oncogene. 1994; 9:1799–1805.

7. Pietrzak M, Puzianowska-Kuznicka M. p53-dependent repression of the human MCL-1 gene encoding an anti-apoptotic member of the BCL-2 family: the role of Sp1 and of basic transcription factor binding sites in the MCL-1 promoter. Biol Chem. 2008; 389:383–393.

8. Findley HW, Gu L, Yeager AM, Zhou M. Expression and regulation of Bcl-2, Bcl-xl, and Bax correlate with p53 status and sensitivity to apoptosis in childhood acute lymphoblastic leukemia. Blood. 1997; 89:2986–2993.

9. Dai M, Clifford GM, Le Calvez F, Castellsagué X, Snijders PJ, Pawlita M, Herrero R, Hainaut P, Franceschi S. Human Papillomavirus Type 16 and TP53 Mutation in Oral Cancer Matched Analysis of the IARC Multicenter Study. Cancer Res. 2004; 64:468–471.

10. Saranath D, Tandle A, Teni T, Dedhia P, Borges A, Parikh D, Sanghavi V, Mehta A. p53 inactivation in chewing tobacco-induced oral cancers and leukoplakias from India. Oral Oncol. 1999; 35:242–250.

11. Polverini P, Nor J. Apoptosis and predisposition to oral cancer. Crit Rev Oral Biol M. 1999; 10:139–152.

12. Xie X, Clausen OPF, Angelis PD, Boysen M. The prognostic value of spontaneous apoptosis, Bax, Bcl-2, and p53 in oral squamous cell carcinoma of the tongue. Cancer. 1999; 86:913–920.

13. Michaud WA, Nichols AC, Mroz EA, Faquin WC, Clark JR, Begum S, Westra WH, Wada H, Busse PM, Ellisen LW. Bcl-2 blocks cisplatin-induced apoptosis and predicts poor outcome following chemoradiation treatment in advanced oropharyngeal squamous cell carcinoma. Clin Cancer Res. 2009; 15:1645–1654.

14. Camisasca DR, Honorato J, Bernardo V, da Silva LE, da Fonseca EC, de Faria PAS, Dias FL, Lourenço SdQC. Expression of Bcl-2 family proteins and associated clinicopathologic factors predict survival outcome in patients with oral squamous cell carcinoma. Oral Oncol. 2009; 45:225–233.

15. Mallick S, Agarwal J, Kannan S, Pawar S, Kane S, Teni T. Bcl-xL protein: Predictor of complete tumor response in patients with oral cancer treated with curative radiotherapy. Head & neck. 2013; 35:1448–1453.

16. Mallick S, Patil R, Gyanchandani R, Pawar S, Palve V, Kannan S, Pathak K, Choudhary M, Teni T. Human oral cancers have altered expression of Bcl-2 family members and increased expression of the anti-apoptotic splice variant of Mcl-1. J Pathol. 2009; 217:398–407.

17. Mallick S, Agarwal J, Kannan S, Pawar S, Kane S, Teni T. PCNA and anti-apoptotic Mcl-1 proteins predict disease-free survival in oral cancer patients treated with definitive radiotherapy. Oral Oncol. 2010; 46:688–693.

18. Palve VC, Teni TR. Association of anti-apoptotic Mcl-1L isoform expression with radioresistance of oral squamous carcinoma cells. Radiat Oncol. 2012; 7:135–145.

19. Palve V, Mallick S, Ghaisas G, Kannan S, Teni T. Overexpression of Mcl-1L Splice Variant Is Associated with Poor Prognosis and Chemoresistance in Oral Cancers. PloS one. 2014; 9:e111927.

20. Thomas LW, Lam C, Edwards SW. Mcl-1; the molecular regulation of protein function. FEBS Lett. 2010; 584: 2981–2989.

21. Ertel F, Nguyen M, Roulston A, Shore GC. Programming cancer cells for high expression levels of Mcl1. EMBO Rep. 2013.

22. Perciavalle RM, Stewart DP, Koss B, Lynch J, Milasta S, Bathina M, Temirov J, Cleland MM, Pelletier S, Schuetz JD. Anti-apoptotic MCL-1 localizes to the mitochondrial matrix and couples mitochondrial fusion to respiration. Nat Cell Biol. 2012; 14:575–583.

23. Jamil S, Mojtabavi S, Hojabrpour P, Cheah S, Duronio V. An essential role for MCL-1 in ATR-mediated CHK1 phosphorylation. Mol Biol Cell. 2008; 19:3212–3220.

24. Jamil S, Stoica C, Hackett TL, Duronio V. MCL-1 localizes to sites of DNA damage and regulates DNA damage response. Cell Cycle. 2010; 9:2915–2927.

25. Thomas RL, Roberts DJ, Kubli DA, Lee Y, Quinsay MN, Owens JB, Fischer KM, Sussman MA, Miyamoto S, Gustafsson ÅB. Loss of MCL-1 leads to impaired autophagy and rapid development of heart failure. Gene Dev. 2013; 27:1365–1377.

26. Nguyen M, Marcellus RC, Roulston A, Watson M, Serfass L, Madiraju SM, Goulet D, Viallet J, Bélec L, Billot X. Small molecule obatoclax (GX15-070) antagonizes MCL-1 and overcomes MCL-1-mediated resistance to apoptosis. P Natl Acad Sci-Biol. 2007; 104:19512–19517.

27. Yecies D, Carlson NE, Deng J, Letai A. Acquired resistance to ABT-737 in lymphoma cells that up-regulate MCL-1 and BFL-1. Blood. 2010; 115:3304–3313.

28. van Delft MF, Wei AH, Mason KD, Vandenberg CJ, Chen L, Czabotar PE, Willis SN, Scott CL, Day CL, Cory S. The BH3 mimetic ABT-737 targets selective Bcl-2 proteins and efficiently induces apoptosis via Bak/Bax if Mcl-1 is neutralized. Cancer cell. 2006; 10:389–399.

29. Chen S, Dai Y, Harada H, Dent P, Grant S. Mcl-1 down-regulation potentiates ABT-737 lethality by cooperatively

inducing Bak activation and Bax translocation. Cancer Res. 2007; 67:782–791.

30. Rahmani M, Aust MM, Attkisson E, Williams DC, Ferreira-Gonzalez A, Grant S. Inhibition of Bcl-2 antiapoptotic members by obatoclax potently enhances sorafenib-induced apoptosis in human myeloid leukemia cells through a Bim-dependent process. Blood. 2012; 119:6089–6098.
31. Huang S, Okumura K, Sinicrope FA. BH3 mimetic obatoclax enhances TRAIL-mediated apoptosis in human pancreatic cancer cells. Clin Cancer Res. 2009; 15:150–159.
32. Smoot RL, Blechacz BR, Werneburg NW, Bronk SF, Sinicrope FA, Sirica AE, Gores GJ. A Bax-mediated mechanism for obatoclax-induced apoptosis of cholangiocarcinoma cells. Cancer research. 2010; 70:1960–1969.
33. O'Brien SM, Claxton DF, Crump M, Faderl S, Kipps T, Keating MJ, Viallet J, Cheson BD. Phase I study of obatoclax mesylate (GX15-070), a small molecule pan–Bcl-2 family antagonist, in patients with advanced chronic lymphocytic leukemia. Blood. 2009; 113:299–305.
34. Schimmer AD, O'Brien S, Kantarjian H, Brandwein J, Cheson BD, Minden MD, Yee K, Ravandi F, Giles F, Schuh A. A phase I study of the pan bcl-2 family inhibitor obatoclax mesylate in patients with advanced hematologic malignancies. Clin Cancer Res. 2008; 14:8295–8301.
35. Parikh SA, Kantarjian H, Schimmer A, Walsh W, Asatiani E, El-Shami K, Winton E, Verstovsek S. Phase II study of obatoclax mesylate (GX15-070), a small-molecule BCL-2 family antagonist, for patients with myelofibrosis. Clin Lymphoma Myeloma Leuk. 2010; 10:285–289.
36. Maiuri MC, Criollo A, Tasdemir E, Vicencio JM, Tajeddine N, Hickman JA, Geneste O, Kroemer G. BH3-only proteins and BH3 mimetics induce autophagy by competitively disrupting the interaction between Beclin 1 and Bcl-2/Bcl-XL. Autophagy. 2007; 3:374–376.
37. Malik S, Orhon I, Morselli E, Criollo A, Shen S, Marino G, BenYounes A, Benit P, Rustin P, Maiuri M. BH3 mimetics activate multiple pro-autophagic pathways. Oncogene. 2011; 30:3918–3929.
38. Moreau K, Luo S, Rubinsztein DC. Cytoprotective roles for autophagy. Curr Opin Cell Biol. 2010; 22:206–211.
39. Yang ZJ, Chee CE, Huang S, Sinicrope FA. The role of autophagy in cancer: therapeutic implications. Mol Cancer Ther. 2011; 10:1533–1541.
40. Vandenabeele P, Galluzzi L, Berghe TV, Kroemer G. Molecular mechanisms of necroptosis: an ordered cellular explosion. Nat Rev Mol Cell Biol. 2010; 11:700–714.
41. Pasparakis M, Vandenabeele P. Necroptosis and its role in inflammation. Nature. 2015; 517:311–320.
42. Tang Y, Hamed HA, Cruickshanks N, Fisher PB, Grant S, Dent P. Obatoclax and lapatinib interact to induce toxic autophagy through NOXA. Mol Pharmacol. 2012; 81:527–540.
43. Yazbeck VY, Li C, Grandis JR, Zang Y, Johnson DE. Single-agent obatoclax (GX15-070) potently induces apoptosis and pro-survival autophagy in head and neck squamous cell carcinoma cells. Oral Oncol. 2014; 50:120–127.
44. Wroblewski D, Jiang CC, Croft A, Farrelly ML, Zhang XD, Hersey P. OBATOCLAX and ABT-737 induce ER stress responses in human melanoma cells that limit induction of apoptosis. PloS one. 2013; 8:e84073.
45. Mizushima N, Yoshimori T. How to interpret LC3 immunoblotting. Autophagy. 2007; 3:542–545.
46. Kimura S, Noda T, Yoshimori T. Dissection of the autophagosome maturation process by a novel reporter protein, tandem fluorescent-tagged LC3. Autophagy. 2007; 3:452–460.
47. Bonapace L, Bornhauser BC, Schmitz M, Cario G, Ziegler U, Niggli FK, Schäfer BW, Schrappe M, Stanulla M, Bourquin JP. Induction of autophagy-dependent necroptosis is required for childhood acute lymphoblastic leukemia cells to overcome glucocorticoid resistance. J Clin Invest. 2010; 120:1310.
48. Kharaziha P, Chioureas D, Baltatzis G, Fonseca P, Rodriguez P, Gogvadze V, et al. Sorafenib-induced defective autophagy promotes cell death by necroptosis. Oncotarget. 2015; 6:37066.
49. Varadarajan S, Butterworth M, Wei J, Pellecchia M, Dinsdale D, Cohen GM. Sabutoclax (BI97C1) and BI112D1, Putative Inhibitors of MCL-1, Induce Mitochondrial Fragmentation Either Upstream of or Independent of Apoptosis. Neoplasia. 2013; 15:568.
50. Christofferson DE, Yuan J. Necroptosis as an alternative form of programmed cell death. Curr Opin Cell Biol. 2010; 22:263–268.
51. Burton TR, Gibson SB. The role of Bcl-2 family member BNIP3 in cell death and disease: NIPping at the heels of cell death. Cell Death Differ. 2009; 16:515–523.
52. Placzek W, Wei J, Kitada S, Zhai D, Reed J, Pellecchia M. A survey of the anti-apoptotic Bcl-2 subfamily expression in cancer types provides a platform to predict the efficacy of Bcl-2 antagonists in cancer therapy. Cell Death Dis. 2010; 1:e40.
53. Mott JL, Bronk SF, Mesa RA, Kaufmann SH, Gores GJ. BH3-only protein mimetic obatoclax sensitizes cholangiocarcinoma cells to Apo2L/TRAIL-induced apoptosis. Mol Cancer Ther. 2008; 7:2339–2347.
54. Zhang H, Guttikonda S, Roberts L, Uziel T, Semizarov D, Elmore S, Leverson J, Lam L. Mcl-1 is critical for survival in a subgroup of non-small-cell lung cancer cell lines. Oncogene. 2011; 30:1963–1968.
55. Luo S, Garcia-Arencibia M, Zhao R, Puri C, Toh PP, Sadiq O, Rubinsztein DC. Bim inhibits autophagy by recruiting Beclin 1 to microtubules. Mol Cell. 2012; 47:359–370.
56. Luo S, Rubinsztein DC. BCL2L11/BIM: a novel molecular link between autophagy and apoptosis. Autophagy. 2013; 9:104–105.
57. F McCoy JH, N McTavish, I Paul, C Barnes, B O'Hagan, K Odrzywol, J Murray, D Longley, G McKerr and DA Fennell. Obatoclax induces Atg7-dependent autophagy

independent of beclin-1 and BAX/BAK. Cell Death Dis. 2010; 1:1–13.

58. Basit F, Cristofanon S, Fulda S. Obatoclax (GX15-070) triggers necroptosis by promoting the assembly of the necrosome on autophagosomal membranes. Cell Death Differ. 2013; 20:1161–1173.
59. Pattingre S, Tassa A, Qu X, Garuti R, Liang XH, Mizushima N, Packer M, Schneider MD, Levine B. Bcl-2 antiapoptotic proteins inhibit Beclin 1-dependent autophagy. Cell. 2005; 122:927–939.
60. Stamelos VA, Fisher N, Bamrah H, Voisey C, Price JC, Farrell WE, Redman CW, Richardson A. The BH3 Mimetic Obatoclax Accumulates in Lysosomes and Causes Their Alkalinization. PloS one. 2016; 11:e0150696.
61. Nakagawa T, Shimizu S, Watanabe T, Yamaguchi O, Otsu K, Yamagata H, Inohara H, Kubo T, Tsujimoto Y. Cyclophilin D-dependent mitochondrial permeability transition regulates some necrotic but not apoptotic cell death. Nature. 2005; 434:652–658.
62. Tait SW, Oberst A, Quarato G, Milasta S, Haller M, Wang R, Karvela M, Ichim G, Yatim N, Albert ML. Widespread mitochondrial depletion via mitophagy does not compromise necroptosis. Cell rep. 2013; 5:878–885.
63. Murphy JM, Czabotar PE, Hildebrand JM, Lucet IS, Zhang JG, Alvarez-Diaz S, Lewis R, Lalaoui N, Metcalf D, Webb AI. The pseudokinase MLKL mediates necroptosis via a molecular switch mechanism. Immunity. 2013; 39:443–453.
64. Omura K. Current status of oral cancer treatment strategies: surgical treatments for oral squamous cell carcinoma. Int J Clin Oncol. 2014; 19:423–430.
65. Chiappori A, Schreeder M, Moezi M, Stephenson J, Blakely J, Salgia R, Chu Q, Malik S, Modiano M, Berger M. A phase Ib trial of Bcl-2 inhibitor obatoclax in combination with carboplatin and etoposide for previously untreated patients with extensive-stage small cell lung cancer (ES-SCLC). J Clin Oncol. 2009; 27:3576.
66. Chang SE, Foster S, Betts D, Marnock WE. DOK, a cell line established from human dysplastic oral mucosa, shows a partially transformed non-malignant phenotype. Int J Cancer. 1992; 52:896–902.
67. Tatake RJ, Rajaram N, Damle R, Balsara B, Bhisey A, Gangal SG. Establishment and characterization of four new squamous cell carcinoma cell lines derived from oral tumors. J Cancer Res Clin. 1990; 116:179–186.
68. Martin CL, Reshmi SC, Ried T, Gottberg W, Wilson JW, Reddy JK, Khanna P, Johnson JT, Myers EN, Gollin SM. Chromosomal imbalances in oral squamous cell carcinoma: examination of 31 cell lines and review of the literature. Oral Oncol. 2008; 44:369–382.
69. Murai M, Toyota M, Suzuki H, Satoh A, Sasaki Y, Akino K, Ueno M, Takahashi F, Kusano M, Mita H. Aberrant methylation and silencing of the BNIP3 gene in colorectal and gastric cancer. Clin Cancer Res. 2005; 11:1021–1027.